CHEMICAL·ENGINEERING
STELLENBOSCH·UNIVERSITY

Oxidant Concentration Effects In the Hydroxylation of Phenol over Titanium-Based Zeolites Al-free Ti-Beta and TS-1

by

Robert M Burton
B. Eng. (Chemical)

Thesis presented in partial fulfillment of the requirements for the degree

of

MASTER OF SCIENCE IN ENGINEERING
(Chemical Engineering)

In the Department of Process Engineering
at the University of Stellenbosch

Supervising Lecturer
DR. L.H. CALLANAN

STELLENBOSCH, SOUTH AFRICA
March 2006

Declaration

I, the undersigned herewith declare that the work presented in this thesis is my own and was completed without assistance from other persons, unless otherwise acknowledged or referenced in a specific section, except for assistance received in formal discussions with the personnel of the Department of Process Engineering, University of Stellenbosch, and the Department of Chemical Engineering, University of Cape Town. To the best of my knowledge it contains neither material previously published or written by another person, nor material which has been accepted for the award of any other degree or diploma of the university or other institute, except where due acknowledgement has been made.

Date submitted: March 28, 2007

Signed: _____

Robert Maynard Burton
U.S. Student No: 12881295

Synopsis

This work focuses on the effects of hydrogen peroxide concentration on the catalytic activity and product selectivity in the liquid-phase hydroxylation of phenol over titanium-substituted zeolites Al-free Ti-Beta and TS-1 in water and methanol solvents. Hydroquinone is typically the desired product, and these solvents employed have previously been shown to be of importance in controlling the selectivity of this reaction.

Different volumetric quantities of an aqueous 30 wt-% peroxide solution were added to either water or methanol solutions containing the catalyst and phenol substrate, and the reaction monitored by withdrawing samples over a period of 6-8 hours.

For Al-free Ti-Beta catalysed reactions, the peroxide concentration affects the selectivity and activity differently in water and methanol solvents. Using methanol solvent, the selectivity to hydroquinone formation is dominant for all peroxide concentrations (p/o-ratio > 1), and is favoured by higher initial peroxide concentrations (> 1.27 vol-%), where p/o-ratios of up to 2 can be reached; in water solvent, increasing the peroxide concentration above this level results in almost unchanging selectivity (p/o-ratio of *ca.* 0.35). For lower peroxide concentrations in water, the p/o-ratio increases slightly, but never exceeds the statistical distribution of *ca.* 0.5. Using water as a solvent, higher phenol conversion is obtained as the initial peroxide concentration increases; in methanol the phenol conversion is largely independent of peroxide concentration.

As expected for the smaller pore TS-1, higher hydroquinone selectivity is obtained in methanol than for Al-free Ti-Beta, which is consistent with shape-selectivity effects enhanced by the use of this protic solvent. Interestingly, with TS-1 the p/o-ratio is higher at lower phenol conversions, and specifically when the initial peroxide concentration is low (p/o-ratio exceeding 3 were obtained at low phenol conversion), and decreases to a near constant value at higher conversions regardless of the starting peroxide concentration. Thus, low peroxide concentrations favour hydroquinone formation when TS-1 is used as the catalyst.

Comparing the performance of the two catalysts using methanol solvent, the phenol conversion on TS-1 is more significantly influenced by higher hydrogen peroxide concentrations than Al-free Ti-Beta. However, with higher initial concentrations the unselective phenol conversion to tars is more severe since the hydroquinone selectivity is not higher at these high peroxide concentrations. The increased tar formation, expressed as tar deposition on the catalyst or as the tar formation rate constant, confirms that the greater

amount of free-peroxide present is mainly responsible for the non-selective conversion of phenol.

Kinetic modelling of the reaction data with an overall second-order kinetic model gave a good fit in both solvents, and the phenol rate constant is independent of changing hydrogen peroxide concentration for the hydroxylation over Al-free Ti-Beta using water as the solvent (k_{Phenol} = 1.93 x 10^{-9} $dm^3/mmol.m^2.s$). This constant value suggests that the model developed to represent the experimental data is accurate. For TS-1 in methanol solvent the rate constant is also independent of peroxide concentration (k_{Phenol} = 1.36 x 10^{-8} $dm^3/mmol.m^2.s$).

The effect of the method of peroxide addition was also investigated by adding discrete amounts over a period of 4.5 hours, and was seen to improve hydroquinone selectivity for reaction on both catalysts, and most significantly for Al-free Ti-Beta in methanol solvent. With TS-1, the mode of peroxide addition had little influence on phenol conversion, but the initial selectivity to hydroquinone was *ca.* 1.6 times higher than for an equivalent single-portion addition (at a similar phenol conversion). Discrete peroxide addition for hydroxylation in methanol over Al-free Ti-Beta gave greatly improved hydroquinone selectivities compared to the equivalent single-dose addition. Compared to TS-1, the initial selectivity was not as high (p/o-ratios of 0.86 and 1.40 respectively at 10 mol-% phenol conversion), but this can be explained on the basis of geometric limitations in the micropores of TS-1 favouring hydroquinone formation. The *final* selectivity, however, is marginally higher (using the same mode of peroxide addition, and at the same phenol conversion).

Pectora roborant cultus recti

Discrete peroxide addition has an additional benefit in that it also reduces the quantity of free-peroxide available for product over-oxidation, and consequently reduces the amount of tars formed.

Thus, the interaction of the effects of peroxide concentration and the solvent composition and polarity on the product selectivity and degree of tar formation is important. Particularly with TS-1, lower peroxide concentrations in bulk methanol solvent are highly beneficial for hydroquinone formation, because of the implicit geometric constraints in the micropores, the lower water concentration, and the decreased tar formation associated with high methanol concentrations. This could have significant reactor design implications, as the results obtained here suggest that the reaction should be terminated after approximately 30 minutes to maximise hydroquinone production (under the conditions evaluated in these experiments), even though the corresponding phenol conversions are low (*ca.* 10 mol-%). The higher hydroquinone selectivities reached at low phenol conversions for the discrete peroxide addition experiments also confirm this. Practically, to enhance the hydroquinone selectivity

for reaction over TS-1, the initial phenol-peroxide molar ratio should be *ca.* 10, methanol should constitute not less than 90 vol-% of the reaction volume, and the peroxide should be added in discrete amounts.

For reaction over Al-free Ti-Beta, methanol solvent also enhances the hydroquinone formation as expected. At low phenol conversions (*ca.* 10 mol-%) hydroquinone is still the preferred product, although in contrast to TS-1 the selectivity increases with phenol conversion, and is higher with higher initial peroxide concentrations. Under the best conditions evaluated here for optimal hydroquinone formation, the initial phenol-peroxide molar ratio should be *ca.* 2.5, with methanol making up at least 90 vol-% of the total volume. Discrete peroxide addition in methanol solvent for the Al-free Ti-Beta catalysed hydroxylation gives excellent improvements in hydroquinone selectivity (2.5 times higher than water solvent), and the addition in more discrete portions might further improve hydroquinone formation, and should therefore be examined.

Opsomming

Die effek van waterstofperoksiedkonsentrasie op die katalitiese aktiwiteit en produk selektiwiteit in die hidroksilering van fenol oor titaan-gesubstitueerde zeoliete Al-vry Ti-Beta en TS-1, word in hierdie werk ondersoek.

Verskillende hoeveelhede van ‘n peroksied-in-water oplossing (30 wt-% H_2O_2) is tot ‘n water- óf metanol bevattende oplossing van die katalis en fenol reaktant bygevoeg. Monsters is oor ‘n tydperk van 6-8 uur geneem om die vordering van die reaksie te volg.

Die peroksiedkonsentrasie beïnvloed die selektiwiet van die reaksie oor Al-vry Ti-Beta katalis op verskillende maniere, afhangende van of water of metanol as oplosmiddel gebruik word. In ‘n metanol oplosmiddel is die selektiwiteit vir die vorming van hidrokinoon oorheersend vir alle peroksiedkonsentrasies (p/o-verhouding > 1), en word deur aanvanklike hoër peroksiedkonsentrasies bevoordeel (> 1.27 vol-% H_2O_2); p/o-verhoudings groter as 2 kan gekry word. In water is die neiging die teenoorgestelde, met ‘n p/o-verhouding van ongeveer 0.35 wat constant bly as dié konsentrasie oorskry word. Vir laer peroksiedkonsentrasie is die p/o-verhouding effens hoër, maar die statistiese verdeling van ongeveer 0.5 is nie oortree nie.

Na verwagting is ‘n hoër selektiwitiet vir hidrokinoon in metanoloplosmiddel oor die kleiner porieë katalis TS-1 as vir Al-vry Ti-Beta gekry. Hierdie verskynsel is in ooreenstemming met struktuur-selektiwiteitseffekte, wat verhoog word deur die gebruik van hierdie protiese oplosmiddel. Dit is opmerkenswaardig dat met TS-1 katalis die p/o-verhouding hoër is by lae fenol omsettings, en spesifiek as die aanvanklike peroksied konsentrasie laag is (p/o-verhoudings wat 3 oorskry is by lae fenol omsettings gekry). Hierdie verhouding neem af na ‘n konstante waarde by hoër omsettings, onafhanklik van wat die aanvanklike peroksiedkonsentrasie is.

Vir die reaksie in ‘n metanol oplosmiddel is die fenol omsetting met TS-1 katalis in ‘n groter mate deur hoër waterstofperoksiedkonsentrasies beïnvloed teenoor Al-vry Ti-Beta. Die nie-selektiewe fenol omsetting na swaar tere is groter by aanvanklike hoër peroksiedkonsentrasies, aangesien die selektiwiteit vir hidrokinoon laer is by dié konsentrasies. Die verhoogde vorming van teer, uitgedruk as teerneerslag op die katalsis, of as die reaksiesnelheidskonstante, bevestig dat die hoër beskikbare hoeveelheid peroksied verantwoordelik is vir die nie-selektiewe omsetting.

Kinetiese modelering van die reaksiekonsentrasiedata met ‘n tweede-graadse kinetiese model, het ‘n goeie passing vir die reaksie in beide oplosmiddels gegee, en die fenol reaksiesnelheidskonstante vir hidroksilering op Al-vry Ti-Beta katalis in water oplosmiddel is onafhanklik van wisselende peroksiedkonsentrasies (k_{Phenol} = 1.93 x 10^{-9} $dm^3/mmol.m^2.s$). Hierdie konstante waarde dui aan dat die model wat die eksperimentele data navorm akkuraat is. Op die TS-1 katalis en in ‘n metanol oplosmiddel is die fenol reaksiesnelheidskonstante ook onafhanklik van die waterstofperoksiedkonsentrasie (k_{Phenol} = 1.36 x 10^{-8} $dm^3/mmol.m^2.s$).

Die effek van peroksied byvoeging in klein hoeveelhede oor ‘n tydperk van 4.5 uur is ook ondersoek, en het ‘n verbetering in die hidrokinoonselektiwiteit oor albei katalisators veroorsaak, veral met die gebruik van die metanol oplosmiddel. Oor die TS-1 katalis het die manier van peroksiedbyvoeging ‘n onbeduidende effek op die fenol omsetting gehad, maar die hidrokinoonselektiwiteit was ongeveer 1.6 keer hoër as toe die peroksied in ‘n enkele porsie bygevoeg was (by dieselfde fenol omsetting). Oor Al-vry Ti-Beta katalis was die hidrokinoonselektiwiteit heelwat hoër toe die peroksied in klein hoeveelhede bygevoeg was, as toe dit in ‘n enkele porsie bygevoeg was. In vergelyking met TS-1 katalis, was die aanvanklike selektiwitiet oor Al-vry Ti-Beta nie so hoog nie (p/o-verhoudings van onderskeidelik 0.86 en 1.40 by 10 mol-% fenol omsetting), maar hierdie verskil kan op grondslag van geometriese beperkinge in die porieë van TS-1 katalis verklaar word. Die finale selektiwiteit is egter effens hoër (met dieselfde peroksied byvoegingstempo, en by dieselfde fenol omsetting).

Pectora roborant cultus recti

Die stadige byvoeging van peroksied verminder ook die konsentrasie van vrye-peroksied wat beskikbaar is vir die verdere oksidasie van die produkte, wat tot gevolg het dat minder tere gevorm word.

Acknowledgements

Firstly, I would like to thank my supervisor, Dr. Linda Callanan, for giving me the opportunity to do this project, and for her professional guidance, encouragement and support throughout the course of this study. I am very grateful for her readily available advice and discussion, without which this work would not have been finished.

I would also like to express my sincere gratitude and appreciation to the following people who have helped in many ways:

Ms. Stephanie La Grange and Mrs. Helen Divey at UCT for their help with HPLC analysis, and for helping to sort out problems with the equipment as fast as possible.

Mrs. Hanlie Botha for all her generous help with HPLC, BET and particle size analysis.

Dr. Silke Sauerbeck of the Catalysis Research Unit at UCT for allowing me the use of her zeolite synthesis equipment, and Marc Wust for all his technical assistance.

Dr. Remy Bucher at iThemba Labs for the XRD spectra.

Mrs. Esmé Spicer for the SEM analysis.

Mr. Mohamed Jaffer at the Electron Microscopy Unit at UCT for TEM analysis.

The admin staff and assistants (especially James, Charles and Vincent) for all they do in helping make Process Engineering a great place to study at.

To my friends for all the great times we have shared over the last two years.

To my parents and sisters for their encouragement and support during the last few months. Thanks for always being there to help in whatever way you can.

I also gratefully acknowledge the NRF (South Africa) and the University of Stellenbosch for the financial support of this project.

Most importantly though, to my loving Lord who has blessed me in more ways than I can possibly ever imagine. This would never have been accomplished without His grace.

TABLE OF CONTENTS

Pectora roborant cultus recti

Nomenclature

Symbols

A_i	Absolute area of species i	[a/u]
C_i	Concentration of species i	[mmol/dm^3]
d	Diameter of particle	[m or μm]
K	Henry's adsorption constant	[-]
k_i	Formation/consumption rate constant of compound i	[dm^3/mmol.m^2.s]
M_r	Molar mass	[g/gmol]
m	Mass	[g]
n_i	Moles of species i	[mol]
r_i	Rate of formation/consumption of compound i	[mmol/s.m^2]
RF_i	Response factor of species i	[-]
S_i	Molar selectivity of species i	[%]
T	Time	[hr, min or s]
t_R	Reaction time	[min]
T	Temperature	[K or °C]
V_i	Volume of compound i	[ml or dm^3]
X_i	Conversion of species i	[mol-%]
x_i	Mass fraction of species i	[-]
y_i	Molar fraction of species i	[-]

Greek

Δ	Difference	[-]
λ	Wavelength	[nm]
θ_{Ox}	Molar ratio of hydrogen peroxide to phenol at t = 0	[-]
ρ_i	Density of compound i	[kg/m^3]

Abbreviations

AAS	Atomic Adsorption Spectroscopy
BET	Brunauer-Emmett-Teller isotherm
EXAFS	X-ray Absorption Fine Structure
GC	Gas Chromatography
HPLC	High Performance Liquid Chromatography
IR	Infra-Red
SEM	Scanning Electron Microscopy
TEM	Transmission Electron Microscopy
TGA	Thermo Gravimetric Analysis
UV-VIS	Ultraviolet-Visible
XANES	X-ray Absorption Near Edge Structure
XRD	X-ray Diffraction

Indices

0	Initial
C	Catechol
Hq	Hydroquinone
m	Meta-hydroxylated isomer (resorcinol)
Ox	Oxidant (hydrogen peroxide)
o	Ortho-hydroxylated isomer (catechol)
p	Para-hydroxylated isomer (hydroquinone)
Ph	Phenol
T	Tars

Pectora roborant cultus recti

1 Introduction

1.1 Selective Oxidation Catalysis

The selective oxidation of hydrocarbons via heterogeneous catalytic reactions is a field of intense interest as it provides a method of functionalising otherwise low value hydrocarbons. Currently approximately 20% of industrial organic chemical processes involve the catalytic oxidation or ammoxidation of hydrocarbons (Shanini, G. H.*, et al.*, 1996), and these selective oxidations are one of the largest industrial scale operations for the production of intermediates, fine chemicals and pharmaceuticals. An increasing amount of attention has focused on the synthesis of fine chemicals and intermediates because the profit margins are higher, and many companies have focused their research efforts into the further development of these catalytic reactions because of their significant industrial relevance.

1.2 Economic Motivation for Selective Oxidations

The reason why a lot of attention has focused on fine-tuning the properties of zeolite catalysts in order to carry out very specific syntheses of high-value chemicals can, to a large extent, be attributed to economics. Ultimately, the purpose of performing these reactions selectively (and in this work the particular focus being on optimisation of the selective oxidation of phenol to produce more hydroquinone) is dictated by economics, in an effort to reduce expenditure and maximise profit. For example, the cost of phenol is approximately R5900 per ton (SRI, 2004), whereas the oxidation products are more valuable – hydroquinone sells for around R772 000 per ton (Sigma-Aldrich, 2005).

Product selectivities are important not only because the cost of feed materials is escalating, but also because one of the most expensive parts of the fine chemicals manufacturing process is the separation of the products. So, if the reaction system can be made to favour the formation of a specific product, then separation costs can be significantly reduced. For commercial processes it is imperative that this selectivity is achieved at acceptably high conversion.

For the hydroxylation of phenol enhanced hydroquinone selectivity has considerable economic advantages, especially when considering that catechol has a market price of just under R357 000 per ton (Sigma-Aldrich, 2005), half that of hydroquinone.

1.2.1 Commercial Applications

World-wide production of hydroquinone, the para-dihydroxybenzene, has been estimated at 35 000 tons per year (IPCS, 1994), with manufacturing facilities in Canada, China, France, Italy, Japan, and the USA. There are three current manufacturing processes for hydroquinone: oxidative cleavage of diisopropylbenzene, oxidation of aniline, and hydroxylation of phenol.

The catalysed hydroxylation of phenol with aqueous H_2O_2 as the oxidising agent, to give hydroquinone and catechol has been an industrial process for numerous years, and was commercialised by EniChem in the early 1990s, operating a 10 000 ton per year plant in Italy (Romano, U.*, et al.*, 1990; Clerici, M. G., 1991; McVey, T. F., 2003). In this process TS-1 – the MFI-structured titanosilicalite – is used as the catalyst.

Hydroquinone has mainly industrial applications. Approximately 25% of all the hydroquinone manufactured is used as an intermediate in the synthesis of antioxidants and antiozonants for use in rubber. Another 25% is used as an intermediate for chemical conversions to inhibitors used to stabilise monomers and prevent polymerisation. It is in the production of fine-chemicals for the photographic and pharmaceutical industries where it finds its major application; 33% is used in the photographic industry including the development of black-and-white photographic film, lithography, and hospital x-ray film. In the pharmaceutical industry it is used for the manufacture of sunscreens and skin lightening creams. Other uses (*ca.* 12%) include chemical conversion to stabilisers for paints, as an anti-coagulant for gas, motor oils and fuels, in the desulphurisation of aqueous ammonium solutions, and for antioxidants for industrial fats and oils (IPCS, 1994).

The synthesis of hydroquinone for use in pharmaceuticals and cosmetics is a lucrative market, even if it only constitutes a small part of the total hydroquinone production. For example, the US market for sunscreen lotions at producer level comes in at just over $640 million per year (Reisch, M. S., 2005); over the past five years this market has been growing at between 5 and 10% per annum. Therefore, there is an increasing surge in this marketplace for this specific oxidation product.

Catechol is mainly used as a raw material for the synthesis of polymerisation inhibitors, in the manufacture of perfumes and drugs, as well as in colour photographic developers as an anti-oxidant and deoxygenating agent. The demand, however, is not as high as for hydroquinone.

1.3 Catalytic Hydrocarbon Oxidations

Catalytic hydrocarbon oxidation reactions can be conducted in either the gas-phase or liquid-phase. Typically, a gas-phase process, using air or oxygen as the oxidant, is always favoured. The low cost of oxygen/air means that large-scale continuous production processes can be performed. However, high reaction temperatures are generally required, which can present a problem for the synthesis of fine chemicals.

Due to the limited thermal stability of fine chemical compounds high temperatures are unfavourable, and consequently a gas-phase synthesis process using air/oxygen should be avoided. Additionally, when one considers that fine chemicals are often produced in batch processes and are high-value chemicals, higher product selectivity will be favoured over the high activity associated with running the process at a higher temperature.

Furthermore, oxygen (or air) exhibits little regioselectivity in reactions with organic substrates; when used as the oxidant in gas-phase reactions the primary oxidation products are generally oxidised more easily than the substrate, and total oxidation of the hydrocarbon substrate and products to water and carbon dioxide also lowers the selectivity of the reaction.

Since product selectivities are very important in fine chemicals syntheses, it is apparent that oxygen is an unsuitable choice of oxidant.

This work is therefore focused on using a liquid-phase oxidant, since relatively mild reaction conditions and high activity/selectivity compared with gas-phase oxidation are possible (Perego, G.*, et al.*, 1986; Sheldon, R. A., 1991).

Traditional methods in fine chemicals synthesis for performing the selective liquid-phase oxidation of hydrocarbons into the corresponding carbonyl compounds generally involve the use of stoichiometric quantities of inorganic oxidants, notably chromium (VI) and manganese reagents (e.g., CrO_3, $KMnO_4$, $K_2Cr_2O_7$), that are simply added to the reaction mixture (Cainelli, G. and Cardillo, G., 1984). However, these methods are not very efficient and also involve the production of large amounts of byproducts, which have both economic and environmental drawbacks further complicated by the difficult recovery of the oxidising salts (Ukrainczyk, L. and McBride, M. B., 1992; Dartt, C. B. and Davis, M. E., 1994). Therefore, more atom efficient catalytic methods employing cleaner oxidants are in growing demand (Sheldon, R. A.*, et al.*, 2000).

Catalytic processes are being increasingly favoured for the development of industrial oxidation reactions. Not only are higher activities and selectivities possible, but the production of reduced quantities of byproducts, and the consequently lower separation costs and environmental effects associated therewith, also has significant economic advantages.

These partial oxidation reactions require the use of a transition metal containing catalyst. While the transformation of organic molecules mediated by well-defined transition-metal complexes as homogeneous catalysts allows a very high selectivity for the catalytic transfer of oxygen from the oxidant to the substrate, a heterogeneously catalysed liquid-phase oxidation process is generally employed because it offers several advantages over homogeneous catalysis. Homogeneous catalysts are typically soluble transition metal complexes and this poses problems. Not only is catalyst recovery difficult and expensive, but these complexes have short life-times and are often toxic, which is an environmental concern (Noreña-Franco, L.*, et al.*, 2002). Furthermore, since the pharmaceutical, veterinary and agro-chemical products produced by these oxidations need to be rigorously free from toxic metals (down to ppm or even ppb levels), the implications for catalyst recovery and leach levels become increasingly noteworthy, and this may be particularly difficult to achieve for homogeneous catalysts (Sanderson, W. R., 2000).

In contrast, heterogeneous catalysts have a higher thermal stability, are more robust and are not incorporated into the oxidation products. Therefore, they can be recovered relatively easily by filtration and regenerated for further use. Catalyst recovery also reduces costs for the separation and purification of the desired products.

Increasingly stringent legislation for the chemical industry has focused attention on developing cleaner and “green” chemical syntheses for industrial application. The demand for sustainable chemistry is increasing, and consequently it is fast becoming a necessity that organic transformations producing fine chemicals are not detrimental to the environment – a worldwide trend towards “green” chemistry. Considerable research has been devoted to making these syntheses more environmentally friendly. Waste management and traditional “end-of-pipe” methods for managing waste at the factory level need to be replaced by waste avoidance techniques (“prevention”), so that the principles of “atom utilisation” or “atom economy” are followed to eliminate waste at the source (Sheldon, R. A., 1997a; Sanderson, W. R., 2000).

The *heterogeneously* catalysed oxidation of hydrocarbons for fine chemicals production offer appreciable methods for minimising the quantity of toxic and environmentally harmful by-products produced.

Therefore the importance of cleaner, heterogeneously catalysed oxidation of hydrocarbons for fine chemical production cannot be ignored in today's stringent operating environment.

2 Scope and Research Objectives

Considerable work has been done investigating the hydroxylation of phenol with aqueous hydrogen peroxide to hydroquinone and catechol, using titanium-substituted molecular sieves. This work has enabled a better understanding of the role of the zeolite structure on the product selectivity and activity of the reaction (Romano, U.*, et al.*, 1990; Tuel, A.*, et al.*, 1991; van der Pol, A. J. H. P.*, et al.*, 1992; Germain, A.*, et al.*, 1996; Mal, N. K. and Ramaswamy, V., 1996; Sanderson, W. R., 2000; Noreña-Franco, L.*, et al.*, 2002; Selli, E.*, et al.*, 2004; Liu, H.*, et al.*, 2005).

Numerous reaction parameters affect the selectivity and activity of the hydroxylation reaction, giving greater flexibility over the reaction. These include, amongst others: (i) type of Ti-Si catalyst used (ii) catalyst acidity and polarity, (iii) catalyst preparation and calcination conditions, (iv) pore geometry (v) crystallite size, (vi) reaction temperature, (vi) solvent type, and (vii) method of peroxide addition (Thangaraj, A.*, et al.*, 1991; van der Pol, A. J. H. P.*, et al.*, 1992; Corma, A.*, et al.*, 1996; Germain, A.*, et al.*, 1996; Ratnasamy, P. and Sivasanker, S., 1996; Blasco, T.*, et al.*, 1998; Wilkenhöner, U., 2001; Callanan, L. H.*, et al.*, 2004).

This research aimed to further study the hydroxylation of phenol over titanium-substituted molecular sieves to gain more insight into the mechanisms governing the catalyst activity and product selectivity.

The pronounced solvent effects observed in aromatic hydroxylations over titanium-substituted zeolites have already been reported, and for the phenol hydroxylation protic solvents have been identified as promoting the preferential hydroquinone formation (Wilkenhöner, U., 2001; Callanan, L. H.*, et al.*, 2004); the current work sought to extend this field of research.

To our knowledge there has been no report about the comparative study concerning the use of Ti-containing zeolites Al-free Ti-Beta and TS-1 in the phenol hydroxylation with different hydrogen peroxide concentrations in different solvents. In this study, particular attention was focused on the use of zeolite Al-free Ti-Beta, and the effect of peroxide concentration on the rate and selectivity was investigated in both water and methanol solvents and co-solvent mixtures. Experiments were also conducted with the medium-pore zeolite TS-1 for comparative purposes, and based on previous findings it was expected to obtain higher hydroquinone selectivity using TS-1 due to the more restrictive pore environment; regardless

of solvent or peroxide concentration, the larger pore Beta catalyst should be expected to give a faster phenol conversion rate than TS-1.

Additionally, the mode of hydrogen peroxide addition was investigated to determine its effects on catalyst activity and product selectivity. While this has been partly investigated for TS-1, where dilute solutions were used in water solvent (Thangaraj, A.*, et al.*, 1991; Ratnasamy, P. and Sivasanker, S., 1996; Wilkenhöner, U., 2001), no reports are made for Al-free Ti-Beta, nor for TS-1 in methanol solvent. Since methanol is known to enhance hydroquinone selectivity, peroxide addition effects in this solvent were deemed necessary of further investigation.

2.1 Hypothesis

Based on the findings in literature the following hypothesis is proposed:

Improved hydroquinone selectivity should be obtained with lower hydrogen peroxide concentrations, and this selectivity will be significantly influenced by the water-methanol co-solvent mixture.

3 Literature Review

3.1 Oxidant

A suitable source of oxygen must be available for the hydroxylation of phenol to occur. While it would be possible to use either oxygen or air, these are regarded as unsuitable oxidants as pointed out earlier in *Section 1.3;* since the hydroxylation of phenol using titanium-substituted molecular sieves is a heterogeneously catalysed liquid-phase reaction, and the use of O_2/air as the oxidant would complicate the procedure through the introduction of a third phase (with consequent more severe mass-transfer limitations).

An alternative oxygen source has to be used. Potential oxidants that can be used for transition metal catalysed hydrocarbon oxidations in the liquid phase are listed in Table 3.1.

Table 3.1: Potential oxygen donating species for selective hydrocarbon oxidations[1]

Potential Oxidant	*Active Oxygen [weight %]*	*Phase*	*By-product of Oxidation*
Hydrogen Peroxide, H_2O_2	47	Liquid	H_2O
Nitrous Oxide, N_2O	36.4	Gas	N_2
Sodium Chlorite, $NaClO_2$	35.6	Liquid	NaCl
Ozone, O_3	33.3	Gas	O_2
Nitric acid, HNO_3	25.4	Liquid	HNO_2
Sodium Chlorate, NaClO	21.6	Liquid	NaCl
Tert-butylhydroperoxide, TBHP	17.8	Liquid	t-BuOH
Sodium Bromate, $NaBrO_3$	13.4	Liquid	NaBr

[1]*Modified from (Wilkenhöner, U., 2001)*

Comparison of these oxidants reveals why hydrogen peroxide is the most suitable oxidant for most hydrocarbon oxidations. Since it offers the highest available active oxygen, it can very effectively be used in the oxidation of the phenol organic substrate. Table 3.2 shows the active oxygen content in solutions of varying H_2O_2 concentration. Under ambient temperature and pressure conditions there is a linear relationship between the hydrogen peroxide concentration and its oxygen liberation capacity on decomposition; the higher the peroxide concentration, the greater its active oxygen content.

Table 3.2: Active oxygen content in H_2O_2 solutions[1]

H_2O_2 concentration [wt-%]	35	50	70	100
Active oxygen content [wt-%]	16.47	23.52	32.92	47.03

[1]*Taken from http://www.h2o2.com (modified)*

Research done in the area of selective liquid-phase oxidation catalysis has focused its attention on the preferential use of aqueous hydrogen peroxide solutions, primarily because it offers the following advantages:

- It has the highest available active oxygen content per weight of the oxidant,
- It is inexpensive, *ca.* R80 per litre (35 wt-% solution) at current prices (2005),
- It can be mixed with water in any proportion, thus making dilution to different concentrations uncomplicated,
- It forms a single liquid phase with phenol and water/methanol solvents, and thus a system of only two phases exists,
- It is non-flammable at any concentration,
- The only oxidation by-product is water, which makes H_2O_2 a very environmentally friendly oxidant, and any residual H_2O_2 is decomposed by UV light, and
- Aqueous H_2O_2 solutions are stable, and safe and easy to handle (Edwards, J. O. and Curci, R., 1992; Sanderson, W. R., 2000; Clyde Corporation, 2005)

With the exception of hydrogen peroxide, nitrous oxide and ozone, all other oxidants listed in the above table yield by-products that would need to be specially handled. Since an increasing amount of attention is being focused on the development of new environmentally safer chemical transformations – by reducing and/or removing the toxic waste and by-products from the chemical processes to make them more ecologically acceptable – hydrogen peroxide is an excellent choice of oxidant because it only generates water as a by-product. This is in line with a worldwide trend towards “greener” organic transformations for the production of fine chemicals.

The use of nitrous oxide and ozone as oxidants should be avoided because both are poisonous gases, and the tri-phase reaction concerns mentioned earlier would also pose a problem.

This project will focus on the use of aqueous hydrogen peroxide solutions as the oxidising reagent in the phenol hydroxylation reaction experiments. This solution is typically commercially available as a 30 to 50 wt-% H_2O_2 aqueous solution, and a stabilised solution was purchased from Sigma-Aldrich.

When considering the mechanism of transition-metal catalysed, liquid-phase oxidations, the nature of the active intermediate species, formed by reaction of the transition metal incorporated in the catalyst with the oxidant, must be taken into account. The transition metal

site can form different types of active species, which initiate different reaction pathways for selectively transferring the oxygen to the substrate in the catalytic reaction.

Metal-catalysed oxidations using hydrogen peroxide as the oxidant can be divided into two categories: those involving a peroxometal active catalyst-oxygen species, or an oxometal species (Sheldon, R. A., 1993). In the peroxometal intermediate pathway the metal ion does not undergo a change in oxidation state during the catalytic cycle, and no stoichiometric oxidation occurs in the absence of hydrogen peroxide. In contrast, oxidations that occur via an oxometal pathway involve a two-electron change in the oxidation state of the metal ion, and in the absence of peroxide a stoichiometric oxidation is observed.

Peroxometal pathways are typical of early transition metals with a d^0 configuration that are relatively weak oxidants, e.g., Ti(IV), Zr(IV), Mo(VI), W(VI), Re(VII). Late and first row transition metal ions, e.g., Cr(VI), Mn(V), Fe(VIII), Ru (VI), Os(VIII), that are strong oxidants in their highest oxidation states, typically react via oxometal intermediates.

The titanosilicate zeolite catalysts, which are the focus of this work, react via an electrophilic peroxometal active intermediate pathway (see also *"Mechanistic Implications"* discussion, *Section 3.5*); this mechanism was confirmed by the lack of oxidation products for the phenol hydroxylation when no peroxide was added to the reaction solution. There is no change in the oxidation state of the titanium site during the course of the reaction, and the metal acts as a Lewis-acid increasing the oxidising power of the peroxo group for the substrate.

The active oxygen-catalyst species and reaction pathway is shown in Figure 3.1 (S represents the organic substrate).

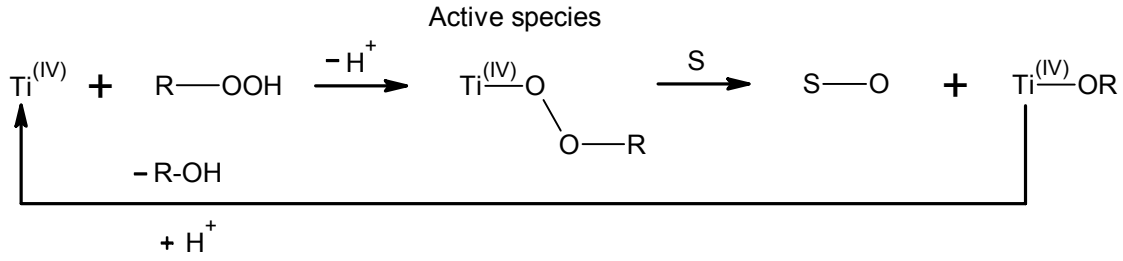

Figure 3.1: Mechanism for the catalytic oxygen transfer by titanium in the liquid phase via an active peroxometal intermediate pathway (Sheldon, R. A., 1997b; Wilkenhöner, U., 2001)

3.2 Catalyst Choice

As mentioned, catalytic oxidation processes require the use of a transition-metal containing catalyst, so that oxygen can be selectively transferred from the oxidant to the organic substrate. For the process to be heterogeneously catalysed, as is desired, the transition metal has to be immobilised. While a variety of methods are available for this immobilisation, all have the associated generic problem of leaching of the transition metal. An additional problem associated with immobilisation methods using transition-metal complexes is regeneration of the catalyst due to the thermal instability of the support material/complex.

Redox molecular sieves, or zeolites, offer a stable environment; the transition metal is chemically bonded to a regular-structured inorganic matrix, which ensures both easy thermal regeneration and increased leaching stability (Sheldon, R. A.*, et al.*, 1998b).

3.2.1 Zeolite Catalysts

Zeolites have become interesting topics for different areas of chemical research, particularly because of their controlled pore architectures and unique porous properties associated with their uniform pore sizes; they are now widely applied in various industrial catalytic applications, for example in the petrochemical industry for crude oil cracking and fuel synthesis, in ion-exchange operations and in the separation and removal of gases and solvents (Heinemann, H., 1981; Dwyer, F. G. and Degnan, T. F., 1993; Zhang, W. and Smirniotis, P. G., 1998). One of their most important applications is as efficient solid acid catalysts in the production of fine chemicals and pharmaceuticals. Being solid gives these materials a distinct advantage over solvated acids: the heterogeneity of the catalyst and the reactants/products facilitates easy catalyst recovery, therefore making them environmentally friendly as pointed out earlier.

By definition, zeolites are crystalline microporous inorganic solids containing large voids and channels, giving the material an internal pore system as well as interstitial spaces between the crystallites. They encompass materials comprising the silicalites, aluminosilicates, aluminophosphates, metalloaluminates and germanates. (IZA, 2005) Pore sizes can vary from approximately 3 Å to 10 Å and it is this microporous structure that allows these materials to act as selective catalysts, and why as a consequence they are synonymously known as molecular sieves (Bell, R. G., 2001; IZA, 2005). Reactions can take place within the pores of the zeolite, which allows for a greater degree of product control because the pore sizes are of the same order of magnitude as the reactant and product molecules.

The well-defined zeolite framework consists predominantly of interconnecting TO_4 tetrahedra (where T represents the tetrahedrally coordinated central metal atom) of transition metal anions strongly bonded at all four corners (4 connected networks of atoms). In the case of silica-based silicalite molecular sieves, $(SiO_2)_n$ is the framework building component, but related to these are other zeolitic material types where different metal ions have been isomorphously substituted for silicon (IV) into the crystalline framework (e.g., aluminium in the aluminosilicates). Other heteroatoms besides aluminium, such as P, V, Ti, Zn and Mo, can also be simultaneously incorporated into the zeolite matrix, e.g., the aluminophosphates which are polymeric frameworks of alternating tetrahedral alumina and phosphate units. When these metal ions are transition metals, the molecular sieves are commonly referred to as *redox* molecular sieves (Bell, R. G., 2001).

The tetrahedral units are created by hydrolysing the precursors (e.g., inorganic salts and oxides or organic sources) to make a sol-gel (Lev, O., 1995; Sonnet, P. E.*, et al.*, 1995) that condenses into crystalline units. If the charge-balancing cation that will reside within the zeolite is an organic molecule (e.g., tetraethylammonium, TEA^+) it may also serve to direct the synthesis to a particular structure; thus, that organic is referred to as a "structure-directing agent" (SDA). Depending on different synthesis conditions (gel composition, crystallisation time, temperature, SDAs, reagent purity) the crystalline units assemble into well-defined structures, which determine the framework dimensionality and pore topology (uni-, bi- or tridirectional pores structures), pore size and shape, and crystal size and habit.

Pectora roborant cultus recti

It is these tetrahedral buildings units that join together in the framework structure forming the linkages of definite crystalline structures, and creating surface pores of uniform diameter. These structures enclose a large number of regular internal cavities and channels, which may themselves be interconnected by a number of still smaller cavities (Corma, A.*, et al.*, 2003). Depending on the chemical composition and crystal structure of the specific zeolite material, these channels have discrete sizes and shapes and control the diffusion of cations and other molecules through the channels within the pore system; the well-defined pore system is ideally able to discriminate between organic molecules with a precision of less than 0.1 nm, thus permitting the diffusion of some atoms and small molecules into the macromolecular structure whilst excluding others that are too large (Lubomira, T., 1999). Not only do the dimensions of the channels limit adsorption to molecules of a certain size, but the cage size (created by interconnecting multidimensional pores) can also significantly influence the accessibility to active sites by offering alternative diffusion paths.

One characteristic that separates redox silicalites from all-silica minerals and other zeolitic materials is the different ionic nature and polarity of their frameworks. The silicalites have a

neutral framework, since the SiO_4 unit has no net charge, whereas generally the zeolites have an overall negatively charged surface and hydrophilic framework that arises from TO_4 tetrahedra containing non-tetravalent metal ions in the zeolite matrix.

The isomorphic incorporation of trivalent aluminium (and other trivalent heteroatoms) in particular generates a charge imbalance in the framework since the TO_4 tetrahedra now contain non-tetravalent metal ions. This charge imbalance is countered by a supplementary counter-cation, M^+, which leads to the generation of an acid site (Brønsted or Lewis), and consequently a hydrophilic framework. The cation can be either inorganic (e.g., Na^+, K^+ resulting in Lewis acidity) or organic (e.g., quaternary ammonium compounds). The contribution of the acid sites has been shown by comparison experiments of hydrogen-exchanged zeolites and their equivalent cation-form zeolites (Windsor, C. M., 1998).

The highly acidic Brønsted-acid sites (produced by the framework-bound proton), combined with the high selectivity arising from shape selectivity and large internal surface area, makes the zeolites ideal industrial catalysts for a wide variety of reactions (olefin polymerization, isomerisation, cracking). Specifically, however, for selective oxidations involving these catalysts the presence of acid sites should be avoided since they result in undesired secondary reactions of the substrate and/or primary products, the high decomposition rate of hydroperoxide, and decreased catalyst activity through coking (this is discussed in more detail in *Section 3.3*).

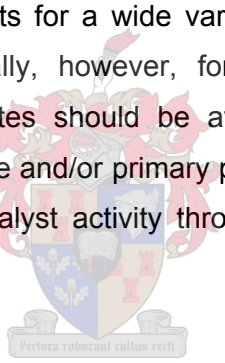

3.2.2 General Considerations

Thus the advantages of zeolites are two-fold: (i) due to their greater thermal stability they can be regenerated more easily, and (ii) their well-defined framework and pore structure means that they are capable of discriminating between organic molecules very precisely.

The latter property offers the greatest advantage to oxidation chemistry employed in the fine chemicals syntheses: since zeolite micropores have a uniform size distribution they are capable of offering more selective reaction pathways through the exclusion of intermediates that require more space than is available in the channels. Their unique shape-selectivity can thus be exploited so that the reaction is driven towards the desired product, and undesired consecutive reactions leading to bulkier products can be excluded.

The shape selectivity of zeolites is attributed to the uniform size distribution of their micropores where most of the reactive centres are located. The molecular sieve effect that is observed in catalytic reactions employing zeolites can be classified as reactant selectivity,

product selectivity or transition-state selectivity. Transition-state shape selectivity effects play a significant role, especially for the zeolite-based oxidation catalysts used in fine chemicals synthesis; the reaction favours that path with the least space-demanding transition state. This, coupled with the fact that the pore system can be one-, two and three-dimensional, can significantly influence the accessibility of the active micropore sites since multi-dimensional pore systems offer alternative diffusion paths. While the pore system offers shape selectivity for the preferential formation of certain reaction products, it should be noted that the active sites on the external surface area are non-selective and therefore offer no size control.

3.2.3 Zeolite Titanium Silicalite-1

Titanium Silicalite-1 (TS-1) is a medium-pore titanium-substituted aluminium-free silicalite with 0.55 nm channels (sinusoidal and straight), in an MFI-type framework structure (analogous to ZSM-5). It was first synthesised by researchers at EniChem in 1983 (Taramasso, M.*, et al.*, 1983; Notari, B., 1988). Industrially, TS-1 found its first application in the production of catechol and hydroquinone from the hydroxylation of phenol.

The catalytic potential of TS-1 as an oxidation catalyst with H_2O_2 has been investigated in numerous publications (Perego, G.*, et al.*, 1986; Clerici, M. and Ingallina, P., 1993; Notari, B., 1993), and while it is an extremely valuable and versatile catalyst, and catalyses a variety of synthetically useful oxidations with 30 wt-% aqueous H_2O_2, (for example, epoxidation, alcohol oxidation, ammoxidation, phenol hydroxylation), it has a major drawback with regards to substrate size limitations, which are limited to small kinetic diameters (< 6 Å). The zeolite channels will not accept o- or m- disubstituted aromatics or tertiary aliphatic compounds, limiting its catalytic potential to linear hydrocarbons or monofunctionalised benzene derivatives only (branched aliphatics pass with difficulty), and which also restricts the desorption of products and therefore the reaction rate (transition-state shape selectivity). Therefore, larger pore alternatives that can accommodate larger substrate molecules and permit greater mobility will allow the oxidation to bulkier products.

3.2.3.1 Framework Structure and Crystallographic Characterisation

TS-1 has a three-dimensional pore structure with interconnecting 10-membered ring channels. Sinusoidal channels parallel to the [100] direction, with pore opening dimensions of 5.1 x 5.5 Å, are interconnected with straight, two-dimensional pore channels (parallel to the [010] direction) with free pore dimensions of 5.3 x 5.6 Å (IZA, 2005).

The framework pore channel structure viewed along the [010] direction is shown in Figure 3.2, and the pore openings in Figure 3.3.

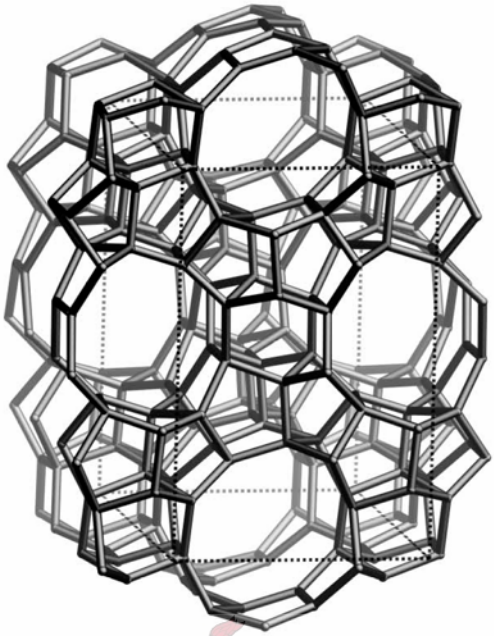

Figure 3.2: Schematic diagram of the MFI TS-1 pore structure viewed along the [010] direction [International Zeolite Association, http://www.iza-structure.org/databases/]

Crystallographic channel characterization: [100] **10** 5.1 x 5.5 Å ↔ [010] **10** 5.3 x 5.6 Å ***

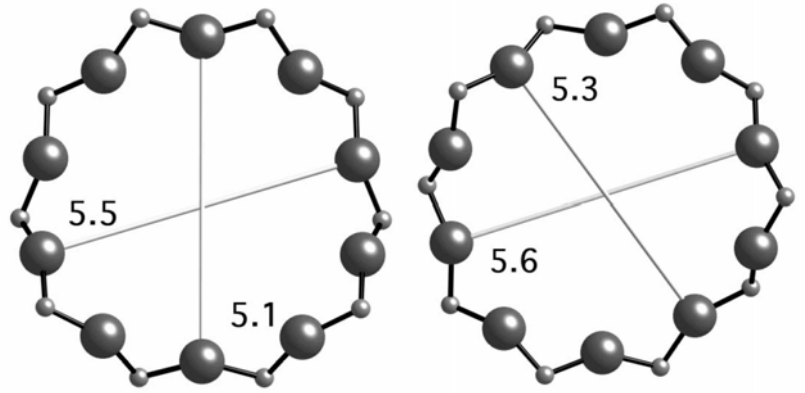

(a) **(b)**

Figure 3.3: Schematic diagram of the 10-membered pore ring openings of TS-1 (a) viewed along the [100] direction, [100] 10 **5.5 x 5.1 Å (b) viewed along the [010] direction, [010]** 10 **5.3 x 5.6 Å [International Zeolite Association, http://www.iza-structure.org/databases/]**

3.2.4 Zeolite Titanium Beta

Titanium Beta is a titanium-based molecular sieve that is frequently used for the oxidation of organic compounds due its well-known activity.

Ti-Beta is a large-pore silicate zeolite with pore dimensions of approximately 0.55-0.66 nm. The advantage of the aluminium-free variant of this zeolite (like TS-1), and other transition-metal incorporated redox silicates, lies in its surface polarity and that it possesses a hydrophobic framework. This offers preferential selectivity towards the adsorption of less polar organic compounds (such as phenol) and excludes polar compounds (such as water and other polar solvents). This not only ensures the enhanced stability of these materials towards leaching (Sheldon, R. A.*, et al.*, 1998a; Sheldon, R. A.*, et al.*, 1998b), but the pores are also maintained in an organic-rich environment. Thus these microporous crystalline solids with hydrophobic properties are particularly important for the phenol hydroxylation reaction studied in this work because they can effectively increase the reaction rate and better catalyse the reaction.

3.2.4.1 Framework Structure and Crystallographic Characterisation

Al-free Ti-Beta (framework type *BEA) is a large pore titanium-substituted molecular sieve. An increasing amount of attention has focused on its use, because it opens the area of heterogeneous oxidation catalysis with aqueous H_2O_2 to more bulky organic molecules that cannot be oxidised in the medium-size pores of TS-1 (which restricts its use to relatively small molecules) (Camblor, M. A.*, et al.*, 1996a).

Ti-beta has a three-dimensional framework, characterised by two interconnecting main channel systems of 12-ring atoms, which make up the rings controlling diffusion through the channels. The two-dimensional straight pore channels parallel to all crystallographically equivalent axes (i.e. along x, y and z) of the cubic structure (the <100> direction), with pore opening dimensions of 6.6 by 6.7 Å, are interconnected with the one-dimensional pore channels, dimensions 5.6 by 5.6 Å, parallel to the [001] direction (IZA, 2005).

The framework pore channel structure viewed along the [010] direction is shown in Figure 3.4, and the pore openings in Figure 3.5.

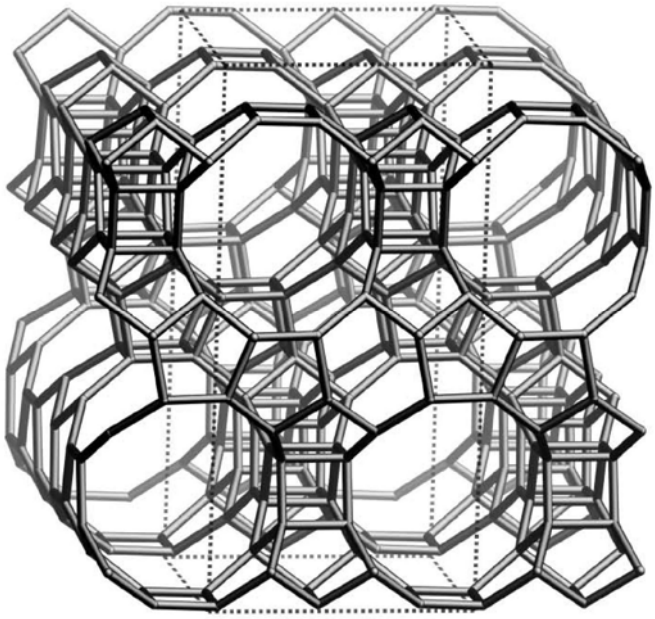

Figure 3.4: Schematic diagram of the *BEA Al-free Ti-Beta pore structure viewed along the [010] direction [International Zeolite Association, http://www.iza-structure.org/databases/]

Crystallographic channel characterization: <100> **12** 6.6 x 6.7 Å ** ↔ [001] **12** 5.6 x 5.6 Å *

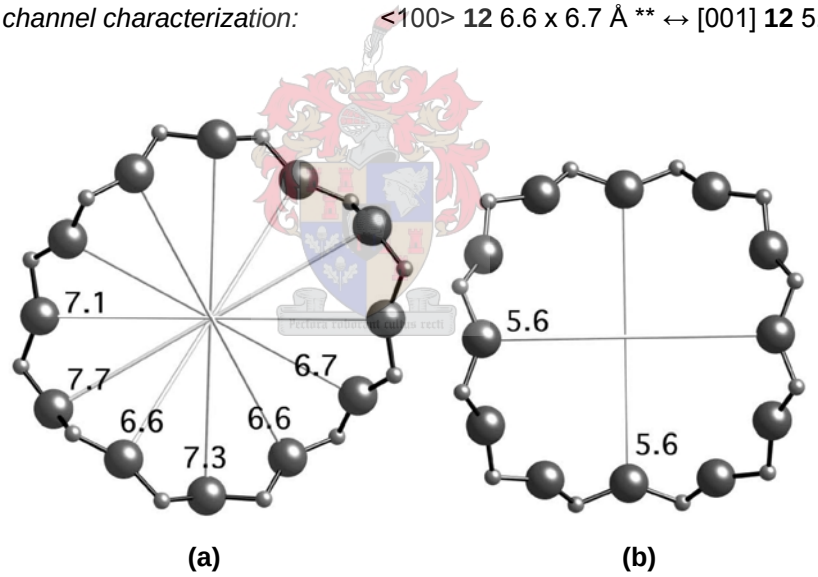

Figure 3.5: Schematic diagram of the 12-ring pore openings of Al-free Ti-Beta (a) viewed along the <100> direction, <100> 12 **6.6 x 6.7 Å ** (b) viewed along the [001] direction, [001]** 12 **5.6 x 5.6 Å * [International Zeolite Association, http://www.iza-structure.org/databases/]**

3.3 Catalyst Synthesis Considerations

The importance of the catalyst synthesis procedure and purity of the reagents used cannot be discounted, because the phenol hydroxylation reaction, as for most selective oxidations involving these titanosilicate zeolite catalysts, is strongly dependent on the quality of the catalyst. Different synthesis parameters affect the activity and selectivity of the catalyst. Therefore, it makes sense that only well-established and reproducible synthesis procedures

are used, and that the catalyst samples obtained are extensively characterized so that reactions can be tailored to meet the selectivities required. Using a reproducible technique will also help towards ensuring easy comparison with other peoples findings using a similar catalyst.

Ti-Beta and other titanium-containing zeolites seem to be particularly sensitive to the presence of phase-impurities such as $(TiO_2)_n$-oligomers since they show inferior catalytic oxidation properties if these are present (van der Pol, A. J. H. P. and van Hooff, J. H. C., 1992; Notari, B., 1996). TiO_2 impurities (mainly occurring as anatase) are formed through hydrolysis and oligomerisation of the titanium source during its addition to the synthesis gel, which leads to poor titanium incorporation. Numerous reproducible synthesis procedures have been developed to ensure that certain conditions are met for proper titanium incorporation, including isomorphous framework substitution, synthesis medium pH, and the use of alkali-free solutions amongst others (Camblor, M. A.*, et al.*, 1992; Blasco, T.*, et al.*, 1993; Camblor, M. A.*, et al.*, 1993b; Blasco, T.*, et al.*, 1996; Camblor, M. A.*, et al.*, 1996b; Blasco, T.*, et al.*, 1998; van der Waal, J. C.*, et al.*, 1998a).

Consideration of essentially six crucial synthesis parameters must be taken into account when producing such titanosilicate zeolite catalysts most suited for use in selective oxidation reactions, namely (i) the method of transition metal incorporation into the silica framework, (ii) the aluminium content of the framework and associated acidity, (iii) the crystallite size obtained, (iv) the purity of the structure-directing template solution, (v) the nature of the synthesis solution coupled with pH effects, and (vi) the presence of connectivity defects in the framework (van der Pol, A. J. H. P.*, et al.*, 1992; Camblor, M. A.*, et al.*, 1993a; Blasco, T.*, et al.*, 1998; Wilkenhöner, U.*, et al.*, 2001; Selli, E.*, et al.*, 2004). The relative effects of each can be determined by catalytic test reactions, adsorption microcalorimetry and spectroscopic characterisation of the catalyst (XRD, IR, UV-VIS, XANES, EXAFS).

3.3.1 Zeolite Framework Modifications

The synthesis of transition-metal incorporated silicates can be done either by post-synthesis modifications to the zeolite Beta framework (the metal is introduced into the lattice *after* zeolite synthesis), or by isomorphous framework substitution of titanium into the interconnected silica tetrahedra via hydrothermal synthesis (achieved by autoclaving the synthesis gel at autogeneous pressure).

The latter method is preferred because it offers ideally perfect incorporation of titanium as metal oxide tetrahedra (TiO_4), and should provide a more stable environment. With grafting

and tethering techniques, and other associated post-synthesis methods, there are fewer bonds between the silica-based zeolite and the transition metal species. Therefore these structures are inherently less stable.

Catalyst deactivation that occurs during oxidation reactions cannot be disregarded. Deactivation of the catalyst occurs through the readsorption of products, with the subsequent formation of undesired high molecular-weight compounds (polymers or tars) in the micropores at or near the active sites, which poisons the catalyst and degrades its performance. These tars also result in pore blockage, which limits the diffusion of reactants and products into and out of the pore system. Therefore, a more stable framework is advantageous because it ensures easy thermal regeneration of the deactivated catalyst due to greater thermally stability of the support – versus the relative instability of the support material if transition metal complexes are used for immobilisation – and the tars can be combusted simply by heating the catalyst in air.

An additional advantage to isomorphously substituting the titanium is the improved stability towards leaching of the metal, since this is a recurrent problem with most varieties of immobilisations. When titanium is chemically bonded to the inorganic zeolite matrix it is less prone to leaching. This is particularly important because leaching of the immobilised transition metal from the catalyst is one of the biggest problems of heterogeneous oxidation catalysis in the *liquid* phase. Particularly with immobilisation methods using ion-exchange of transition metal complexes, the metal can rapidly dissolve in the reaction medium, a problem that is exacerbated in the presence polar solvents (Sheldon, R. A., 1997b; Sheldon, R. A.*, et al.*, 1998a; Sheldon, R. A.*, et al.*, 1998b).

The isomorphous substitution of Si^{IV} by Ti^{IV} in tetrahedral co-ordination can be confirmed using physiochemical analyses (XRD, XANES) by indicating the presence of the single Beta crystalline phase, with no competition of other crystalline phases (intense XRD peaks at 2θ of approximately 7.5 and 23) (Blasco, T.*, et al.*, 1998).

Framework incorporation of titanium can be confirmed (after calcination of the catalyst) by the presence of a sharp, single adsorption band in the 205-220 nm ultraviolet spectrum, using diffuse reflectance ultraviolet analysis (DRUV-VIS) (Blasco, T.*, et al.*, 1998). The narrow band is assigned to isolated framework titanium. The poor incorporation of titanium, which results in the formation of amorphous TiO_2 impurities as anatase, can indirectly be determined from XRD spectra, since these impurities lead to framework defects that result in poor crystallinity. Titanium incorporation is also characterised in IR spectroscopy by the appearance of three infrared bands in the region near 960 cm^{-1}.

3.3.2 Acid Sites in Zeolite Beta: Framework Aluminium Content

Under typical conditions, as developed by Camblor *et al.* (1993b), Ti-Beta zeolite crystallises with some aluminium as a framework constituent (Si/Al molar ratios ≤ 150). This leads, after calcination, to the presence of acid sites (Brønsted and Lewis sites). Subsequent catalytic studies have demonstrated the existence of a specific combination of Brønsted- and Lewis-acid sites, whose strength are affected by the procedures that are used for zeolite Beta synthesis and temperature activation (Kiricsi, I*., et al.*, 1994; Kuehl, G. H. and Timken, H. K. C., 2000; Muller, M*., et al.*, 2000). The temperature programmed desorption (TPD) of ammonia is frequently used for characterisation of the zeolite acidity, and the total number and strength of acid sites can be determined from the amount of desorbed ammonia molecules adsorbed directly on the acid sites (Niwa, M*., et al.*, 1995). The disadvantage of this method is that the type and structure of acid site cannot be distinguished. However, using a combination of infrared (IR) and mass spectrometry (MS) together with TPD, it has become possible to determine the amount and strength of each kind of acid site (Niwa, M*., et al.*, 2005).

As mentioned, the micropores of zeolites are formed by corner sharing of SiO_4 and AlO_4 tetrahedron, and when aluminium atoms (Al^{3+}) replace silicon (Si^{4+}) in tetrahedral co-ordination the framework becomes negatively charged due to the excess negative charge on the aluminium tetrahedra. This net negative charge must be stabilised by a nearby positive ion such as a proton, and typically neutrality is achieved by incorporating metal cations (inorganic/organic) outside the framework. The alkali cations (Na^+/K^+) countering the negative charge of the framework can be exchanged for ammonium ions (present in the structure-directing template, or by ion-exchange through washing with ammonium nitrate/chloride solution), and after high-temperature calcination (approximately 600 °C), ammonia is released and the zeolite is in its protonic form; the protons act as Brønsted-acid sites. Additionally, Al-sites located at the external surface, probably terminated by hydroxyl groups, also require a charge compensating proton, thus producing Brønsted acidity as well (Jansen, J. C*., et al.*, 1997), so it is concluded that Brønsted acidity is present both on the internal and external surfaces, and the concentration of tetrahedral aluminium is proportional to the concentration of the Brønsted-acid sites.

Lewis-acid sites are present predominantly on the internal surface, and arise from extra-framework aluminium and local defects (crystallographic faulting and disordered stacking) that comprise partially coordinated aluminium atoms (Jansen, J. C*., et al.*, 1997). Jansen *et al.* (1997) confirmed this micropore Lewis acidity with the catalytic data obtained from acid-

catalysed reductions over zeolite Beta using a bulky probe-molecule too large to enter the micropores.

Therefore, with more aluminium in the framework and present on the external surface, there is an increased concentration of these acid sites.

While this can be useful for bifunctional acid/redox catalytic processes where both an active oxidative metal site and acid component are required (e.g., for isomerization, cracking and polymerization reactions of olefins) (Corma, A.*, et al.*, 1995; Alvarez, F.*, et al.*, 1997; Magnoux, P.*, et al.*, 2000), these acid sites can have a detrimental effect on the activity and selectivity of zeolite TS-1 and Ti-Beta catalysts in selective oxidation reactions like epoxidations. It has been seen that specifically these acid sites lower the selectivity to the epoxide during oxidation of alkenes with H_2O_2, due to its catalysing the hydrolysis and opening of the epoxirane ring to produce 1,2-diols and other rearrangement products (Sato, T.*, et al.*, 1994; van der Waal, J. C.*, et al.*, 1998b; Uguina, M. A.*, et al.*, 2000; Hulea, V. and Dumitriu, E., 2004; Zhuang, J.*, et al.*, 2004).

For hydroxylation reactions acidity, though not directly involved in the hydroxylation, plays a major role in determining catalyst deactivation and lifetime (Selli, E.*, et al.*, 2004). The rate of deactivation is influenced by the different active species present in the catalyst and surface acid sites are known to be involved in catalyst deactivation by coking (Meloni, D.*, et al.*, 2003). Selli *et al.* (2004) investigated benzene hydroxylation to phenol over Fe-MFI catalysts, and found that coke formation, which is triggered by further undesired condensation-polymerisation reactions of phenol, is favoured by the strong adsorption of phenol on Lewis-acid sites, restraining its diffusion out of the zeolite pores. Thus, for applications like these, and similarly for the phenol hydroxylation reaction, it is necessary to suppress the acidity of the catalyst, as it leads to fouling of the catalyst by over-oxidised products.

The best way to circumvent the acid-catalysed secondary reactions would be the total elimination of aluminium from the zeolite; therefore, there was strong incentive for the production of Al-free Ti-Beta catalysts by clean and reproducible direct synthesis methods for such oxidation reactions, and this was first done by Camblor *et al.* in 1996 (Camblor, M. A.*, et al.*, 1996b; Camblor, M. A.*, et al.*, 1996a).

The design of this synthetic procedure developed from the observation that during the syntheses in the presence of aluminium and the tetraethylammonium ion, titanosilicate zeolite Beta continued to grow and nucleate after all the aluminium was incorporated into the framework (Camblor, M. A.*, et al.*, 1993b). However, under these reaction conditions it was

not possible to synthesise the material in the absence of aluminium, which suggested that Al-free Ti-Beta could not grow and nucleate. A novel and reproducible procedure whereby dealuminated zeolite-Beta seeds are added to the synthesis gels allows Al-free Ti-Beta to grow over the seeds, thus promoting its growth and nucleation, and resulted in high yields of a hydrophobic Al-free Ti-Beta oxidation catalyst.

The aluminium content of these seeds determines the total aluminium content in the reaction mixture (and ultimately the acid strength of catalyst), which can be reduced to trace levels (total Si/Al molar ratios > 10 000) if dealuminated zeolite-Beta crystals are used as seeds. Dealumination by acid leaching at elevated temperature using an organic/inorganic acid can be used to remove most of the (extra-) framework aluminium, and depending on the type, strength and concentration of acid used, and the number of treatments, a variable silica/alumina ratio (50-4000) can be obtained (Fajula, F.*, et al.*, 1994; Saxton, R. J.*, et al.*, 1996; Taylor, B., 2004).

The effect of a reduced aluminium content and acid strength was confirmed when it was shown that the Al-free Ti-Beta produced an enhanced activity and a much higher selectivity to the epoxide during the oxidation of alkenes in the presence of H_2O_2 (Camblor, M. A.*, et al.*, 1996b).

3.3.3 Reagent Purity

Purity of the reagents is another key factor to be considered when synthesising the catalyst. Al-free Ti-Beta, and other titanosilicates such as TS-1, can be obtained from a variety of silica- and titanium-sources with good results, but the structure-directing template, tetraethylammonium hydroxide (TEAOH), has to be of a very high purity.

The exclusion of alkali ions (K^+ and Na^+) is crucial because the presence of even trace amounts of these ions in the template solution can result in catalyst samples with poor catalytic properties, even though spectroscopic characterisation indicates a high purity material. Alkali cations have been shown to poison the titanium sites, since for zeolite TS-1 the catalytic performance decreases as a function of the alkali metal cations content in the synthesis gel (Taramasso, M.*, et al.*, 1983; Notari, B., 1988; Bellussi, G.*, et al.*, 1991). Commercially supplied template solutions should therefore be tested using AAS to confirm their alkali content; concentrations less than 50 ppm are ideal. Defect-free Ti-substituted zeolite Beta has been prepared in the absence of alkali cations to produce stable nanocrystallites (Camblor, M. A.*, et al.*, 1997).

3.3.4 Crystallite Dimensions

Seeding has distinct advantages. Firstly, it allows the crystallisation time to be reduced from 20 days to 4 days. More importantly it allows smaller crystallites to be obtained. Typically, the Ti-Beta zeolites crystallised from aqueous gels in the absence of seeds have an average crystal size in the 2-5-μm range, but this can be reduced to less than 1 μm by seeding the gels with nanocrystalline zeolite Beta seeds with an average crystal size of about 50 nm.

Crystallite dimensions are important because their dimensions can influence the catalytic performance (van der Pol, A. J. H. P.*, et al.*, 1992; Wilkenhöner, U.*, et al.*, 2001). It has been observed by Wilkenhöner *et al.* (2001) that the reaction rates and selectivities for oxidation reactions over Al-free Ti-Beta with H_2O_2 became increasingly diffusion mass-transfer limited for large crystals (due to very low intracrystalline diffusivity values for phenol), and were consequently lower. Due to the larger surface to volume ratio in smaller crystallites, diffusion mass-transfer resistance can be reduced.

3.3.5 Catalytic Test Reaction: Catalyst Characterisation

Calcined Al-free Ti-Beta zeolite displays the typical spectroscopic features of zeolite Ti-Beta: amongst others, the 960 cm^{-1} IR band (assigned to Si-OH defect groups promoted by framework titanium), and the narrow diffuse reflectance UV band at 205-225 nm (assigned to isolated framework titanium) (Camblor, M. A.*, et al.*, 1993c; Boccuti, M. R.*, et al.*, 1998). It is thus indistinguishable from previously synthesized Ti-β zeolite containing aluminium, except for its chemical composition (which is determined by AA spectroscopy).

In order to examine possible differences in its activity and selectivity for catalytic oxidations, Camblor *et al.* (1996b) studied the 1-hexene epoxidation to 1,2-epoxyhexane with aqueous H_2O_2 in methanol solvent, over a series of Ti-Beta samples with different aluminium contents. It was seen that as the aluminium content decreases the selectivity to the epoxide increases, which is due to the decreasing concentration of strong acid-centres which can catalyze the hydrolitic opening of the epoxirane ring to yield methyl glycol ether, by addition of one molecule of methanol. Thus the selectivity to the epoxide is at a maximum for the Al-free Ti-Beta catalyst. Furthermore, a very high efficiency for H_2O_2 utilisation (selectivity > 95%) was obtained on Al-free Ti-Beta, which confirms this epoxide selectivity. This epoxide selectivity as a function of aluminium content can be seen in Figure 3.6.

Cleavage of the epoxide ring, although slow, still occurs on the Al-free Ti-Beta material. This is attributed to the formation of Brønsted-acid sites related to framework titanium, that are

developed in the presence of H_2O_2 in polar solvents (alcoholic solutions) due to alcohol co-ordination to the active site to give a cyclic penta-coordinated Ti-hydroperoxo active intermediate species stabilised by H-bonding.

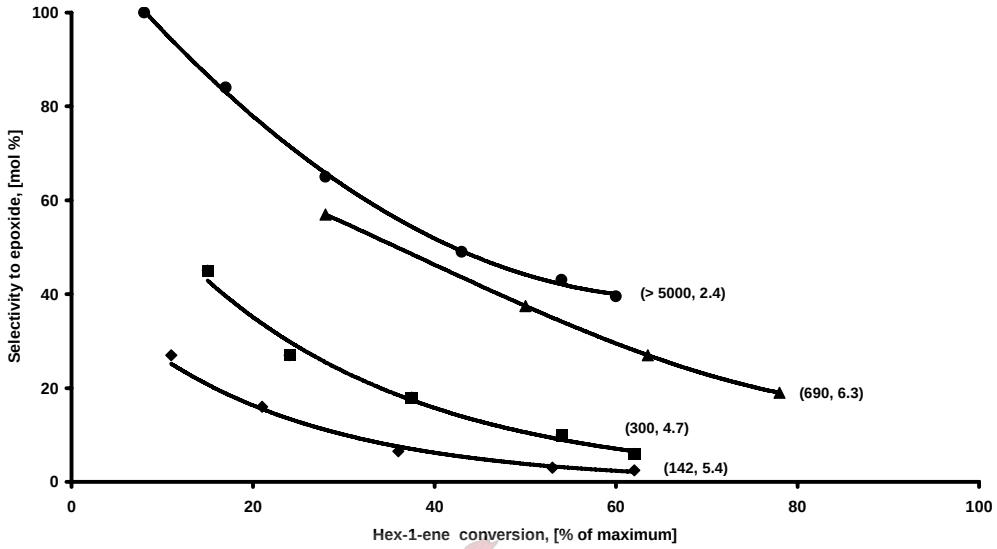

Figure 3.6: Selectivity to the epoxide as a function of conversion in the oxidation of hex-1-ene with aqueous H_2O_2 using Ti-Beta catalyst. The numbers near each trace represent the Si/Al ratio and Ti content (as mass % TiO_2) in the different catalysts (redrawn and modified from (Camblor, M. A.*, et al.*, 1996b))

It was also observed that opening of the epoxide ring, although slow, still occurred on the Al-free catalyst, which suggests that in Ti-Beta zeolite there are sites other than bridging hydroxy groups that are capable of catalysing the opening of the oxirane ring. Bellussi *et al.* (1992) reported that the aluminium-free zeolite TS-1 develops acid centres in the presence of H_2O_2 in alcoholic or aqueous solutions. These acid centres are related to framework titanium and are developed in the presence of H_2O_2 in polar solvents, due to co-ordination of the solvent to the active titanium site yielding a cyclic penta-coordinated species (see later discussion on the reaction mechanism). These acid centres were able to catalyse the opening of *cis* and *trans*-2,3-epoxybutane.

To quantify the effects observed with Al-free Ti-Beta, and to account for the contribution of both types of acid centres, Camblor thus synthesised a pure silica Beta-zeolite without introducing titanium in the gel mixture. When 1,2-epoxyhexane was reacted on both catalyst samples no epoxide conversion to methyl glycol was observed on the all-silica zeolite, while the oxirane ring was substantially opened on the Al-free Ti-Beta sample.

From these results it was possible for Camblor *et al.* (1996b) to conclude that it was the acid centres associated to framework titanium that were mostly responsible for opening the epoxide ring during the epoxidation of alkenes with H_2O_2 on Al-free Ti-Beta, and not bridging of hydroxy groups of the silanol defects located on the catalyst surface.

3.3.6 Synthesis Medium

Incorporation of titanium into the framework of Al-free zeolite Beta is done in hydrogen fluoride medium in the presence of tetraethylammonium ions, and at near neutral pH (8-9).

This is because there is a fundamental difference between Beta materials synthesised in fluoride medium, Beta(F), and in hydroxide medium, Beta(OH). Blasco *et al.* (1998) demonstrated this using a combination of powder XRD, adsorption microcalorimetry and spectroscopic techniques, and catalytic testing experiments.

The lack of silanol connectivity defects in Beta(F) samples, as opposed to the very high concentration of such defects in Beta(OH) samples, shows the strict hydrophobic nature of Beta zeolites synthesised in F^- medium, and the enhanced hydrophilicity when the materials are synthesised in OH^- medium.

The difference is a consequence of the resistance to hydrolysis of the Ti-O-Si bonds in Ti-beta(F) to form Si-OH and Ti-OH groups. This resistance is due to the lack of nearby Si-OH groups (or surface oxygens) to stabilise the hydrolysed $TiOH(OSi)_3$ + SiOH situation by hydrogen bonding to the silanol produced. This means that the stable 4-coordinated form of titanium, the unhydrolised $Ti(OSi)_4$ species, predominates in F^- medium.

In Beta(F) only Si-OH moieties ascribed to terminal groups in the external surface of the crystallite exist. There is no dependence of the Si-OH concentration on the titanium content of the sample, suggesting that hydrolysis of Si-O-Ti bonds does not occur to a large extent.

^{29}Si CP MAS NMR spectroscopy confirms that no hydrolysis of Si-O-Ti bonds occurs in Ti-Beta zeolites prepared by the fluoride route; the spectrum does not have a band at *ca.* -102 ppm, assigned to Si-OH groups (also confirmed by IR analysis). More conclusively, $^1H \rightarrow {}^{29}Si$ CP MAS NMR cross-polarisation experiments, which are more sensitive to Si-OH groups, revealed the presence of only a small concentration of these groups in fluoride-synthesised materials, and this concentration appeared to be dependent on the crystal size but not on the titanium concentration. Therefore, Blasco *et al.* (1998) assigned these bands to Si-OH

groups at the external surface of the crystallites. Silanol groups are however a significant feature of Ti-Beta(OH) samples, as evidenced by spectroscopy.

This difference in Si-OH concentration determines the different polar character of materials synthesised in F^- and OH^- media, as demonstrated by adsorption microcalorimetric experiments. While pure silica zeolite Beta(F) is strictly hydrophobic, the presence of titanium in the Ti-beta(F) samples increases their hydrophilicity. The enhanced hydrophilicity is due to the titanium centres themselves which when tetrahedral in the zeolite framework can expand their first co-ordination sphere by bonding to ligands with electron donor properties (like water), and thus act as Lewis-acid sites (electron-pair acceptors). Experiments strongly suggest the comparatively strong heterogeneous adsorption of precisely one water molecule per Ti site, followed by only weak adsorption of additional water molecules which occurs by mere condensation (Blasco, T.*, et al.*, 1998).

According to XANES and adsorption experiments (Blasco, T.*, et al.*, 1998), in the Beta(OH) samples, more than one water molecule can adsorb on each site. The significant contribution of the hydrophilic Si-OH groups also cannot be ignored, which in addition also cause the titanium sites to co-ordinate with more than one water molecule.

The hydrophobic character of the Ti-Beta(F) zeolite is crucial for reactions involving the oxidation of organics in the presence of highly polar species (water/methanol), since the pores will exclude the highly polar molecules and be maintained in an organic-rich environment. Blasco demonstrated this ease of diffusion and adsorption of less polar organics in the micropore channels, and related it to the more efficient H_2O_2 use observed than was observed for a Ti-Beta(OH) catalyst (Blasco, T.*, et al.*, 1998).

Thus the high hydrophobicity of Ti-Beta(F) materials means that they can advantageously replace Ti-Beta(OH) catalysts in the oxidation of organic substrates containing a polar moiety, and this enhanced hydrophobicity can determine their activity and selectivity.

3.4 Mechanistic Implications

The hydroxylation of phenol to dihydroxybenzenes is given schematically in Figure 3.7. There are essentially two products formed during this reaction, namely catechol and hydroquinone (theoretically resorcinol can form as well, but the probability for this meta-substituted derivative is low; see discussion in *Section 3.4.2*).

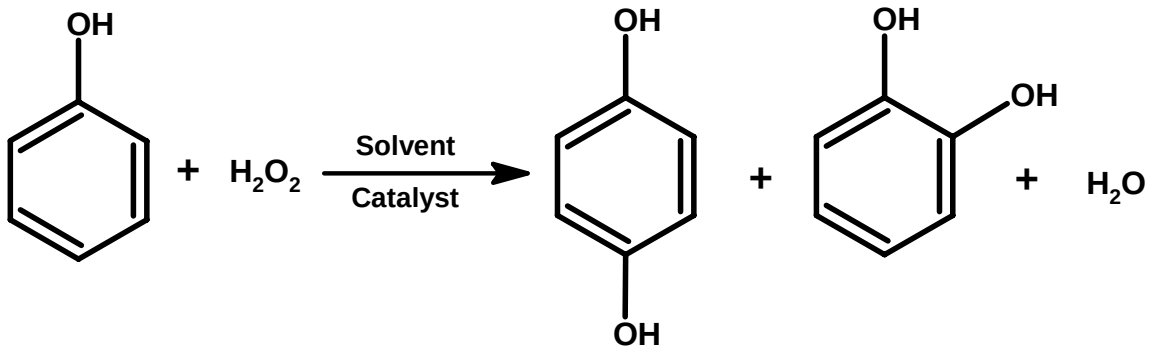

Figure 3.7: Hydroxylation of phenol with aqueous hydrogen peroxide to hydroquinone and catechol

While it is known that the two main oxidation products in the phenol hydroxylation are hydroquinone and catechol, the reaction path and product selectivity observed need clarification, since they depend to a large extent on the pore size of the catalyst used, as well as the nature of the solvent (protic vs. aprotic, polar vs. non-polar, co-solvent mixtures).

The possible electrophilic, aromatic substitution mechanisms that have been proposed, and that qualitatively account for the different effects observed, need to be explained.

3.4.1 Substituent Effects

Firstly, the hydroxy substituent group plays a significant role in determining the regioselectivity. It is a strongly activational species since it has a dominant electron-*donating* resonance effect (+R) that is most pronounced at the ortho and para positions, and that outweighs a weaker electron-*withdrawing* inductive effect (–I), due to the high electro-negativity of the O atom bonded to the aromatic ring. The resonance structures of phenol can be seen in Figure 3.8.

This resonance effect consequently increases the electron concentration and charge density in the aromatic system by donation of an electron pair from the oxygen atom of the hydroxy substituent through the pi bond, thereby making phenol a stronger nucleophile than

unsubstituted benzene, so that it is more readily attacked by an electrophile, and predominantly at the (electron-rich) ortho and para positions.

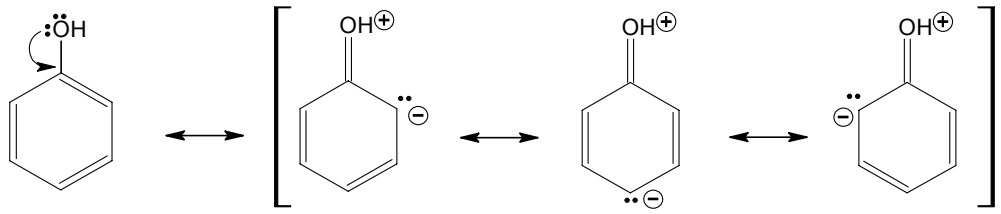

Figure 3.8: Resonance structures of phenol. The increased charge density at the ortho and para positions occurs due to the donation of electrons from the oxygen atom through π bonds (McMurry, J., 1996)

3.4.2 Carbocation Intermediates

The different resonance stabilised carbocation intermediates formed in the phenol hydroxylation by electrophilic attack of the terminal OH of the titanium hydroperoxo group are *all* stabilised by resonance. These carbocations can be seen in Figure 3.9.

All possible carbocation intermediates are stabilised by resonance, but the ortho and para complexes are stabilised the most by intermediates in which the positive charge in the benzene ring is stabilised by delocalisation through the donation of an electron pair from the oxygen atom (structures in bold in Figure 3.9). The ortho and para intermediates are thus lower in energy than the meta-substituted complex and therefore form faster, rendering the probability for the meta intermediate less significant. Therefore, only ortho- and para-substituted products should theoretically be obtained when phenol is hydroxylated according to an electrophilic attack mechanism.

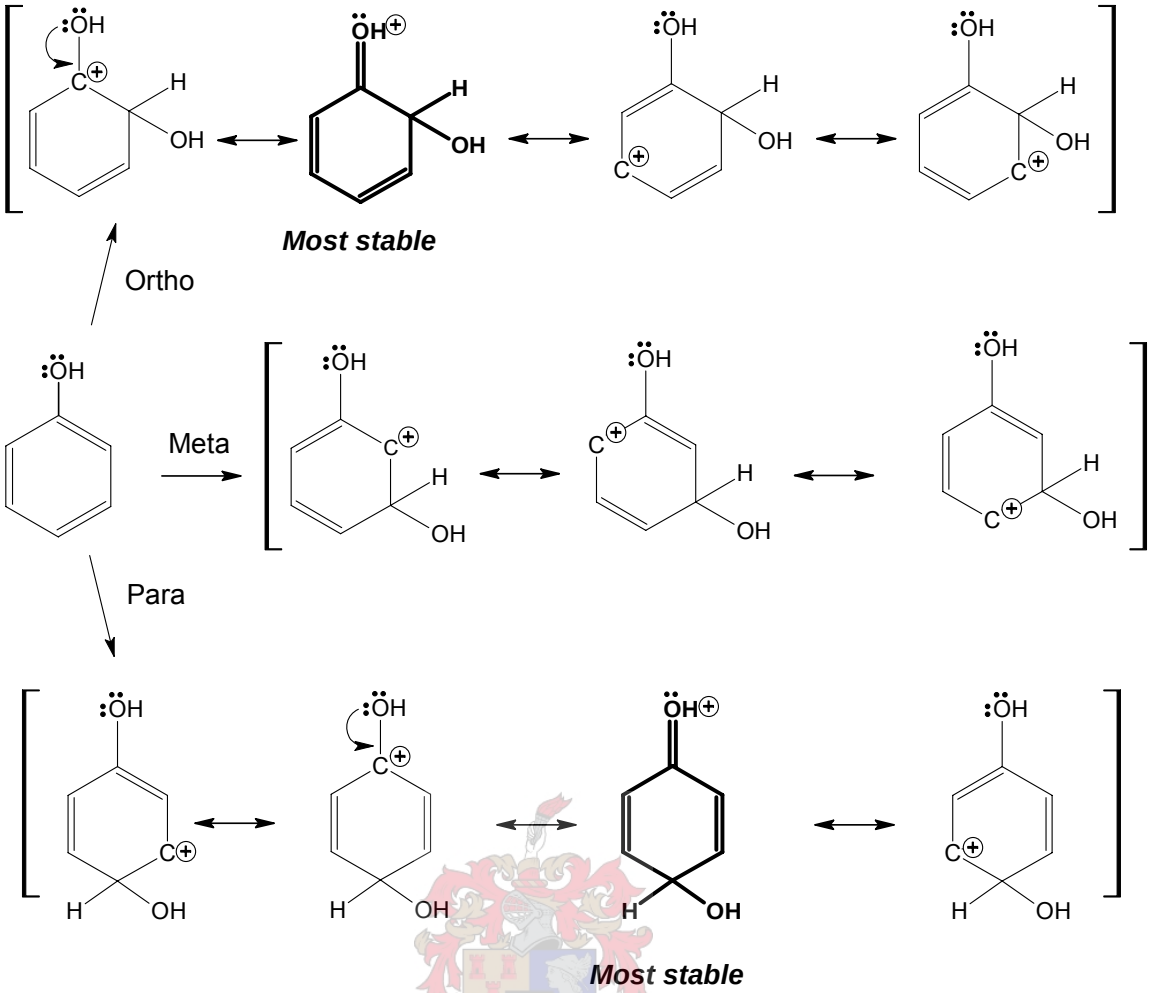

Figure 3.9: Carbocation intermediates formed in the hydroxylation of phenol. Resonance donation of electrons stabilises the ortho- and para-complexes. Modified from (McMurry, J., 1996)

3.5 Proposed Mechanisms

When using a non-selective catalyst, the probability for the reaction is 2:1 in favour of catechol formation since there are two ortho positions and one para position, all with approximately equivalent energies (66% ortho, 33% para formation). From an economic viewpoint (as discussed earlier), catechol is, however, typically the undesired product, and enhanced hydroquinone selectivity is favoured.

The titanium silicalite zeolites TS-1 and Al-free Ti-Beta have been gainfully employed to change the selectivity of the reaction by reversal of the regioselectivity, so that predominantly hydroquinone is obtained when the reaction is carried out in a protic solvent.

While reaction mechanisms for epoxidations, alkane oxidations and ammoximations over TS-1 and Al-free Ti-Beta have been proposed in the literature, Wilkenhöner *et al.* (2001) and Clerici (1991) have proposed the only detailed mechanisms for aromatic hydroxylations.

The absence of resorcinol from the phenol hydroxylation product mixture, which is detected only in trace amounts, indicates that the heterolytic, electrophilic, aromatic substitution mechanism that has been proposed by these authors is favoured. Since only low meta-isomer concentrations are detected, indicating a lack of formation of any significant quantities of free-radical intermediates, it seems that a radical mechanism pathway is unlikely, although its occurrence cannot be completely disqualified. A radical pathway should be avoided since free-radical chemistry does not usually exhibit selective oxygen transfer, and side reactions to undesired products become significant.

TS-1 and Al-free Ti-Beta catalysed phenol hydroxylations are only possible using hydrogen peroxide as the oxidant. While the pores of TS-1 are too small to accommodate the larger organic peroxide *tert*-butylhydroperoxide (TBHP), there is sufficient space in the pores of Ti-Beta to activate the titanium sites, as has been observed for epoxidation reactions (Blasco, T.*, et al.*, 1998). However, no phenol hydroxylation occurred with Al-free Ti-Beta when TBHP was the oxidant (Wilkenhöner, U.*, et al.*, 2001), which strongly suggests that the aromatic hydroxylation over titanium substituted molecular sieves follows a different reaction mechanism than proposed for epoxidation reactions.

Protic solvents have been seen to favour the formation of hydroquinone, whereas more catechol is formed in aprotic solvents, such as acetone. For TS-1 in all solvents, it was observed that hydroquinone was preferentially formed on the internal surface titanium sites (Wilkenhöner, U.*, et al.*, 2001), which suggested a geometric constriction for the reaction taking place in the pore system of the TS-1 catalyst. It was also observed that hydroquinone formation was favoured for hydroxylations over Al-free Ti-Beta in methanol solvent (Callanan, L. H.*, et al.*, 2004), despite its larger pores, which would be able to accommodate the bulkier intermediate leading to the formation of catechol.

The effects of different solvents for the phenol hydroxylation over TS-1 and Al-free Ti-Beta are illustrated in Figure 3.10.

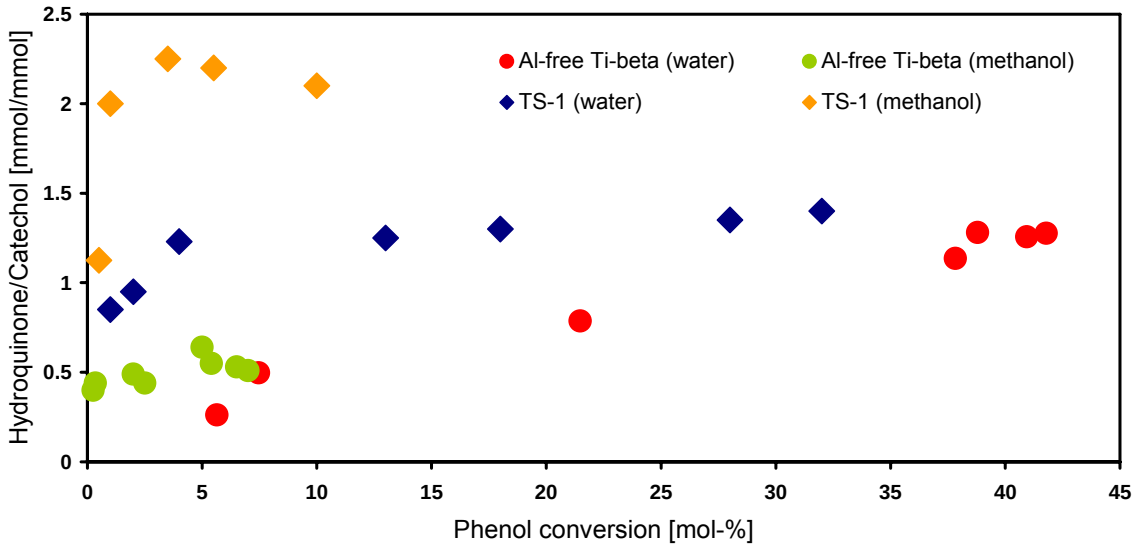

Figure 3.10: The effects of water and methanol solvents on the hydroquinone-to-catechol selectivity in the hydroxylation of phenol over Al-free Ti-Beta (Wilkenhöner, U., *et al.*, 2001; Callanan, L. H., *et al.*, 2004)

Catalyst: TS-1/Al-free Ti-β; $m_{catalyst}$ = 0.12 g; m_{phenol} = 1.2 g; T_R = 60 °C; Solvent: water/methanol; V_{H2O2} = 0.6 ml; V_{total} = 5.5 ml

The mechanism for this selective reaction, and the active role played by the different solvents used and size of the zeolite micropores where the active sites are located in determining the product selectivities, are discussed in the following sections.

3.5.1 Solvent Effects

The reaction mechanisms presented attempt to account for the solvent effects observed in the aromatic phenol hydroxylation reaction. It has been seen that the solvent greatly influences the rate and product selectivity of the reaction, and this is predominantly to do with their profound influence on the local environment of the active titanium cation sites (Mal, N. K. and Ramaswamy, V., 1996).

The size and special environment size of the zeolite micropores where the active sites are located also has to be taken into account to explain their active role in affecting the product distribution and selectivity.

Consider the reaction in protic solvents such as alcohols (e.g., methanol) and water.

Firstly, the active site must be considered. The formation of peroxo species with tetrahedral titanium has been well documented by numerous authors (Bellussi, G.*, et al.*, 1992; Clerici, M. and Ingallina, P., 1993; Sato, T.*, et al.*, 1994), and many titanium compounds produce peroxo species on reaction with basic, neutral and acidic solutions of hydrogen peroxide.

The active site in the titanium-substituted silicates is also thought to be a titanium-peroxo species formed by reaction of hydrogen peroxide with titanium incorporated in the silica environment (Clerici, M. G., 1991), as shown in Figure 3.11. Aprotic solvents (like acetone and acetonitrile) cannot form stable complexes with the titanium metal sites, thus limiting formation of the peroxo intermediates at the active sites in the pores, so that catechol formation at the external surface sites dominates (see discussion later in this section).

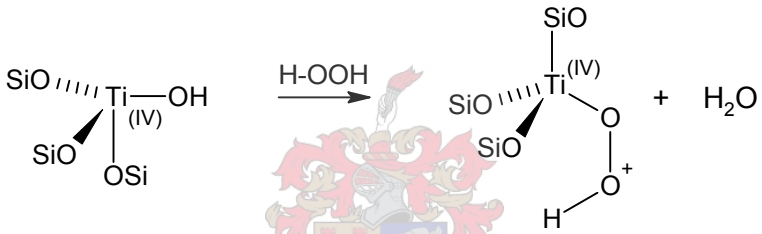

Figure 3.11: Titanium-hydroperoxo active site species with a tetracoordinate tetrahedral configuration (in the absence of a protic solvent molecule (Clerici, M. G., 1991)

An electrophilic attack of the aromatic ring using this species as the active intermediate has been suggested by Wilkenhöner *et al.* (2001), similar to the mechanism suggested by Reddy and Jacobs (1996) for the selective oxidation of secondary amines to the corresponding hydroxylamines.

When protic solvents molecules such as alcohols and water are present, they co-ordinate to the peroxo group at the active titanium site and form a larger penta-coordinated active intermediate complex stabilised by hydrogen bonding, as shown in Figure 3.12. The co-ordinating polar protic molecules expand the co-ordination sphere of titanium to 5 or 6 (Bonneviot, L.*, et al.*, 1993; Davis, R. J.*, et al.*, 1995). A five-membered ring with hydrogen bonds between methanol and the peroxo group at the titanium site has been proposed as the active complex for a TS-1 catalysed reaction (Martens, J. A.*, et al.*, 1993).

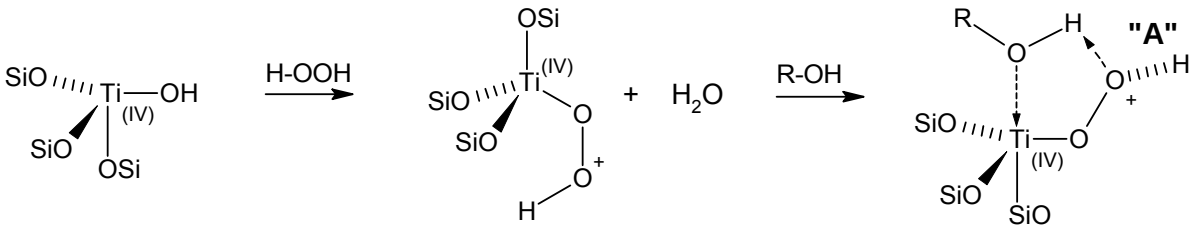

Figure 3.12: Penta-coordinated active intermediate complex with a trigonal bipyramidal configuration (active site with co-ordination of 1 protic solvent molecule, R=H/CH_3) (Wilkenhöner, U.*, et al.*, 2001)

It has been proposed that the terminal OH of the titanium hydroperoxo group in this 5-membered ring (labeled “A” in the above diagram) is the electrophile that attacks the aromatic ring (Wilkenhöner, U.*, et al.*, 2001).

This complex significantly increases the size of the Ti site, which could substantially narrow the TS-1 or Ti-Beta micropore channels and lead to a geometric constraint for an approaching phenol molecule. With the OH group pointing away from the bulky active titanium centre, the para-position is closer to the active site and para-hydroxylation, giving hydroquinone, occurs. This orientation can be further enhanced if the phenolic OH group is also hydrogen-bonded to OH groups of protic solvent molecules, thereby enlarging the phenol molecule and hindering ortho-hydroxylation. This scenario corresponds to a transition-state shape selectivity induced by protic solvent molecules.

The reaction mechanism for the formation of hydroquinone in the hydroxylation of phenol in the presence of protic solvent molecules is shown in Figure 3.13.

The reason why little catechol is produced in protic solvents is because of competition between the solvent and phenol molecules for co-ordination to the active site. The para-substitution pathway dominates because of the hydrogen bonds that can form between phenol and the protic solvent, which makes the molecule too bulky, inhibiting its access to, and movement within, the pores. Furthermore, if coordinated protic molecules close to the peroxo species form hydrogen bonds with the active site, this with destabilise hydrogen bonding between the titanium site and phenol molecules (which assists ortho-hydroxylation; see mechanism schemes in Figure 3.14 and Figure 3.15).

A reaction pathway for ortho-hydroxylation to catechol is made possible by the co-ordination of phenol to the active site, as shown in Figure 3.14. In aprotic solvents (such as acetone and acetonitrile) this reaction pathway will dominate since phenol can take over the role of

the protic solvent molecule. Titanium sites without protic molecules co-ordinated (see Figure 3.11) are present, and via co-ordination of phenol to these titanium peroxo species a penta-coordinated phenol-titanium site is formed, yielding catechol. Protic solvents compete with phenol so that this reaction pathway doesn't dominate in these solvents.

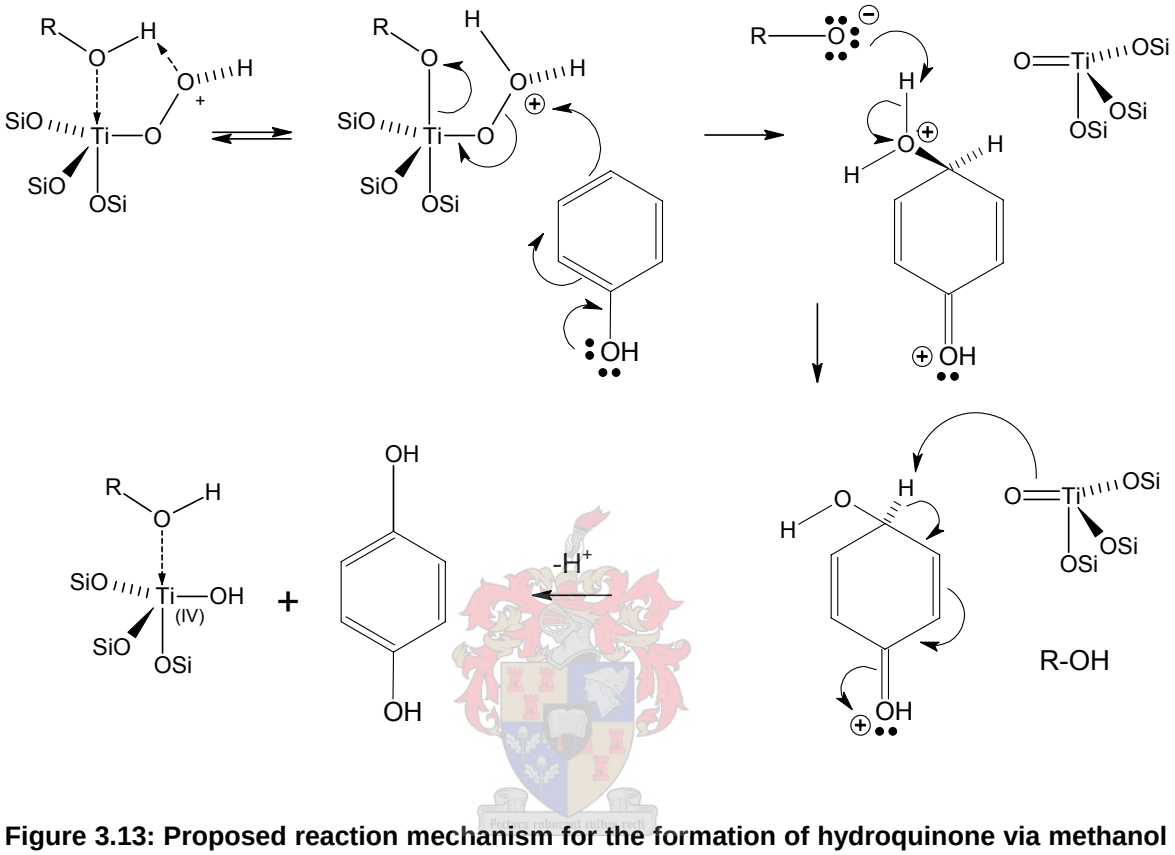

Figure 3.13: Proposed reaction mechanism for the formation of hydroquinone via methanol co-ordination to the Ti-OOH active site (R=H/CH_3) (Wilkenhöner, U.*, et al.*, 2001)

An alternative mechanism for catechol formation occurs via direct attack of the weakly electrophilic hydroperoxo group on the phenol ring giving a six-membered transition state. This reaction scheme is shown in Figure 3.15. In aprotic solvents the mechanisms depicted in Figure 3.14 and Figure 3.15 will dominate, so that catechol will be the preferred product.

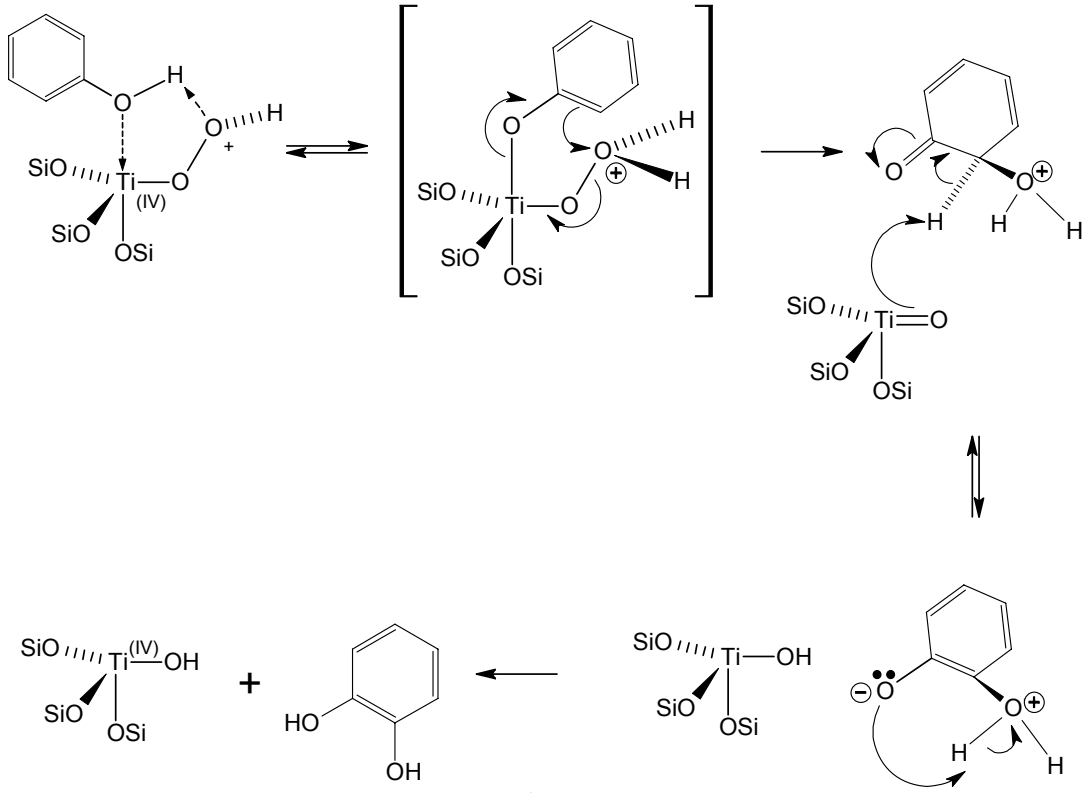

Figure 3.14: Proposed reaction mechanism for the formation of catechol via phenol co-ordination to the Ti-OOH active site (Wilkenhöner, U.*, et al.*, 2001)

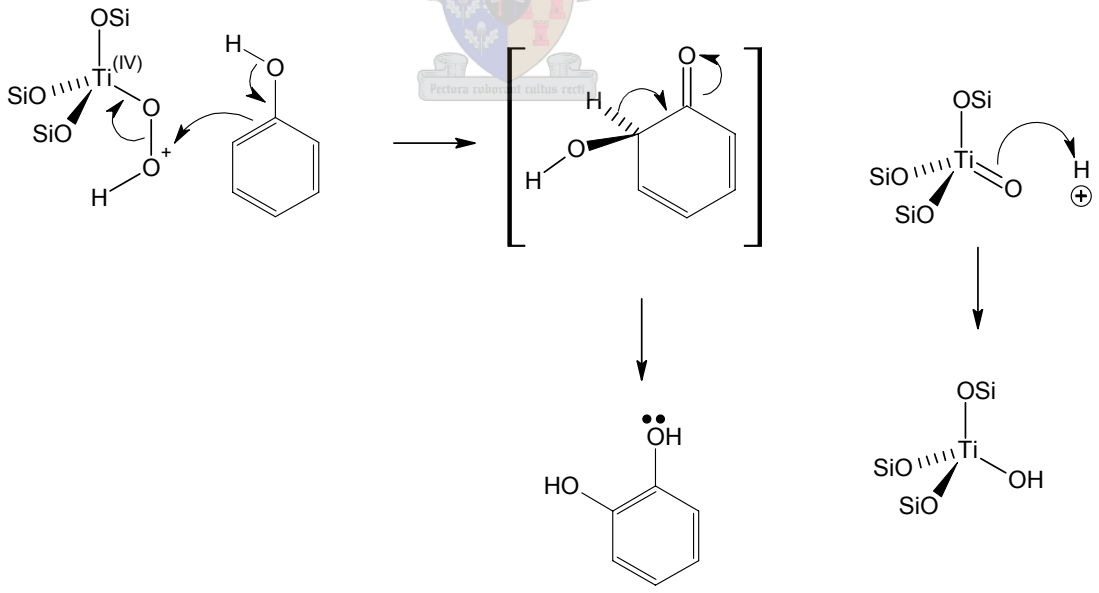

Figure 3.15: Proposed reaction mechanism for the formation of catechol without phenol co-ordination to the active site (Wilkenhöner, U.*, et al.*, 2001)

3.5.2 Geometric Effects

Comparison of product selectivities obtained with the medium-pore titanium silicalite TS-1 and the large pore Al-free Ti-Beta can indicate whether shape selectivity effects and the role of pore geometry are influential in the hydroxylation reaction. If the pore geometry imposes a geometric constraint on the reaction, then different product distributions should be obtained with both catalysts.

Wilkenhöner *et al.* (2001) found that for TS-1 and Al-free Ti-Beta crystals with similar diffusional path lengths, the p/o-ratio was almost three times higher for hydroxylation over TS-1 than Al-free Ti-Beta in water solvent (1.3 and 0.5 respectively at 5.8% phenol conversion). The preferential formation of hydroquinone in TS-1 and catechol in Al-free Ti-Beta in this solvent was seen as proof of the existence of geometric constraints (shape selectivity) in the pores of TS-1 limiting the formation of catechol.

3.5.2.1 TS-1

While the highly polar phenolic OH would be expected to point towards the hydrophilic Ti-peroxo site, favouring the ortho-position for electrophilic attack, the presence of hydrogen-bonded or co-ordinated methanol molecules at the Ti-peroxo site favours a configuration where it is repelled by the active site and points towards the TS-1 zeolite wall (hydrophobic). In this configuration the para-position of the molecule is closer to active centre and para-hydroxylation, yielding hydroquinone, preferentially occurs.

In TS-1 pores, co-ordinating protic solvent molecules increase the size of the titanium active site, narrowing the pore channels and significantly restricting the space available for phenol in the reaction zone. Therefore, more para-isomer is obtained (as seen in the first reaction mechanism, Figure 3.13). This phenomenon can also be partially explained by the fact that the electron-withdrawing inductive effect (–I), although weak, decreases the electron concentration more at the ortho position (thereby deactivating it) than at the para position, making it less susceptible to attack by the electrophile (Ti-OOH). The para position is thus slightly more electron-rich, and favoured for electrophilic attack. The phenol molecule has to adopt a ‘flat’ configuration with the OH group in the line channel direction, and it is unlikely for the molecule to be in an orientation where the OH group is perpendicular to the channel direction.

Without co-ordinated protic solvent molecules at the titanium hydroperoxo active site there is more space available for the phenol molecule so that the phenolic OH can hydrogen-bond to the active site. The ortho-position of the phenol molecule is closer to the Ti-OOH group, and

catechol formation is favoured. This is the case when water is used as the solvent; the lower p/o-ratios thus obtained can also be explained by the higher polarity of water compared to methanol, which means it is more strongly excluded from the hydrophobic pore environment, the active site formed is consequently smaller, and with resulting higher phenol concentrations in the vicinity of the active site ortho-hydroxylation is favoured.

Thus, hydroquinone is formed in a more selective way under the limiting geometric conditions found in the pores of TS-1, and is strongly influenced by hydrogen bonding effects with polar protic solvents (Wilkenhöner, U.*, et al.*, 2001).

3.5.2.2 *Al-free Ti-Beta*

In the larger pore Al-free Ti-Beta pores Wilkenhöner *et al.* (2001) hypothesised that the phenol molecule can adopt a different configuration than in TS-1, and can rotate into a position where it is perpendicular to the channel direction and the polar OH group points in the direction of the hydrophilic Ti-peroxo site. The higher amount of catechol that formed with Al-free Ti-Beta than with TS-1 was consistent with this theory. Thus, Al-free Ti-Beta was concluded to have a less restrictive pore environment.

Thus, for less restricted geometric titanium active sites found in the wider-pore Beta molecular sieve, catechol will be the preferred product. This will also be the case for the external surface titanium sites, and in aprotic solvents.

Pectora roborant cultus recti

3.6 Co-solvent Considerations

The correct choice of a solvent is particularly important in the phenol hydroxylation reaction, because it potentially offers reversed regioselectivity of the reaction, promoting hydroquinone production. As discussed, protic solvents play a very active role in controlling the reaction path determining product selectivities; through co-ordination to the active titanium site they stabilise the Ti-peroxo complex by hydrogen bonding and amplify transition-state shape selectivity.

Wilkenhöner *et al.* (2001) showed that that in protic solvents hydroquinone is the favoured product, while in aprotic solvents (acetone was investigated) catechol is favoured. The catalyst activity and reaction rate were higher when using pure water as the solvent as opposed to methanol, but that the hydroquinone selectivity was lower.

In aprotic solvents the bulkier catechol is favoured as the product because the solvent molecules do not form stable complexes with the titanium metal sites (internal sites), thus limiting the formation of the peroxo intermediate at the active sites in the pores.

Since it was known that the nature of the solvent (polarity and protic/aprotic nature) had a strong influence on the activity and selectivity of the reaction, the effect of varying the ratio of water to methanol in the solvent was investigated in order to quantify the relative effects of water and methanol in mixtures of the two on the overall reaction rate for the production of hydroquinone (Callanan, L. H.*, et al.*, 2004). van der Waal and van Bekkum (1997) did similar work in the epoxidation of alkenes, and it was seen that the 1-octene epoxidation exhibited a maximum in the reaction rate with the percentage alcohol in the solvent mixture. Their work, however, focused on the use of different alcohols as co-solvents in alcohol/acetonitrile mixtures, and thus investigated the difference between percentage protic/aprotic solvent.

Callanan *et al.* (2004) showed that the effect of varying the fraction of water in the solvent mixture had opposite effects on the desired activity and selectivity of the reaction. Increasing the amount of water yielded a higher reaction rate and phenol conversion, but decreased the selectivity for hydroquinone.

Increasing the amount of water in the solvent, which has a higher polarity than methanol, effectively makes the solvent mixture more polar, thus increasing the relative amount of phenol that adsorbs on the catalyst, and consequently yielding a higher reaction rate. In contrast, increasing the amount of water necessarily decreases the amount of methanol, relative to phenol in the reaction system and, hence, decreases the percentage of active sites coordinated with methanol giving larger penta-coordinated Ti active sites, which would favour the formation of hydroquinone due to amplified transition-state shape selectivity. This is because there is a competitive adsorption between methanol and phenol at the Ti-hydroperoxo active site as the methanol fraction in the solvent increases, which affects whether hydroxylation occurs on the para-position yielding hydroquinone (methanol dominating in the adsorption dynamics), or ortho-position yielding catechol (phenol dominating in the adsorption dynamics) (Callanan, L. H.*, et al.*, 2004).

In terms of optimising the methanol-water ratio, a series of experiments was done with different fractions of water in the solvent (Callanan, L. H.*, et al.*, 2004). The ratio of water to methanol in the initial solvent was adjusted so that there was between 7 and 100 vol-% water in the final solvent mixture.

Their findings suggested that it might not be possible to obtain optimal water to methanol ratio since the range of water percentages in which the desired activity and selectivity overlap do not coincide (see Figure 3.16).

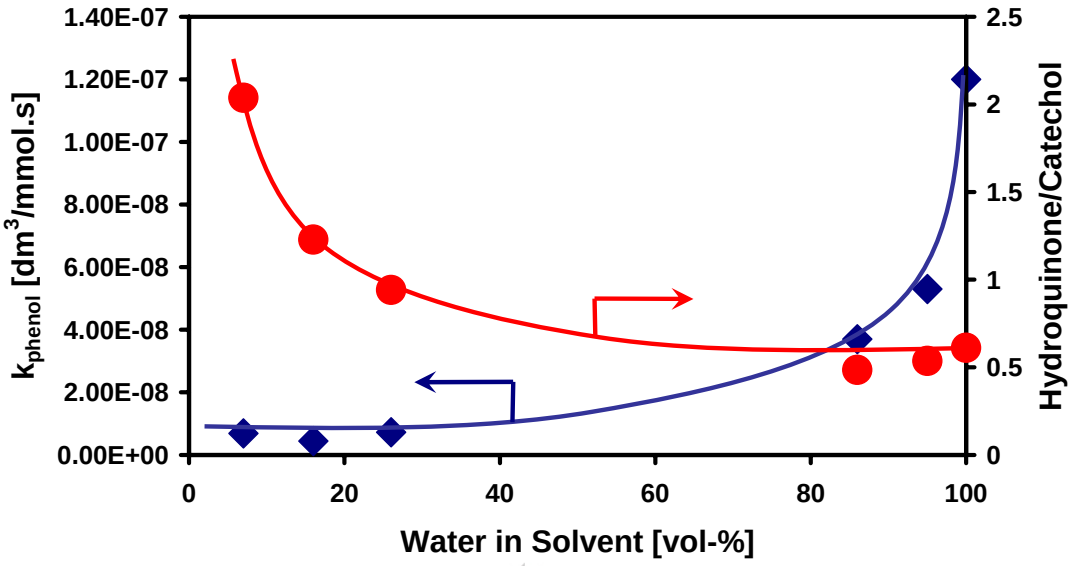

Figure 3.16: Phenol rate constant and hydroquinone selectivity plotted as function of the percentage water in the solvent mixture at 8% phenol conversion (Callanan, L. H.*, et al.*, 2004)

Catalyst: Al-free Ti-β; $m_{catalyst}$ = 0.12 g; m_{phenol} = 1.2 g; 4.6 mmol H_2O_2; Solvent: water/methanol; V_{total} = 5.5 ml; T_R = 60 °C

Keeping in mind that protic solvents favour the formation of hydroquinone, the focus of the current work will be exclusively on the use of these solvents.

3.7 Key Consideration

Hydrogen peroxide is favoured as the oxidant of choice for this liquid-phase hydroxylation because it is a versatile and environmentally compatible oxidising agent. Furthermore, the lower operating temperatures possible and limited mass-transfer limitations in the liquid phase are advantageous for the highly selective synthesis of fine-chemicals.

The use of acid-free, hydrophobic zeolites is crucial for partial oxidation reactions, and has been observed to result in greatly improved catalyst activity, product selectivity, and hydrogen peroxide efficiency. In light of the reduced catalyst lifetime and potentially higher separation costs associated with tar formation on acid catalysts, the catalysts used for the phenol hydroxylation reaction should be free of any framework aluminium. TS-1 and Al-free Ti-Beta have been shown to be suitable, and the strength of their unique activity lies in a combination of isolated tetrahedrally coordinated titanium atoms in a silicate structure and a

hydrophobic and non-acidic environment. The catalysts essentially differ with regards to their pore size, TS-1 being a medium-pore and Al-free Ti-Beta being a large-pore silicate zeolite. The difference in pore size can affect the formation of different transition-states and geometric constraints in the pores of TS-1 are thus more limiting, a situation which can be enhanced by the use of different solvents.

The choice of solvent for the phenol hydroxylation is known to be critical. The complete inversion of selectivities in protic and aprotic solvents is an interesting phenomenon and due to different interactions between the solvent molecules with the active metal catalyst sites. Catechol formation is preferred in aprotic solvents like acetone, and dominates at the non-selective active sites at the catalyst surface. Protic solvents play a more active role in determining micropore selectivity and by co-ordinating to the active site, transition-state shape selectivity is increased so that hydroquinone is the preferred product with these solvents. Since hydroquinone is the desired product the use of protic solvents like methanol and water is favoured. It should, however, be noted that the polarity of these protic solvents also needs consideration as the contrasting effects of water and methanol in co-solvent mixtures on the activity and selectivity of the reaction over Al-free Ti-Beta have shown; higher water fractions result in a higher reaction rate but lower hydroquinone selectivity, whereas higher methanol concentrations greatly enhance hydroquinone formation.

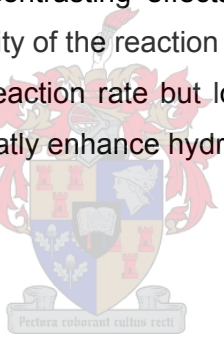

4 Research Design and Experimental Methodology

This section details the experimental apparatus and setup, experimental conditions and procedure, and analysis techniques that were used in this work.

4.1 Catalyst Synthesis and Preparatory Treatment

The importance of the catalyst synthesis procedure, and the dependence of the selectivity of oxidation reactions on the catalyst quality and activity, has been discussed in *Section 3.3*. Although this was not a synthesis project where one was developing a catalyst and investigating its specific properties, it was still necessary to attempt to prepare the Al-free Ti-Beta catalyst. It was therefore essential that the catalyst also be well characterised, as has been previously pointed out, to confirm that it has the required properties.

Blasco *et al.* (1998) developed the procedure for synthesis of the hydrophobic Al-free Ti-Beta that was used in this work. Essentially, the method involves the seeding of a synthesis mixture containing the silicon precursor (tetraethyl orthosilicate, TEOS), the titanium precursor (tetraethyl orthotitanate, $Ti(OEt)_4$) and the structure-directing template (tetraethylammonium hydroxide solution, TEOH), with dealuminated nanoscale zeolite Beta crystals in fluoride medium (HF, the mineraliser) and at near neutral pH (8-9). The resulting gel subsequently undergoes crystallisation to produce the catalyst crystals, followed by calcination to destructively remove the template.

The synthesised catalyst has a Si/Ti ratio of approximately 40. Particles with an average diameter of approximately 1 μm or less were used to minimise the effect that internal diffusion constraints within the catalyst particle could play on the results observed for oxidation reactions over Al-free Ti-Beta (Wilkenhöner, U., *et al.*, 2001; Wilkenhöner, U., *et al.*, 2002).

The importance of reagent purity has already been discussed in *Section 3.3.3.* Of particular importance is the exclusion of alkali metal cations from the synthesis gel, since their presence results in poor catalytic performance. The alkali concentrations in the template solution used were confirmed by AAS elemental analysis to be well below 50 ppm (*ca.* 5-10 ppm).

4.1.1 Synthesis and Dealumination of Nanoscale Zeolite (Al-) Beta Seeds

Small crystallites of Al-free Ti-Beta (diameter of *ca.* 1 μm) were synthesised by adding dealuminated zeolite Beta seeds at the end of the gel preparation, prior to autoclaving and crystallisation. For seeding, 0.05 g of nanoscale (*ca.* 15 nm) Beta seeds was added per gram of silica final synthesis gel. Not only does this allow smaller crystallites to nucleate and grow, but it also reduces the crystallisation time from 20 to 5 days (Wilkenhöner, U., 2001).

Zeolite Beta seeds are obtained by crystallising a starting gel of the following approximate molar ratio composition (accounting for water evaporated during the removal of ethanol as well as water consumed in the hydrolysis of TEOS):

1 SiO_2 : 0.040 Al : 0.56 TEAOH : 6.47 H_2O

In a typical synthesis, 45.24 g of tetraethylammonium hydroxide (35 wt-% aqueous solution, Aldrich), 1.85 g of metal aluminium chloride hexahydrate (Aldrich) and 4.33 g of deionised water were first mixed gently under magnetic stirring (100 rpm) in a polypropylene container at 25 °C until the aluminium source had dissolved completely, and a homogenous solution was obtained.

40.00 g tetraethylorthosilicate (TEOS, 99%+, Aldrich) was then slowly added dropwise under continued stirring, and a suspension of clear droplets in a milky solution was formed. This solution was kept stirring (100-150 rpm) at 25 °C until the ethanol formed in the hydrolysis of TEOS was completely evaporated (35.33 g ethanol). Two molecules of water per molecule of TEOS hydrolysed were consumed during this hydrolysis (6.91 g water), and approximately 5.3 g of water was also evaporated during evaporation of the ethanol. This water loss was not compensated. While the hydrolysis can take in excess of 6 hours at ambient room temperature it was accelerated by the heating the solution to 50 °C, and using a gentle purge flow of nitrogen through the solution (*ca.* 100 ml (NTP)/min). As time evolves, the solution became more milky-white and after approximately 1 hour the droplets disappeared, forming a clear, viscous solution (due to the hydrolysis of TEOS and water evaporation). Condensate was visible on the sides of the container (indicative of ethanol and water evaporation), and once the desired mass loss had been achieved and ethanol could not be smelt, the hydrolysis was assumed to be complete. The resulting solution had a pH of 12-14.

The crystallisation was carried out in 24 ml Parr PTFE-lined stainless steel autoclaves. The solution was loaded into the autoclaves and heated to 413 ± 0.1 K and at autogeneous pressure under mild rotation (60 rpm) for 72 to 90 hours.

After the required heating time the autoclaves were cooled and quenched in water, yielding a translucent, stable colloidal suspension with a pH of 11-12. This suspension was centrifuged at 18 000 rpm for 90 minutes to separate the suspended particles from the mother liquor. The gel-like appearance of the undried crystalline solids thus obtained was due to their very small particle size, and no solid particles were observed. The (solid) zeolite was then washed with deionised water (and subsequently centrifuged) repeatedly until the decanted supernatant liquid was *ca.* pH 8-9. Finally, the solids were dried at 70 °C for 12 hours, yielding agglomerated off-white zeolite crystals.

Acid leaching was used to dealuminate the as-made, dried zeolite-Beta crystals (Bourgeat-Lami, E.*, et al.*, 1993; Fajula, F.*, et al.*, 1994). The dealumination treatment was carried out in a 500 ml glass reactor equipped with a condenser at reflux conditions under vigorous stirring, using aqueous 11 M nitric acid (55 wt-%, Merck). 1 g of zeolite Beta seeds was treated with 60 g of acid and the solution kept under magnetic stirring and reflux at 75 °C for 24 hours. The solid seeds were recovered by centrifuging at 18 000 rpm (90 minutes), and washed with distilled water (with subsequent centrifuging) until the supernatant had near neutral pH (7-8). Finally, the sample was dried at 70 °C for 12 hours, yielding the dealuminated nanocrystalline zeolite-Beta crystals.

Two successive dealumination treatments, similar to the series of treatments done with different acids by Roberge *et al.* (2002), were also performed to investigate the effect on the degree of aluminium removal.

4.1.2 Al-free Ti-Beta Synthesis

Ti-Beta zeolite was prepared in a fluoride-assisted hydrothermal synthesis from a starting gel with the following chemical composition:

1 TiO_2 : 25.03 SiO_2 : 14.06 TEAOH : 8.59 H_2O_2 : 193.28 H_2O : 14.05 HF.

This molar composition corresponds to the final synthesis gel, i.e. water consumed in the hydrolysis of TEOS and TEOT has been accounted for, and water evaporated during the evaporation of the ethanol has been compensated.

In a typical synthesis, 45.37 g of tetraethylammonium hydroxide (TEAOH, 35 wt-% aqueous solution, Aldrich), 7.47 g of aqueous hydrogen peroxide solution (30 wt-% solution in water, Aldrich), 1.22 g of deionised water, and 40.00 g of tetraethylorthosilicate (TEOS, 99%+, Aldrich) were gently mixed under magnetic stirring (100 rpm) in a polypropylene beaker to

form a colloidal suspension of clear droplets in solution. The solution mixture was stirred for 2 hours at room temperature (25 °C), becoming slightly more viscous and milky-white, and during this time water condensate was visibly formed on the sides of the beaker and ethanol could be smelt evaporating, indicative of TEOS hydrolysis. The pH of the solution was in the range 12-14.

1.75 g of tetraethylorthotitanate ($Ti(OEt)_4$, Fluka) was then slowly added dropwise under continued stirring. To avoid pre-hydrolysis of the $Ti(OEt)_4$, and subsequent TiO_2 formation, it was added directly from the bottle to the beaker containing the synthesis solution. The titanium source dissolved slowly to form a very pale yellow solution. This solution was then stirred (100-150 rpm) at room temperature until complete dissolution of the titanium source had been attained, and the ethanol formed in the hydrolysis of TEOS and $Ti(OEt)_4$ was evaporated (36.74 g of ethanol). While this process can take several hours, it was accelerated as was done during the Al-Beta seed preparation (heating the solution to 50 °C under a gentle purge flow of nitrogen). After approximately 10 hours, ethanol evaporation was complete, and a homogeneous, clear pale-yellow solution was obtained. During the evaporation of the ethanol, water was also evaporated (5.3 g of water), and the loss of this water was taken into account and compensated for by adding deionised water prior to autoclaving.

5.40 g of hydrofluoric acid solution (40 wt-% solution in water, Merck) was then added to the prepared solution dropwise and slowly, and a thick, bright-yellow paste/gel was obtained, that could not be stirred magnetically. This thick paste was stirred mechanically to ensure uniform incorporation of the HF into the paste. Prior to crystallisation, this paste was seeded by adding dealuminated nanoscale zeolite Beta seeds to the gel with a mass ratio seeds/SiO_2 of 0.05 (0.58 g of seeds per gram of silica formed were used, to constitute a 1.00 wt-% seed composition in the final gel mixture).

This paste was transferred to Parr PTFE-lined stainless steel 24 ml autoclaves and heated at 413 ± 0.1 K under mild rotation (60 rpm) and autogeneous pressure for 5 days. Extended crystallisation times of up to 8-10 days were also used.

After crystallisation the autoclaves were quenched in cold water, and a light-brown solid product in solution was obtained. The pH of the mother-liquor was in the range 9-10. This material, and all washings from the autoclaves, was diluted with deionised water and the resulting solid product was then recovered by filtration on 0.45-μm Millipore filters. The solid was again mixed and washed extensively with deionised water (approximately 1500 ml) until

neutral filtrate (*ca.* pH 6-7) was obtained, and then dried at 80 °C for 10 hours to yield an off-white Ti-Beta sample.

Calcination of the prepared catalyst before use, to remove moisture, the organic template molecules and fluoride anions occluded in the solids, was done by heating the dehydrated sample to 400 °C in static air (temperature ramp 2 °C/min), and holding it at this temperature for 8 hours. It was observed that at approximately 220-230 °C the sample turned a dark orange-brown colour, and there was a strong, pungent ammonia-like smell, which is likely attributed to template burn-off. After the required holding time, the sample was cooled down to ambient temperature at the same rate.

4.1.3 TS-1

Small crystallites of TS-1 catalyst, synthesised by Wilkenhöner (2001) according to the method described by Thangaraj *et al.* (1990), were used. The crystallites have a cubic morphology with an average diameter of about 0.1 μm, as determined by scanning electron microscopy.

4.2 Catalyst Characterisation

Several physiochemical spectroscopic techniques have been used for physical and chemical characterisation of the dehydrated seeds and calcined catalyst samples.

4.2.1 Catalyst Chemical Composition

Elemental analysis, for determining the silicon, aluminium, titanium and alkali cation (Na^+ and K^+) contents of the samples, was determined using a Varian Spectra AA-100 spectrometer, attached to a DSD-30 data station.

Samples were prepared by weighing and placing approximately 20 mg of calcined and detemplated solids into a 24 ml teflon Parr acid digestion bomb and wetting them with 2 ml of deionised water. 4 ml of cold 40 wt-% HF solution (Merck, Saarchem) was added, the Parr bomb closed, and left for 2 hours to digest the zeolite (at room temperature). The solution was then transferred to a polypropylene volumetric flask and diluted to 50 ml with deionised water.

Standards in the range 0 to 100 ppm were prepared. Samples out of the standard calibration range were diluted with deionised water and then analysed.

4.2.2 Catalyst Structure and Morphology

4.2.2.1 Adsorption Measurements

N_2-BET adsorption isotherms, obtained using a Micromeritics ASAP 2010 adsorption apparatus equipped with a Micromeritics VacPrep 061 Sample Degas System, were used to measure the specific surface area, pore size and micropore volume of the calcined catalyst. Prior to N_2 adsorption, 0.5 g of the catalyst sample was first dried at 90 °C for 1 hour and then 300 °C under vacuum for 20 hours, and degassed at 77 K for 16-24 hours, and the anhydrous weight of the sample was taken. Nitrogen was then adsorbed at liquid nitrogen temperature until ambient pressure was reached.

4.2.2.2 Particle Size Distribution

Particle size distributions of the parent and calcined Al-free Ti-Beta samples (analysis of Beta seeds was not done) were obtained using a Saturn Digisizer 5200. Samples were suspended in Tetra Sodium PyroPhosphate (TSPP) using ultrasound (120 seconds) prior to analysis.

4.2.2.3 Powder X-ray Diffraction

Powder X-ray diffraction spectra of the Beta seeds (Al-containing and dealuminated), and the as-synthesised and calcined Ti-Beta catalysts were obtained on a Bruker D8 Advance Powder Diffractometer to examine their crystallinity and determine the phase purity.

The instrument generated monochromatic Cu-Kα radiation (λ = 0.1542 nm), and was operated at 40 kV and 25 mA. Scanning was done in the range 4 to 55° 2θ, with a step size of 0.02° 2θ and a 30 second counting time. A slit divergence of 3° was used.

Better resolution of the spectra was obtained using a narrower aperture (1° divergence), a step width of 0.04°, and an extended counting time of 120 seconds.

4.2.2.4 Scanning Electron Microscopy

Crystallite morphologies and crystal sizes were determined from electron micrographs, obtained using a Leo 1430VP Scanning Electron Microscope.

Samples were mounted on aluminium stubs (5 mm diameter) and subsequently sputter-coated with a thin gold film prior to scanning the images to prevent surface charging, and also to protect from thermal damage from the electron beam. The instrument was operated at

an accelerating voltage of 40 keV, a tilt angle of 0° and an aperture size of 30 μm, and a working distance of 7 mm.

4.2.2.5 Transmission Electron Microscopy

Transmission electron micrographs (TEM) were obtained using a LEO/Zeiss EM 912 TEM. The samples were dispersed in methanol by ultrasound, and this suspension was then transferred onto a Cu-grid coated with thin polymeric film, and the solvent allowed to evaporate before scanning.

4.2.2.6 Thermal Gravimetry Analysis

Thermo-gravimetric spectra for the calcination of the fresh, as-synthesised catalyst, and the combustion of deposited coke (i.e. organic tars) on the spent catalyst after reaction to determine the tar content, were obtained using a Shimadzu TGA-50H thermogravimetric analyser equipped with a TA-60WS thermal analyser (TGA/DTA).

For analysis of the tar content on the spent catalyst after reaction, the catalyst sample was first recovered by filtration on a 0.45 μm Millipore® disk filter, extensively washed with deionised water (approximately 500 ml per 0.12 g catalyst sample), and dried at room temperature.

A sample mass of 20 mg and a carrier gas flow rate of 60 ml (NTP)/min was used. In the thermal analyser, the sample was first heated in nitrogen at 5 °C/min to 150 °C, and held at this temperature for 60 minutes to desorb any water and light components. Subsequently, the carrier gas was changed to a mixture of air (80 ml (NTP)/min) and nitrogen (15 ml (NTP)/min), and the sample was heated further at 5 °C/min to 550 °C, and kept at this temperature for 6 hours to burn off all tar and coke.

4.3 Experimental Reactions

4.3.1 Apparatus and Setup

The apparatus in which the phenol hydroxylation reaction was conducted essentially consisted of a 24 ml glass closed-batch reactor that was immersed in a water bath. The water bath, which was placed on a magnetic stirrer/heater unit, ensured that the reaction mixture was maintained at the correct temperature. The reactor vessel was equipped with a Mininert® valve teflon sample port so that reaction aliquots could be withdrawn to monitor the

reaction. The use of teflon sample ports with silicon septa ensured that samples were only in contact with glass and teflon, as well as to minimise any evaporation losses.

While the accuracy of the temperature control can be increased by utilising a heating unit equipped with a thermocouple and PID temperature controller, this equipment was not available. Consequently, prior to conducting any experiments the heater plate had to be calibrated so that the correct temperature could be attained. The heater-water batch was calibrated, and five settings in the 55 °C to 70 °C range were obtained so that the temperature could be manipulated with relative ease. The water bath was also fitted with a lid to prevent evaporation of the water, and to maintain a uniform temperature.

Since a negligible temperature variance of about 1-2 °C was observed with this method of temperature control, its accuracy was sufficient.

Figure 4.1 shows a schematic drawing of the experimental setup that was used.

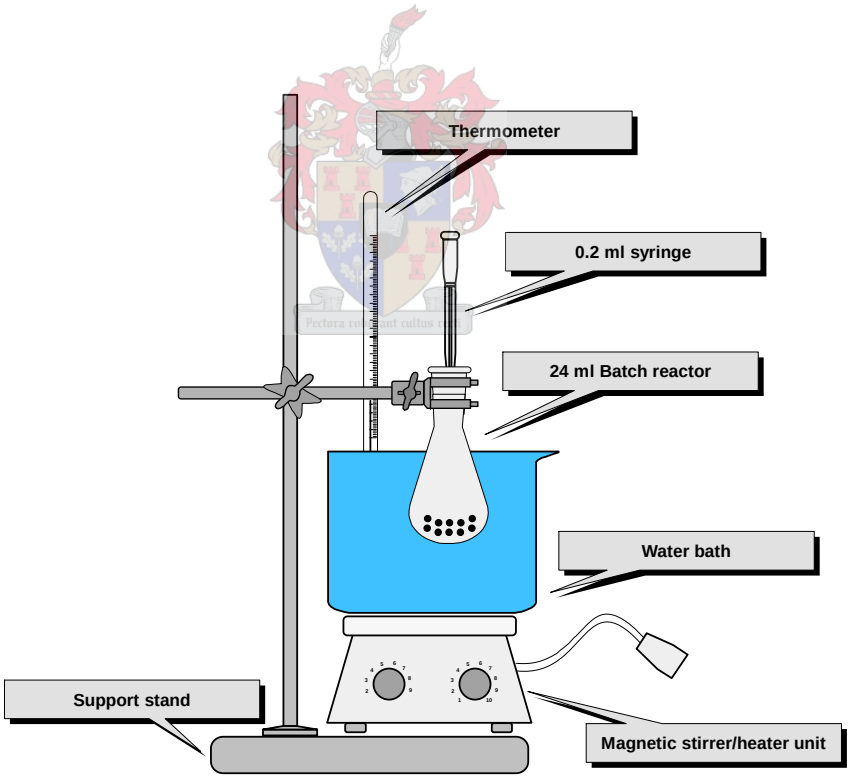

Figure 4.1: Experimental setup used in the phenol hydroxylation reactions

4.3.2 Experimental Conditions and Procedure

All phenol hydroxylation reactions were carried out batchwise at atmospheric pressure under air environment, at a temperature of 60 °C, and under continuous magnetic stirring.

Initially, 1.2 g of phenol crystals (Assoc. Chem. Enterprises, AR, min. assay 99.9%) was mixed in the appropriate amount of solvent and dissolved to a homogeneous solution under stirring (effective starting concentration *ca.* 2300 mmol/dm^3). 0.12 g of the calcined Al-free Ti-Beta catalyst was then added (phenol/catalyst ratio *ca.* 10) and adsorption equilibrium was attained at the reaction temperature by allowing the suspension to stabilise for 12-16 hours prior to reaction. The suspension turned a pale cream-yellow in colour during this stabilisation period.

To start the catalytic hydroxylation reaction hydrogen peroxide, as a 30 wt-% aqueous solution (Sigma-Aldrich, AR, 30 wt-% stabilised solution) was added at time zero to the catalyst and phenol-solvent solution. The peroxide was added in a single portion. Depending on the desired concentration of peroxide in the initial reaction solution, different volumetric quantities were added, and the total volume of the reaction solution (solvent and hydrogen peroxide) at the start of the reaction was kept constant at 5.50 ml. For experiments investigating peroxide addition effects, the reactor was operated in pseudo semi-batch mode, with discrete amounts of peroxide solution added at regular intervals over a period of 4.5 hours at either 0.1 ml per hour or 0.05 ml per half hour.

Periodically a representative aliquot sample (0.2 ml) of the vigorously stirred reaction solution (*including* the catalyst) was withdrawn through a septum with a microlitre syringe for analysis. The sample was injected into a 4 ml sample vial (fitted with Teflon-lined septa), diluted with 3 ml distilled water, and then filtered over a sterile 0.22-μm Millipore filter (Millex-GV). The samples were cooled to 0 °C to prevent further reaction and peroxide decay prior to analysis. Under the semi-batch method of reactor operation sampling was done prior to addition of the next portion of peroxide solution.

The frequency of sampling followed a power-law type pattern with more samples being taken at the earlier reaction times. Samples were taken at 5, 10, 15, 30 and 60 minutes, and then at 60-minute intervals for an additional 7 hours. Each experimental run was concluded after 8 hours total reaction time. The spent catalyst was subsequently recovered by filtration on a 0.45 μm Millipore® disk filter, extensively washed with deionised water, and dried at room temperature prior to TGA analysis.

4.4 Product and Sample Analysis

The following analytical techniques were used: standard iodometric titration (H_2O_2), high-performance liquid chromatography (organics), and thermal gravimetry (deposited tars, as discussed in *Section 4.2*).

4.4.1 Standard Iodometric Titration

A standard iodometric titration was used to monitor the residual H_2O_2 content in the aliquot samples, and hence determine the quantity used during the reaction and its degree of conversion. Skoog and West (1976) report that this titration method has been widely employed for the analysis of oxidants such as hydrogen peroxide, and under these conditions hydrogen peroxide should react completely with iodine to liberate iodide, without any side reactions.

Titrations to determine peroxide concentrations were performed immediately after withdrawing and filtering the samples, since peroxide decay continues in the samples, even after removal from the reactor.

The oxidation-reduction process applicable in this work involves the indirect iodometric titration method (termed iodometry); in principle, it occurs via a two-step procedure, namely the titration of iodine liberated in a chemical reaction involving the hydrogen peroxide. In this redox reaction, before titration of the oxidising agent (iodine) by the thiosulphate solution (reducing agent) can be carried out, it is necessary for a potassium iodide solution to be reduced by an oxidant to ensure that the substance being titrated (iodine) is in a suitable lower oxidation state.

The first step of the procedure involves the oxidation of iodide (in potassium iodide solution) to iodine by hydrogen peroxide. Hydrogen peroxide is a strong oxidising agent (oxidant) and when reacted/treated in acid solution with a large (unmeasured) excess of the iodide ion, the latter reacts as a reducing agent (reductant) and the peroxide will be quantitatively reduced. A chemically equivalent molar quantity of iodine (to the amount of peroxide) is liberated from the oxidation of iodide, and thus serves as the basis for the titration analysis.

The partial half-cell equation for the reduction of hydrogen peroxide is:

$$H_2O_2 + 2H^+ + 2e^- \Leftrightarrow 2H_2O \qquad [4.1]$$

The partial half-cell equation for the oxidation of iodide is:

$$2I^- \Leftrightarrow I_2 + 2e^- \quad [4.2]$$

Adding [4.1] and [4.2] the reaction equation becomes:

$$H_2O_2 + 2H^+ + 2I^- \Leftrightarrow 2H_2O + I_2 \quad [4.3]$$

Using sulphuric acid as the proton source, this can be expressed as:

$$H_2O_2 + H_2SO_4 + 2KI \Leftrightarrow 2H_2O + I_2 + K_2SO_4 \quad [4.4]$$

The iodine thus formed is then titrated with a standard sodium thiosulphate solution incorporating a suitable indicator to indicate the end-point, at which point the titration is concluded. Thiosulphate is a strong oxidising agent with a much lower reduction potential than iodine and so will react completely and rapidly with the iodine, even in the acid solution.

The partial half-cell reaction for sodium thiosulphate, which behaves as a reducing agent (i.e. is itself oxidised) is:

$$2S_2O_3^{2-} \Leftrightarrow S_4O_6^{2-} + 2e^- \quad [4.5]$$

The partial half-cell reaction for the reduction of iodine is:

$$I_2 + 2e^- \Leftrightarrow 2I^- \quad [4.6]$$

Thus, adding [4.5] and [4.6] gives the overall reaction equation:

$$2S_2O_3^{2-} + I_2 \Leftrightarrow S_4O_6^{2-} + 2I^- \quad [4.7]$$

Including all ionic species gives:

$$2Na_2S_2O_3 + I_2 + \text{indicator} \Leftrightarrow Na_2S_4O_6 + 2NaI \quad [4.8]$$

oxidised form colour — reduced form colour

It is important that the titration of the iodine with thiosulphate is performed in an acidic solution with a pH below approximately 8. This is because in alkaline medium there are

competing reactions with the iodine. Reaction of iodine with hydroxide ions results in the formation of the unstable hypoiodite ion:

$$I_2 + 2OH^- \Leftrightarrow I^- + IO^- + H_2O \qquad [4.9]$$

The hypoiodite ion may subsequently disproportionate to iodate and iodide:

$$2IO^- + 2OH^- \Leftrightarrow IO_3 + I^- + H_2O \qquad [4.10]$$

The quantitative conversion of thiosulphate to the tetrathionate ion, given by expression [4.7], is almost unique with iodine. Other oxidising agents tend to carry the oxidation to sulphate ion; the reaction with hypoiodous acid demonstrates this stoichiometry:

$$4HOI + S_2O_3^{2-} + H_2O \Leftrightarrow 2SO_4^{2-} + 4I^- + 6H^+ \qquad [4.11]$$

The occurrence of these reactions can cause serious errors in the titration, since the presence of the hypoiodite ion in slightly alkaline solutions will seriously upset the stoichiometry of the iodine-thiosulphate reaction. Consequently, the titrations are performed in acidic solution.

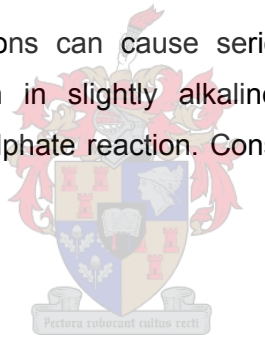

4.4.1.1 Titration Procedure

The titration method is critical, as has been seen previously (Callanan, L. H.*, et al.*, 2004). Two particular considerations that need to be taken into account to avoid errors are: (i) the loss of iodine owing to its considerable volatility, and (ii) acid solutions of iodide are oxidised by oxygen from the air.

To negate the influence of iodine's volatility the titrations were performed in cold solutions and in conical flasks as opposed to open beakers.

The rate of oxidation of iodide by atmospheric oxygen,

$$4I^- + O_2 + 4H^+ \Leftrightarrow 2I_2 + 2H_2O \qquad [4.12]$$

becomes significant as the pH of the solution decreases, and is catalysed by strong light and heat. Low pHs cannot however be avoided since acidification of the peroxide sample is

essential to ensure the complete reaction of hydrogen peroxide with the iodide to liberate iodine, otherwise the amounts of peroxide actually present will be underestimated. However, to minimise the effect on oxygen on the iodide oxidation, bubbling nitrogen gas through the solution produces an inert reaction atmosphere. Additionally, all solutions containing iodide were stored in cool place out of direct light, and the titrations were also not performed in direct sunlight.

The modified indirect iodometric titration, developed by Pan (Pan, Y.*, et al.*, 2003) was used in this current work, and the results obtained appear more reliable than before.

Preparation methods of the chemical reagents used in the titration are detailed in APPENDIX A.

In a typical titration, 50 ml of dilute sulphuric acid solution (0.1 M) was first placed in a 250 ml Erlenmeyer flask, and nitrogen gas was bubbled through the flask (200 ml (NTP)/min) into the solution for 5 minutes to purge any oxygen and carbon dioxide from the titration environment prior to injecting the reaction sample.

1 ml of the diluted aliquot sample was then added to the flask, and the nitrogen stream slowed to approximately 100 ml (NTP)/min, ensuring that it was bubbled directly into the solution.

5 ml of a 1 wt-% potassium iodide solution was then added slowly and the solution was gently agitated using a magnetic stirrer to ensure complete mixing, whilst minimising the loss of iodine through evaporation. 0.5 to 1 ml of a 2 wt-% ammonium molybdate solution was added to accelerate the reaction velocity and decomposition of the hydrogen peroxide and liberation of iodine; 5-10 minutes was allowed for the reaction to reach equilibrium and for the solution to turn a reddy-brown colour (occasionally with the formation of a visible precipitate), indicating complete iodine liberation.

This mixture was then titrated with a dilute sodium thiolsulphate solution (*ca.* 0.004019 N or less) at a rate of approximately 1 ml/min using a peristaltic pump, until the rust-brown colour was nearly discharged and the solution was pale orange-yellow, indicating the approach of the endpoint. 1 ml of starch indicator was then added slowly under further mixing to yield a deep violet/blue solution. The mixture was then titrated further with the thiosulphate solution (0.75 ml/min) until the colour of the solution changed to the first permanent murky white or colourless, indicating that the endpoint had been reached. An additional 0.5 ml of starch was added, and the solution left for 5 minutes. If the solution regained a tinge of purple it was

further titrated with thiosulphate until the endpoint. The volume of sodium thiosulphate titre required to reach the endpoint was recorded.

4.4.2 High Performance Liquid Chromatography

High performance liquid chromatography (HPLC) was used to determine the concentration of the phenol and dihydroxybenzene aromatics (and any other reaction species) present in the samples. Typical HPLC operating conditions are detailed in *Section 10.1.2* (APPENDIX B).

Syringes used for introducing the liquid samples onto the column were fitted with filters (sterile Millex®-GV 0.22 μm Millipore filter tips) to remove any catalyst that could potentially damage the apparatus.

Wilkenhöner *et al.* (2001) reported that HPLC is a better choice for the analysis of reaction mixtures of aromatic hydrocarbons with H_2O_2 than gas chromatography (GC) is. It has been found that GC analysis of the reaction products in the phenol hydroxylation, when hydrogen peroxide had not been completely converted (and especially at low H_2O_2 conversions), detected high concentrations of para-benzoquinone. HPLC analysis, in contrast, found only small quantities. These findings suggested that residual H_2O_2 in the reaction mixture reacted with phenol and its hydroxylation products in the high-temperature injector port of the gas chromatograph system, and which resulted in the over-estimated phenol conversion, para-benzonquinone concentration, and o/p selectivity (Ma, N.*, et al.*, 2002). These authors also reported that in the GC system hydroquinone could be oxidised by a trace amount of O_2 in the N_2 carrier gas, so even in the absence of residual hydrogen peroxide the para-benzoquinone yield and o/p selectivity obtained might be higher than the true values.

Earlier work done by van der Pol *et al.* (1992; 1993) reported similar observations, and these authors also concluded that a probable explanation for this discrepancy was the occurrence of a reaction between hydroquinone and hydrogen peroxide during GC analysis.

Since GC analysis results have been found to be dependent on the injector temperature when phenol hydroxylation reaction mixtures still containing residual H_2O_2 were injected, HPLC was identified as the preferred analysis technique for samples that were generated in this work. This was because complete phenol and hydrogen peroxide conversions could not be guaranteed, especially at some of the higher initial peroxide concentrations used. Furthermore, HPLC is favoured over GC for analysis of these samples because the major reaction products formed, hydroquinone and catechol, are generally too large for typical GC columns.

4.5 Kinetic Modelling

A kinetic study was conducted fitting the concentration-time profile data obtained from the phenol hydroxylation reactions, and rate constants were determined using initial reaction rates.

The hydroxylation of phenol to dihydroxybenzenes can be expressed by the following independent reactions:

$$\underset{\text{phenol}}{C_6H_5OH} + \underset{\text{peroxide}}{H_2O_2} \xrightarrow{k_{hyroquinone}} \underset{\text{hydroquinone}}{C_6H_4(OH)_2} + H_2O \qquad \text{(Reaction 1)}$$

$$\underset{\text{phenol}}{C_6H_5OH} + \underset{\text{peroxide}}{H_2O_2} \xrightarrow{k_{catechol}} \underset{\text{catechol}}{C_6H_6O_2} + H_2O \qquad \text{(Reaction 2)}$$

Hydrogen peroxide also undergoes a non-selective decay/decomposition in the presence of light according to the following reaction (presumably second order):

$$H_2O_2 \xrightarrow{uv} 2 \cdot H_2O + O_2$$

However, for the purpose of modelling the data, the hydrogen peroxide was assumed to be reacting only with phenol to form hydroquinone and catechol, since in the presence of phenol, which blocks access to the catalyst surface, these reactions are inhibited.

Assuming that the reaction can be modelled by an overall second-order kinetic expression with first-order dependency on both phenol and hydrogen peroxide, the kinetic reaction rate law expressions for reactants and products are:

$$-r''_{Ph} = \frac{1}{S_T} \cdot \frac{dC_{Ph}}{dt} = k_{Ph} \cdot C_{Ph} \cdot C_{Ox} \qquad [4.13]$$

$$r''_{C} = \frac{1}{S_T} \cdot \frac{dC_{C}}{dt} = k_{C} \cdot C_{Ph} \cdot C_{Ox} \qquad [4.14]$$

$$r''_{Hq} = \frac{1}{S_T} \cdot \frac{dC_{H}}{dt} = k_{Hq} \cdot C_{Ph} \cdot C_{Ox} \qquad [4.15]$$

$$-r''_{Ox} = \frac{1}{S_T} \cdot \frac{dC_{Ox}}{dt} = -k_{Ph} \cdot C_{Ph} \cdot C_{Ox} \qquad [4.16]$$

Where r_i" = Rate of consumption/generation per unit external surface area of catalyst [mmol/s.m^2],
C_i = Concentration of species i [mmol/dm^3],
k_i = Reaction rate constant [dm^3/(mmol.m^2.s)],
t = Time [s], and
S_T = Total external surface area of catalyst [m^2].

The following symbols are used to identify the reactants and products:

Ph = Phenol
Ox = Oxidant (hydrogen peroxide)
C = Catechol, and
Hq = Hydroquinone

The differential form of the design equation for the batch reactor, written in terms of the conversion of phenol, is described by:

$$N_{ph,0} \cdot \frac{dX_{Ph}}{dt} = -r_{Ph} \cdot V \qquad [4.17]$$

For the liquid-phase reaction, where the reactor volume remains constant, the design equation can be expressed as:

$$-r_{Ph} = C_{ph,0} \cdot \frac{dX_{Ph}}{dt} \qquad [4.18]$$

For the irreversible liquid-phase reaction, the rate law is given by:

$$-r_{Ph} = k_{Ph} \cdot C_{Ph,t} \cdot C_{Ox,t} \qquad [4.19]$$

The phenol and hydrogen peroxide concentrations at time t can be expressed in terms of the phenol conversion, and initial phenol concentration ($C_{Ph,0}$) and molar ratio of hydrogen peroxide to phenol (θ_{Ox}) at the start of the reaction:

$$C_{ph,t} = C_{ph,0} \cdot (1 - X_{ph}) \qquad [4.20]$$

$$C_{Ox,t} = C_{ph,0} \cdot (\theta_{Ox} - X_{ph}) \qquad [4.21]$$

Substituting these concentrations into the phenol rate expression, the rate law for phenol consumption can be rewritten as:

$$-r_{Ph} = k_{Ph} \cdot C_{ph,0}^{2} \cdot (1 - X_{ph}) \cdot (\theta_{Ox} - X_{Ph}) \quad [4.22]$$

Substituting into equation [4.18], the design equation for the batch reactor, written in terms of the phenol conversion, can be expressed as:

$$\frac{dX_{Ph}}{dt} = k_{Ph} \cdot C_{Ph,0} \cdot (1 - X_{Ph}) \cdot (\theta_{Ox} - X_{Ph}) \quad [4.23]$$

Solving this equation for the conversion term, X_{Ph}, gives the following expression:

$$\frac{dX_{Ph}}{(1 - X_{Ph}) \cdot (\theta_{Ox} - X_{Ph})} = k_{Ph} \cdot C_{Ph,0} \cdot dt \quad [4.24]$$

Integrating over the boundaries t_1 and t_2 gives the following equation:

$$\frac{1}{(\theta_{Ox} - 1)} \cdot \ln \frac{\theta_{Ox} - X_{Ph}}{\theta_{Ox} \cdot (1 - X_{Ph})}\Bigg|_{X_{t1}}^{X_{t2}} = k_{Ph} \cdot C_{Ph,0} \cdot (t_2 - t_1) \quad [4.25]$$

Raising the exponent, gives:

$$\frac{\theta_{Ox} - X_{Ph}}{\theta_{Ox} \cdot (1 - X_{Ph})} = \exp\left[k_{Ph} \cdot C_{Ph,0} \cdot \Delta t \cdot (\theta_{Ox} - 1)\right] \quad [4.26]$$

Rearranging, and solving for X_{Ph}, yields the following expression after simplification:

$$X_{Ph} = \frac{\theta_{Ox} \cdot \left(1 - \exp\left[k_{Ph} \cdot C_{Ph,0} \cdot \Delta t \cdot (\theta_{Ox} - 1)\right]\right)}{1 - \theta_{Ox} \cdot \exp\left[k_{Ph} \cdot C_{Ph,0} \cdot \Delta t \cdot (\theta_{Ox} - 1)\right]} \quad [4.27]$$

Using equation [4.27], together with equation [4.20], it is possible to calculate a theoretical phenol concentration at every time t.

The rate constant for phenol consumption is then found by solving to minimise the error between the theoretical and measured concentrations, by changing the value of the rate constant.

Non-linear least-squares regression was used to determine the rate constant for phenol consumption. Solver® in Microsoft Excel was used, and the sum of squares of the differences between the phenol conversion calculated from experimental data and the model theoretical conversion was minimised by varying the rate constant. The rate constant was constrained to be greater than zero.

The catechol and hydroquinone formation rate constants were calculated numerically using equations [4.14] and [4.15] respectively. The derivatives were calculated by taking the value of dC/dt to be the straight-line gradient between two consecutive concentration points, at the time halfway between the times of the individual points. Average phenol and hydrogen peroxide concentrations at this average interval time were calculated by interpolation. Thus, rate constants for each data pair were calculated, and the average of these taken as the overall rate constant for the particular experimental run.

Subsequent over-oxidation of hydroquinone and catechol to high-molecular compounds (tars) was accounted for, and the rate constant representing tar formation was obtained by subtracting the rate constants for hydroquinone and catechol formation from the phenol consumption rate constant:

$$k_{Tars} = k_{Ph} - k_{Hq} - k_{C} \qquad [4.28]$$

The rate constants presented in the following sections are calculated relative to the total BET surface area of the catalysts. The BET surface area of the Al-free Ti-Beta and TS-1 catalysts samples used are 574 m^2/g and 442 m^2/g respectively.

5 Results and Discussion

5.1 Physical and Chemical Catalyst Characterisation

5.1.1 Zeolite Beta Seeds

After 72-90 hours at the crystallisation temperature, zeolite Al-Beta seeds were obtained in moderate yield; approximately 22.5 ± 0.2 g of solid zeolite (washed and dried) per 100 g of the initial reaction gel mixture was obtained, with Si/Al = *ca.* 18.4, and amounting to an approximately 51 % incorporation of silica into the zeolite (90% on inorganic oxides and aluminium), after 90 hours. This is in accordance with Blasco *et al.* (1998), who synthesised seeds with a Si/Al ratio of *ca.* 21.

Only a marginally decreased amount of zeolite was produced at the shorter crystallisation time of 72 hours (*ca.* 17.6 g per 100 g gel), whilst the crystallinity of the recovered solids remains unchanged. This is in agreement with the crystallisation kinetics data obtained by Camblor *et al.* (1997) for the synthesis of nanocrystalline zeolite Beta from a gel with an initial Si/Al molar ratio of 25 (the same as for the synthesis gel used in this work). These authors noted that once the maximum yield of Beta was produced the system was very stable for extended periods of time at the crystallisation temperature, and the yield of the zeolite, its crystallinity and its chemical composition, as well as the physical properties of the colloidal suspension obtained, were not affected.

It is worth mentioning that recovery of the crystals from the colloidal suspension at the end of crystallisation by high-speed centrifuging (18 000 rpm, 90 min) was only effective if water was added to the suspension prior to centrifuging. This water addition had the effect of lowering the viscosity of the solution and the pH (from *ca.* 12 to near-neutral), and also allowed for recovery at a lower centrifuging speed (10 000 rpm), which is a definite advantage. Without water addition, solid yields were very low (equivalent of 2.33 g per 100 g starting mixture), which was attributed to too viscous a suspension for coagulation and precipitation of the suspended particles.

Dealumination of the Al-seeds (with one acid leaching treatment) led to an approximate 18 wt-% loss from the seeds after washing and drying, giving an overall yield of 18.6 ± 0.5 g solid Al-free Ti-Beta seeds per 100 g of the initial batch synthesis gel mixture. After two successive leaching treatments an overall equivalent yield of 17.5 ± 0.5 g dealuminated seeds per 100 g synthesis gel was obtained. The final Si/Al ratio of the seeds increased to

231 for a single dealumination (from 25 in the synthesis gel), and to 369 after two treatments. Thus, even though the strength of the acid did not change from the first to the second leaching treatment, the amount of aluminium extracted from the framework was still approximately 1.5 times higher, confirming that a series of treatments is effective in achieving dealumination, without significantly impacting the crystal structure (crystallinity of the seeds is discussed later in this section). While a stronger acid solution (≥ 20 M) could be used to obtain a higher degree of dealumination in a more severe subsequent treatment, it is widely known that too severe a treatment can impact negatively on the crystal structure resulting in reduced crystallinity, porous volume and thermal stability (Fajula, F.*, et al.*, 1994; Taylor, B., 2004); thus, dealumination using nitric acid is typically done with concentrations below 15 M, as was done in this study.

The crystal size of the seeds has been estimated from SEM and TEM micrographs. The crystal size is very small and the crystallites tend to aggregate, making it difficult to get an accurate crystal size distribution. While literature data (Blasco, T.*, et al.*, 1998) reports that the seeds have an average crystal size of *ca.* 30-50 nm, the seeds synthesised here were considerably smaller (*ca.* 15 nm). Beta seeds synthesised on different occasions from fresh silica sources all gave these smaller crystallites. It is possible that by increasing the crystallisation time further larger seeds could be obtained, though this needs to be confirmed. The smaller than desired size of these seeds could be responsible for the poor crystallisation of the Al-free Ti-Beta catalyst (see *Section 5.1.2*). This would suggest that 30 nm is the critical size of seeds for Al-free Ti-Beta to grow over, and that the smaller 15 nm seeds might not be sufficiently large to promote the growth and nucleation of Al-free Ti-Beta and accelerate its formation.

Figure 5.1 shows a typical SEM micrograph of the zeolite Beta seed crystals. There is a significant amount of intergrowth, as illustrated by the rough and irregular edges, which suggests that the crystals are not individual but agglomerates of smaller crystallites. The average size of these larger agglomerates is estimated to be in the range 1-3 μm.

TEM analysis confirms the nanoscale size of these particles. While the bulk of the material is 15 nm particles, irregularly shaped particles ranging in size from *ca.* 1-3 μm are also observed. The edges are coarse and uneven, and closer examination reveals that very small 11-15 nm round-shaped particles aggregate to form these larger clusters. The TEM micrograph in Figure 5.2 illustrates this.

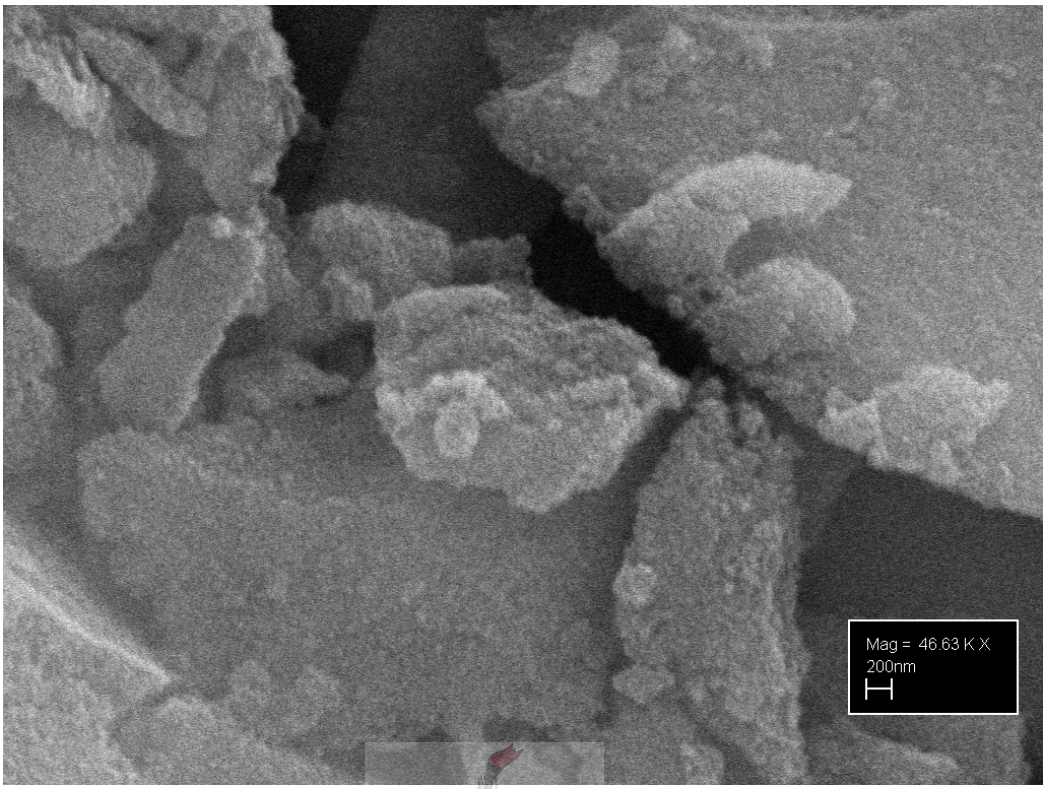

Figure 5.1: SEM micrograph of dealuminated (Si/Al=370) zeolite Beta seed agglomerates (scale bar represents 200 nm)

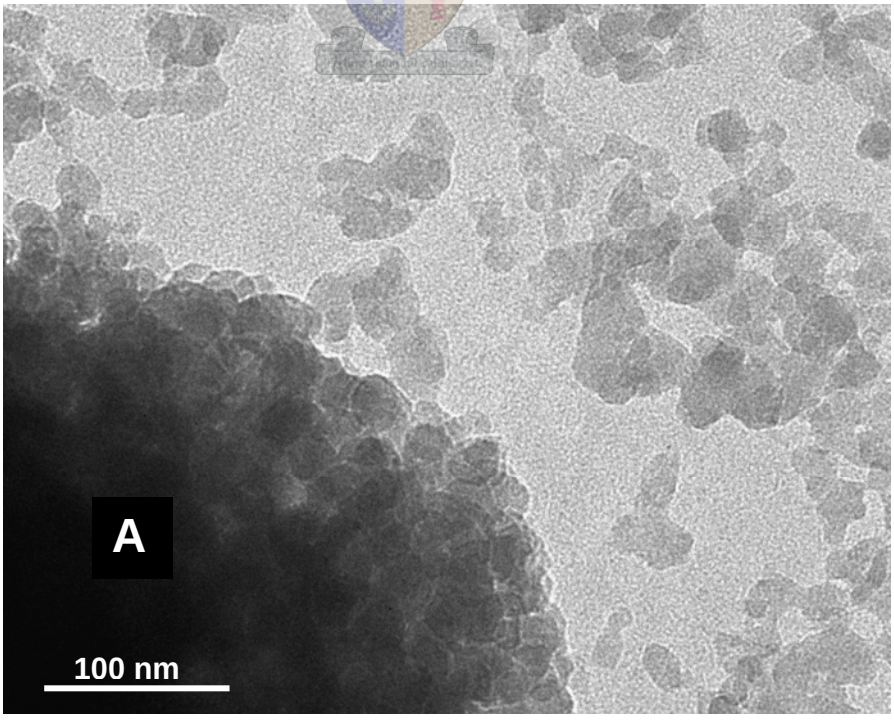

Figure 5.2: TEM micrograph of zeolite Beta seeds, depicting the individual seeds and a crystallite agglomerate (denoted "A") (scale bar represents 100 nm)

The X-ray diffraction patterns of the as-synthesised solid zeolite Al-Beta seeds correspond well with those obtained by Newsam *et al.* (1998), Higgins *et al.* (1998) and Camblor *et al.* (1991; 1991), and show the typical structural features of zeolite Beta with sharp and broad reflections characteristic of an intergrowth of different polymorphs. The samples exhibit all peaks characteristic of the Beta zeolite material, with intense diffraction peaks at 2θ = 7.5° and 2θ = 22.4°, typical of the Beta phase (see Figure 11.1, APPENDIX C). The position of these peaks and their relative intensities compared to the reference confirms that the material synthesised belongs to the Beta crystalline phase, and no other competing phases can be identified. The broad "hump" observed in the low-angle range 11 to 14° 2θ is due to the influence of the perspex sample-holder, and not amorphous material present in the sample scanned. This was confirmed when it was found that if an aluminium sample-holder was used this peak is absent.

Diffraction patterns of the dealuminated Beta seeds show similar peaks to that of standard zeolite Beta (reference) and the as-synthesised Al-Beta, although marginally less intense. The position of the main peaks did not change significantly upon acid leaching. This would suggest that there was a minimal loss in crystallinity upon acid leaching with concentrated HNO_3 to selectively remove aluminium from the zeolite framework and on the external surface area, and that the parent and modified (dealuminated) materials are identical in phase. From a crystallinity and phase point of view, the XRD patterns indicate that acid leaching has no marked detrimental effect on the structure of the Beta zeolite. Figure 5.3 illustrates typical XRD diffraction patterns obtained for the parent and dealuminated Beta seeds. An XRD pattern of the dealuminated material after two successive acid treatments is included in APPENDIX C (see Figure 11.1).

Pectora roborant cultus recti

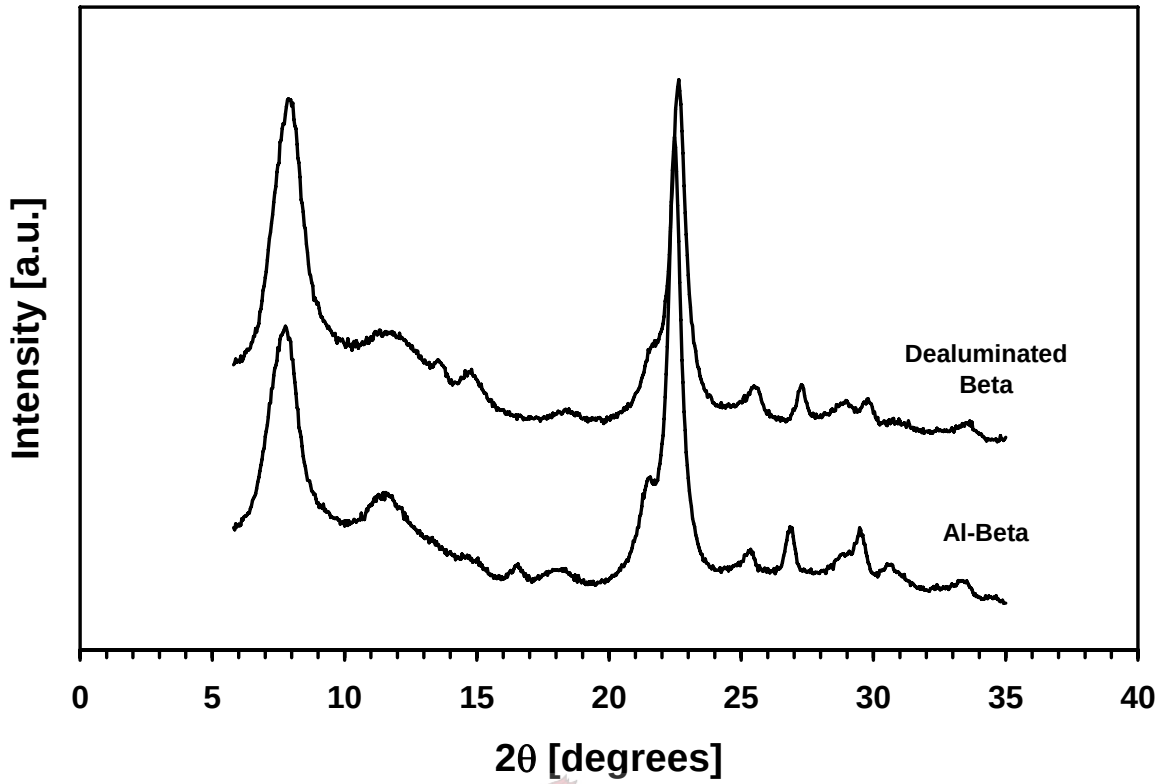

Figure 5.3: XRD diffraction pattern of as-synthesised (Al)-Beta (bottom) and dealuminated Beta seeds

5.1.2 Al-free Ti-Beta

After 5-6 days at the crystallisation temperature, zeolite Al-free Ti-Beta was obtained in moderately high yield; approximately 31.8 ± 0.1 g of solid (after washing and drying) were obtained per 100 g of the initial reaction mixture charged to the autoclaves.

Taking into account a further 15.15 % mass loss upon calcinations at 400 °C, this translates into a yield of approximately 27.0 ± 0.1 g of solid zeolite per 100 g of initial gel mixture.

Chemical analysis of the calcined material reveals that the total Si/Ti molar ratio is 53.

It is, however, felt that the material synthesised here is not completely crystallised Al-free Ti-Beta, for a number of reasons.

Nitrogen adsorption measurements on catalyst samples synthesised on different occasions, and from fresh silica sources, give a total BET area of 380-404 m^2/g, a micropore volume of 0.0989-0.114 cm^3/g and an external surface area of 151.65-163 m^2/g. The external surface area is much higher than reported by Wilkenhöner *et al.* ((2001) (8 m^2/g), and only *ca.* 62% of the total surface area is located in the pores of the crystals, compared to 98% for

Wilkenhöner's samples. Thus, these samples would appear to have incompletely developed pore systems, which could, amongst others, be due to too short a crystallisation time.

SEM and TEM imaging results show that the bulk of the material is composed of small 25 nm crystallites, which agglomerate to form larger crystals. The edges of these larger crystals are not well-defined, and there is intergrowth between them indicative of their nanoparticle, clustered make-up. A few of the truncated square bipyramids expected to crystallise were identified, although they were not very well-faceted, and had irregular edges. Those that were identified were approximately 2 μm in size. A TEM micrograph such a crystallite is included in APPENDIX C (see Figure 11.2)

XRD patterns of the samples are poorly resolved, and the only significant peak observed is that at 2θ=22.4°, which suggests that the material is not fully crystallised Beta.

Characterisation experiments on different catalyst batches confirm the poor Beta nature of the synthesised material; low phenol conversions to hydroquinone and catechol, (X_{Phenol} < 2 mol-%), as well as low peroxide conversions ($X_{peroxide}$ < 30 mol-%), were obtained. Rapid catalyst deactivation, as indicated by a significant amount of coke/tar formation early on in the reaction, would point to poor catalyst durability and explain the low conversions attained.

Consequently, only well-synthesised and characterised Al-free Ti-Beta catalyst (previously synthesised at the Catalysis Research Unit in the Department of Chemical Engineering, UCT, $d_{crystal} \approx 1$ μm) was used in all reactions performed.

5.2 Batch Phenol Hydroxylation

Analysis of the aliquots taken through the course of the reactions was done using HPLC, and the evaluation of this data is explained in *Section 10.1.2* (see APPENDIX B). A typical chromatogram obtained from analysis of the reaction mixture can be seen in Figure 10.1, and a typical concentration profile of the reactants and products constructed from this data is shown in Figure 12.1 (see APPENDIX D).

5.2.1 Al-free Ti-Beta

The results for the phenol conversion over Al-free Ti-Beta, plotted as a function of the reaction time for different starting hydrogen peroxide volumetric fractions, are shown in Figure 5.4 (water solvent) and Figure 5.5 (methanol solvent).

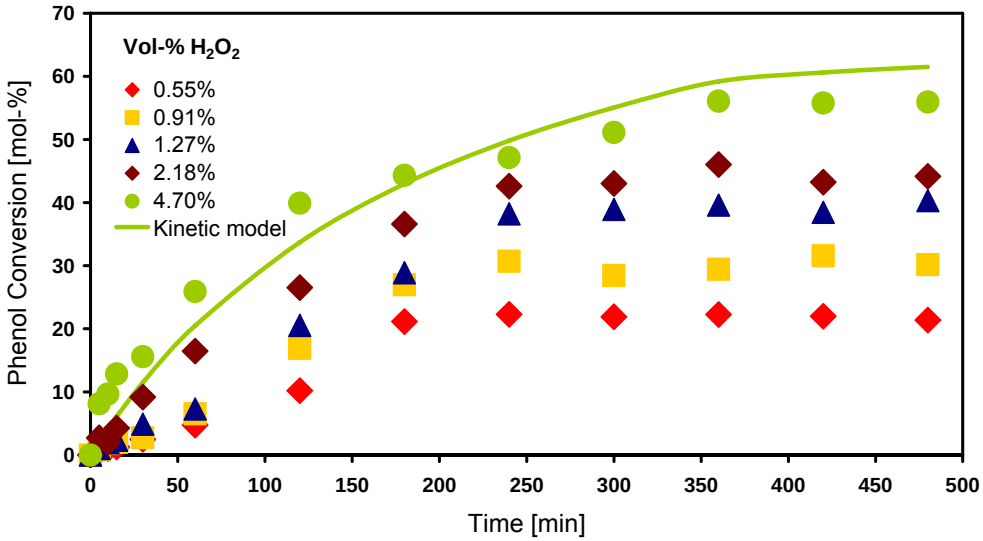

Figure 5.4: Phenol conversion vs. reaction time for different initial volumetric fractions of hydrogen peroxide in water solvent over Al-free Ti-Beta

Catalyst: Al-free Ti-β; $m_{catalyst}$ = 0.12 g; m_{phenol} = 1.2 g; T_R = 60 °C; Solvent: water; V_{total} = 5.5 ml

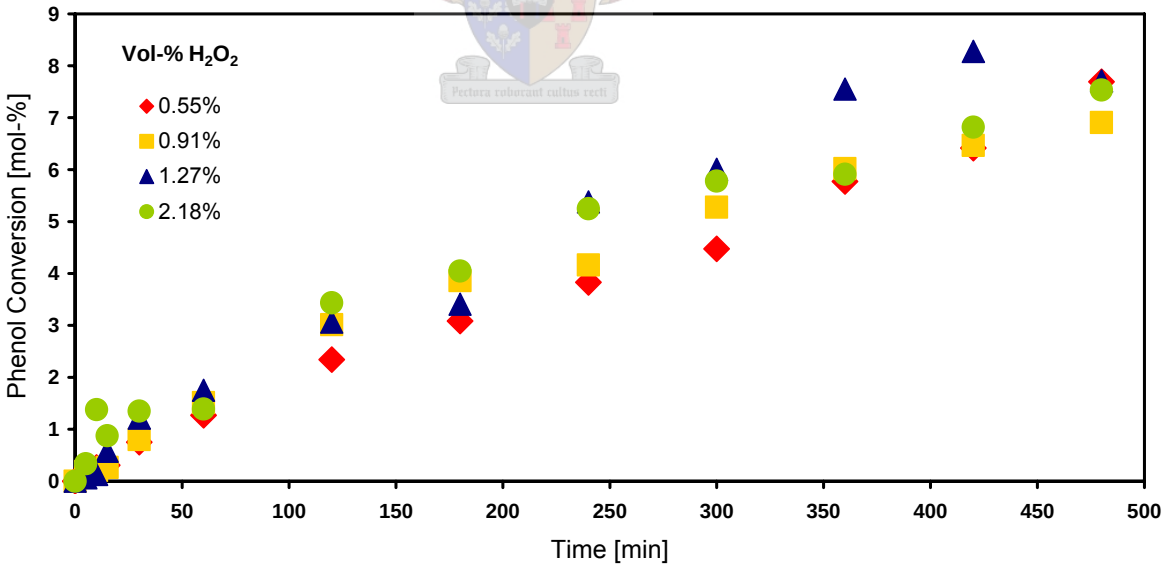

Figure 5.5: Phenol conversion vs. reaction time for different initial volumetric fractions of hydrogen peroxide in methanol solvent over Al-free Ti-Beta

Catalyst: Al-free Ti-β; $m_{catalyst}$ = 0.12 g; m_{phenol} = 1.2 g; T_R = 60 °C; Solvent: methanol; V_{total} = 5.5 ml

It is apparent that the phenol conversion increases with time in both water and methanol solvent media, but that peroxide concentration effects are more evident when water is used as the solvent.

The effect of initial peroxide concentration on the rate and degree of phenol conversion is more pronounced in water; increasing the initial peroxide concentration enhanced the phenol conversion, and considerably higher conversions are achieved than in methanol for equivalent starting peroxide concentrations; the lowest overall conversion reached in water solvent (*ca.* 21 mol-% with an initial peroxide concentration of 0.55 vol-%) exceeds even the highest conversion achieved in methanol with the highest initial peroxide concentration (*ca.* 7.5 mol-% at 2.18 vol-% initial peroxide concentration). The terminal phenol conversion obtained with an initial peroxide concentration of 4.70 vol-% is close to the maximum, although a marginal improvement in phenol conversion could be obtained with the maximum initial hydrogen peroxide concentration possible in this work (5.04 vol-%); the theoretical conversion with an initial peroxide concentration of 5.04 vol-% is 65.4 mol-% after complete reaction, compared to the 61.5 mol-% for an initial concentration of 4.70 vol-%.

The improved conversion in water solvent can be attributed to the peroxide itself, since the solvent contains no methanol and there are thus no competitive adsorption effects occurring between methanol and the other reactants at the reactive sites. Furthermore, the volumetric fraction of water changes insignificantly from *ca.* 99.5 to 97.5 vol-% as the quantity of peroxide solution is increased. Thus, it is proposed that with higher peroxide volumetric fractions present in the solution there is an increased amount of peroxide interaction with the titanium sites to give a greater number of Ti-hydroperoxo active sites that are available for phenol co-ordination and oxidation. Hence the higher phenol conversions obtained. The higher phenol conversion obtained at the start of the reaction when the initial peroxide concentration is higher supports this; at an initial peroxide concentration of 4.70 vol-% the phenol conversion within 1 hour is already *ca.* 26 mol-%, compared to only *ca.* 5 mol-% for an initial concentration of 0.55 vol-%.

The changes in phenol conversion with the volumetric fraction of peroxide in methanol solvent are more interesting, and are observed to be largely independent of peroxide concentration. Although lower conversions than in water are expected – due to the lower polarity of methanol meaning that phenol is not driven as strongly into the pores as in the case of water – it is interesting that the conversion remains largely unchanged, which suggests a possible zero-order dependence on peroxide concentration. The answer to the unchanging activity lies in the fact that there is insufficient water present in the reaction system. The water fraction changes from 2.24 vol-% to 8.96 vol-% (bulk volume still

methanol) as more aqueous peroxide solution is used, and from previous work it was seen that the fraction of water must increase to above at least 60-70 vol-% for there to be any positive influence on the phenol rate constant and level of phenol conversion (Callanan, L. H., *et al.*, 2004). Thus, the observations made are consistent with the previous findings.

The effect of peroxide concentration on the selectivity for hydroquinone formation is shown in Figure 5.6 (water solvent) and Figure 5.7 (methanol solvent), as a function of phenol conversion for different initial hydrogen peroxide volumetric fractions. As seen in previous work, it is expected that the hydroquinone selectivity would increase with phenol conversion, regardless of the solvent. This effect seems more pronounced with higher peroxide concentrations, and it is also clear that a higher hydroquinone-to-catechol ratio is achieved in methanol solvent at higher peroxide concentrations than when using water solvent (as to be expected, mechanistic explanation given in *Section 5.2.1.3*).

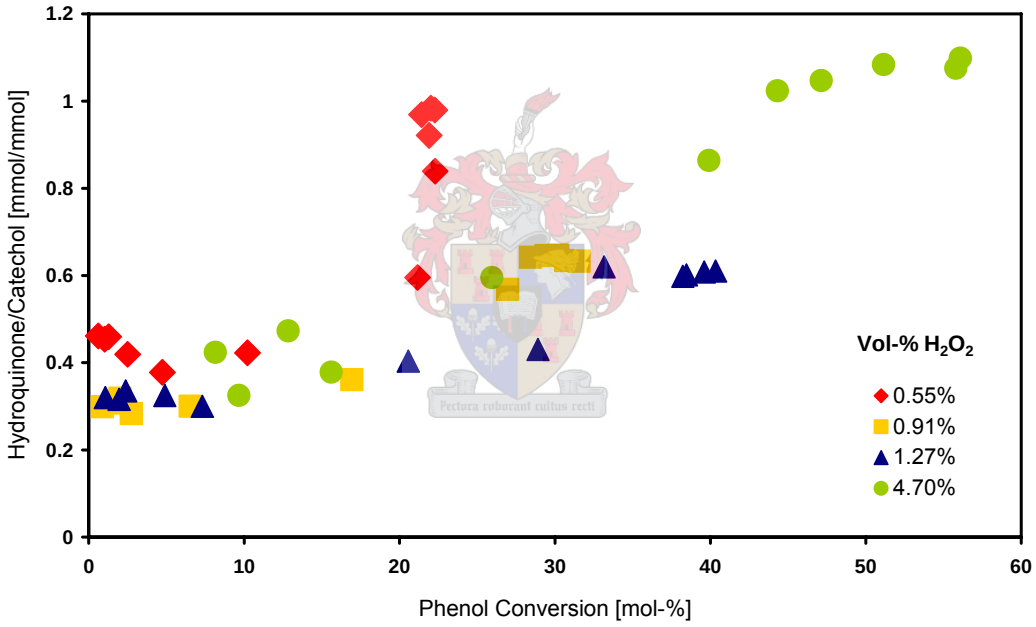

Figure 5.6: Hydroquinone selectivity as a function of phenol conversion for different initial volumetric fractions of hydrogen peroxide in water solvent over Al-free Ti-Beta

Catalyst: Al-free Ti-β; $m_{catalyst}$ = 0.12 g; m_{phenol} = 1.2 g; T_R = 60 °C; Solvent: water; V_{total} = 5.5 ml

While in water the selectivity to hydroquinone increases with phenol conversion regardless of the initial peroxide concentration, it never increases beyond a value of approximately 1.1 even at maximum phenol conversion. Thus, catechol is still the preferred product when using water as a solvent, even when peroxide concentrations are increased.

In comparison, when methanol is used as the solvent higher hydroquinone selectivities are achieved (p/o-ratio ≥ 1), even at low phenol conversions with the lowest initial peroxide concentration. Thus, methanol offers enhanced selectivity for hydroquinone production and should therefore be present in the reaction system for there to be a positive influence on the reaction selectivity for hydroquinone. As the initial peroxide concentration is increased to 2.18 vol-% the selectivity increases more significantly.

If the hydroquinone-to-catechol ratio is estimated by fitting the data in Figure 5.6 and Figure 5.7 at a fixed level of phenol conversion, the hydroquinone selectivity can be plotted as a function of the initial peroxide volumetric fraction. Figure 5.8 shows the hydroquinone selectivity in water solvent (fitted at X_{Phenol} = 10%) and Figure 5.9 the hydroquinone selectivity in methanol solvent (fitted at X_{Phenol} = 7%, the highest common conversion for all peroxide concentrations).

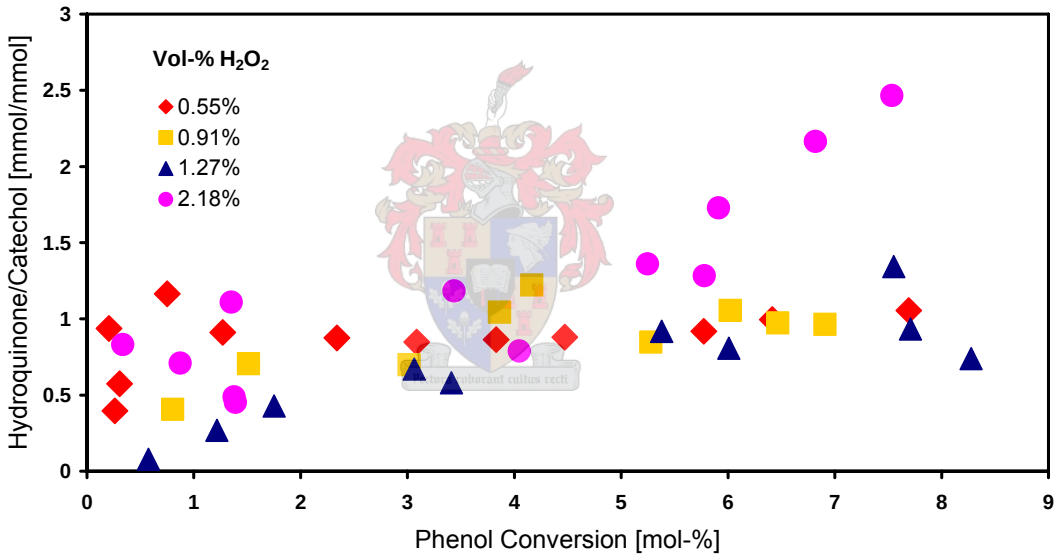

Figure 5.7: Hydroquinone selectivity as a function of phenol conversion for different initial volumetric fractions of hydrogen peroxide in methanol solvent over Al-free Ti-Beta

Catalyst: Al-free Ti-β; $m_{catalyst}$ = 0.12 g; m_{phenol} = 1.2 g; T_R = 60 °C; Solvent: methanol; V_{total} = 5.5 ml

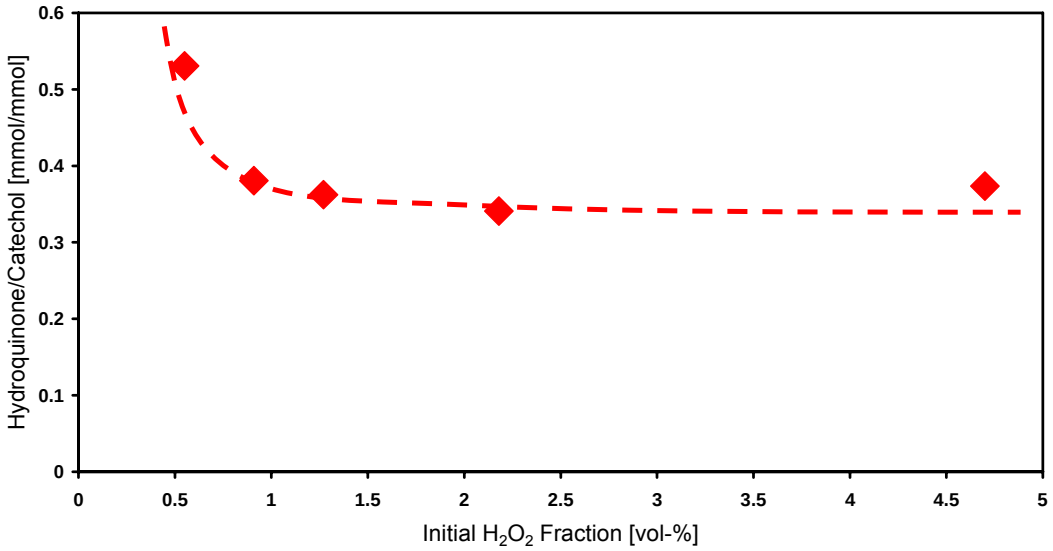

Figure 5.8: Ratio of hydroquinone-to-catechol formed at 10% phenol conversion in water solvent for varying initial hydrogen peroxide volumetric fractions

Catalyst: Al-free Ti-β; $m_{catalyst}$ = 0.12 g; m_{phenol} = 1.2 g; T_R = 60 °C; Solvent: water; V_{total} = 5.5 ml

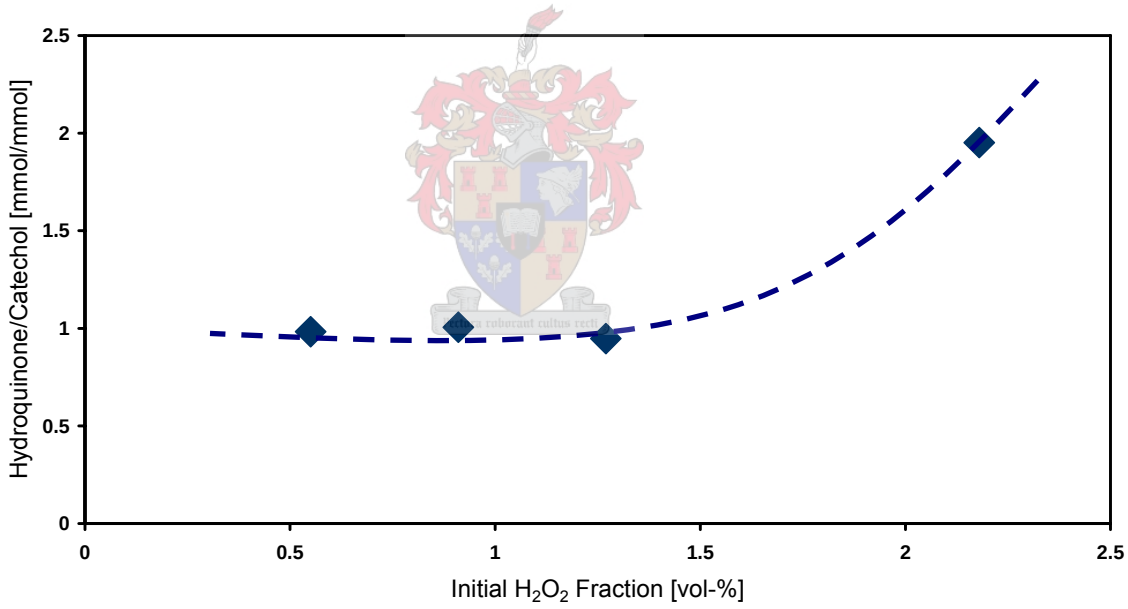

Figure 5.9: Ratio of hydroquinone-to-catechol formed at 7% phenol conversion in water solvent for varying initial hydrogen peroxide volumetric fractions

Catalyst: Al-free Ti-β; $m_{catalyst}$ = 0.12 g; m_{phenol} = 1.2 g; T_R = 60 °C; Solvent: methanol; V_{total} = 5.5 ml

It is apparent that the effect of peroxide concentration on the selectivity towards hydroquinone is opposite in water and methanol solvents, and that in each solvent 1.27 vol-% hydrogen peroxide appears to be a threshold concentration. In water, increasing the peroxide fraction above 1.27 vol-% results in unchanging selectivity (*ca.* 0.35); below this concentration a maximum selectivity ratio of 0.53 is obtained, which is approaching the

statistical distribution and confirms that shape-selectivity effects are less restrictive in the Beta pores. In methanol solvent, hydroquinone selectivity is significantly enhanced as the peroxide concentration increases above 1.27 vol-% (the p/o-ratio increases to *ca.* 2); for peroxide fractions below this threshold concentration, it appears that equal amounts of catechol and hydroquinone are formed (p/o-ratio *ca.* 1).

Previous work by Callanan *et al.* (2004) investigating the influence of solvent composition for varying water fractions, postulated that water should constitute less than *ca.* 30 vol-% of the reaction volume to have any significant influence on increasing hydroquinone selectivity (p/o-ratio > 1). For water fractions above 60 vol-% a ratio of *ca.* 0.5 was observed (at 10% phenol conversion). The peroxide concentration, however, remained constant at 2.10 vol-% as the solvent composition varied, and methanol always constituted a part of the solvent, so direct comparison with the current work done here (where both peroxide and water concentrations change simultaneously) is difficult; however, as the water fraction is increased the hydroquinone selectivity is still seen to decrease. With methanol solvent, and an initial peroxide concentration of 2.18 vol-%, water constitutes an equivalent 8.96 vol-% of the initial reaction volume, and a p/o-ratio of 1.95 is obtained (X_{Phenol} = 7%), which compares favourably with a selectivity of *ca.* 1.65 (X_{Phenol} = 8%) obtained by Callanan *et al.* (2004).

5.2.1.1 Kinetics and Rate Fitting

Phenol rate constants were calculated by solving the differential equation obtained after fitting the concentration-time data to an overall second-order rate equation.

The fit of the conversion estimated with the model to the experimental data is important, because one wants an accurate rate constant that fits the experimental data well. It was seen that if the phenol conversion was modeled over the initial 2 hours of the reaction (i.e. obtaining a rate constant by least-squares regression of the experimental and theoretical phenol conversion over those data points up to 2 hours reaction only), while a very close and accurate fit was obtained at the shorter reaction times, the model gave a poor fit at extended reaction times. Fitting the data over the complete 12 hours of reaction gave a slightly more reasonable kinetic fit over *all* conversion points, and was thus considered more accurate. A comparison between the two is shown in Figure 5.10 for an initial peroxide concentration of 4.70 vol-%.

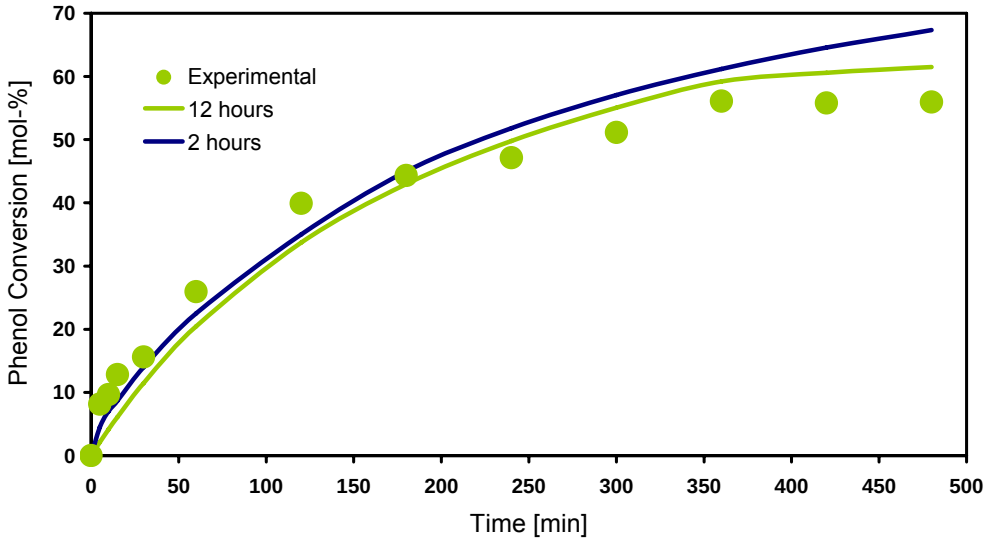

Figure 5.10: Comparison between the theoretical phenol conversions obtained by fitting the model over the initial 2 hours and total 12 hours reaction for the hydroxylation reaction over Al-free Ti-Beta in water solvent

Catalyst: Al-free Ti-β; $m_{catalyst}$ = 0.12 g; m_{phenol} = 1.2 g; T_R = 60 °C; Solvent: water; V_{total} = 5.5 ml

The rate constants calculated for phenol consumption, and hydroquinone, catechol and tar formation are summarised in Table 5.1 for the different experiments using water as a solvent.

Table 5.1: Influence of initial hydrogen peroxide concentration on the observed rate constants for phenol hydroxylation in water solvent over Al-free Ti-Beta[1]

H_2O_2 concentration	k_{Phenol}	$k_{Hydroquinone}$	$k_{Catechol}$	k_{Tars}
[vol-%]	[$dm^3/mmol.m^2.s$]			
0.55	2.036×10^{-9}	2.860×10^{-10}	3.445×10^{-10}	1.406×10^{-9}
0.91	2.202×10^{-9}	6.242×10^{-10}	7.939×10^{-10}	7.832×10^{-10}
1.27	2.067×10^{-9}	6.422×10^{-10}	9.551×10^{-10}	4.690×10^{-10}
2.18	1.702×10^{-9}	3.291×10^{-10}	6.534×10^{-10}	7.198×10^{-10}
4.70	1.637×10^{-9}	1.089×10^{-10}	1.349×10^{-10}	1.394×10^{-9}

[1]**Catalyst: Al-free Ti-β; $m_{catalyst}$ = 0.12 g; m_{phenol} = 1.2 g; T_R = 60 °C; Solvent: water; V_{total} = 5.5 ml**

The rate constant for phenol consumption, k_{Phenol}, is largely independent of changing peroxide concentration, and is averaged to a value of 1.93×10^{-9} $dm^3/mmol.m^2.s$. This constant value suggests that the model fitted is indeed correct, because the rate constant should not depend on the reactant concentration. For comparison, when pure water solvent

was used and the peroxide concentration was fixed at 2.10 vol-%, a value of 1.95 x 10^{-9} $dm^3/mmol.m^2.s$ was obtained (Callanan, L. H., *et al.*, 2004).

For reaction in methanol solvent, the concentration-time data was also fitted to an overall second-order kinetic model. Additionally, since the conversion profiles show little change with peroxide concentration, suggesting that it is even questionable whether there is any effect of the peroxide concentration on phenol conversion when methanol is used as the solvent, an overall first-order model was also fitted (i.e. a model independent of hydrogen peroxide concentration was tested to confirm or refute this possibility).

It was found that the second-order model still gave a better overall fit, despite the curves in Figure 5.5 suggesting possible zero-order peroxide concentration dependence. Using an overall first-order model is adequate for predicting phenol conversion when the initial peroxide concentration is low (small volumes of H_2O_2 injected into the reactor), but gives a poor overall fit for higher initial concentrations, and overestimates the final phenol conversion. A comparison between the first-order and second-order kinetic fits of the phenol conversion is included in APPENDIX D (see Figure 12.3) for one such case.

The rate constants calculated for phenol consumption, and hydroquinone, catechol and tar formation are summarised in Table 5.2 for the different experiments using methanol as the solvent.

Table 5.2: Influence of initial hydrogen peroxide concentration on the observed rate constants for phenol hydroxylation in methanol solvent over Al-free Ti-Beta[1]

H_2O_2 concentration	k_{Phenol}	$k_{Hydroquinone}$	$k_{Catechol}$	k_{Tars}
[vol-%]	*[$dm^3/mmol.m^2.s$]*			
0.55	2.803 x 10^{-10}	3.648 x 10^{-11}	3.150 x 10^{-11}	2.122 x 10^{-10}
0.91	1.583 x 10^{-10}	1.968 x 10^{-11}	2.806 x 10^{-11}	1.106 x 10^{-10}
1.27	1.205 x 10^{-10}	2.998 x 10^{-11}	2.918 x 10^{-11}	6.128 x 10^{-11}
2.18	8.982 x 10^{-11}	3.431 x 10^{-11}	3.256 x 10^{-11}	2.296 x 10^{-11}

[1]Catalyst: Al-free Ti-β; $m_{catalyst}$ = 0.12 g; m_{phenol} = 1.2 g; T_R = 60 °C; Solvent: methanol; V_{total} = 5.5 ml

The phenol consumption rate constant for hydroxylation in methanol solvent does not appear to be independent of the peroxide concentration, as was observed for a purely water-based reaction, but decreases slightly with peroxide concentration. This might possibly be due to changing polarity effects in the solvent as more water is added.

5.2.1.2 Tar Analysis

Thermogravimetric analysis on the spent catalyst after reaction was performed to determine the influence of increased peroxide concentrations on the extent of tar formation.

The exact interpretation of the weight loss is difficult since the loss of water is overlapped with the loss of organic compounds. However, assuming that the weight loss below 150 °C is due to weakly adsorbed water, the remaining weight loss can be attributed to the organic material.

An example of the TGA curves for the combustion of the deposited tar on the catalyst with different initial peroxide concentrations is included in APPENDIX D (see Figure 12.6), from which tar formation is determined.

Table 5.3 summarises the quantity of tars deposited on the catalyst surface after 12 hours reaction time.

Table 5.3: Quantity of tar deposited on the surface of Al-free Ti-Beta in the hydroxylation of phenol in water and methanol solvents[1]

H_2O_2 Concentration [vol-%]	Tar formation [$mg/g_{catalyst}$]*	
	Water	*Methanol*
0.55	102.52	64.94
0.91	84.91	76.52
1.27	38.98	99.11
2.18	105.83	103.47
4.70	371.37	

[1]Catalyst: Al-free Ti-β; $m_{catalyst}$ = 0.12 g; m_{phenol} = 1.2 g; T_R = 60 °C; Solvent: water/methanol; V_{total} = 5.5 ml; *total reaction time = 12 hours

As expected, the amount of tar deposition is higher in water solvent since the tar components/precursors are less soluble in this solvent (more polar than methanol). It is particularly evident that for reaction in methanol solvent, low peroxide concentrations limit the amount of tar formation. Tar formation is highest when the initial peroxide concentration is the greatest, which can be accounted for by the higher free-peroxide concentration available for consecutive product oxidation, as well as the increased water concentration that increases the solvent polarity.

5.2.1.3 Mechanistic Implications

The generally enhanced selectivity for hydroquinone in methanol (p/o-ratio ≥ 1) can largely be attributed to steric constraints arising from the co-ordination of methanol to the titanium active intermediate species making it more bulky (Species II, Figure 5.11), and which is enhanced by the higher concentration of active sites formed as the peroxide concentration increases. The increased size of the titanium site significantly narrows the pore channels and imposes additional restrictions on the diffusional path of the approaching phenol molecule within the pores. Thus, an arrangement with the phenolic OH group pointing away from the active centre is favoured, so hydroxylation of the para position occurs, leading to preferential hydroquinone formation.

Lower hydroquinone selectivities in water (p/o-ratio < 0.5) can be explained on the basis of solvent polarity and/or co-ordination of water to the active site (Species I, Figure 5.11).

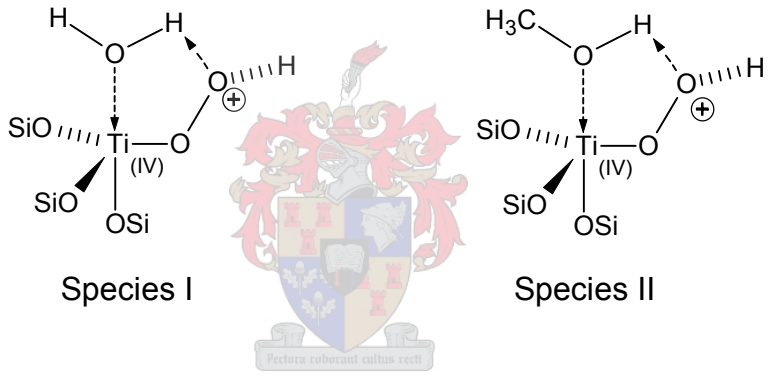

Figure 5.11: Active intermediate species with water (Species I) and methanol (Species II) molecules co-ordinated to the active titanium-hydroperoxo site

The highly polar phenolic OH group would be expected to point towards the hydrophilic titanium centre, favouring electrophilic attack by the terminal OH group of the active intermediate at the ortho position. This is the case in water. Being a stronger polar solvent than methanol, co-ordination of a water molecule to the active site does not occur as readily because it is more strongly excluded from the hydrophobic pore environment. This favoured ortho-hydroxylation is also explained by the Henry's constants for phenol adsorption on Al-free Ti-Beta in water and methanol; the Henry's constant for the adsorption of phenol in pure water is 17.2, compared to 1.3 for the adsorption of phenol from pure methanol. Thus, in water solvent the adsorption of phenol dominates, the pores are maintained in a more phenol-rich environment, and a phenol molecule approaches more easily with its OH group pointing towards the titanium-hydroperoxo group, resulting in ortho-hydroxylation and consequent catechol formation.

Additionally, if water does coordinate to the active site (Species I, Figure 5.11), it is still relatively less bulky than the corresponding methanol-coordinated species with the larger methyl group (Species II, Figure 5.11), so phenol can still approach the active site in a configuration where it is perpendicular to the pore channel and ortho-hydroxylation occurs.

Increasing the initial peroxide concentration by adding more hydrogen peroxide solution causes the hydroquinone selectivity to decrease in water solvent because one is effectively increasing the solvent polarity.

5.2.2 TS-1

Figure 5.12 shows the conversion profiles obtained over TS-1 ($d_{crystal} \approx 0.1$ μm) in methanol solvent for different initial concentrations of hydrogen peroxide.

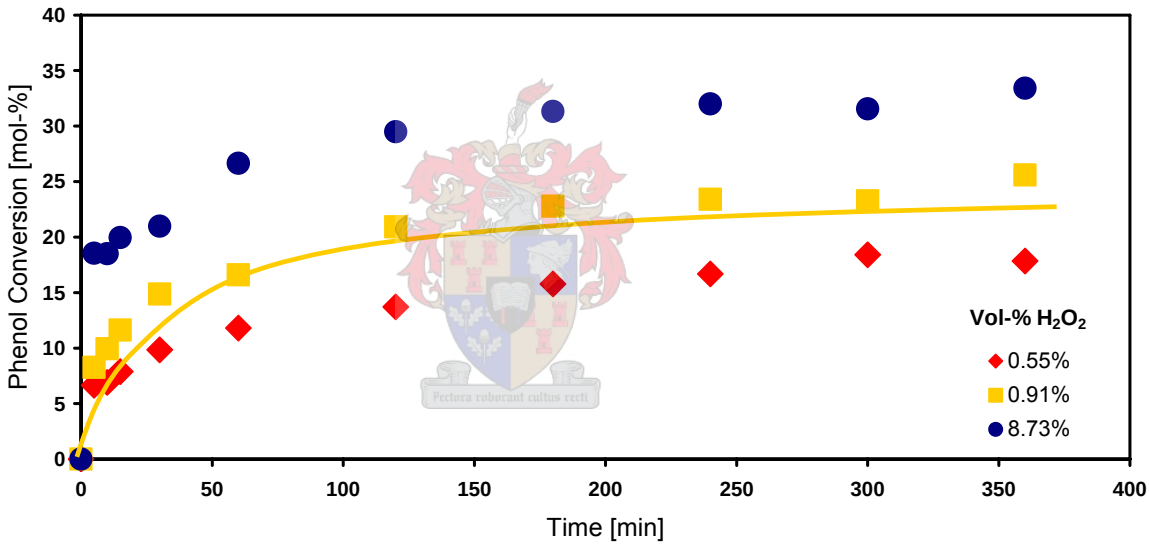

Figure 5.12: Phenol conversion vs. reaction time for different initial volumetric fractions of hydrogen peroxide in methanol solvent over TS-1

Catalyst: TS-1; $m_{catalyst}$ = 0.12 g; m_{phenol} = 1.2 g; T_R = 60 °C; Solvent: methanol; V_{total} = 5.5 ml

Comparing Figure 5.5 and Figure 5.12, phenol conversions in methanol solvent over TS-1 are more significantly influenced by the initial peroxide concentration than over Al-free Ti-Beta; considerably higher conversions are obtained at the same initial peroxide concentration.

From the profiles in Figure 5.12 it is also noteworthy that the phenol is more rapidly converted on TS-1 at short reaction times when the initial peroxide concentration is higher. At

an initial volumetric fraction of 8.73 vol-%, a phenol conversion of *ca.* 20 mol-% is obtained within the first 15 minutes, compared with only *ca.* 8 mol-% at an initial concentration of 0.55 vol-%. This can be attributed to more titanium-hydroperoxo active sites being formed with higher peroxide concentrations, and which are therefore available for phenol co-ordination.

The effect of peroxide concentration on hydroquinone selectivity is illustrated in Figure 5.13 as a function of phenol conversion.

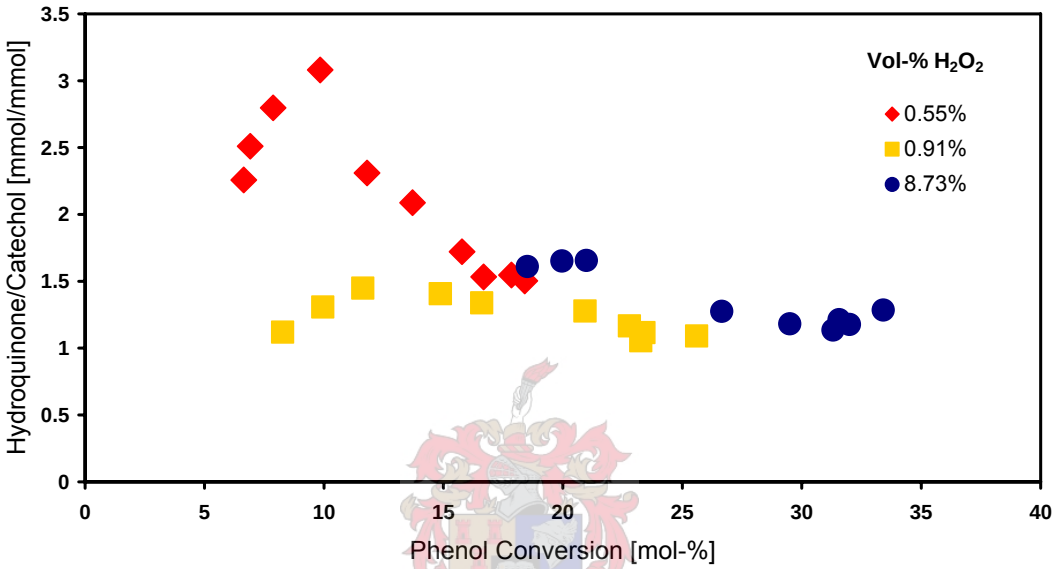

Figure 5.13: Hydroquinone selectivity as a function of phenol conversion for different initial volumetric fractions of hydrogen peroxide in methanol solvent over TS-1

Catalyst: TS-1; $m_{catalyst}$ = 0.12 g; m_{phenol} = 1.2 g; T_R = 60 °C; Solvent: methanol; V_{total} = 5.5 ml

Significantly higher hydroquinone selectivity is obtained with TS-1 than Al-free Ti-Beta, as can be expected. Compared to the large-pore Al-free Ti-Beta (whose micropores are able to accommodate larger molecules and product transition-states like those producing catechol), using TS-1 the reaction is more shape selective due to the more restrictive pore environment where the micropores are only able to accommodate smaller molecules (< 6 Å), and which is amplified by protic solvents. This is particularly evident at the lowest peroxide concentration (0.55 vol-%), where p/o-ratios of up to 3 are obtained. Initial peroxide concentrations above this level do not significantly enhance the product selectivity for hydroquinone, and the selectivity curves for the 0.91 and 8.73 vol-% peroxide fractions are almost identical, except that with higher peroxide concentrations there is a shift to higher phenol conversions.

Particularly interesting is the tendency for the selectivity to initially increase and reach a maximum at lower phenol conversions (and reaction times) and then decrease to an almost

constant and equivalent level at higher conversions for all peroxide concentrations. A selectivity plot as a function of reaction time is included in APPENDIX D (see Figure 12.4), where the maxima in p/o-ratios can clearly be seen occurring within 30 minutes reaction for all peroxide concentrations (although there is a shift to higher phenol conversions as the initial peroxide concentration increases). The initial p/o-ratio increase is most noticeable when less peroxide is used, and a maximum ratio of 3.1 is obtained for 0.55 vol-% peroxide, compared to only *ca.* 1.5 for the 0.91 and 8.73 vol-% cases. This 'rise-decline' trend was also seen by Wilkenhöner (2001), and is unique to phenol hydroxylations in methanol solvent over TS-1; over both TS-1 and Al-free Ti-Beta this effect is not observed using water solvent. No explanation, however, can be found in the literature. This effect will be discussed further when considering the process mechanism in *Section 5.2.2.2*.

5.2.2.1 Kinetics and Rate Fitting

Similarly to the Beta-catalysed reactions, the concentration-time data was fitted to an overall second-order kinetic model to determine the phenol consumption, and hydroquinone, catechol and tar formation rate constants. These rates are summarised in Table 5.4, and it appears that the phenol rate constant (as for reaction on Al-free Ti-Beta) is largely independent of the initial peroxide concentration ($k_{Phenol} \approx 1.36 \times 10^{-8}$ $dm^3/mmol.m^2.s$). Thus, the model accurately models the experimental data.

Table 5.4: Influence of initial hydrogen peroxide concentration on the observed rate constants for phenol hydroxylation in methanol solvent over TS-1[1]

H_2O_2 concentration	k_{Phenol}	$k_{Hydroquinone}$	$k_{Catechol}$	k_{Tars}
[vol-%]	*[$dm^3/mmol.m^2.s$]*			
0.55	1.443×10^{-8}	1.501×10^{-9}	7.666 x 10-^{10}	1.216×10^{-8}
0.91	1.418×10^{-8}	1.237×10^{-9}	1.023×10^{-9}	1.192×10^{-8}
8.73	1.217×10^{-8}	1.064×10^{-10}	6.833×10^{-11}	1.246×10^{-8}

[1]Catalyst: TS-1; $m_{catalyst}$ = 0.12 g; m_{phenol} = 1.2 g; T_R = 60 °C; Solvent: methanol; V_{total} = 5.5 ml

Deposition TGA measurements suggest that tar formation increases with increasing hydrogen peroxide concentration: 60.97, 70.31 and 88.08 mg/$g_{catalyst}$ tar was formed after 12 hours of reaction with the respective initial peroxide concentrations. This is consistent with the greater free peroxide concentration that is available for the over-oxidation of reaction products as the initial peroxide fraction increases, as well an increased water concentration (percentage water in reaction mixture increases as the quantity of peroxide solution increases) that increases the solvent polarity and reduces the solvent's ability to dissolve the

tars (since the tars and precursors are more soluble in pure methanol than water). The higher phenol conversions reached with the highest initial peroxide concentration (8.73 vol-%) are likely the result of the non-selective phenol conversion to tars as opposed to the desired reaction products, since the rate constants for hydroquinone and catechol formation are the lowest and the tar formation rate constant is the highest at this concentration. This is confirmed by the TGA measurements.

5.2.2.2 Mechanistic Implications

Similarly to hydroxylation over the Beta catalyst, it is proposed that with methanol in such large excess at the start of the reaction (up to 97 vol-%) the concentration of methanol relative to hydrogen peroxide in the vicinity of the titanium sites is much higher (a methanol-peroxide ratio of *ca.* 176 when the solution contains 0.55 vol-% peroxide). Thus, the proportion of active sites co-ordinating with methanol to form the larger penta-coordinated active intermediate (Species II, Figure 5.11) is therefore significantly greater than those forming the titanium-hydroperoxo sites alone. Thus, phenol will approach the electrophilic terminal OH group of the titanium-hydroperoxo site with its OH group pointing away towards the zeolite wall, and as a result hydroquinone will be formed. This situation is enhanced by phenol also being hydrogen bonded to methanol solvent molecules, which significantly increases the steric hindrance for ortho-hydroxylation. As a result the hydroquinone selectivity is high. This explains the high p/o-ratio obtained for the case when 0.55 vol-% hydrogen peroxide is used.

At higher initial peroxide concentrations, there is increasingly more water present in the reaction system (constituting a part of the aqueous peroxide solution), and water comprises up to *ca.* 36 vol-% of the total volume for the highest initial peroxide concentration. Therefore, an intermediate with co-ordinated water will also be formed (Species I, Figure 5.11), and due to its smaller size, favour ortho-hydroxylation yielding catechol. This explains why initial selectivities are noticeably lower at higher peroxide fractions. Furthermore, with higher amounts of water present the relative amount of phenol co-ordination increases over that of methanol (since the increased solvent polarity effectively drives more phenol into the pores), so that the reaction rate is higher (as seen in Figure 5.12) but selectivity is lower.

The increased p/o-ratio for low peroxide concentrations can also be partly explained by decreased tar formation on the catalyst early on in the reaction. With less peroxide present, less over-oxidation of the products to tars occurs, which is further enhanced by the high methanol concentration in which the tars are soluble. Therefore, tars do not block the catalyst pores and the shape-selective reaction occurring within them (and promoting the formation of

hydroquinone) occurs relatively unhindered so that the relative amount of hydroquinone formed rapidly increases. The less dramatic 'rise-decline' at higher peroxide fractions has already been explained by the greater amount of free peroxide and water present in the system; the relative amount of tars formed is higher and they are less soluble in the solvent, thereby blocking the pores and hindering hydroquinone formation.

5.3 Peroxide Addition Effects

The influence of the mode of hydrogen peroxide addition in a pseudo semi-batch reactor was also investigated in this work.

Although for a different selective oxidation reaction and different catalysts, the addition of hydrogen peroxide in more discrete amounts has been shown to be advantageous. Fraile *et al.* (2003) showed that in the epoxidation of cyclohexene using dilute hydrogen peroxide as oxidant, the slow addition (over 2.5 and 6 hours) gave improved selectivity to the epoxide, while suppressing side reactions and radical mechanism pathways (oxidation at allylic position, ring opening, epoxide rearrangement), and resulting in a reduced carbon content on the recovered catalyst.

While peroxide concentration effects have been partly investigated by Wilkenhöner *et al.* (2001) for TS-1 using water as a solvent and under dilute conditions (using 30 ml solvent and addition over 35 minutes), no reports were made for Al-free Ti-Beta for different methods of peroxide addition, nor for TS-1 using methanol as solvent.

Previous work done by Wilkenhöner (2001) and Thangaraj *et al.* (1991) showed that higher hydroquinone selectivities and peroxide efficiencies could be achieved on TS-1 using a dropwise addition of H_2O_2 compared with addition in a single portion (p/o-ratio of 1.42 vs. 1.13 respectively at X_{Phenol} = 28%). Using one of the methods of peroxide addition in this current study (0.1 ml per hour), a hydroquinone selectivity of *ca.* 1.30 was obtained in water solvent at a similar phenol conversion, which is close to that obtained by Wilkenhöner (2001). Both these authors, however, gave no indication of *initial* product selectivities (i.e. p/o-ratios at low phenol conversions/short reaction times), or the selectivity as a function of conversion. This is important, and as the results for the batch hydroxylations over TS-1 with different initial peroxide concentrations show, initial selectivities are high and decrease with increasing phenol conversion, particularly when the peroxide concentration is low (see *Section 5.2.2*); this effect was seen again when peroxide was added in more discrete portions.

In this work, aqueous hydrogen peroxide solution was added as discrete amounts at either 0.1 ml per hour or 0.05 ml per half hour from the start of the reaction, and until a total of 0.5 ml solution had been added. A typical concentration-time profile of the reactants and products obtained from such a reaction is included in APPENDIX D (see Figure 12.2).

For reactions over both catalysts higher initial p/o-ratios were obtained in both water and methanol solvents when the peroxide was added in more discrete amounts, which confirms that the formation of hydroquinone is favoured at low hydrogen peroxide concentration levels (see also the discussion in *Section 5.2.2*). This is discussed further in *Section 5.3.1.*

The influence of the mode of peroxide addition on phenol conversion can be seen in Figure 5.14 (TS-1) and Figure 5.15 (Al-free Ti-Beta).

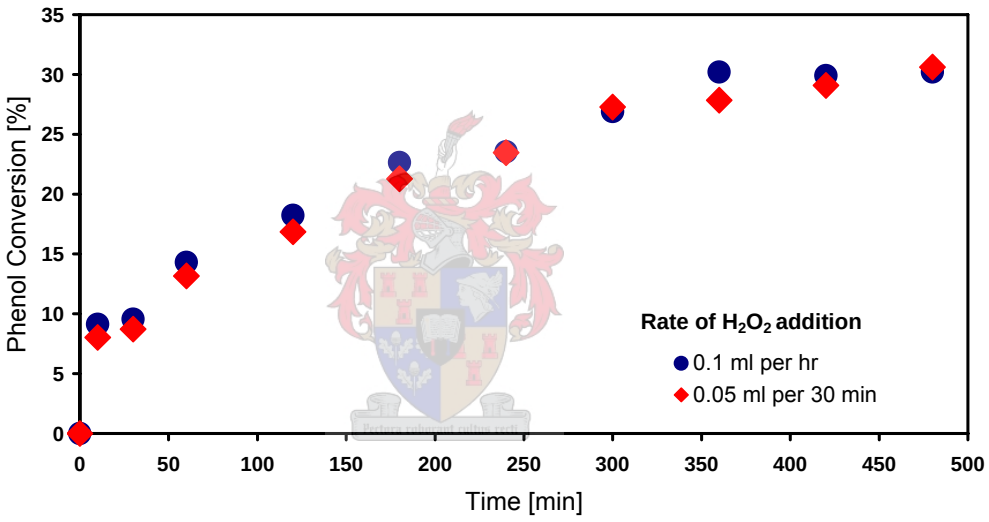

Figure 5.14: Phenol conversion vs. reaction time for different rates of hydrogen peroxide addition in methanol solvent over TS-1

Catalyst: TS-1; $m_{catalyst}$ = 0.12 g; m_{phenol} = 1.2 g; T_R = 60 °C; Solvent: methanol; $V_{peroxide}$ = 0.5 ml (total volume, 30 wt-% in water); V_{total} = 5.5 ml

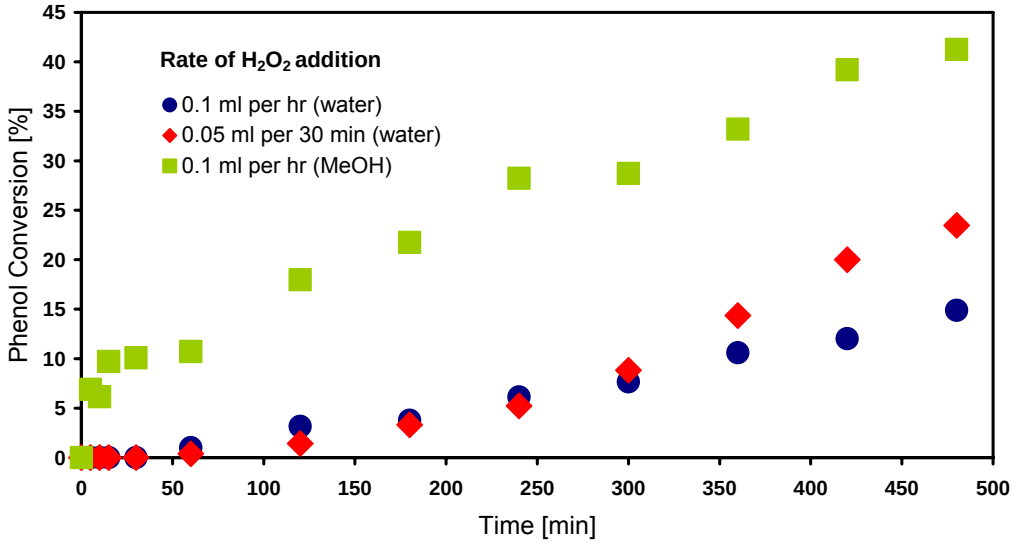

Figure 5.15: Phenol conversion vs. reaction time for different rates of hydrogen peroxide addition in methanol solvent over Al-free Ti-Beta

Catalyst: Al-free Ti-β; $m_{catalyst}$ = 0.12 g; m_{phenol} = 1.2 g; T_R = 60 °C; Solvent: water/methanol; $V_{peroxide}$ = 0.5 ml (total volume, 30 wt-% in water); V_{total} = 5.5 ml

Over both Al-free Ti-Beta and TS-1 the phenol conversion increases with reaction time, as expected.

For TS-1, the rate of peroxide addition has negligible influence on the observed rate of phenol conversion in methanol solvent, with *ca.* 30 mol-% conversion reached after 12 hours reaction. In methanol, and under the same mode of H_2O_2 addition, the catalytic activity of Al-free Ti-Beta is higher, and the final conversion reached is higher (X_{Phenol} = 41.3%). This can be explained by the larger pore of Beta zeolite facilitating the access of organic phenol molecules to the active sites, while diffusion limitations of phenol and shape-selectivity towards different transition states can be taken into account to explain the lower activity of medium-pore TS-1. Additionally, independently measured Henry's constants for the adsorption of phenol from pure methanol are 0.7 and 1.3 on TS-1 and Al-free Ti-Beta respectively. Thus, the adsorption of phenol is stronger on Al-free Ti-Beta than TS-1, which explains the higher activity observed over Al-free Ti-Beta.

It is apparent that the addition of peroxide in more discrete amounts in water and over Beta catalyst has a positive effect on phenol conversion (*ca.* 23.5% final conversion when H_2O_2 is added at 0.05 ml every 30 minutes vs. 14.9% at 0.1 ml per hour). Using methanol as solvent, a significantly higher conversion is achieved than in water at the same rate of addition; this is anomalous to what one would have expected since water is more polar, and a higher activity

is therefore expected in water than in methanol (Henry's constants for phenol adsorption of 17.2 and 1.3 in water and methanol respectively).

However, it is worth noting that the Beta catalysed hydroxylation is incomplete even after 8 hours, as suggested by the conversion profiles that show no sign of leveling off. Thus, terminal conversions in water solvent could increase further should the reaction time be extended beyond 8 hours. Particularly for reaction in water solvent, the phenol conversions appear to be increasing greatly only from *ca.* 6 hours reaction. As a consideration for future work it is thus worth bearing in mind that 8 hours is possibly insufficient time for complete reaction in Beta catalysed systems when peroxide is added in discrete portions.

As mentioned, higher hydroquinone selectivity was obtained when peroxide was added in more discrete amounts. However, product selectivities using the two catalysts are contrary, and a complete inversion in the product selectivity trends over Beta and TS-1 catalyst was observed. Figure 5.16 (TS-1) and Figure 5.17 (Al-free Ti-Beta) show the p/o-ratios as a function of phenol conversion obtained under the different modes of peroxide addition.

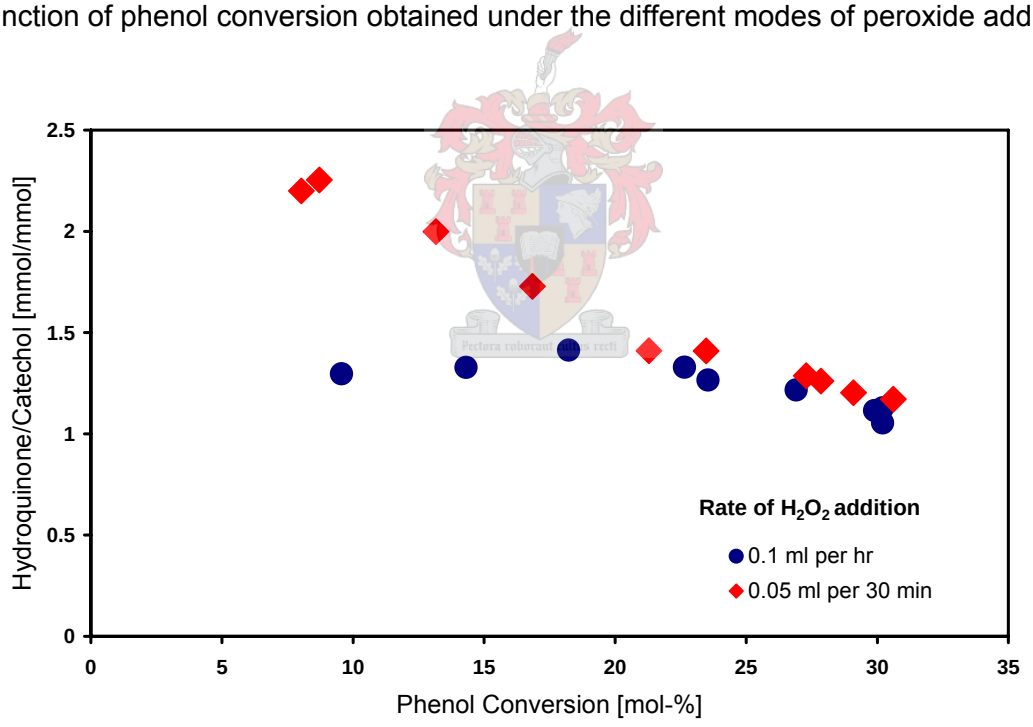

Figure 5.16: Hydroquinone selectivity as a function of phenol conversion in methanol solvent over TS-1 for different modes of H_2O_2 addition

Catalyst: TS-1; $m_{catalyst}$ = 0.12 g; m_{phenol} = 1.2 g; T_R = 60 °C; Solvent: methanol; $V_{peroxide}$ = 0.5 ml (total volume, 30 wt-% in water); V_{total} = 5.5 ml

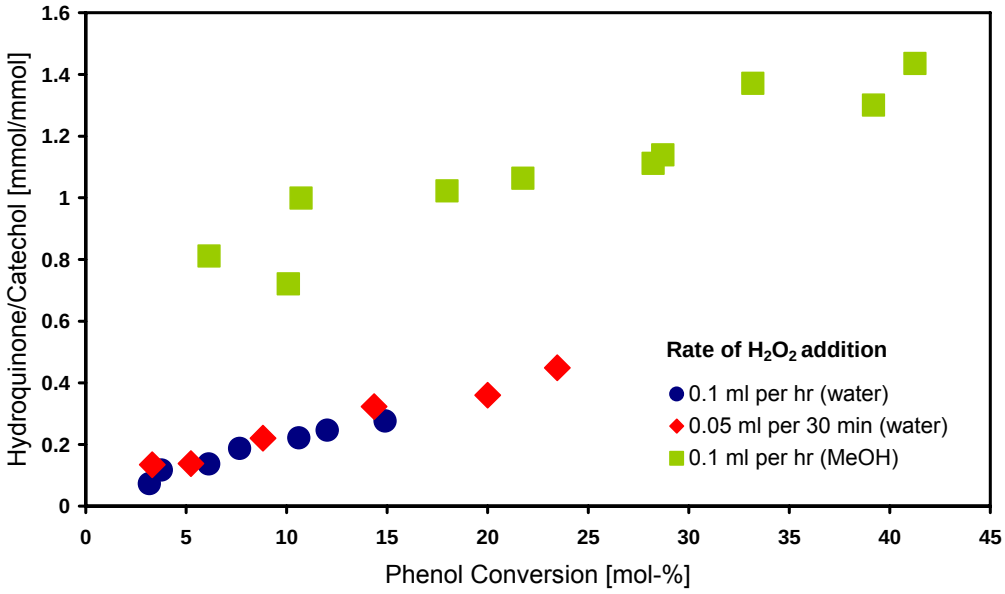

Figure 5.17: Hydroquinone selectivity as a function of phenol conversion in water and methanol solvent over Al-free Ti-Beta for different modes of H_2O_2 addition

Catalyst: Al-free Ti-β; $m_{catalyst}$ = 0.12 g; m_{phenol} = 1.2 g; T_R = 60 °C; Solvent: water/methanol; $V_{peroxide}$ = 0.5 ml (total volume, 30 wt-% in water); V_{total} = 5.5 ml

Over Al-free Ti-Beta, the p/o-ratio *increases* with increasing phenol conversion in both solvents (see Figure 5.17); it can be seen that the p/o product-ratio increases linearly with conversion (residuals of 0.87-0.98 are obtained for straight-line fitting to this experimental data). In water solvent, the selectivity seems largely independent of the mode of peroxide addition, and p/o-ratios above *ca.* 0.45 are not achieved even when the peroxide solution is added in more discrete amounts (0.05 ml every 30 minutes). Thus, catechol formation is dominant (p/o-ratios < 1) despite the p/o-ratio increasing. The selectivity to hydroquinone is, however, marginally enhanced at all levels of phenol conversion when H_2O_2 is added more discretely and the p/o-ratio reaches a final value slightly over 1.5 times larger (0.45 vs. 0.28 for the faster rate of addition). Compared to a single-dose addition, discrete peroxide addition offers a slight improvement in hydroquinone selectivity; p/o-ratios of 0.45 and 0.36 respectively were obtained (X_{Phenol} = 23.5%).

In contrast to water, when using methanol as the solvent hydroquinone formation is greatly favoured (p/o-ratios > 1) and the selectivity to hydroquinone is some 2.5 times higher than was obtained in water under identical reaction conditions and at the same phenol conversion (X_{Phenol} = 23.5%). Furthermore, the final selectivity to hydroquinone even exceeds that obtained on TS-1 in methanol using the same mode of peroxide addition, and at the same phenol conversion (a p/o-ratio on TS-1 of 1.13 vs 1.20 on Al-free Ti-Beta at X_{Phenol} = 30% was obtained).

Comparing the selectivity profiles for the two catalysts (see also Figure 12.5, APPENDIX D), a higher selectivity for hydroquinone formation is achieved over TS-1 at shorter reaction times (and similar phenol conversion levels) than on Al-free Ti-Beta. However, the selectivity trend over TS-1 (in methanol solvent) is contrasting to that for Al-free Ti-Beta, and *decreases* with increasing phenol conversion. As for single-portion peroxide addition on TS-1 (see *Section 5.2.2*), the formation of hydroquinone is favoured at the shorter reaction times (and low phenol conversions) when effectively less peroxide is present in the reaction volume. Comparing the two modes of peroxide addition, the initial hydroquinone selectivity (at X_{Phenol} = 10%) is 1.5 times higher for the slower rate of H_2O_2 addition (0.05 ml per 30 min) compared with the faster addition rate (0.1 ml per hour). The p/o-ratio, however, decreases more rapidly with increasing conversion for the slower, more discrete rate of peroxide addition. As for single-portion addition, a near constant and equivalent selectivity is obtained at higher phenol conversions, and for both rates of H_2O_2 addition the terminal p/o-ratio is the same (*ca.* 1.2 at X_{Phenol} = 30%). As for reactions on Al-free Ti-Beta, comparing the discrete mode of peroxide addition with a single-portion addition of an equivalent amount of peroxide for reaction over TS-1, it is apparent that the slower addition does offer enhanced hydroquinone selectivity. At a phenol conversion of 10 mol-% p/o-ratios of 2.11 and 1.28 are obtained for discrete and batch-mode additions respectively. At a terminal phenol conversion of 25.6 mol-%, the p/o-ratio is still marginally higher for the discrete rate of peroxide addition (1.35 vs. 1.09 for single-dose addition). Compared with the discrete vs. batch-mode addition results for Al-free Ti-Beta, the slower addition on TS-1 gives a larger improvement in selectivities than when the peroxide solution is added in a single portion.

Table 5.5 (TS-1) and Table 5.6 (Al-free Ti-Beta) summarise the results obtained over the two catalysts when the hydrogen peroxide solution was added at different rates.

Table 5.5: Influence of the method of hydrogen peroxide addition over TS-1[1]

H_2O_2 rate [ml]	X_{Phenol} [mol-%]	S_{Phenol}[2] [mol-%]	S_{H2O2}[2] [%]	p/o-ratio[2] [mol/mol]	Tars[3] [mg/g_{cat}]
0.1/hr	30.20	63.68	56.83	1.40	62.66
0.05/30 min	30.61	50.91	69.04	2.11	53.57

[1]Catalyst: TS-1; $m_{catalyst}$ = 0.12 g; m_{phenol} = 1.2 g; T_R = 60 °C; Solvent: methanol; $V_{peroxide}$ = 0.5 ml (total volume, 30 wt-%); V_{total} = 5.5 ml
[2]At X_{Phenol} = 10%
[3]Quantity of tar deposited on TS-1 after 12 hours reaction

Table 5.6: Influence of the method of hydrogen peroxide addition over Al-free Ti-Beta[1]

H_2O_2 rate [ml]	X_{Phenol} [mol-%]	S_{Phenol}[2] [mol-%]	S_{H2O2}[2] [%]	p/o-ratio[2] [mol/mol]	Tars[3] [mg/g_{cat}]
0.1/hr	14.89	85.47	47.38	0.21	114.22
0.05/30 min	23.46	81.60	41.25	0.23	99.09
0.1/hr (MeOH)	41.26	26.19	36.74	0.86	96.29

[1]Catalyst: Al-free Ti-β; $m_{catalyst}$ = 0.12 g; m_{phenol} = 1.2 g; T_R = 60 °C; Solvent: water/methanol; $V_{peroxide}$ = 0.5 ml (total volume, 30 wt-% solution); V_{total} = 5.5 ml
[2]At X_{Phenol} = 10%
[3]Quantity of tar deposited on Al-free Ti-β after 12 hours reaction

It is clear from this information that for TS-1 improved hydroquinone selectivities and peroxide efficiencies can be attained if the peroxide solution is added in more discrete portions. Thus, lower peroxide concentrations offer favourable conditions for hydroquinone formation. Tar deposition on the used catalyst is also lower when peroxide is added at 0.05 ml every 30 minutes, which is likely related to less peroxide decomposition, and lower concentrations being available for the over-oxidation of the reaction products leading to the formation of higher-molecular compounds. Visually, it was also confirmed that by 60-120 minutes reaction time, the reaction solution was already a dark-brown colour when peroxide was added at 0.1 ml per hour, while only fawn-brown at the slower rate of addition at the same time, which also suggests a higher amount of tar formation when higher peroxide concentrations are present. Compared to single-portion peroxide additions, the quantity of tar formed is also significantly reduced at the most discrete H_2O_2 addition rate.

Over Al-free Ti-Beta in water solvent, the p/o-ratio remains effectively unchanged for different modes of peroxide addition. A marginally lower peroxide efficiency and phenol selectivity is obtained for the slower rate of addition (0.05 ml per 30 minutes). In methanol, while the p/o-ratio is initially 4 times higher than it is in water at the same rate of addition (0.1 ml per hour), both peroxide efficiency and phenol selectivity are significantly reduced.

Tar deposition on Al-free Ti-Beta is also reduced by a more discrete mode of peroxide addition. Compared with the single-portion addition of peroxide (addition of an equivalent 0.5 ml peroxide solution at the start of the reaction) where 105.83 mg/$g_{catalyst}$ tar was formed, a marginally reduced amount was produced when peroxide was added at 0.05 ml every 30 minutes. For reaction in methanol solvent, the quantity of tar formed is also lower than the 103.47 mg/$g_{catalyst}$ formed for batch-mode peroxide addition.

Thus, the lower peroxide concentrations maintained with addition over a period of 4.5 hours results in improved p/o-ratios and reduced tar formation on both TS-1 and Al-free Ti-Beta in both water and methanol solvents.

5.3.1 Mechanistic Implications

The higher p/o-ratio obtained at all conversion levels over TS-1 (p/o-ratio > 1) can be attributed to geometric and shape-selective effects induced in the smaller zeolite channels, and which favours the production of hydroquinone. Over the larger pore Al-free Ti-Beta catalyst, the reaction is governed much less by a geometric constriction in the pore system, so that the formation of the bulky intermediate leading to catechol can dominate in the micropores. Furthermore, catechol is also the preferred product on the external catalyst surface, as seen by Wilkenhöner (2001), so its formation is expected to dominate overall on Al-free Ti-Beta and lead to lower hydroquinone selectivity. This is observed where the initial p/o-ratio is less than 1 for reaction over Beta catalyst (see Figure 5.17).

For reaction in methanol solvent, methanol is initially in great excess (over 98 vol-%, compared to *ca.* 0.15 vol-% peroxide and *ca.* 0.90 vol-% water at t = 0), and is thus found in a much larger concentration in the reaction zone than either peroxide or water. Furthermore, due its small size the methanol molecule can easily penetrate the TS-1 pores and will be easily adsorbed onto the active titanium-hydroperoxo site. With such great excess, the relative amount of titanium active sites with an alcohol molecule co-ordinated is substantially greater than the titanium-hydroperoxo sites alone. Due to the increased size of this active site, and the restricted space for phenol in the pores (considerable diffusion limitations), the phenolic OH will be repelled by the titanium-hydroperoxo site and point towards the TS-1 zeolite wall. Consequently, para-hydroxylation occurs, and hydroquinone is preferentially formed in the TS-1 micropores. This explains the high p/o-ratios obtained initially when the peroxide is added in discrete amounts (p/o-ratio ≈ 2.3).

On Al-free Ti-Beta, the bulky intermediate with phenolic OH pointing towards the hydrophilic active site can be accommodated and shape-selectivity effects are less restrictive, so ortho-hydroxylation and catechol formation occurs as well. The initial p/o-ratio is closer to the expected statistical distribution.

As more hydrogen peroxide solution is added with time, both the relative amounts of peroxide and water increase. Therefore, a competitive adsorption between water and methanol at the active site also exists and a cyclic species can be formed in which water is also co-ordinated as a ligand of titanium, and which is much smaller than the corresponding

methanol-titanium co-ordinated species. Consequently, with this smaller water-titanium co-ordinated species there is more space available in the pores in the vicinity of the active site for a phenolic OH to hydrogen-bond to it; the ortho position is consequently closer to the active site and ortho-hydroxylation occurs so that catechol is thus increasingly formed. In this way, shape selectivity towards a particular transition state in the micropores is reduced. As the relative amount of catechol being formed in the pores increases in this way, the hydroquinone-to-catechol ratio on TS-1 decreases.

It is also worth noting that the active intermediate species with co-ordinated water molecules is more electrophilic due to the lower donor properties of water with respect to methanol; therefore, not does it only offer less steric hindrance to ortho-hydroxylation, but it also has a higher intrinsic reactivity, which also explains the increasing phenol conversion with peroxide addition (and increasing water fraction).

Exactly why the hydroquinone selectivity decreases with phenol conversion over TS-1 can possibly also be attributed to tar formation on titanium sites in the pore mouths or inside the micropores; tar poisoning of these active sites will block access to/from the pores (where hydroquinone formation is favoured), so that catechol formation at the external surface sites will dominate as interporous hydroquinone formation is restricted. When there is little peroxide in the system at the start of the reaction, tar formation from consecutive over-oxidation reactions is limited, and this together with the high methanol concentration favouring tar dissolution, means that hydroquinone formation occurs easily. However, with increasing peroxide and water concentrations product over-oxidation is more likely, so that the concentration of tars is greater. Since the solvent is more polar as a result of the increased water fraction, these tars are not dissolved and block the pores where hydroquinone is formed. Thus, the amount of hydroquinone formed decreases and/or remains unchanged; catechol formation dominates and the p/o-ratio decreases accordingly. Looking at the concentration-time profiles (a typical profile is shown in Figure 12.2, APPENDIX D), it appears that the hydroquinone concentration levels-off after approximately 180-240 minutes, while the catechol concentration continues to increase. Thus, the catechol concentration increases relative to (constant) hydroquinone.

6 Conclusions

The effect of hydrogen peroxide concentration on the hydroxylation of phenol over Al-free Ti-Beta and TS-1 catalysts was investigated with the aim of understanding how a changing concentration influences the activity and selectivity of the reaction. Reactions were performed in water and methanol solvents, and the peroxide added either as a single portion or in more discrete amounts over 4.5 hours.

It was observed that the conversion of phenol over zeolite Al-free Ti-Beta is enhanced by higher hydrogen peroxide concentrations, especially in water solvent. This is due to the increased number of active sites formed between titanium and hydrogen peroxide, resulting in a larger number of titanium-hydroperoxo active species that which are available for co-ordination and phenol oxidation.

In methanol, the phenol conversion remained largely unchanged despite an almost four-fold increase in initial peroxide concentration, and final conversions did not exceed *ca.* 8 mol-% for all peroxide concentrations. With methanol in such large excess, there is insufficient water present in the reaction volume to maintain the micropores in a phenol-rich environment, so methanol also co-ordinates to the active sites, inhibiting the access of phenol to the micropores and resulting in decreased conversions.

Pectora roborant cultus recti

Kinetic modelling of the reaction data with an overall second-order kinetic model gave a good fit in both solvents, and despite unchanging conversion in methanol solvent indicating a possible zero-order dependence on peroxide concentration; model fits for methanol-based reactions were not as accurate when an overall first-order model was fitted to the data, and overestimated phenol and hydrogen peroxide conversions.

The rate constant for phenol consumption was extracted from the experimental data, and is independent of varying hydrogen peroxide concentration for the hydroxylation of phenol over Al-free Ti-Beta using water as the solvent. A value of 1.93×10^{-9} $dm^3/mmol.m^2.s$ was obtained, which corresponds well with the literature. Results are inconclusive in methanol solvent over Al-free Ti-Beta, but for TS-1 in methanol, the phenol rate constant is also independent of peroxide concentration (*ca.* 1.36×10^{-8} $dm^3/mmol.m^2.s$). These unchanging rate constants confirm that the kinetic model developed to represent the experimental data is correct.

Selectivity to the para isomer exhibits contrasting trends in water and methanol solvent as the initial peroxide fraction changes. For Al-free Ti-Beta in water solvent, catechol formation dominates (p/o-ratios < 1), and is enhanced by using higher initial peroxide concentrations. Above 1.27 vol-% peroxide a constant p/o-ratio of *ca.* 0.35 is obtained (at X_{Phenol} = 10%). Lower initial concentrations cause the p/o-ratio to increase slightly, but the selectivity for hydroquinone formation never becomes dominant. In contrast, using a methanol solvent, hydroquinone selectivity is significantly improved for initial peroxide concentrations *above* 1.27 vol-%; the selectivity for hydroquinone formation dominates for all peroxide concentrations (p/o-ratio > 1), and ratios of up to 2 are obtained.

With TS-1 using methanol solvent, the phenol conversion is more significantly influenced by higher hydrogen peroxide concentrations than Al-free Ti-Beta, but with higher initial concentrations unselective phenol conversion/decomposition to tars is more severe since the hydroquinone selectivity is not higher at these concentrations. The increased tar formation, expressed as tar deposition on the catalyst or as tar formation rate constant, supports the idea that the greater amount of free peroxide is mainly responsible for the non-selective conversion of phenol.

The higher selectivity towards hydroquinone with TS-1 than Al-free Ti-Beta is consistent with a shape selectivity effect in the pores; the p/o-ratio is higher at low peroxide concentrations (p/o-ratios up to 3 were obtained at low phenol conversions), and decreases to a constant value at higher conversions. The higher p/o-ratios obtained initially can be explained by the high methanol concentration. With methanol in such large excess at the start of the reaction the proportion of active sites co-ordinating with methanol molecules is high, resulting in the bulky active-intermediate promoting hydroquinone formation.

Addition of hydrogen peroxide solution in discrete amounts confirms that the formation of hydroquinone is favoured at low peroxide concentrations. However, a reversal in product selectivity is observed over the two catalysts; with TS-1 higher selectivities are obtained at low phenol conversions, and over Al-free Ti-Beta the p/o-ratio increases with phenol conversion. Methanol is initially in great excess, resulting in increased co-ordination to the active site, and the associated geometric limitations allow hydroquinone formation to dominate; high p/o-ratios are therefore obtained initially. On Al-free Ti-Beta, shape-selectivity effects are less restrictive so catechol formation in the pores occurs more readily, and the initial p/o-ratio is closer to the statistical distribution.

As more peroxide solution is added competitive adsorption effects at the active site increase because the water fraction increases simultaneously. Smaller water-co-ordinated active

species result in phenol being able to increasingly adopt a configuration which is favourable for catechol formation.

For both catalysts, discrete peroxide addition results in favourable p/o-ratios compared to single-portion additions, particularly for reaction on Al-free Ti-Beta in methanol solvent For TS-1, while the mode of peroxide addition had negligible influence on the phenol conversion, at low phenol conversions a hydroquinone selectivity of *ca.* 1.6 higher was obtained when the peroxide solution was added discretely, compared to the single-portion addition of an equivalent volume.

Furthermore, tar formation is also reduced with discrete peroxide addition, which is due to lower amounts of free-peroxide initially available for the consecutive oxidation of the reaction products, and the high methanol concentration that favours dissolution of the tars.

Thus, the interaction of the effects of peroxide concentration and the solvent composition and polarity on the product selectivity and degree of tar formation is important. Particularly with TS-1, lower peroxide concentrations in bulk methanol solvent are highly beneficial for hydroquinone formation, because of the implicit geometric constraints in the micropores, the lower water concentration, and the decreased tar formation associated with high methanol concentrations. This could have significant reactor design implications, as the results obtained here suggest that the reaction should be terminated after approximately 30 minutes to maximise hydroquinone production (under the conditions evaluated in these experiments), even though the corresponding phenol conversions are low (*ca.* 10 mol-%). The higher hydroquinone selectivities reached at low phenol conversions for the discrete peroxide addition experiments also confirm this. Practically, to enhance the hydroquinone selectivity for reaction over TS-1, the initial phenol-peroxide molar ratio should be *ca.* 10, methanol should constitute not less than 90 vol-% of the reaction volume, and the peroxide should be added in discrete amounts.

For reaction over Al-free Ti-Beta, methanol solvent also enhances the hydroquinone formation as expected. At low phenol conversions (*ca.* 10 mol-%) hydroquinone is still the preferred product, although in contrast to TS-1 the selectivity increases with phenol conversion, and is higher with higher initial peroxide concentrations. Under the best conditions evaluated here for optimal hydroquinone formation, the initial phenol-peroxide molar ratio should be *ca.* 2.5, with methanol making up at least 90 vol-% of the total volume. Discrete peroxide addition in methanol solvent for the Al-free Ti-Beta catalysed hydroxylation gives excellent improvements in hydroquinone selectivity (2.5 times higher than water

solvent), and the addition in more discrete portions might further improve hydroquinone formation, and should therefore be examined.

7 Recommendations

As far as the phenol hydroxylation reaction is concerned a great deal is now known; several authors in the literature have investigated a variety of different catalysts, reaction conditions, solvents, and co-solvent mixtures amongst others, in an attempt to understand the key parameters influencing catalyst activity and product selectivity in aromatic hydroxylations over these unique catalysts, and to develop appropriate kinetic models. This current work focused on the effects of the reactant concentration, namely hydrogen peroxide.

As far as future work is concerned, it is suggested that the focus is broadened to include other substrates. The epoxidation of α-olephins is particularly attractive with Al-free Ti-Beta because of its large pore structure.

A literature investigation for the epoxidation of 1-octene and 1-hexene over TS-1 Al-free Ti-Beta has revealed that hydrogen peroxide concentration effects have not fully been investigated, which could be a possible future project. What is clear thus far is that aprotic solvents (such as acetonitrile and acetone) are favoured because they limit cleavage of the epoxide ring, resulting in higher epoxide selectivity and inhibiting by-product formation. Methanol and water present in the reaction system result in cleavage of the ring, and undesired diol formation. Thus, it is suggested that any investigations undertaken should be done using a more concentrated peroxide solution (50 and 70 wt-% aqueous solutions are available), or ideally a solution of peroxide in acetonitrile/acetone. This will overcome the effects of water on catalyst deactivation and give an improvement in activity and product selectivity. Furthermore, a basic solvent should also preferentially be used; while not fully confirmed, the basic solvent is thought to poison and neutralise catalyst acid sites and suppress acid-catalysed ring opening.

It has to be noted that synthesis of the Al-free Ti-Beta catalyst should be resolved, as problems were encountered in this work. While the Al-free Beta seeds used for seeding the (HF)-synthesis gel in Ti-Beta preparation were successfully prepared, a catalyst favourable for the phenol hydroxylation reactions conducted in this study was not made. Catalyst batches synthesised on different occasions and from fresh TEOS and TEOT sources were not fully crystallised Beta phase. It is suggested that the crystallisation time might also be increased to the full 20 days (as done for the non-HF assisted synthesis) to see if this has a positive effect, something that time constraints of this work prevented.

8 References

1. Alvarez, F., Silva, A. I., Ribeiro, F., Ramoa, F., Ginannetto, G., and Guisnet, M., *Stud. Surf. Sci. Catal.* **108**, 609 (1997).

2. Bell, R. G., "British Zeolite Association. http://www.bza,org/zeolites", 2001.

3. Bellussi, G., Carati, A., Clerici, M., and Esposito, A., *Stud. Surf. Sci. Catal.* **63**, 421 (1991).

4. Bellussi, G., Carati, A., Clerici, M. G., Maddinelli, G., and Millini, R., *J. Catal.* **133**, 220 (1992).

5. Blasco, T., Camblor, M. A., Corma, A., Esteve, P., Guil, J. M., Martínez, A., Perdigón-Melón, J. A., and Valencia, S., *J. Phys. Chem. B* **102** (No. 1), 75 (1998).

6. Blasco, T., Camblor, M. A., Corma, A., Esteve, P., Martínez, A., Prieto, C., and Valencia, S., *Chem. Commun.*, 2367 (1996).

7. Blasco, T., Camblor, M. A., Corma, A., and Pérez-Pariente, J., *J. Am. Chem. Soc.* **115** (No. 25), 11806 (1993).

8. Boccuti, M. R., Rao, K. M., Zecchina, A., Leofanti, G., and Petrini, G., *Stud. Surf. Sci. Catal.* **48**, 133 (1998).

9. Bonneviot, L., Trong On, D., and Lopez, A., *J. Chem. Soc., Chem. Commun.*, 685 (1993).

10. Bourgeat-Lami, E., Fajula, F., Anglerot, D., and Des Courieres, T., *Mic. Mes. Mat.* **1**, 237 (1993).

11. Cainelli, G., and Cardillo, G., "Chromium Oxidations in Organic Chemistry", First Ed., Springer, Berlin, 1984.

12. Callanan, L. H., Burton, R. M., Wilkenhöner, U., and van Steen, E., "Proceedings of the 13th International Zeolite Conference", (E. van Steen, L. H. Callanan and M. Claeys, Eds.), p. 2596. Cape Town, 2004.

13. Camblor, M. A., Constantini, M., Corma, A., Gilbert, L., Esteve, P., Martínez, A., and Valencia, S. "In The Roots of Organic Development". (J. R. Desmurs and S. Ratton, Eds.), Elsevier, Amsterdam, 1996a.

14. Camblor, M. A., Constantini, M., Corma, A., Gilbert, L., Esteve, P., Martínez, A., and Valencia, S., *Chem. Commun.* **11**, 1339 (1996b).

15. Camblor, M. A., Corma, A., Martínez, A., and Pérez-Pariente, J., *J. Chem. Soc., Chem. Commun.* (No. 8), 589 (1992).

16. Camblor, M. A., Corma, A., Martínez, A., Pérez-Pariente, J., and Primo, J., *Studies in Surface Science and Catalysis* **78 (Heterogeneous Catalysis and Fine Chemicals III)**, 393 (1993a).

17. Camblor, M. A., Corma, A., Mifsud, A., Pérez-Pariente, J., and Valencia, S., *Stud. Surf. Sci. Catal.* **105**, 341 (1997).

18. Camblor, M. A., Corma, A., and Pérez-Pariente, J., *Zeolites* **13**, 82 (1993b).

19. Camblor, M. A., Corma, A., and Pérez-Pariente, J., *J. Chem. Soc., Chem. Commun.*, 557 (1993c).

20. Camblor, M. A., Mifsud, A., and Pérez-Pariente, J., *Zeolites* **11**, 792 (1991).

21. Camblor, M. A., and Pérez-Pariente, J., *Zeolites* **11**, 202 (1991).

22. Clerici, M., and Ingallina, P., *J. Catal.* **140** (No. 1), 71 (1993).

23. Clerici, M. G., *Appl. Cat.* **68**, 249 (1991).

24. Corma, A., Esteve, P., and Martínez, A., *J. Catal.* **161**, 11 (1996).

25. Corma, A., Iglesias, M., and Sánchez, F., *J. Chem. Soc., Chem. Commun.*, 1635 (1995).

26. Corma, A., Rey, F., Valencia, S., Jordá, J. L., and Rius, J., *Nature Materials* **2**, 493 (2003).

27. Clyde Corporation, USA, 2005.

28. Dartt, C. B., and Davis, M. E., *Ind. Eng. Chem. Res.* **33**, 2887 (1994).

29. Davis, R. J., Liu, Z., Tabora, J. E., and Wieland, W. S., *Catal. Lett.* **34**, 101 (1995).

30. Dwyer, F. G., and Degnan, T. F., *Stud. Surf. Sci. Catal.* **76**, 499 (1993).

31. Edwards, J. O., and Curci, R., Catalytic Oxidations with Hydrogen Peroxide as Oxidant. (G. Strukul, Eds.), Kluwer Academic Publishers, Dordrecht, 1992.

32. Fajula, F., Bourgeat-Lami, E., Zivkov, C., Des Courieres, T., and Anglerot, D., US Pat. 5,310,534 A1, 1994.

33. Fraile, J. M., García, J. I., Mayoral, J. A., and Vispe, E., *Appl. Cat. A: General* **245**, 363 (2003).

34. Germain, A., Allain, M., and Figueras, F., *Catal. Today* **32**, 145 (1996).

35. Heinemann, H., *Catal.: Sci. Technol.* **1**, 1 (1981).

36. Higgins, J. B., LaPierre, R. B., Schlenker, J. L., Rohrman, A. C., Wood, J. D., Kerr, G. T., and Rohrbaugh, W. J., *Zeolites* **8**, 446 (1998).

37. Hulea, V., and Dumitriu, E., *Appl. Cat. A: General* **277**, 99 (2004).

38. IPCS, "SIDS Initial Assessment Report", 1994.

39. IZA, "International Zeolite Association. Database of Zeolite Structures, http://www.iza-structure.org/databases/", 2005.

40. Jansen, J. C., Creyghton, E. J., Njo, S. L., van Koningsveld, H., and van Bekkum, H., *Catal. Today* **38**, 205 (1997).

41. Kiricsi, I., Flego, C., and Pazzuconi, G., *J. Phys. Chem. B* **98**, 4624 (1994).

42. Kuehl, G. H., and Timken, H. K. C., *Mic. Mes. Mat.* **35-36**, 521 (2000).

43. Lev, O., *Analytical Chemistry* **67** (No. 1), 22A (1995).

44. Liu, H., Lu, G., Guo, Y., and Wang, J., *Chem. Eng. Journal* **108**, 187 (2005).

45. Lubomira, T. "Zeolite Macrostructures". Department of Chemical and Metallurgical Engineering. Sweden, Luleå University of Technology. 1999.

46. Ma, N., Ma, Z., Yue, Y., and Gao, Z., *J. Mol. Cat. A: Chemical* **184**, 361 (2002).

47. Magnoux, P., Lavaud, N., Melo, L., Giannetto, G., Silva, A. I., Alvarez, F., and Guisnet, M., *Stud. Surf. Sci. Catal.* **130C**, 3011 (2000).

48. Mal, N. K., and Ramaswamy, V., *J. Mol. Cat. A: Chemical* **105**, 149 (1996).

49. Martens, J. A., Buskens, P. H., Jacobs, P. A., van der Pol, A. J. H. P., van Hooff, J. H. C., Ferrini, C., Kouwenhoven, H. W., Kooyman, P. J., and van Bekkum, H., *Appl. Cat. A: General* **99**, 71 (1993).

50. McMurry, J., "Organic Chemistry", Fourth Ed., Brooks/Cole Publishing Company, New York, 1996.

51. McVey, T. F. Hydroquinone from Phenol Using Ti-Si Catalyst, PEP Review, SRI Consulting, http://www.sriconsulting.com/PEP (2003).

52. Meloni, D., Monaci, R., Solinas, V., Berlier, G., Bordiga, S., Rossetti, I., Oliva, C., and Forni, L., *J. Catal.* **214**, 169 (2003).

53. Muller, M., Harvey, G., and Prins, R., *Mic. Mes. Mat.* **34**, 135 (2000).

54. Newsam, J. M., Treacy, M. M. J., Koetsier, W. T., and de Gruyter, C. B., *Proc. R. Soc. London A* **420**, 375 (1998).

55. Niwa, M., Katada, N., Sawa, M., and Murakami, Y., *J. Phys. Chem. B* **99**, 8812 (1995).

56. Niwa, M., Nishikawa, S., and Katada, N., *Mic. Mes. Mat.* **82**, 105 (2005).

57. Noreña-Franco, L., Hernandez-Perez, I., Aguilar-Pliego, J., and Maubert-Franco, A., *Catal. Today* **75**, 189 (2002).

58. Notari, B. Synthesis and catalytic properties of titanium containing zeolites. Stud. Surf. Sci. Catal. P. J. In Grobet. Amsterdam, Elsevier Science Publishers B.V. **47:** 413 (1988).

59. Notari, B., *Catal. Today* **18**, 163 (1993).

60. Notari, B., *Adv. Catal.* **41**, 253 (1996).

61. Pan, Y., Xie, H., Tan, X., Liu, L., and Zheng, C., *39* **No. 7**, 404 (2003).

62. Perego, G., Bellussi, G., Corno, C., Taramasso, M., Buonomo, F., and Esposito, A., *Stud. Surf. Sci. Catal.* **28**, 129 (1986).

63. Ratnasamy, P., and Sivasanker, S., 5493061, 1996.

64. Reddy, J. S., and Jacobs, P. A., *Catal. Lett.* **37** (No. 3-4), 213 (1996).

65. Reisch, M. S., *Chemical & Engineering News* **83** (No. 15), 18 (2005).

66. Roberge, D. M., Hausmann, H., and Hölderich, W. F., *Phys. Chem. Chem. Phys.* **4**, 3128 (2002).

67. Romano, U., Esposito, A., Maspero, F., Neri, C., and Clerici, M., *Stud. Surf. Sci. Catal.* **55**, 33 (1990).

68. Sanderson, W. R., *Pure Appl. Chem.* **72** (No. 7), 1289 (2000).

69. Sato, T., Dakka, J., and Sheldon, R. A., *Stud. Surf. Sci. Catal.* **84**, 1853 (1994).

70. Saxton, R. J., Crocco, G. L., and Zajacek, J. G., US Pat. 5,508,019 A1, 1996.

71. Selli, E., Rossetti, I., Meloni, D., Sini, F., and Forni, L., *Appl. Cat. A: General* **262**, 131 (2004).

72. Shanini, G. H., Gunardson, H. H., and Easterbrook, N. C., *Chem. Eng. Prog.*, 66 (1996).

73. Sheldon, R. A., *Stud. Surf. Sci. Catal.* **59**, 33 (1991).

74. Sheldon, R. A., *Top. Curr. Chem.* **164**, 23 (1993).

75. Sheldon, R. A., *Chem. Ind.* **12** (1997a).

76. Sheldon, R. A., "Proceedings of the 3rd World Congress on Oxidation Catalysts", (R. K. In Grasselli, S. T. Oyama, A. M. Gaffney and J. E. Lyons, Eds.), p. 151. Amsterdam, 1997b.

77. Sheldon, R. A., Arends, I. W. C. E., and Dijksman, A., *Catal. Today* **57**, 157 (2000).

78. Sheldon, R. A., Arends, I. W. C. E., and Lempers, H. E. B., *Catal. Today* **41**, 387 (1998a).

79. Sheldon, R. A., Wallau, M., Arends, I. W. C. E., and Schuchardt, U., *Accounts of Chemical Research* **31**, 485 (1998b).

80. Sigma-Aldrich, *Sigma-Aldrich* (2005).

81. Skoog, D. A., and West, D. M., "Fundamentals of analytical chemistry", 3rd Ed., Rinehart and Winston, New York, 1976.

82. Sonnet, P. E., Laukin, M. E., and McNeill, G. P., *J. Am. Oil Chem. Soc.* **72**, 199 (1995).

83. SRI, "Chemical Economics Handbook, SRI Consulting, http://www.sriconsulting.com/CEH/", 2004.

84. Taramasso, M., Perego, G., and Notari, B., US Pat. 4,410,501 A1, 1983.

85. Taylor, B. Dealumination of Nanoporous Catalysts (2004).

86. Thangaraj, A., Kumar, R., Mirajkar, S. P., and Ratnasamy, P., *J. Catal.* **130**, 1 (1990).

87. Thangaraj, A., Kumar, R., and Ratnasamy, P., *J. Catal.* **131**, 294 (1991).

88. Tuel, A., Moussa-Khouzami, S., Ben Taârit, Y., and Naccache, C., *J. Mol. Cat. A: Chemical* **68**, 45 (1991).

89. Uguina, M. A., Serrano, D. P., Sanz, R., Fierro, J. L. G., Lopez-Granados, M., and Mariscal, R., *Catal. Today* **61**, 263 (2000).

90. Ukrainczyk, L., and McBride, M. B., *Clays Clay Miner.* **40**, 157 (1992).

91. van der Pol, A. J. H. P., and van Hooff, J. H. C., *Appl. Cat. A: General* **92**, 93 (1992).

92. van der Pol, A. J. H. P., Verduyn, A. J., and van Hooff, J. H. C., *Appl. Cat. A: General* **92**, 113 (1992).

93. van der Pol, A. J. H. P., Verduyn, A. J., and van Hooff, J. H. C., *Appl. Cat.* **96**, L13 (1993).

94. van der Waal, J. C., Kooyman, P. J., Jansen, J. C., and van Bekkum, H., *Mic. Mes. Mat.* **25**, 43 (1998a).

95. van der Waal, J. C., Rigutto, M. S., and van Bekkum, H., *Appl. Cat. A: General* **167**, 331 (1998b).

96. van der Waal, J. C., and van Bekkum, H., *J. Mol. Cat. A: Chemical* **124**, 137 (1997).

97. Wilkenhöner, U. "Aromatic hydroxylations over titanium-substituted crystalline silicates". Department of Chemical Engineering. Cape Town, University of Cape Town. 2001.

98. Wilkenhöner, U., Gammon, D. W., and van Steen, E., **142**, 619 (2002).

99. Wilkenhöner, U., Langhendries, G., van Laar, F., Baron, G. V., Gammon, D. W., Jacobs, P. A., and van Steen, E., *J. Catal.* **203**, 201 (2001).

100. Windsor, C. M. Computational Studies of Zeolite Catalysis (1998).

101. Zhang, W., and Smirniotis, P. G., *Appl. Cat. A: General* **168** (No. 1), 113 (1998).

102. Zhuang, J., Ma, D., Yan, Z., Liu, X., Han, X., Bao, X., Zhang, Y., Guo, X., and Wang, X., *Appl. Cat. A: General* **258**, 1 (2004).

9 APPENDIX A

9.1 Titration Reagent Preparation

Chemical solutions used in the titrations were prepared as detailed below.

Ammonium Molybdate Tetrahydrate

A 2 wt-% ammonium molybdate solution was prepared by dissolving 1.0 g of ammonium molybdate tetrahydrate ($H_{24}Mo_7N_6 \cdot 4H_2O$, Fluka) in 50 ml of distilled water.

Potassium Iodide

Approximately 1.0 g of potassium iodide crystals (KI, Merck) were dissolved in 100 ml of distilled water to give a 1 wt-% per volume solution. The solution was stored in a glass-stoppered flask and kept out of the direct light in a cool place to prevent oxidation of iodide by atmospheric oxygen.

Sodium Thiosulphate

Sodium thiosulphate solutions prepared with ordinary distilled water are particularly unstable because the distilled water usually contains an excess of carbon dioxide, which may cause a slow decomposition to take place resulting in the formation of sulphur. Consequently boiled-out distilled water was used.

An approximately 0.04019 mol per litre (0.04019-*N*) sodium thiosulphate ($Na_2S_2O_3 \cdot 5H_2O$) solution was prepared by dissolving 4.9866 g of sodium thiosulphate crystals in a little boiled-out distilled water, and making up with 500 ml of boiled distilled water in a graduated round-bottom flask. Three drops of chloroform was added to stabilise and improve the keeping qualities of the solution by inhibiting microbial decomposition.

Exposure to light, which hastens the decomposition, was avoided by storing the flask in a dark cupboard.

For titration of the representative samples, where the peroxide concentration is not as high due to the fact that it is continuously being consumed as the reaction progresses, a more dilute thiosulphate solution is required (Callanan, L. H., *et al.*, 2004). Consequently, when

such small quantities of peroxide are present, the stoichiometric end-point is reached too quickly when using a concentrated thiosulphate solution, since the volume required may be less than that of a single drop. As a result, the titration may be relatively inaccurate since a single drop may exceed the *actual* theoretical volume required to attain equivalence.

By using a more dilute standard thiosulphate solution a quantitatively more measurable and accurate volume will be required. This will also ensure that there is a good range between the volumes required for the sequential samples.

A more dilute solution is prepared by diluting the standarised 0.04019-*N* solution 1 to 10 with boiled distilled water, giving an approximately 0.004019 mol per litre solution.

Starch

An aqueous suspension of starch is a commonly used indicator for iodometry. β-amylose present in the indicator reacts with iodine to form an intensely blue-coloured complex.

A 1 wt-% per volume solution of starch indicator was prepared by dissolving 1.0 g of soluble starch ($(C_6H_{10}O_5)_n$, Fluka) in a little distilled water to give a paste, which was added with constant stirring to 100 ml of boiled distilled water. The solution was kept in a stoppered bottle and stored out of direct light.

Aqueous starch solutions decompose within a few days, primarily because of bacterial action. Furthermore, the decomposition products may consume iodine, as well as interfere with the indicator properties of the preparation. While the rate of decomposition and bacterial degradation of the starch solution is greatly inhibited by adding chloroform to act as a bacteriostat, a fresh indicator suspension was prepared for each run of titrations.

Sulphuric Acid

A dilute sulphuric acid solution was prepared by slowly adding 2.75 ml of sulphuric acid (98 mass %) to 500 ml of distilled water under constant stirring. This yielded an approximately 0.1 M solution.

10 APPENDIX B

10.1 Data Evaluation and Workup

10.1.1 Iodometric Titration

An oxidation-reduction reaction was used in the titrimetric analysis. A standardised sodium thiosulphate solution of known concentration was used as the titrant, and the hydrogen peroxide concentration was determined quantitatively from the thiosulphate volume required for equivalence, and the known laws of stoichiometry.

The moles of thiosulphate required to reach the end-point can be calculated from:

$$n_{Na_2S_2O_3} = C_{Na_2S_2O_3} \cdot V_{equivalence} \qquad [10.1]$$

From expression [4.7], two moles of thiosulphate reduce one mole of iodine, and consequently the moles of iodine formed through the oxidation of potassium iodide by hydrogen peroxide can be calculated.

From expression [4.3], a chemically equivalent molar quantity of peroxide is consumed to the quantity of iodine liberated by the iodide oxidation.

Thus, the moles of peroxide quantitatively reduced are given by equation [10.2]:

$$n_{H_2O_2} = 0.5 \cdot C_{Na_2S_2O_3} \cdot V_{equivalence} \qquad [10.2]$$

Knowing the aliquot volume and degree of dilution, the peroxide concentration in the reactor can therefore be determined.

10.1.2 Aromatics Analysis

All samples withdrawn from the reaction mixture were diluted with 3 ml of water/methanol and filtered on a 0.45 μm Millipore filter to remove the catalyst prior to HPLC analysis.

A Beckman HPLC was used to quantify the aromatic compounds present in the each sample. The HPLC was equipped with a Luna C_{18} 5 μm reverse-phase column as the stationary

phase, using an acetonitrile/water solution (30 vol-% acetonitrile) as the mobile phase (1 ml/min), and a Beckman 168 diode array detector operating at 220/280 nm. The mobile phase was buffered with 1 ml tetraethylamine (TEA) and 0.8 ml orthophosphoric acid (85% H_3PO_4) per 1000 ml water.

Figure 10.1 shows a typical chromatogram from HPLC analysis of the reaction samples.

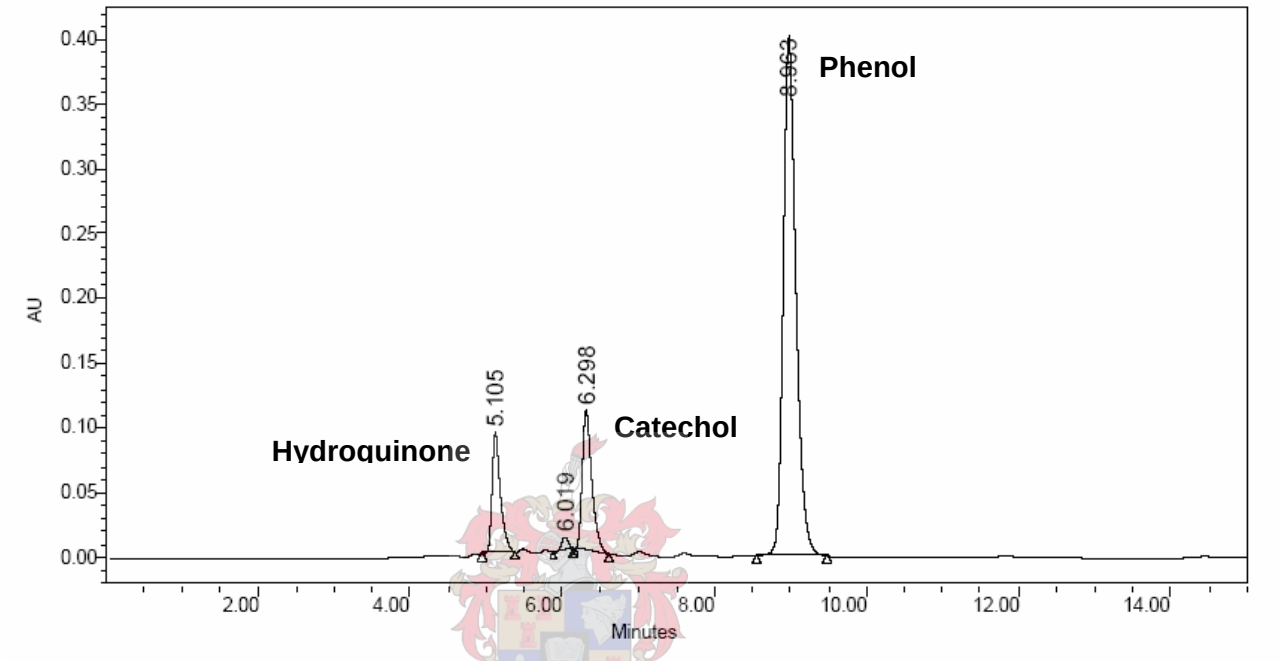

Figure 10.1: A typical chromatogram from HPLC of the phenol hydroxylation reaction mixture

Species concentrations were determined relative to calibration standards of known concentration, and the aromatics were identified qualitatively by comparison of their retention times with those of phenol, hydroquinone, catechol and resorcinol in the standards. Fresh calibration solutions were prepared prior to each analysis.

Linear calibration curves for phenol, hydroquinone, catechol and resorcinol were generated by plotting the absolute peak areas as a function of concentration each component. A typical plot obtained for hydroquinone is shown in Figure 10.2.

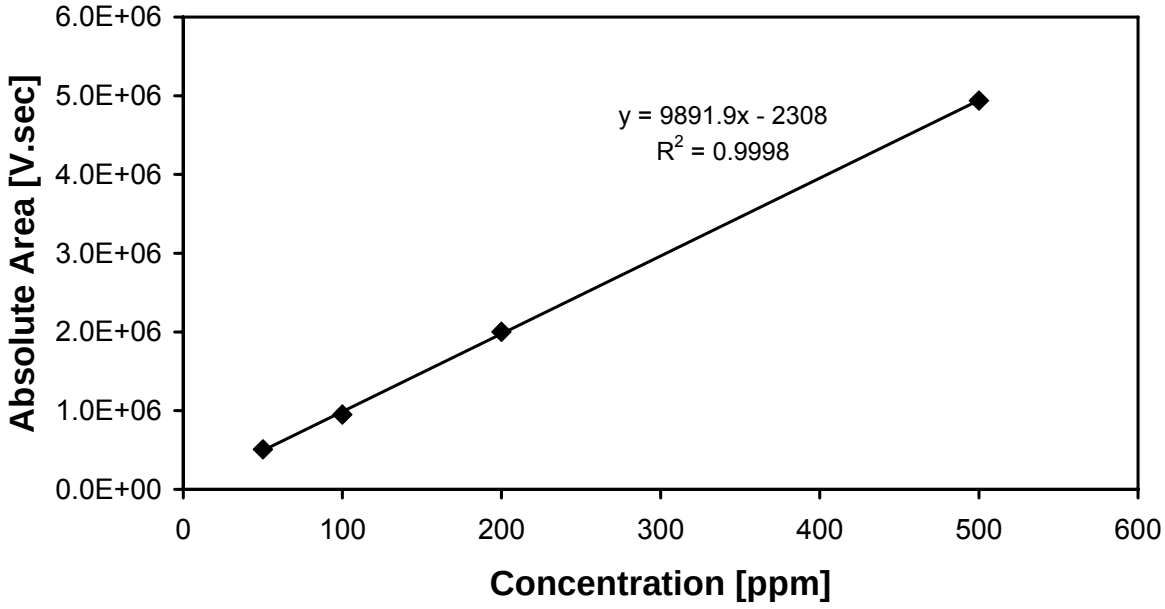

Figure 10.2: Linear concentration calibration curve of hydroquinone

Taking the gradient of these curves the average standard response factors of compound i can be calculated relative to phenol (which is arbitrarily assigned a response factor of 1) using equation [10.3]:

$$RF_i = \left(\frac{\text{Abs. area}_i}{\text{ppm}_i}\right) \cdot \left(\frac{\text{ppm}_{\text{Phenol}}}{\text{Abs. area}_{\text{Phenol}}}\right) \qquad [10.3]$$

The peaks in each sample analysed that are positively identified as phenol, hydroquinone and catechol, based upon comparison of their retention times with those of the calibration solution species, are assigned these response factors. Unidentified compounds are assigned a response factor of 1.

An adjusted absolute peak area for each species was obtained by dividing the measured peak area by the response factor. The mass fraction of compound i, was calculated by dividing this adjusted peak area by the sum of all adjusted absolute peak areas in the sample, as given by equation [10.4]:

$$x_i = \frac{\left(\frac{\text{Abs. area}_i}{RF_i}\right)}{\sum_{i=1}^{n} \frac{\text{Abs. area}_i}{RF_i}} \qquad [10.4]$$

Molar fractions (y_i) were subsequently calculated based on the molar masses of the species.

Phenol conversions were calculated on a concentration basis using equation [10.5]:

$$X_{Phenol} = \frac{C_{Phenol,0} - C_{Phenol}(t)}{C_{Phenol,0}} \cdot 100 \qquad \text{[mol-\%]} \qquad [10.5]$$

Since the concentration at time t can be calculated using the initial phenol concentration and the mole fraction already calculated, equation [10.5] reduces to:

$$X_{Phenol} = (1 - y_{Phenol}) \cdot 100 \qquad \text{[mol-\%]} \qquad [10.6]$$

The concentration of species i can then be calculated using the following equation:

$$C_i = \frac{(n_{Phenol,0} - X_{Phenol} \cdot n_{Phenol,0})}{V_{reaction}} \cdot \left(\frac{y_i}{y_{Phenol}} \right) \qquad \text{[mmol/dm}^3\text{]} \qquad [10.7]$$

where $n_{Phenol,0}$ is the initial moles phenol, and $V_{reaction}$ is the total reaction volume.

10.1.3 Additional Calculations

Once species concentrations have been determined, the following equations can be used to determine selectivities, hydrogen peroxide selectivity (efficiency conversion), the product p/o-ratio, and product yields:

$$S_i(t) = \frac{C_o(t) + C_p(t)}{C_{i,0} - C_i(t)} \cdot 100 \qquad \text{[\%]} \qquad [10.8]$$

$$S_{H_2O_2}(t) = \frac{C_o(t) + C_p(t)}{C_{H_2O_2,0} - C_{H_2O_2}(t)} \cdot 100 \qquad \text{[\%]} \qquad [10.9]$$

$$p/o - ratio(t) = \frac{C_{Hydroquinone}(t)}{C_{Catechol}(t)} \qquad \text{[mmol/mmol]} \qquad [10.10]$$

$$Y_i(t) = \frac{C_{Phenol,0} - C_{Phenol}(t)}{C_{i,0} - C_i(t)} \cdot 100 \qquad \text{[\%]} \qquad [10.11]$$

11 APPENDIX C

11.1 Physio-Chemical Catalyst Characterisation

11.1.1 X-Ray Diffraction

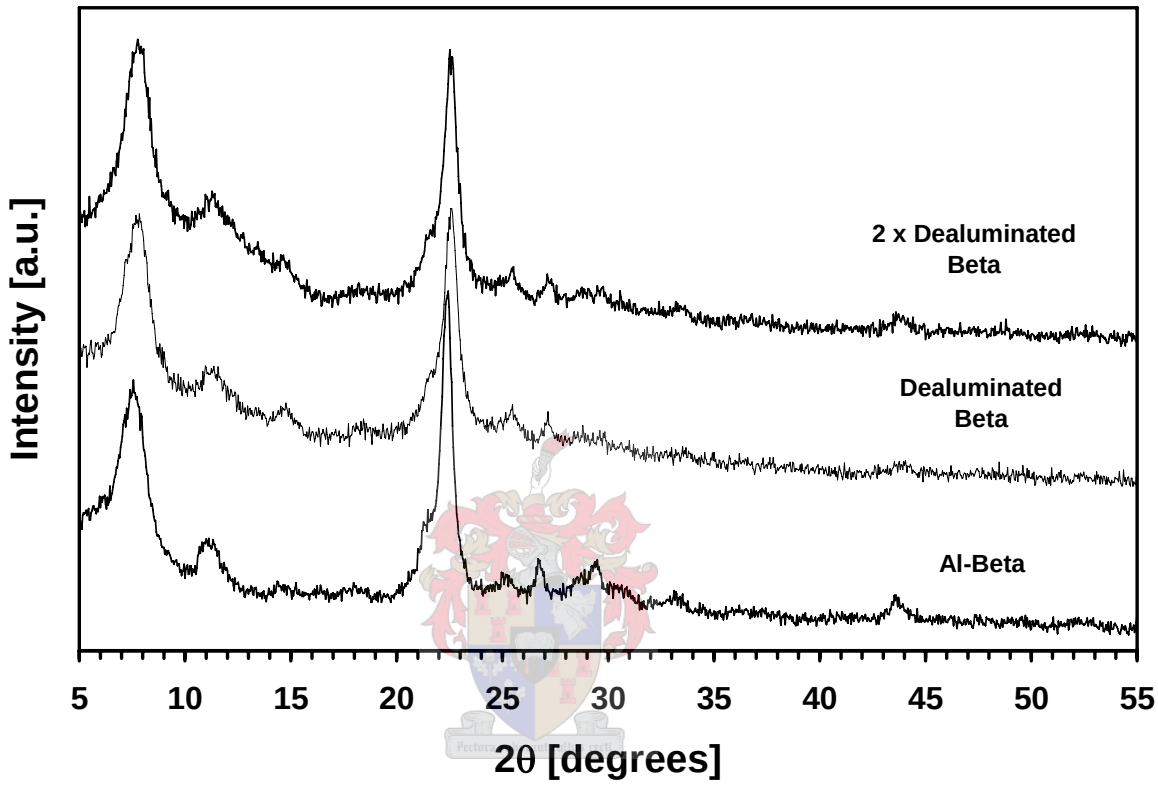

Figure 11.1: XRD diffraction patterns of (Al)-Beta (bottom), and dealuminated Beta seeds after one (middle) and two (top) successive HNO_3 acid leaching treatments

11.1.2 TEM Imaging

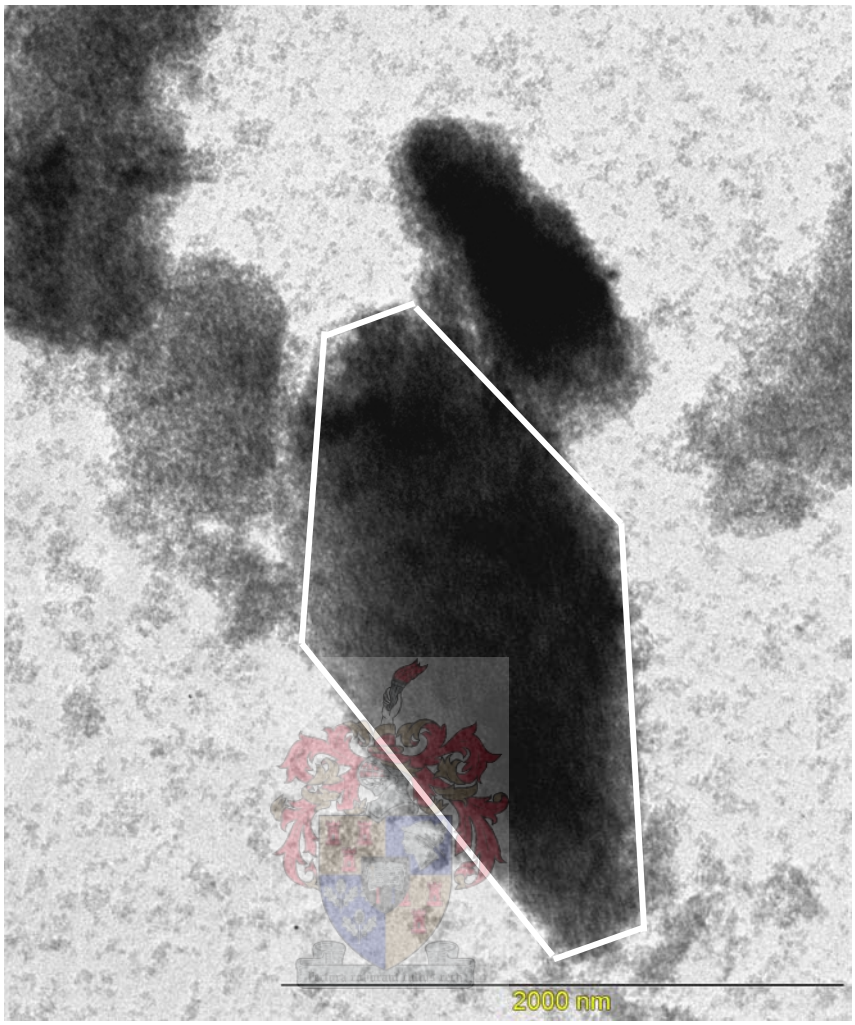

Figure 11.2: TEM micrograph of Al-free Ti-beta crystallite (scale bar represents 2000 nm). A coffin-shaped crystallite *ca.* 2.3 x 1.2 μm is outlined

12 APPENDIX D

12.1 Concentration-time Profiles

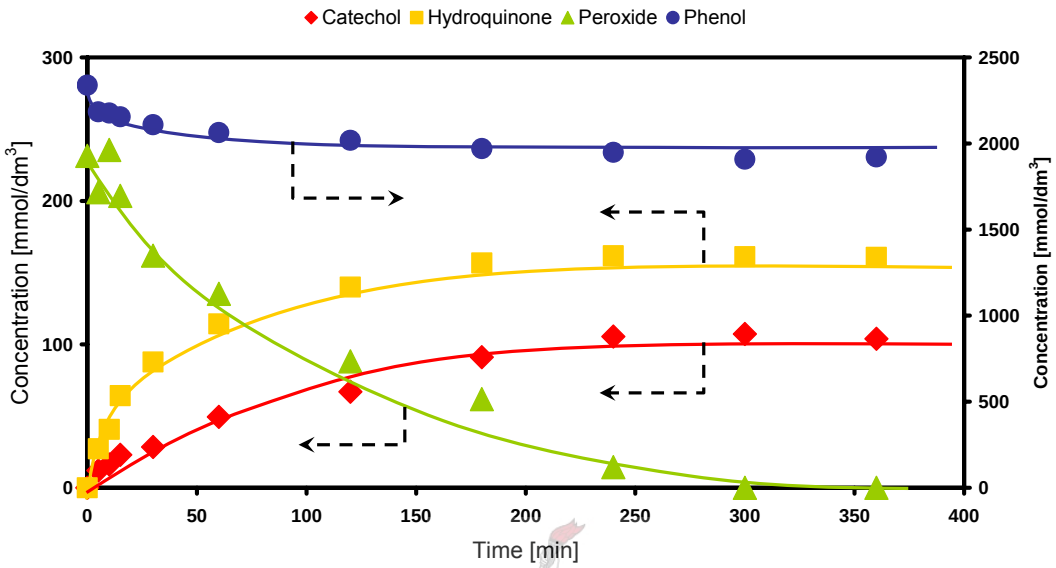

Figure 12.1: Concentration-time profile for the batch hydroxylation of phenol over TS-1

Catalyst: TS-1; $m_{catalyst}$ = 0.12 g; m_{phenol} = 1.2 g; T_R = 60 °C; Solvent: methanol; $V_{peroxide}$ = 0.15 ml; V_{total} = 5.5 ml

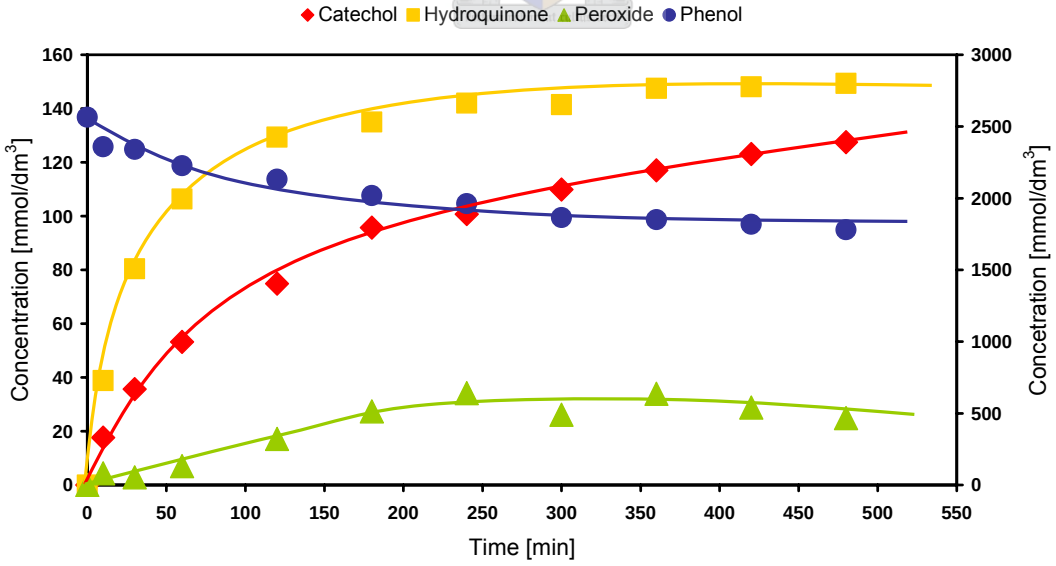

Figure 12.2: Concentration-time profile for the hydroxylation of phenol over TS-1 under semi-batch operation with H_2O_2 added to the reactor at a rate of 0.05 ml per 30 minutes

Catalyst: TS-1; $m_{catalyst}$ = 0.12 g; m_{phenol} = 1.2 g; T_R = 60 °C; Solvent: methanol; $V_{peroxide}$ = 0.5 ml (total); V_{total} = 5.5 ml

12.2 Kinetic Modelling

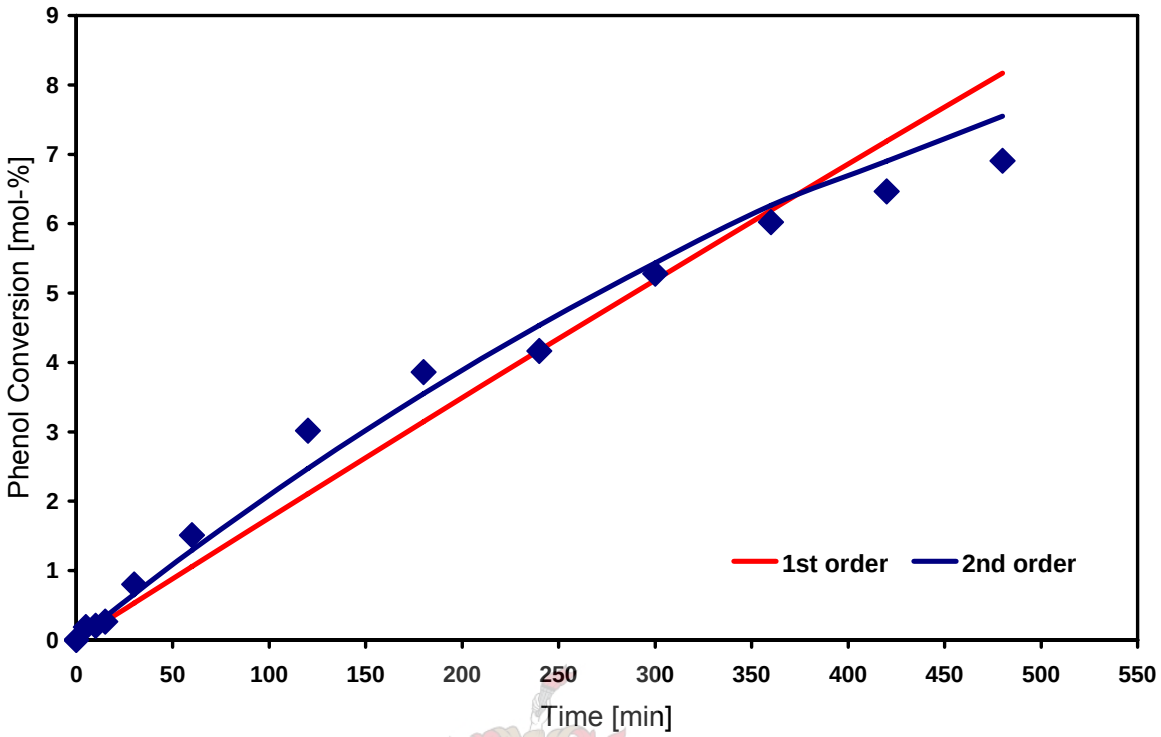

Figure 12.3: Comparison between an overall first-order and second-order kinetic fit of the phenol conversion for the hydroxylation reaction over Al-free Ti-Beta in methanol solvent

Catalyst: Al-free Ti-β; $m_{catalyst}$ = 0.12 g; m_{phenol} = 1.2 g; T_R = 60 °C; Solvent: methanol; $V_{peroxide}$ = 0.35 ml; V_{total} = 5.5 ml

12.3 Product Selectivity

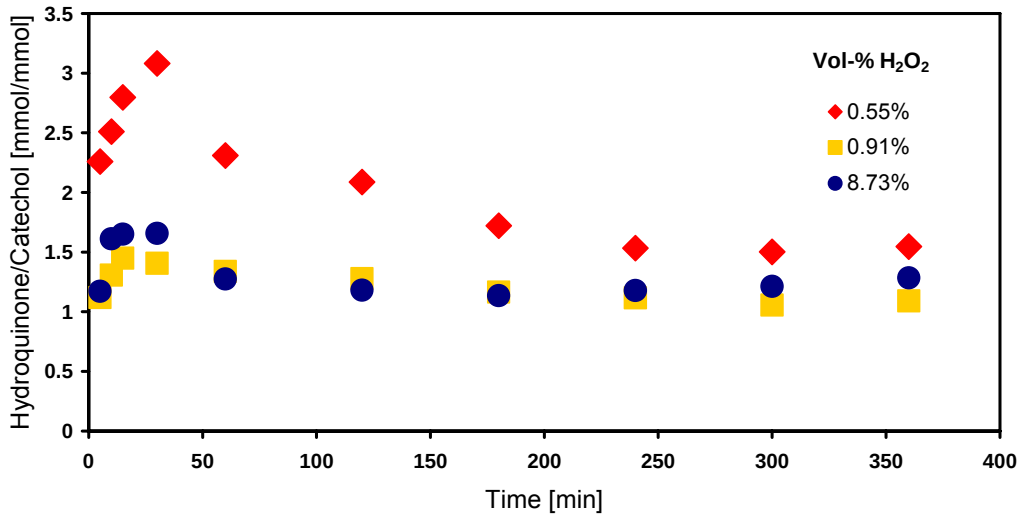

Figure 12.4: Ratio of hydroquinone-to-catechol formed as a function of reaction time over TS-1 for differential initial hydrogen peroxide concentrations

Catalyst: TS-1; $m_{catalyst}$ = 0.12 g; m_{phenol} = 1.2 g; T_R = 60 °C; Solvent: methanol; V_{total} = 5.5 ml

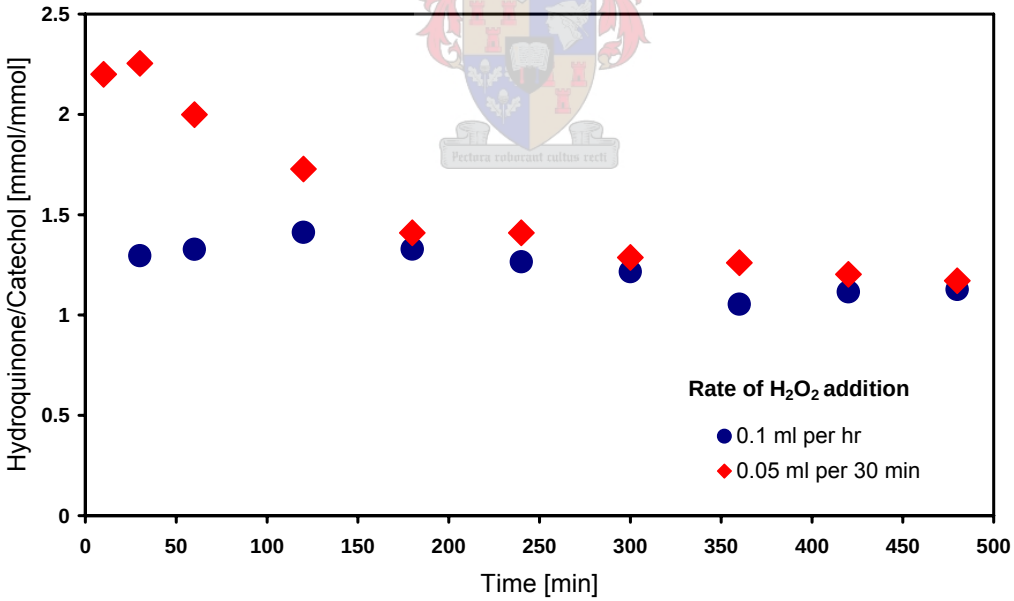

Figure 12.5: Ratio of hydroquinone-to-catechol formed as a function of reaction time over TS-1 for different methods of hydrogen peroxide addition

Catalyst: TS-1; $m_{catalyst}$ = 0.12 g; m_{phenol} = 1.2 g; T_R = 60 °C; Solvent: methanol; $V_{peroxide}$ = 0.5 ml (total); V_{total} = 5.5 ml

12.4 TGA Analysis

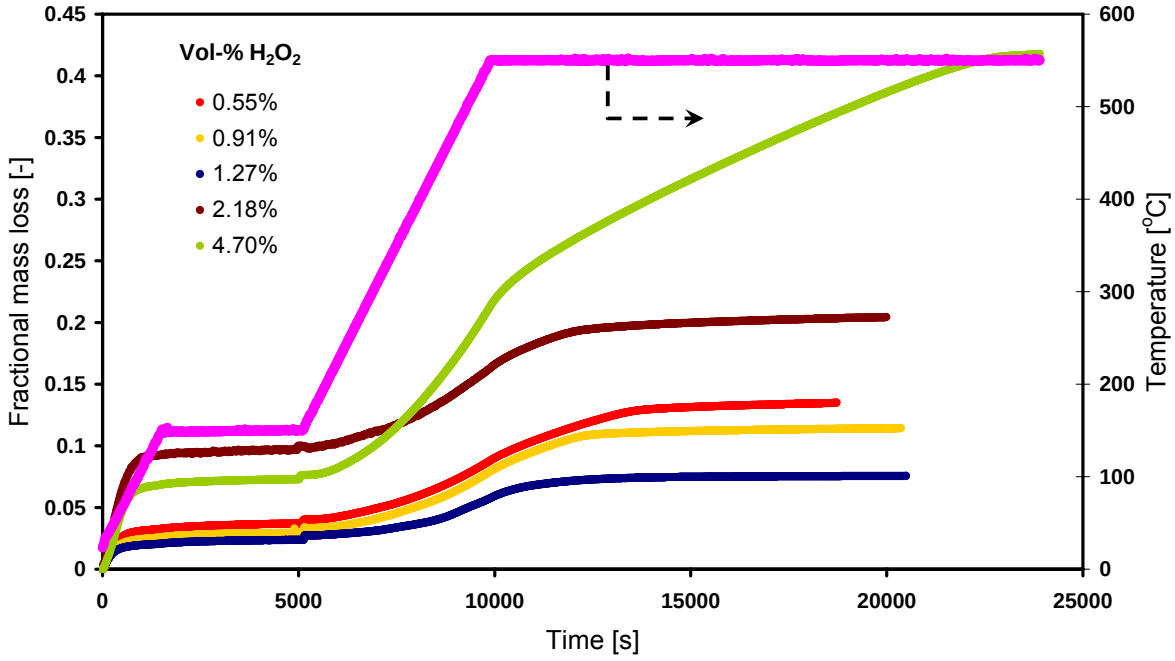

Figure 12.6: TGA curves obtained for determining the deposition of tars on the Al-free Ti-Beta catalyst surface after 12 hours hydroxylation reaction using water solvent

Catalyst: Al-free Ti-β; $m_{catalyst}$ = 0.12 g; m_{phenol} = 1.2 g; T_R = 60 °C; Solvent: water; V_{total} = 5.5 ml

13 APPENDIX E

13.1 List of Chemicals

Table 13.1: List of chemicals

Chemical	*Purity*	*Supplier*
Aluminium Chloride Hexahydrate	p.a.	Sigma-Aldrich
Ammonium Molybdate Tetrahydrate	Puriss p.a. ≥ 99%	Fluka
Catechol	99.9%	Saarchem
Hydrofluoric Acid	40 wt-% aqueous solution, p.a.	Merck
Hydrogen Peroxide	30 wt-% aqueous solution, p.a.	Sigma-Aldrich
Hydroquinone	99.9%	BDH Laboratory Supplies
Methanol	99.9%+, HPLC grade	Sigma-Aldrich
Nitric Acid	55 wt-% aqueous solution	Saarchem, Merck
Phenol	Min. assay 99.9%	Assoc. Chem. Enterprises
Phosphoric acid	85 wt-% aqueous solution, p.a.	BDH Laboratory Supplies
Potassium Iodide	Min. assay 99.8%, p.a.	BDH Laboratory Supplies
Sodium Thiosulphate	Min. assay 99%	NT Laboratory Supplies
Starch	–	Fluka
Sulphuric acid	Min. assay 98%	KIMIX
Tetraethylammonium hydroxide (TEAOH)	35 wt-% aqueous solution (Na^+,K^+ < 50 ppm)	Sigma-Aldrich
Tetraethylorthosilicate (TEOS)	99%+	Sigma-Aldrich
Tetraethylorthotitanate (TEOT)	99%+	Fluka

Oxidant Concentration Effects in the Hydroxylation of Phenol over Ti-based Zeolite Catalysts

The effect of H_2O_2 on the Reaction Activity and Product Selectivity of Al-free Ti-β and TS-1 catalysts

Presented by Robert Burton
Supervisor: Dr. Linda H. Callanan

Department of Process Engineering
University of Stellenbosch

M.Sc. Presentation, 27 February 2006, Stellenbosch

CHEMICAL·ENGINEERING
STELLENBOSCH·UNIVERSITY

BACKGROUND

Selective Oxidation Reactions: Why the Interest and Concern?

- **Partial oxidation catalysis**
  - *Ranges from large-scale production of commodities to fine-chemicals and pharmaceuticals synthesis*
- **Research motivators for selective oxidations**
  - *Oxidations are complex reactions, difficult to control: improved control is advantageous*
  - *Increased pressure of environmental legislations: Alternative process development to traditional stoichiometric oxidations*
  - *Importance of separation costs: by-product waste elimination*
  - *Synthesis of high-value chemicals: enhanced selectivity for most valuable products is possible $\Rightarrow$ economic gains*

PHENOL HYDROXYLATION

Reaction Scheme & Product Uses: Why Enhance The Selectivity?

- **Hydroxylation to dihydroxybenzenes**
  - *Mixture of hydroquinone and catechol, and residual resorcinol*

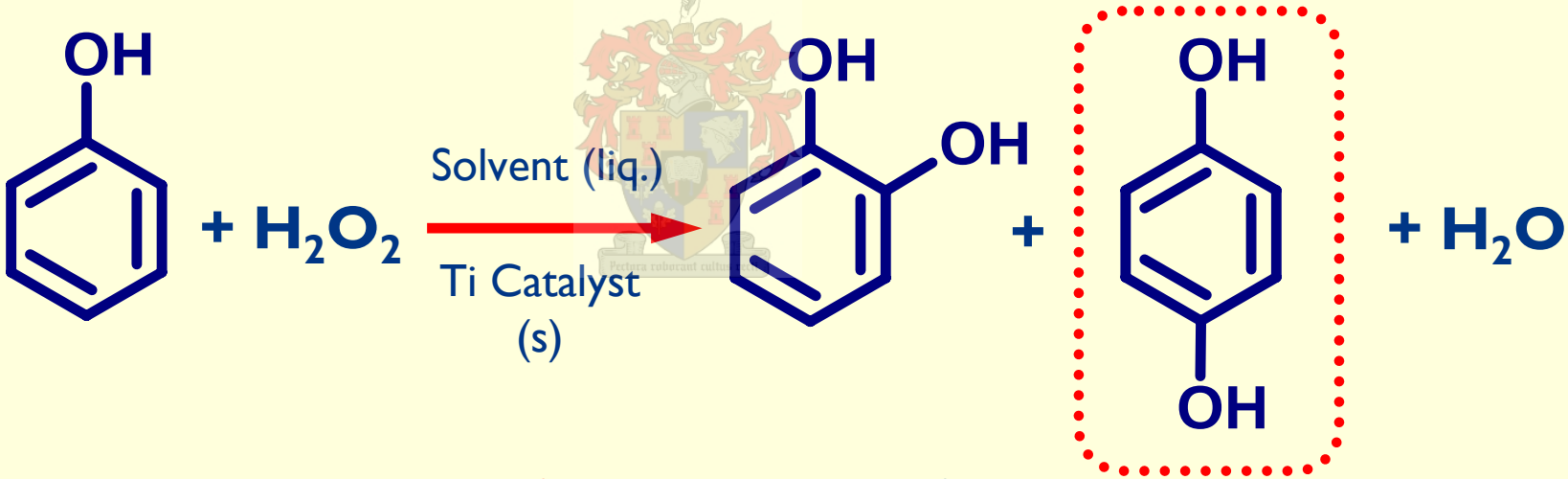

- **Enhance hydroquinone production**
  - *R772 000 per ton vs. catechol's R357 000 per ton (2005)*
- **Factors affecting efficiency/selectivity of reaction**
  - *Oxidant, catalyst preparation, solvent, temperature*

USES OF HYDROQUINONE

Industrial, Pharmaceutical, Fine-Chemicals

- **World-wide hydroquinone production is *ca.* 35 000 tons per year**
- **Broad range of industrial uses**

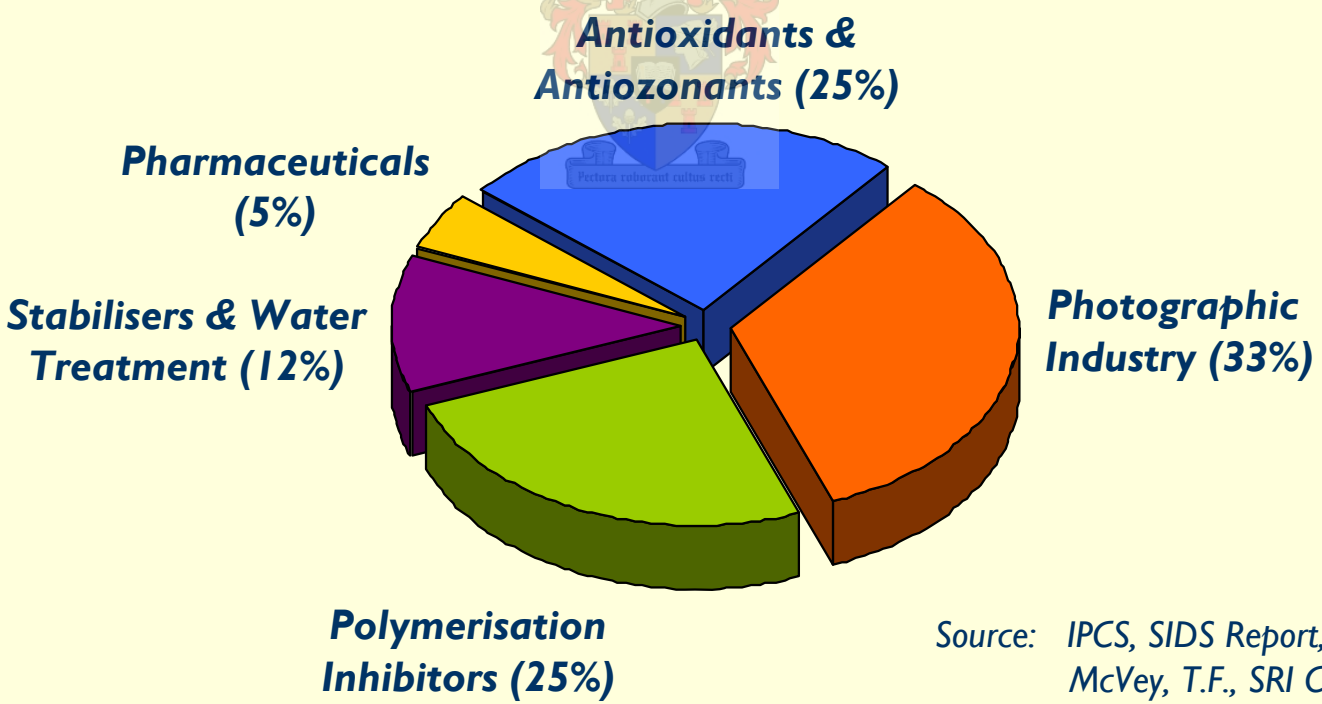

Source: IPCS, SIDS Report, 1994
McVey, T.F., SRI Consulting, 2003

OXIDISING AGENT

Choice of H_2O_2 as Oxidising Medium

- **Choices for oxidation reactions**
  - *Oxygen/air (g), H_2O_2, long-chain organic hydro-peroxides (e.g., TBHP)*
- **H_2O_2 as oxidant offers several advantages …….**
  - *Safe and easy to handle*
  - *Mild reaction temperatures ⇒ higher product selectivity possible*
  - *Relatively inexpensive*
  - *High active-oxygen content*
  - *Multi-phase mass-transfer problems can be avoided*
  - *Only reaction by-product is water ⇒* ***"green" chemistry***

CATALYST PROPERTIES

Choice and Synthesis of Suitable Ti-substituted Zeolites

- **Framework topology & pore geometry**
  - *Accessibility to active sites inside the micropores, e.g., TS-1 (0.55 nm) vs. Ti-β (0.65 nm): 'molecular-sieve' effect offers selective reaction pathways*
- **Framework modifications**
  - *Post-synthesis vs. isomorphous substitution of Ti into SiO_2 framework*
- **Framework[1, 2] & surface acidity[3]**
  - *Acidic impurities, e.g., $Al^{3+}/Fe^{3+} \Rightarrow$ unfavourable to selective oxidations*
- **Crystallite dimensions[4, 5]**
  - *Small crystallites offer less M/T limitations ॐ better catalytic performance*
- **Catalyst polarity[6]**
  - *Enhanced mobility and adsorption of organics in hydrophobic channels*

[1] Camblor et al., 1993 [2] Camblor et al., 1996 [3] Selli et al., 2004 [4] Wilkenhöner et al., 2001 [5] van der Pol et al., 1992 [6] Blasco et al., 1998

CATALYST PROPERTIES

Influence of Acid Sites: Consecutive Oxidation of Products

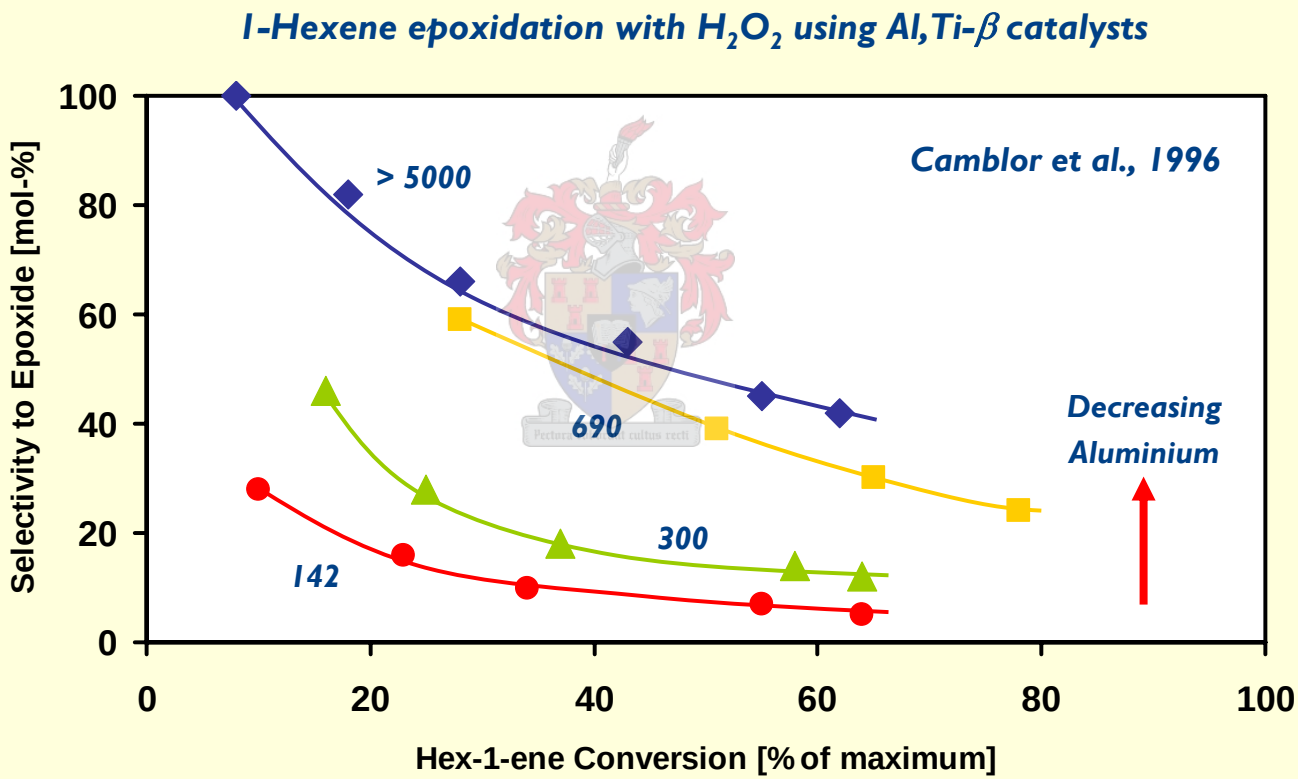

Simultaneous presence of Al decreases efficiency of catalytic process ⇒ use of *Al-free* samples suppresses acidity

MECHANISTIC IMPLICATIONS

Active Site Formation & Coordinated Active Site Complexes

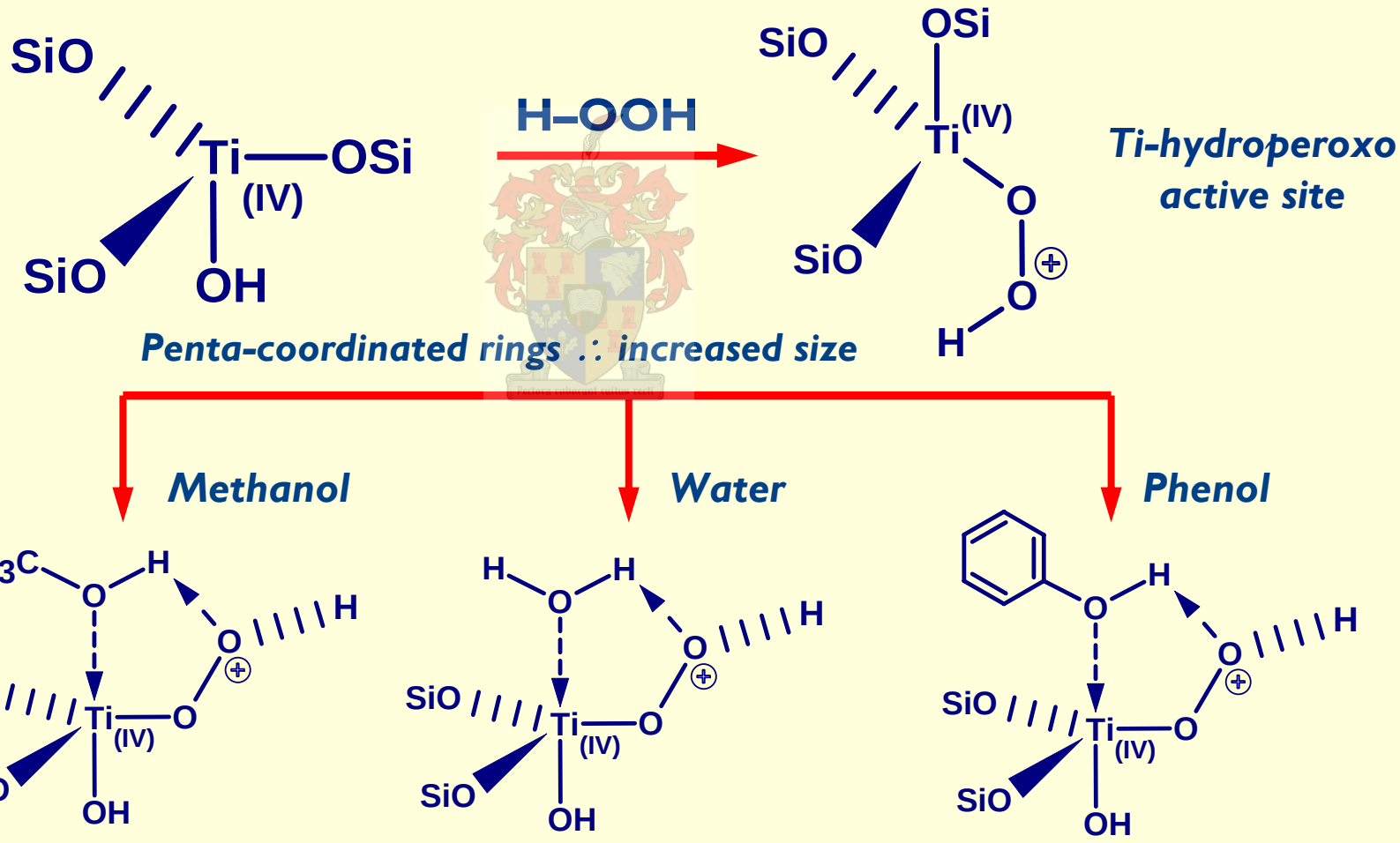

SOLVENT CONSIDERATIONS

Observed Effects in Different Solvents Of Ti-Silicalites

- **Solvent strongly influences activity and product selectivity[7, 8, 9]**
  - *Protic vs. non-protic molecules interact differently with active metal site*
  - *Protic ⇒ Mainly Hydroquinone; Aprotic ⇒ Mainly Catechol at surface sites*

- **Relative effects on selectivity and activity of water and methanol in co-solvent mixtures are contrasting[10]**
  - *Competitive adsorption at Ti-hydroperoxo sites as methanol fraction increases*
  - ***Pure water:*** *Increases relative adsorption of phenol over methanol ⇒ higher reaction rate & phenol conversion, lower hydroquinone selectivity*
  - ***Pure methanol:*** *Active site coordination with methanol over phenol ⇒ bulky intermediate ⇒ geometric constraint promotes hydroquinone selectivity*

[7] Wilkenhöner et al., 2001 [8] Mal et al., 1995 [9] van der Waal et al., 1997 [10] Callanan et al., 2004

SOLVENT COMPOSITION

Selectivity & Activity Effects over Al-free Ti-β

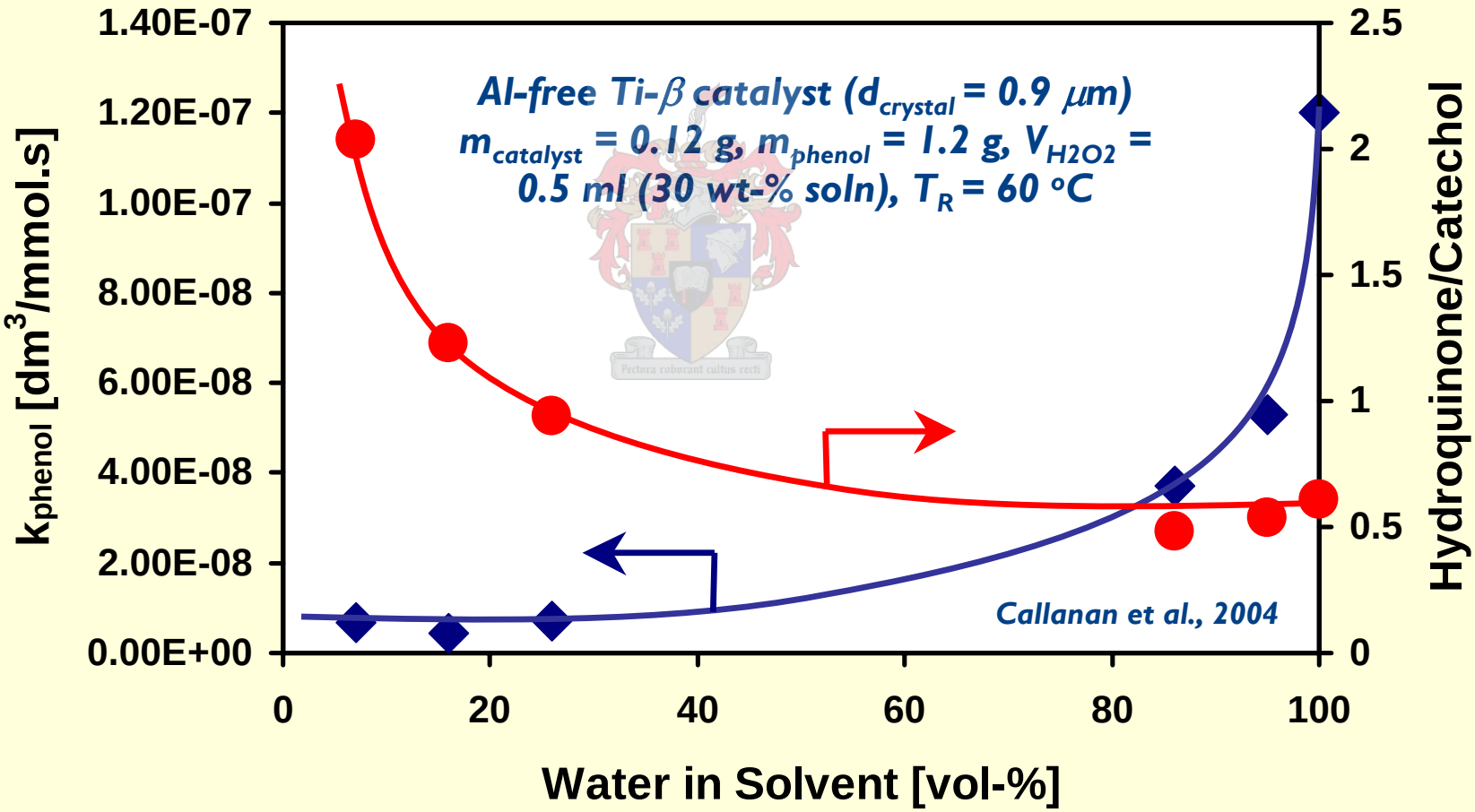

PRODUCT SELECTIVITY

TS-1 vs. Al-free Ti-β in Water & Methanol Solvents

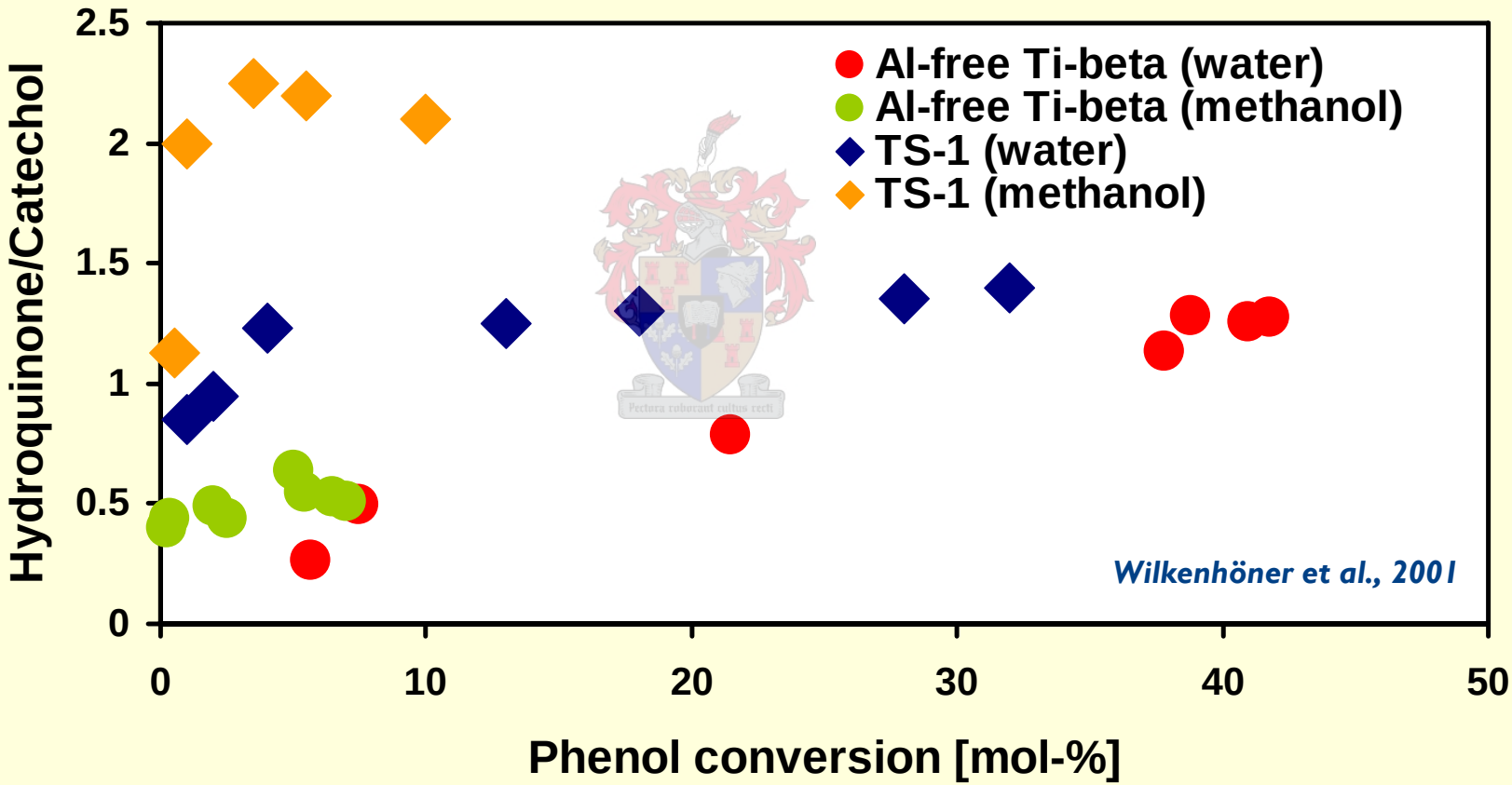

$m_{catalyst}$ = 0.12 g, m_{phenol} = 1.2 g, V_{H2O2} = 0.6 ml (30 wt-% soln), T_R = 60 °C

PEROXIDE ADDITION EFFECTS

How Does the Mode of H_2O_2 Addition Affect the Reaction?

- **Cyclohexene epoxidation on silica-supported catalysts[11]**
  - *Slow H_2O_2 addition improves yield and selectivity for direct epoxidation products over hydrophobic catalysts, and reduces catalyst deactivation*
- **Addition of dilute H_2O_2 solution for phenol hydroxylation over TS-1[12,13,14]**
  - *Single-portion vs. drop-wise addition effects on peroxide efficiency and product distribution*
  - *Higher H_2O_2 efficiency and hydroquinone selectivity under drop-wise addition*
  - *Product selectivity as a function of phenol conversion …???*

Low addition concentration levels of H_2O_2 are advantageous

[11] Fraile et al., 2003 [12] Thangaraj et al., 1991 [13] Ratnasamy et al., 1996, 2003 [14] Wilkenhöner et al., 2001

PROBLEM STATEMENT & HYPOTHESIS

- Currently no comparative study with Ti-zeolites varying the initial H_2O_2 concentration and in different solvents/co-solvent mixtures
- Currently no investigation of peroxide addition effects using Al-free Ti-β
- Currently no study of peroxide addition in water/methanol co-solvent mixtures for Al-free Ti-β or TS-1

SPECIFIC OBJECTIVES

AIMED TO INVESTIGATE:

- **Peroxide concentration effects in phenol hydroxylation over Al-free Ti-β and TS-1 in methanol and water solvent**
  - *Initial concentration varied in range 0.55 to 5 vol-% of total volume*
  - *Phenol-H_2O_2 ratio in range 10 to 1.1*
- **Combined effects of solvent composition and peroxide concentration on product selectivity and catalyst activity**
- **Effects of method of peroxide addition in a pseudo semi-batch reactor: Is it at all advantageous?**
  - *H_2O_2 added in discrete amounts over 4-4½ hours: 0.1 ml per hr & 0.05 ml per 30 min*

EXPERIMENTAL SETUP

Experimental Setup & Product Analysis

- **24 ml glass batch-reactor**
- **Continuous stirring (1000 rpm)**
- **0.2 ml samples at intervals**
  - *Reaction terminated after 12 h*
- **Analysis**
  - *HPLC → aromatics content*
  - *Iodometric titration → residual H_2O_2 concentration*
  - *TG analysis → tar attached to deactivated/used catalyst*

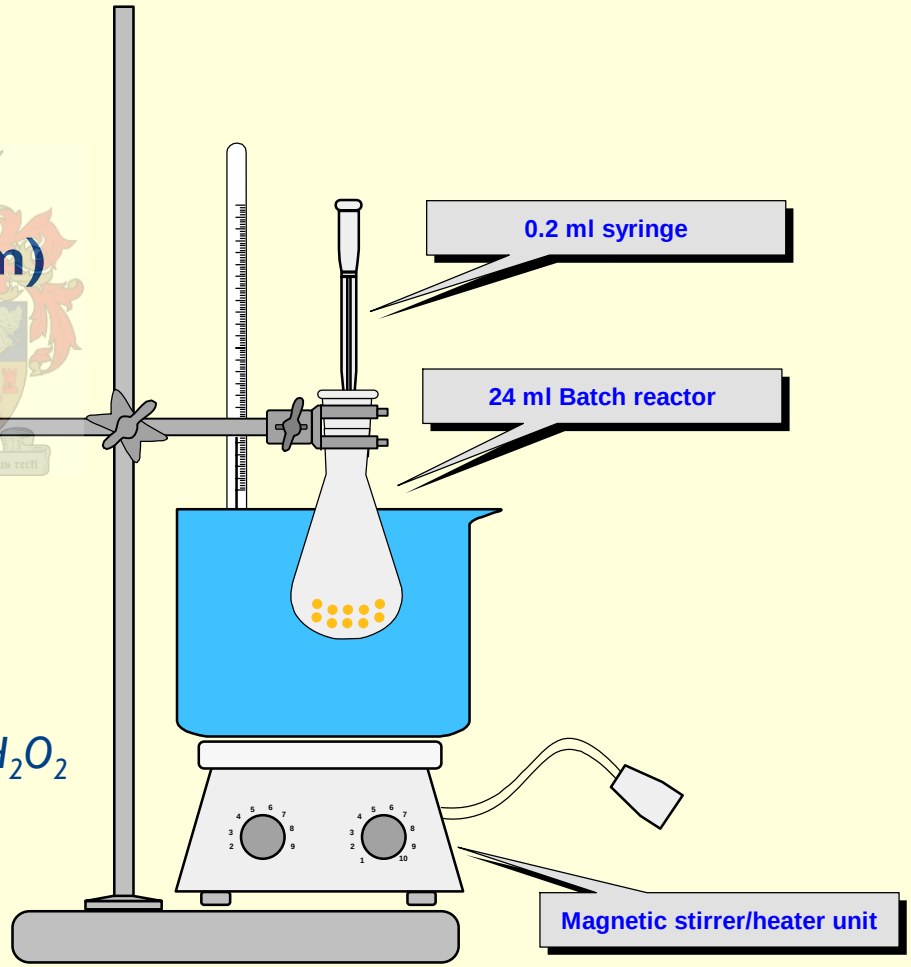

CRYSTALLITE MORPHOLOGY & CRYSTAL SIZE

SEM Micrographs of Zeolite Beta & TS-1 Crystals

Al-free Ti-β
Square bibyramids, $d_{Crystal}$ ≈ 0.9 μm

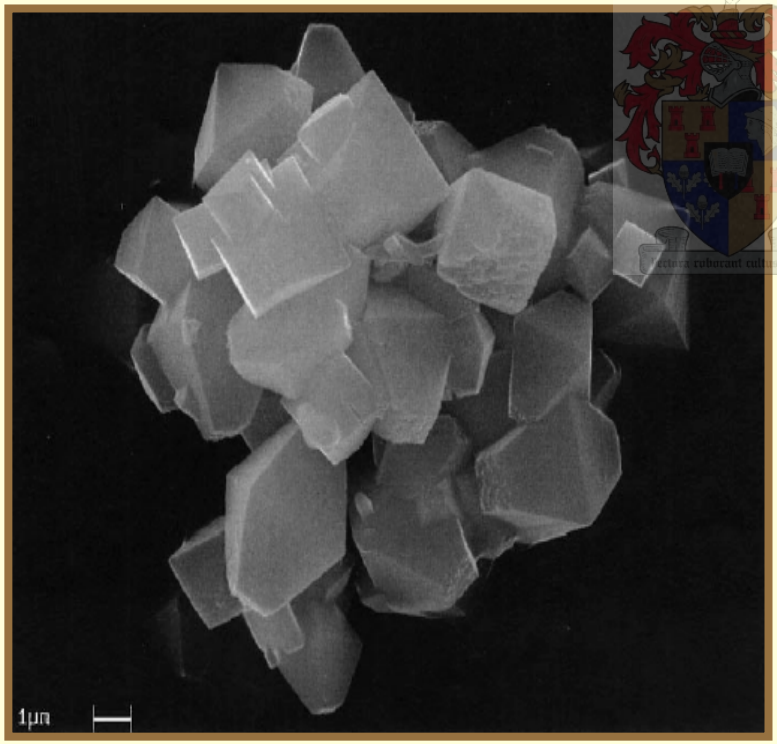

TS-1
Cubic morphology, $d_{Crystal}$ ≈ 0.1 μm

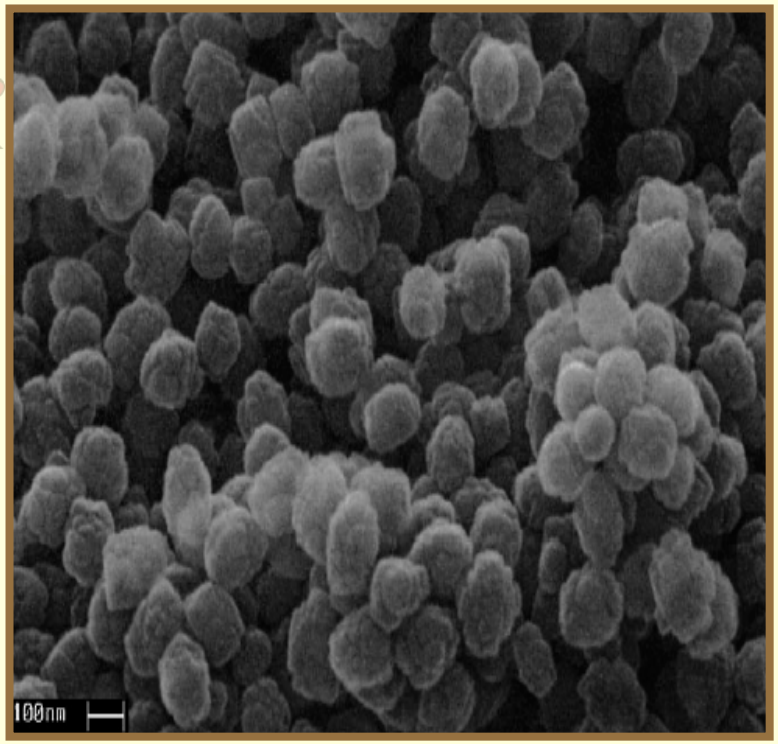

PHENOL CONVERSION

Al-free Ti-β Catalyst, Water Solvent

Phenol conversion vs. time for different starting volumetric fractions of H_2O_2 (WATER solvent)

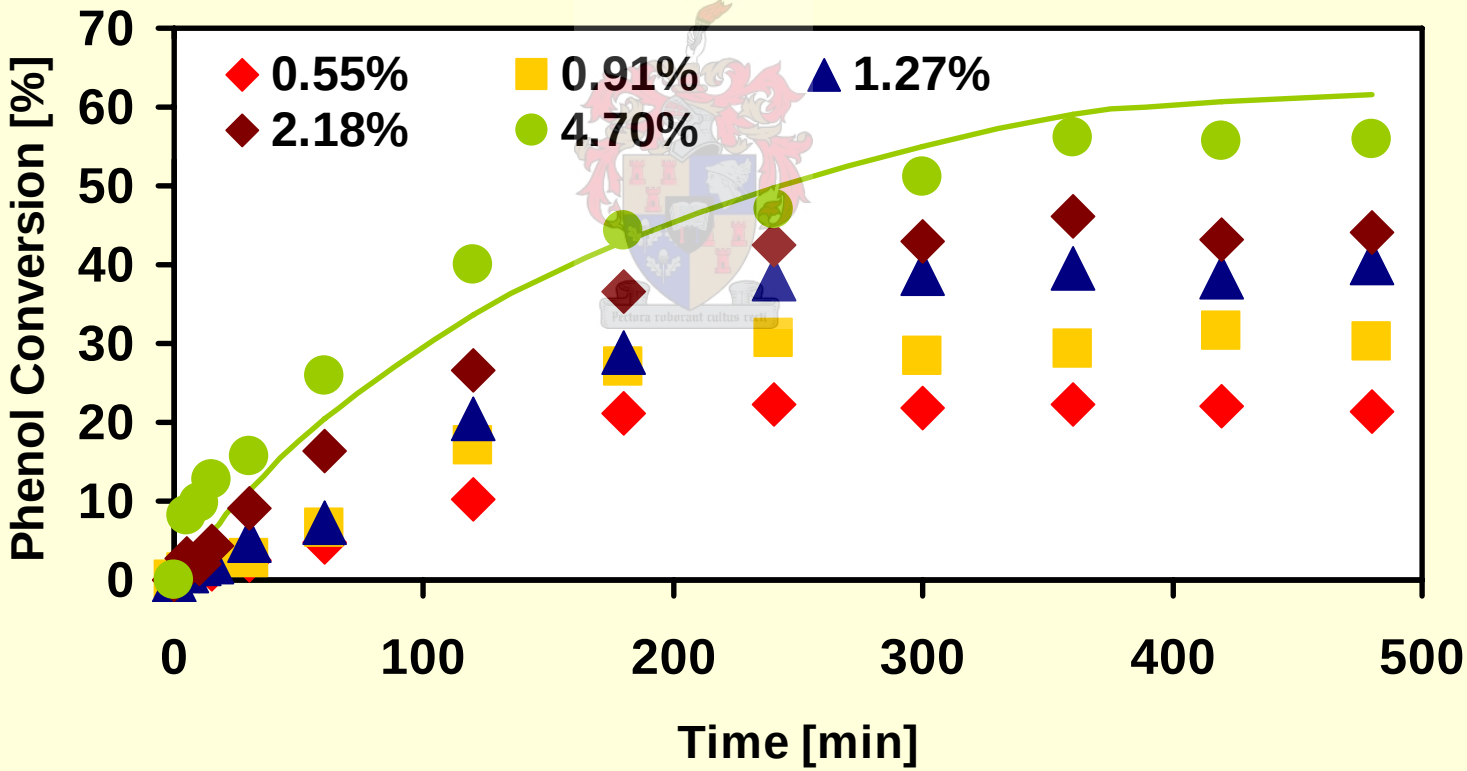

Al-free Ti-beta ($d_{crystal}$ = 0.9 μm), $m_{catalyst}$ = 0.12 g, m_{phenol} = 1.2 g, T_R = 60 °C

PHENOL CONVERSION

Al-free Ti-β Catalyst, Methanol Solvent

Phenol conversion vs. time for different starting volumetric fractions of H_2O_2 (METHANOL solvent)

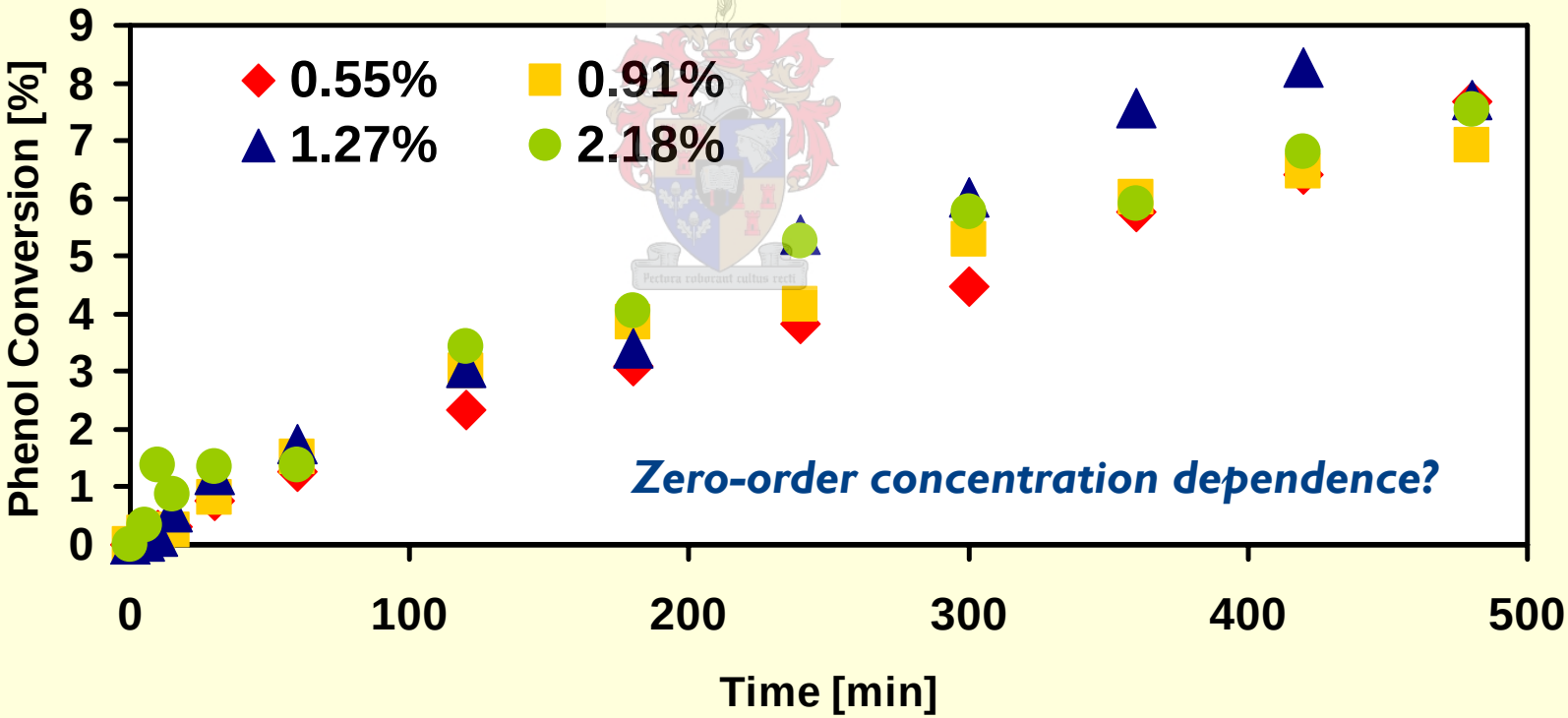

Al-free Ti-beta ($d_{crystal}$ = 0.9 μm), $m_{catalyst}$ = 0.12 g, m_{phenol} = 1.2 g, T_R = 60 °C

RATE FITTING & KINETICS (WATER)

Phenol Rate Constants for 2nd Order Reaction Kinetics

$$-r_{Ph} = k_{Ph} \cdot C_{Ph} \cdot C_{Ox} = C_{Ph,0} \cdot \frac{dX_{Ph}}{dt}$$

2nd order model

$$\Rightarrow \frac{dX_{Ph}}{dt} = k_{Ph} \cdot C_{Ph,0} \cdot (1 - X_{Ph}) \cdot (\theta_{Ox} - X_{Ph})$$

k_{Phenol} [dm³/mmol.s]		
H_2O_2 [vol-%]	Fitted for 480 min	Fitted for 120 min
0.55	1.256×10^{-7}	1.018×10^{-7}
0.91	1.358×10^{-7}	9.114×10^{-8}
1.27	1.275×10^{-7}	7.765×10^{-8}
2.18	1.050×10^{-7}	7.508×10^{-8}
4.70	1.010×10^{-7}	4.882×10^{-8}

- Overall 2nd order kinetics fit best in water solvent
  - *Better overall kinetic fit obtained over 480 minutes*

Rate constant is independent of changing H_2O_2 concentration

RATE FITTING & KINETICS (MeOH)

Phenol Rate Constants for 2nd and 1st Order Reaction Kinetics

$$-r_{Ph} = k_{Ph} \cdot C_{Ph} \cdot C_{Ox} = C_{Ph,0} \cdot \frac{dX_{Ph}}{dt}$$ *1st order model*

$$\Rightarrow \frac{dX_{Ph}}{dt} = k_{Ph} \cdot C_{Ph,0} \cdot (1 - X_{Ph})$$

k_{Phenol} [dm^3/mmol.s]		
H_2O_2 [vol-%]	2nd order kinetics	1st order kinetics
0.55	1.729×10^{-8}	2.73×10^{-6}
0.91	9.766×10^{-9}	2.96×10^{-6}
1.27	7.4×10^{-9}	3.3×10^{-6}
2.18	5.540×10^{-9}	3.02×10^{-6}

- 1st order kinetics provides a good fit only for low initial H_2O_2 concentrations in methanol → 2nd order is still overall best fit for all concentrations

RATE FITTING & KINETICS (MeOH)

Model Comparison

1st and 2nd order kinetic fits of the phenol conversion in methanol solvent

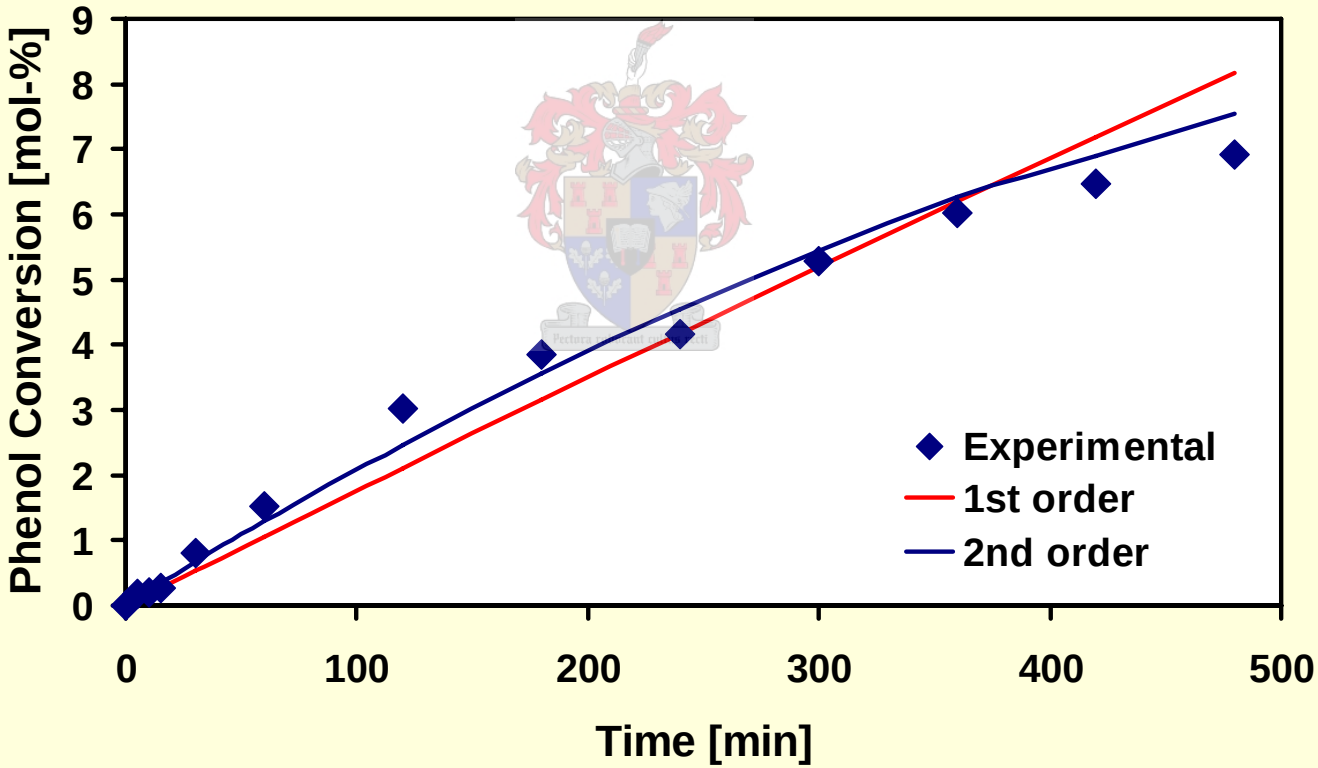

Al-free Ti-β ($d_{crystal}$ = 0.9 μm), $m_{catalyst}$ = 0.12 g, m_{phenol} = 1.2 g, V_{H2O2} = 0.35 ml, V_{MeOH} = 0.15 ml, T_R = 60 °C

HYDROQUINONE SELECTIVITY

Al-free Ti-β Catalyst

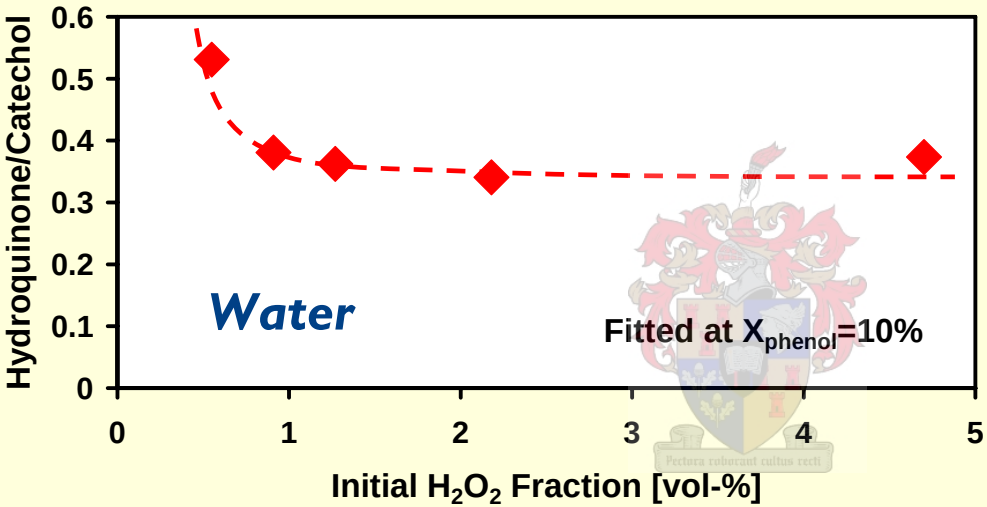

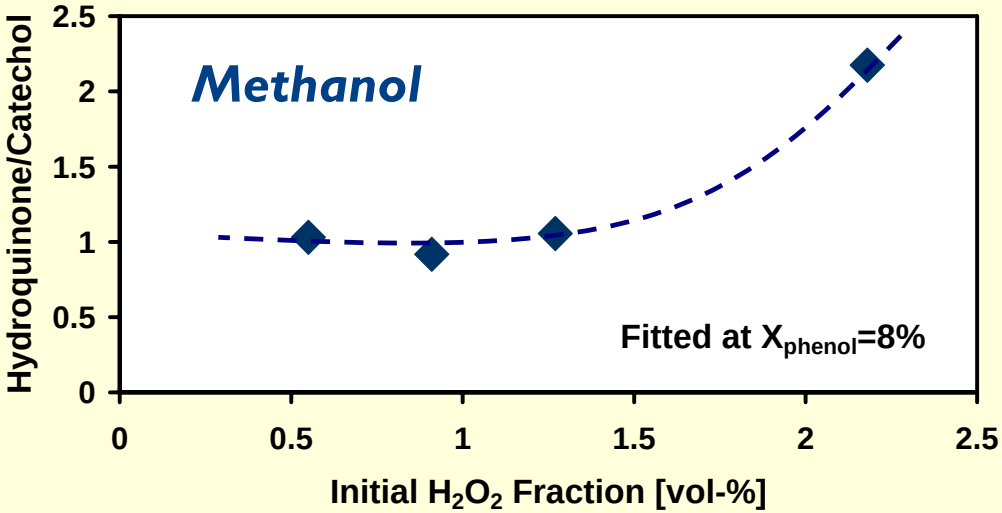

Hydroquinone formation favoured in methanol solvent

1.27 vol-% H_2O_2 appears to be a threshold concentration in both solvents

OPPOSITE effects on selectivity in each solvent above this volume fraction

***WATER:* const. selectivity**
***METHANOL:* selectivity ↑**

PHENOL CONVERSION

TS-1 Catalyst, Methanol Solvent

Phenol conversion vs. time for different starting volumetric fractions of H_2O_2 (METHANOL solvent)

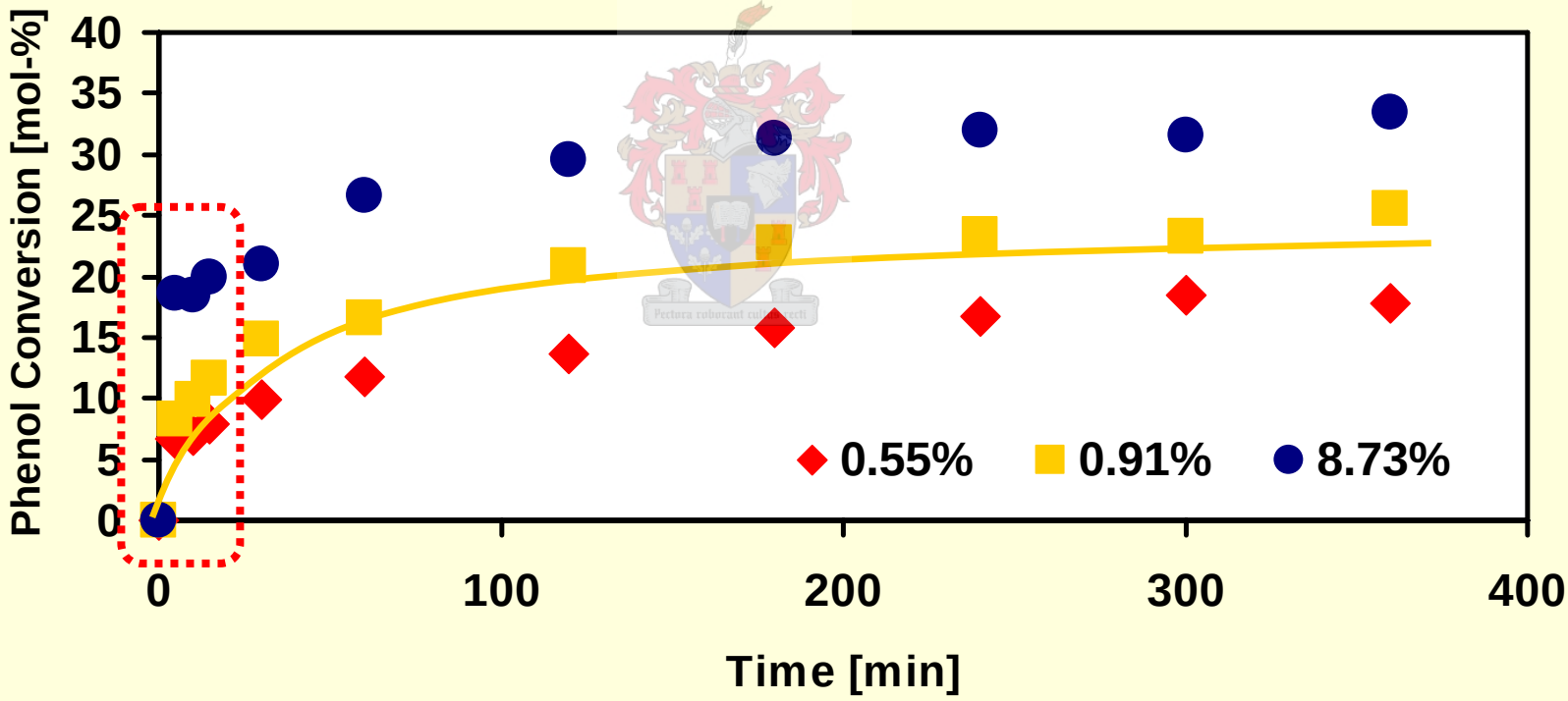

TS-1 ($d_{crystal}$ = 0.1 μm), $m_{catalyst}$ = 0.12 g, m_{phenol} = 1.2 g, T_R = 60 °C

More rapid phenol conversion as initial H_2O_2 concentration increases

HYDROQUINONE SELECTIVITY

TS-1 Catalyst

Hydroquinone selectivity vs. phenol conversion for different starting volumetric fractions of H_2O_2 (METHANOL solvent)

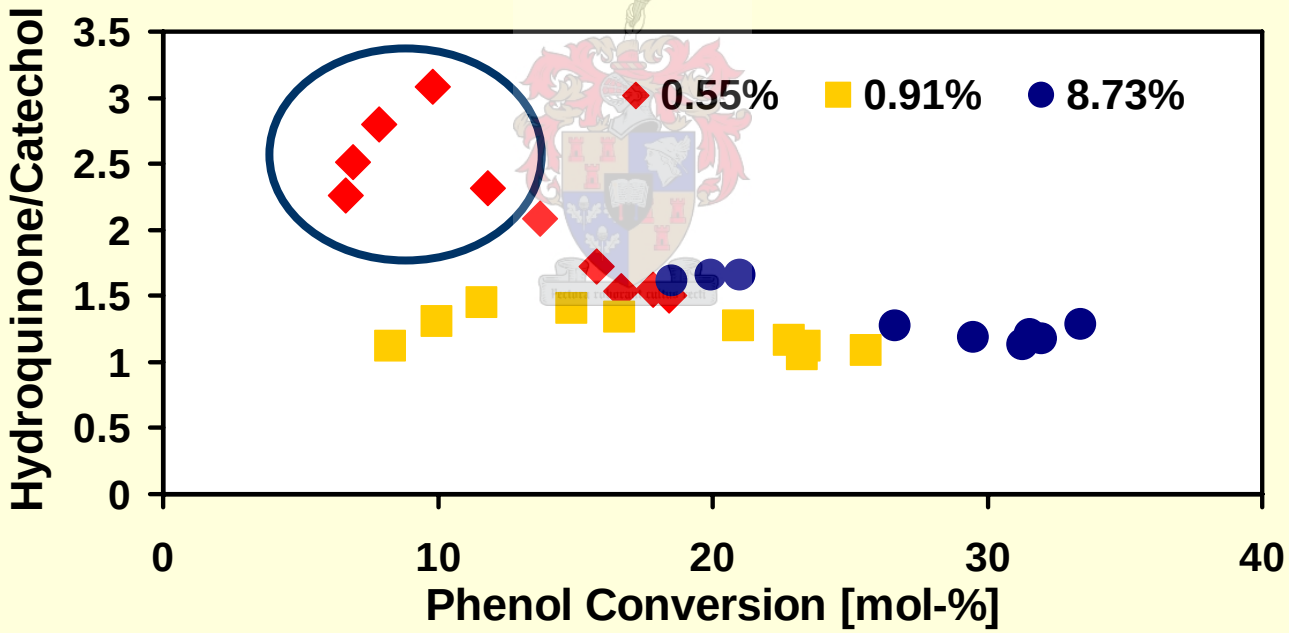

- Initial increase most pronounced at low initial H_2O_2 concentrations
- Constant selectivity approached at higher phenol conversions

MECHANISTIC IMPLICATIONS

Steric Hindrance of Coordinated Active Site Complexes

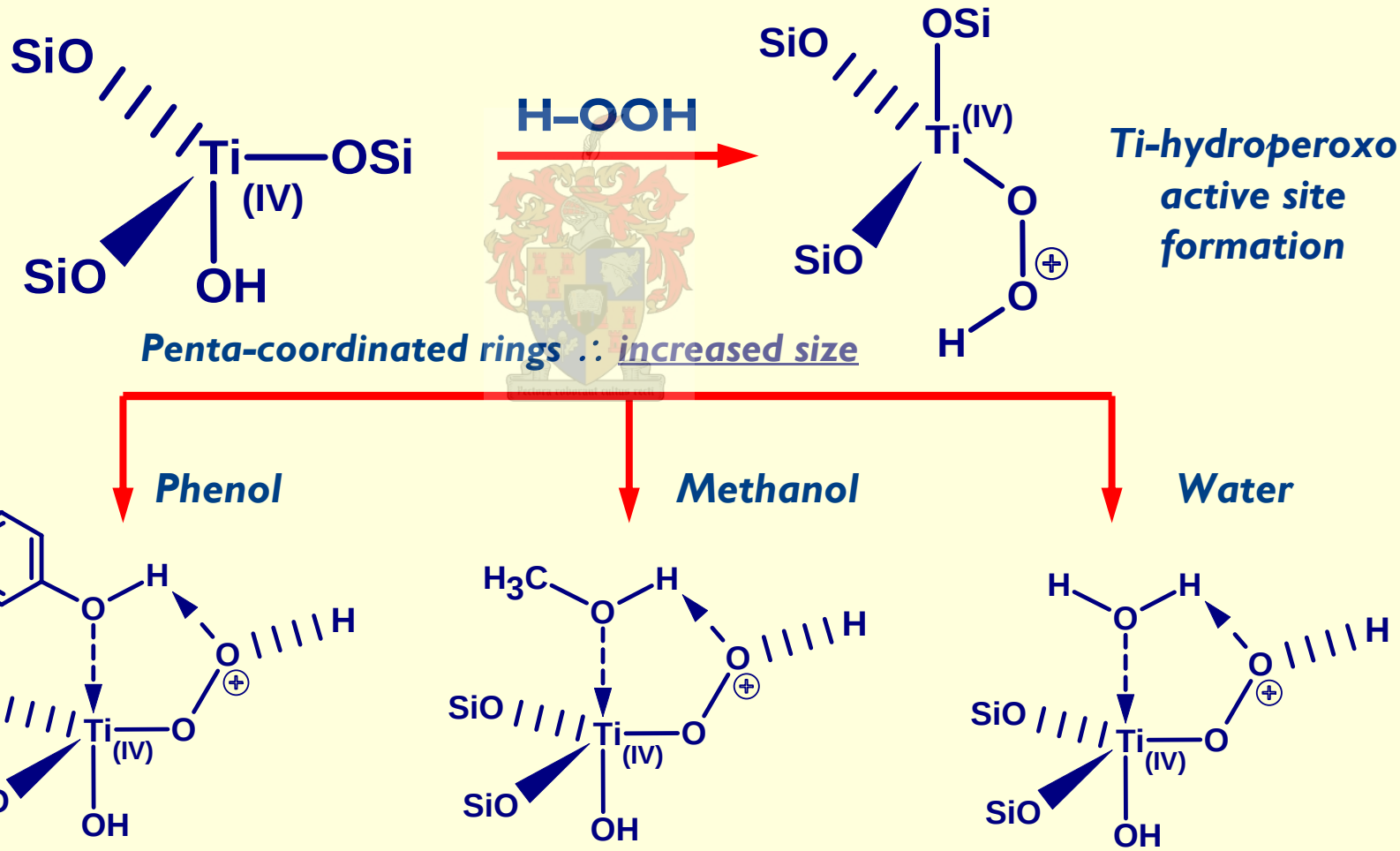

PEROXIDE ADDITION EFFECTS

Phenol Conversions for Al-free Ti-β & TS-1 Catalysts

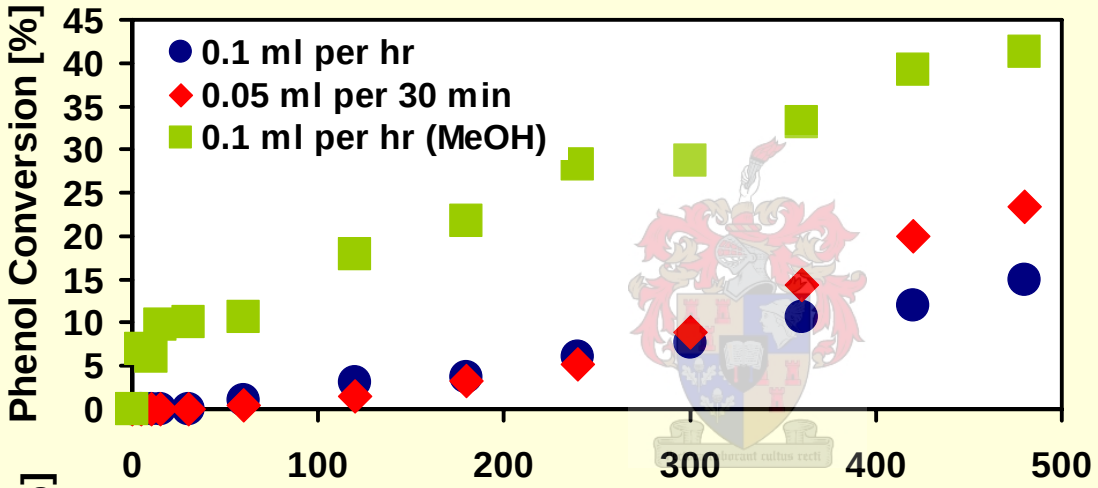

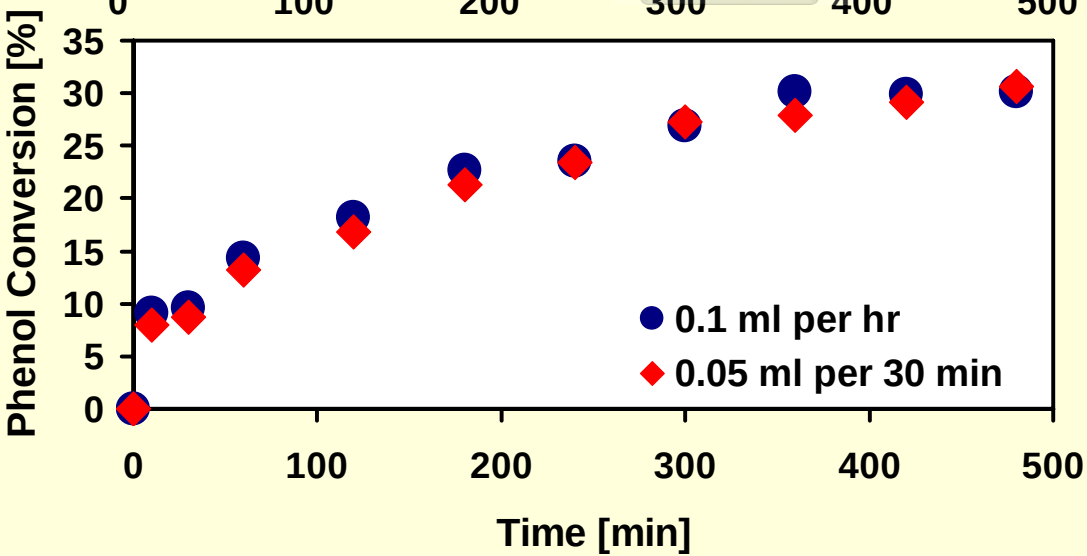

Al-free Ti-β

Positive effect of more discrete addition in water on conversion

Incomplete reaction?

TS-1

Little influence of H_2O_2 addition on rate of conversion

PEROXIDE ADDITION EFFECTS

Product Selectivities

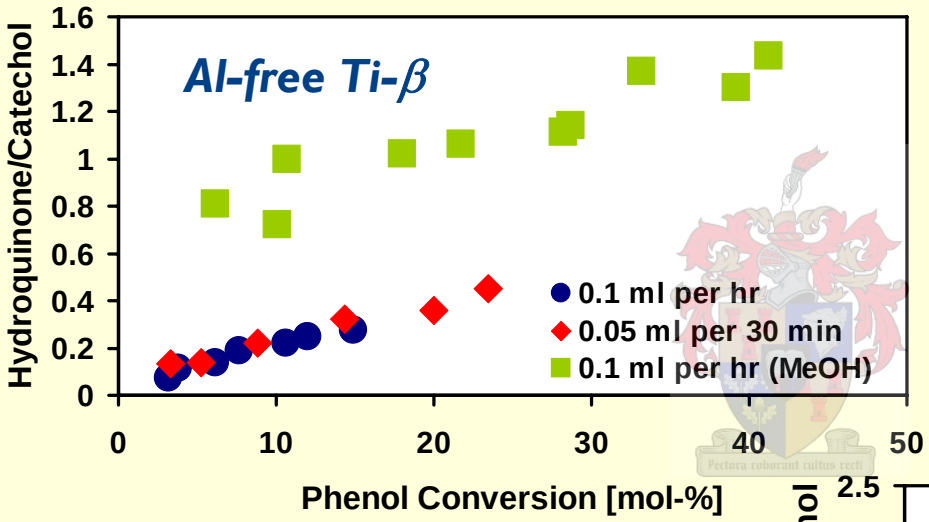

- *Ti-β:* *- selectivity ↑ as X_{phenol} ↑*
  - p/o < 0.4 in water
  - p/o >1 in methanol
  - Improvement over TS-1
- *TS-1:* *- selectivity ↓ as X_{phenol} ↑*

- *Methanol adsorption dominates at low conversions*
- *Favoured for more discrete H_2O_2 additions*
- *Reduced shape selectivity*
- *Constant selectivity is approached at high conversions*

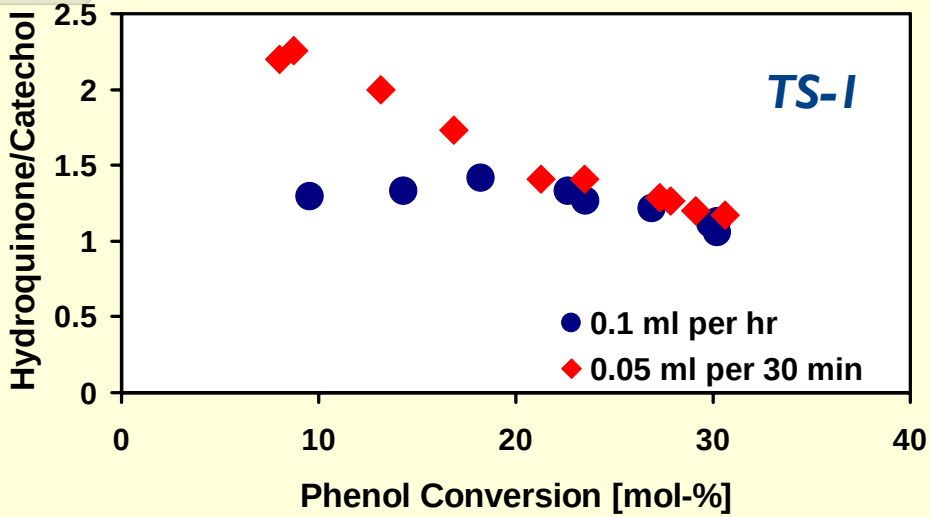

TAR FORMATION

Effect of H_2O_2 Concentration & Solvent Polarity

- **Tar formation is reduced with lower initial H_2O_2 concentrations in both solvents for TS-1 and Al-free Ti-β**
  - *Less free-peroxide for consecutive product over-oxidation*
  - *Reduced solvent polarity with lower water concentrations increases solubility*
- **Less polar methanol favours tar dissolution**
  - *Hydroquinone selectivity in micropores is favoured with high methanol fractions in the solvent in which tars are soluble*
- **Discrete H_2O_2 addition also promotes reduced tar formation**
  - *Visual confirmation of less tar formation early on in the reaction for slower peroxide addition rate*
  - *Less tar compared to single-portion additions*

BATCH vs. DISCRETE ADDITION

Relative Hydroquinone Selectivity

- **Discrete peroxide addition improves hydroquinone selectivity**

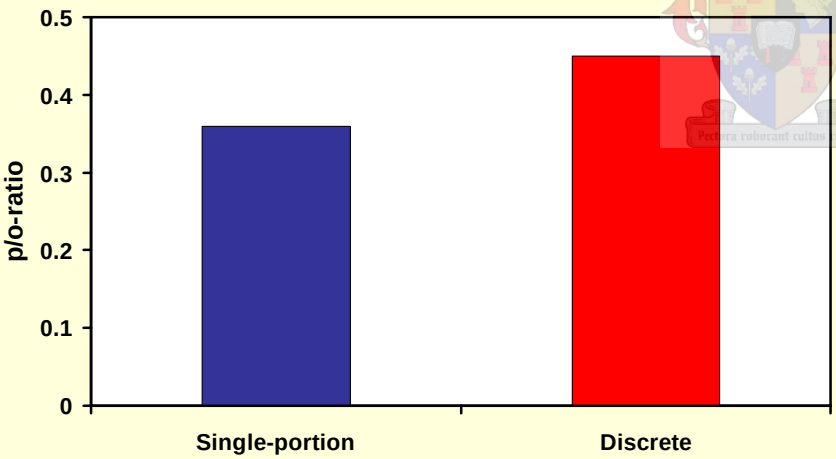

Al-free Ti-β

Water solvent

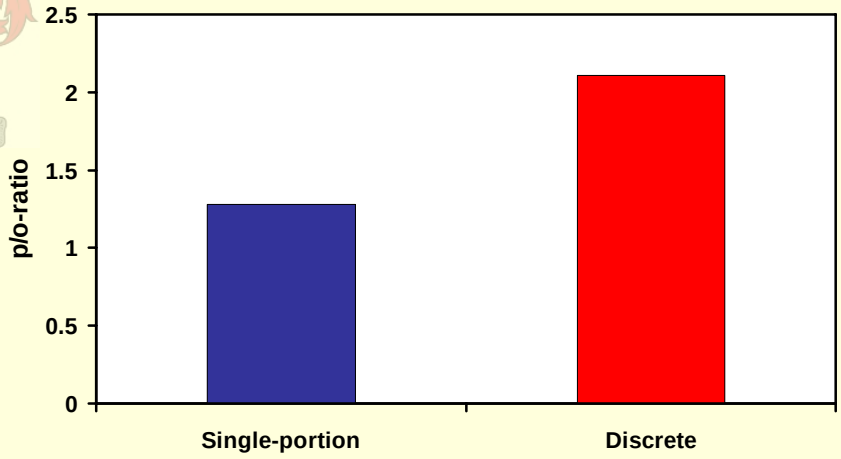

TS-1

Methanol solvent

SUMMARISED CONCLUSIONS

Batch-mode Hydroxylation Reactions

- Phenol conversion over Al-free Ti-β is enhanced by higher peroxide concentrations, especially in water solvent
- Over Al-free Ti-β methanol solvent inhibits phenol access in micropores resulting in lower conversions → conversion largely independent of peroxide concentration
- Second-order kinetic modelling fits experimental data well in both solvents
- Reaction rate constant is independent of H_2O_2 concentration in water solvent over Al-free Ti-β and TS-1, confirming accuracy of kinetic model
- Using TS-1 phenol reaction rate is also independent of peroxide concentration.
- Over Al-free Ti-β, hydroquinone selectivity in methanol is enhanced by higher initial H_2O_2 concentrations
- In water and over Al-free Ti-β, hydroquinone selectivity is below *ca.* 0.6 for all H_2O_2 fractions → no positive influence on selectivity
- Over TS-1, higher selectivity is obtained at lower initial H_2O_2 concentrations (p/o-ratios exceeding 3); constant selectivity is reached at higher X_{phenol}

SUMMARISED CONCLUSIONS

Discrete Peroxide Addition

- **Discrete addition confirms that hydroquinone formation is favoured at low peroxide concentrations**
- **Over Al-free Ti-β, hydroquinone selectivity increases, while over TS-1 selectivity to catechol increases with X_{phenol}**
- **Competitive adsorption effects become increasingly important as more peroxide is added → favourable for catechol formation**
- **Slow peroxide addition offers preferential hydroquinone formation compared to single-portion additions (p/o-ratio *ca.* 2 times higher)**
- **Lower peroxide concentrations with addition over 4.5 hours result in reduced tar formation on both catalysts in both solvents**

ACKNOWLEDGMENTS

- My supervisor, Dr. Linda Callanan
- Ms. Stephanie La Grange & Mrs. Helen Divey for assistance with HPLC analysis (UCT)
- Mrs. Hanlie Botha for assistance with HPLC analysis (US)
- NRF & Stellenbosch University for financial assistance

END OF PRESENTATION

Thank you

Questions ……

ADDITIONAL SLIDES

- Mechanistic Implications of Hydroquinone Formation
- Carbocation Intermediates
- Hydroquinone Selectivity (TS-1 Catalyst)
- Concentration-time Profile

MECHANISTIC IMPLICATIONS

Reaction Mechanism for Hydroquinone Formation

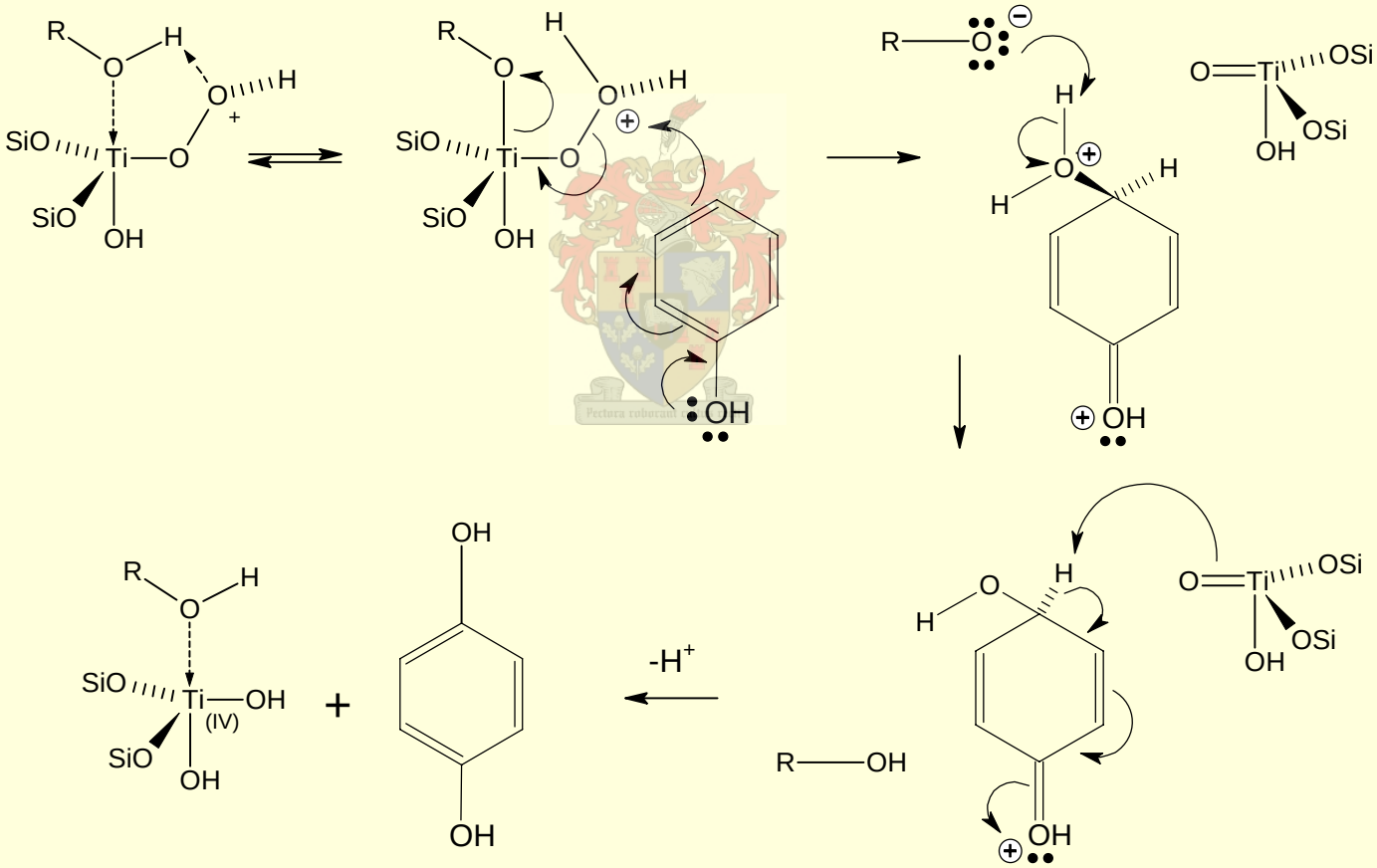

CARBOCATION INTERMEDIATES

Resonance Stabilisation at ortho and para positions

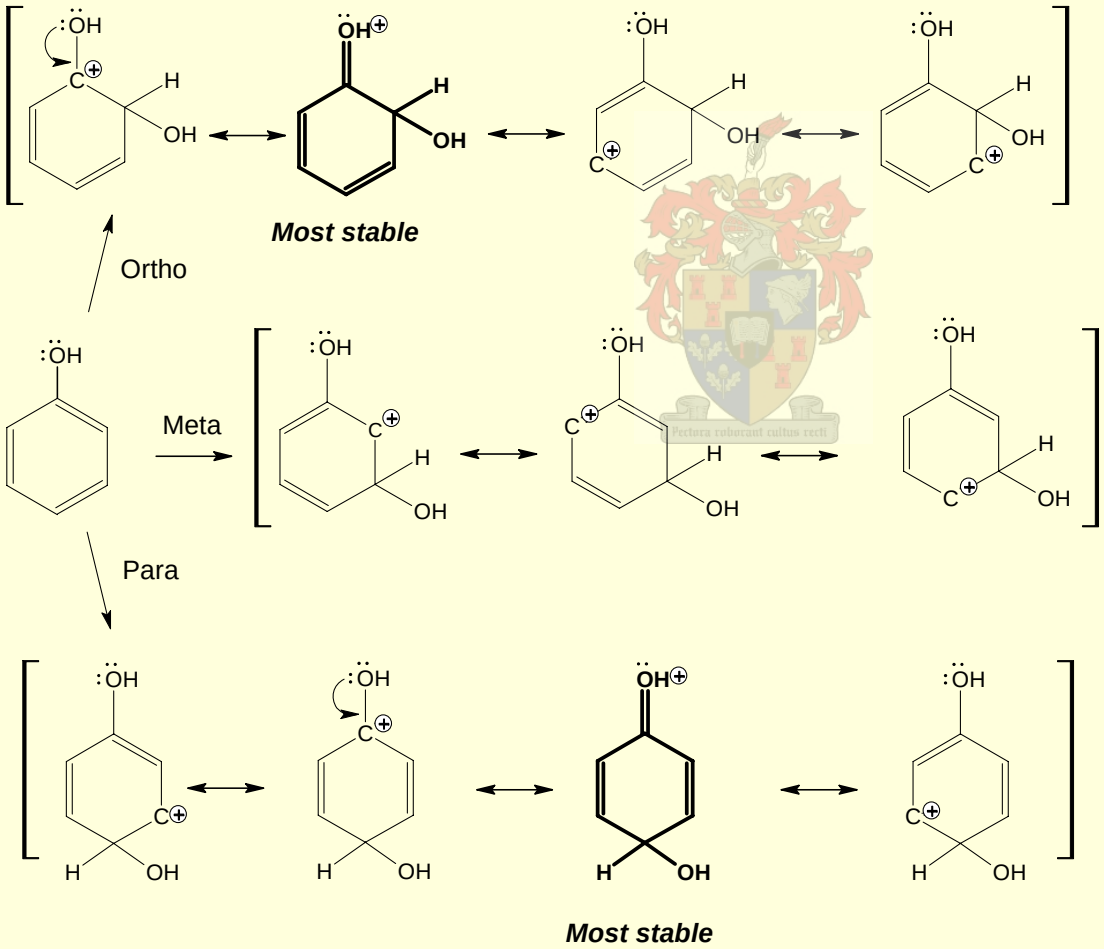

- *Ortho & para complexes are stabilised through delocalisation of the positive charge in the benzene ring*
- *These positions are lower in energy → form faster than meta-substituted complex*
- *Probability for resorcinol formation is thus lower than hydroquinone or catechol*

HYDROQUINONE SELECTIVITY

TS-1 Catalyst

Hydroquinone selectivity vs. time for different starting volumetric fractions of H_2O_2 (METHANOL solvent)

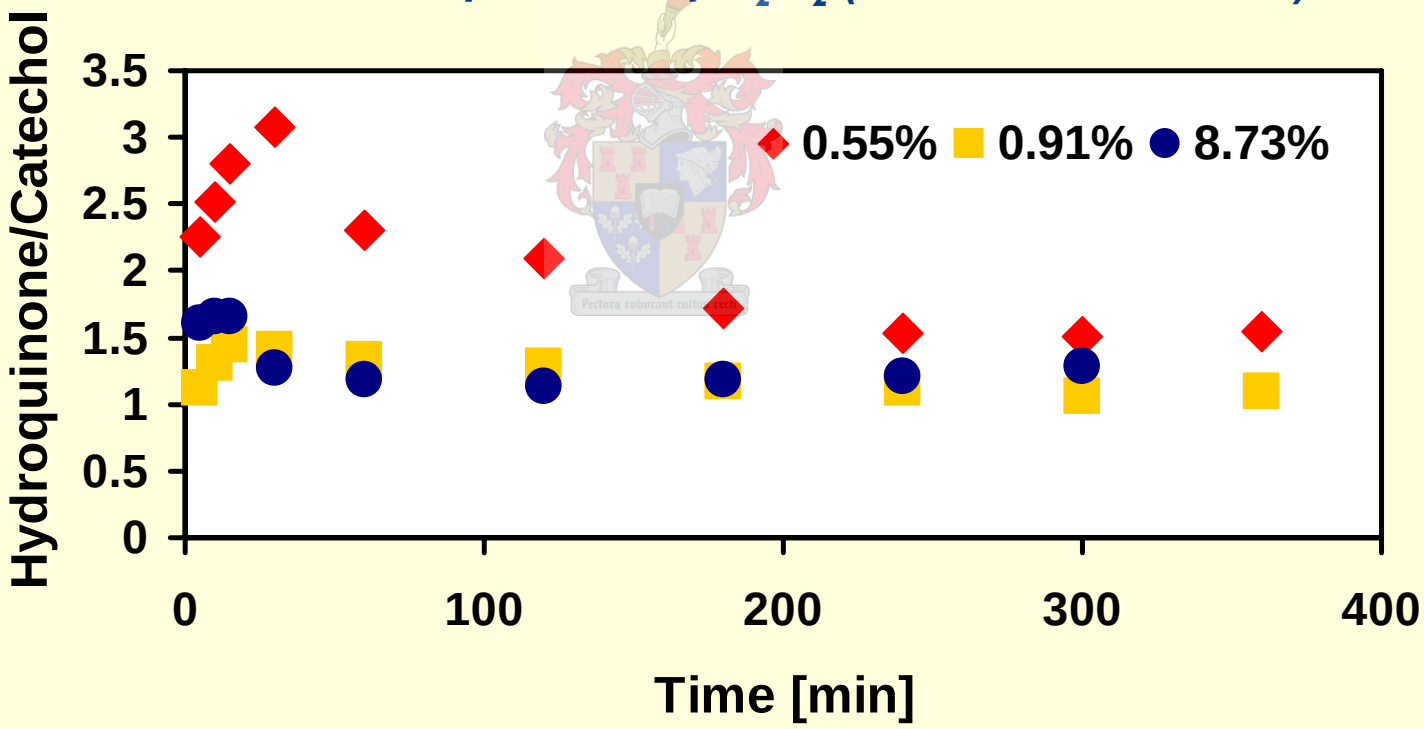

TS-1 ($d_{crystal}$ = 0.1 μm), $m_{catalyst}$ = 0.12 g, m_{phenol} = 1.2 g, T_R = 60 °C

CONCENTRATION-TIME PROFILE

TS-1 Catalyst, 0.55 vol-% H_2O_2, Methanol Solvent

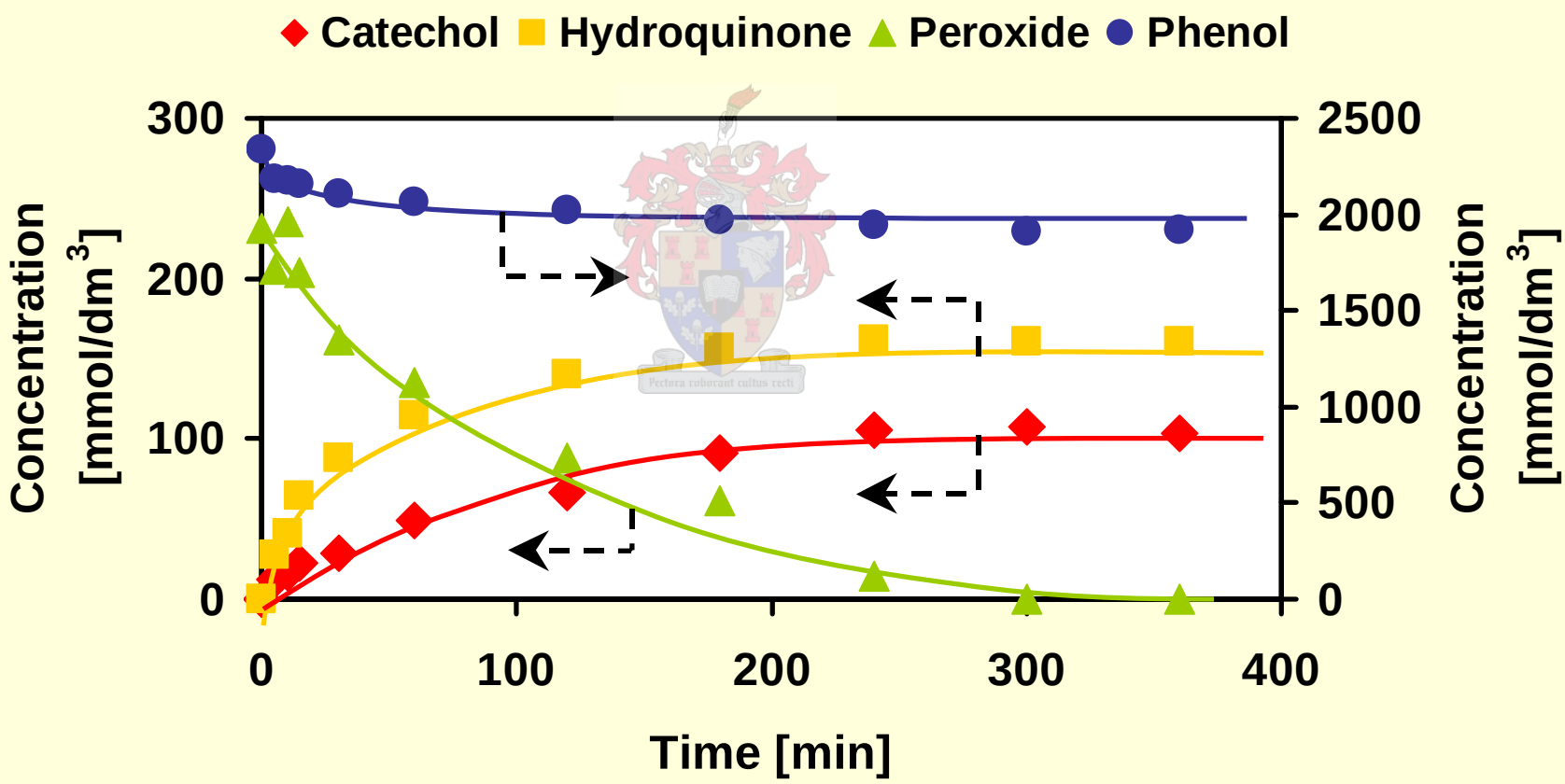

TS-1 ($d_{crystal}$ = 0.1 μm), $m_{catalyst}$ = 0.12 g, m_{phenol} = 1.2 g, V_{H2O2} = 0.15 ml, V_{MeOH} = 5.35 ml, T_R = 60 °C

Oxidant Concentration Effects in the Hydroxylation of Phenol over Ti-based Zeolite Catalysts

The effect of H_2O_2 on the Reaction Activity and Product Selectivity on Al-free Ti-β and TS-1 catalysts

Robert Burton & Linda H. Callanan
Department of Process Engineering
University of Stellenbosch

14 November 2005, CATSA Conference, Johannesburg

BACKGROUND

Selective Oxidation Reactions: Why the Interest and Concern?

- **Partial oxidation catalysis**
  - *Ranges from large-scale production of commodities to fine-chemicals and pharmaceuticals synthesis*
- **Research motivators for selective oxidations**
  - *Oxidations are complex reactions, difficult to control: improved control is advantageous*
  - *Alternative process development to current stoichiometric oxidations: increased pressure from environmental legislation*
  - *Importance of separation costs: by-product waste elimination*
  - *Synthesis of high-value chemicals: enhanced selectivity for most valuable products*

PHENOL HYDROXYLATION

Reaction Scheme & Product Uses: Why Enhanced Selectivity?

- **Hydroxylation to dihydroxybenzenes**
  - *Mixture of hydroquinone and catechol, and residual resorcinol*

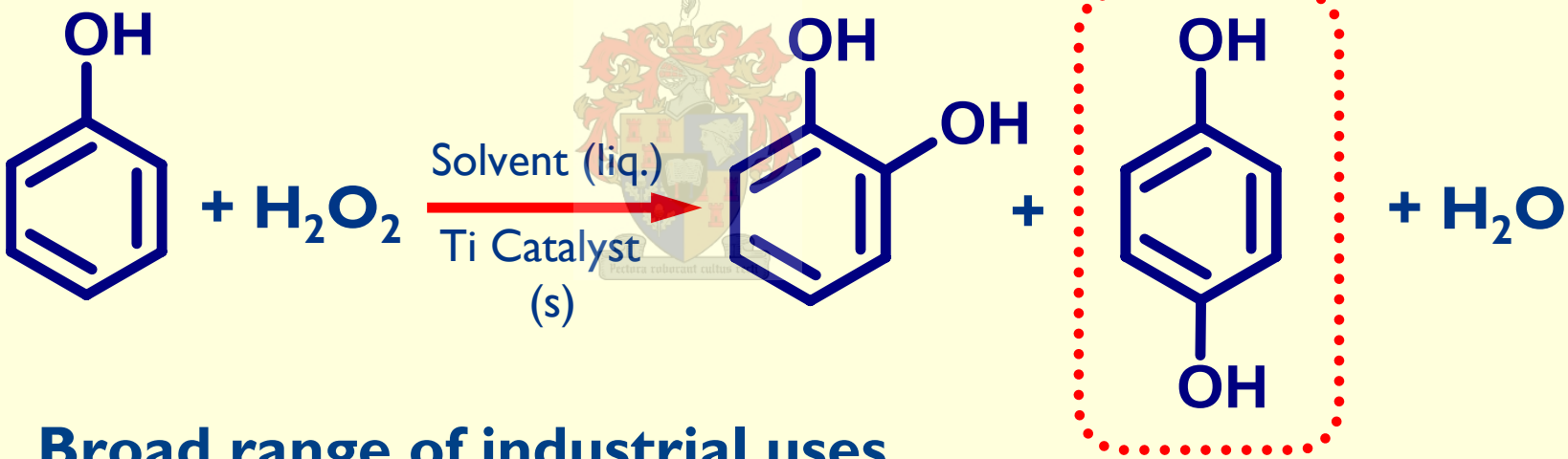

- **Broad range of industrial uses**
- **Enhance hydroquinone production!**
  - *R772 000 per ton vs. catechol's R357 000 per ton (2005)*
- **Factors affecting efficiency of reaction**
  - *Oxidant, catalyst preparation, solvent, temperature*

OXIDISING AGENT

Choice of H_2O_2 as Oxidising Medium

- **Choices for oxidation reactions**
  - *Oxygen/air, H_2O_2, long-chain hydro-peroxides etc.*
- **H_2O_2 favoured as oxidant …… liquid-phase reaction**
  - *Easy to handle*
  - *Mild reaction temperatures*
  - *Inexpensive*
  - *High active-oxygen content*
  - *Multi-phase mass-transfer problems can be avoided*
  - *Only reaction by-product is water* $\Rightarrow$ ***"green" chemistry***

CATALYST PROPERTIES

Choice and Synthesis of Suitable Ti-substituted Zeolites

- **Framework topology & pore geometry**
  - *Accessibility to active sites inside the micropores, e.g., TS-1 (0.55 nm) vs. Ti-β (0.65 nm)*
- **Framework modifications**
  - *Post-synthesis vs. isomorphous substitution of Ti into SiO_2 framework*
- **Framework[1] & surface acidity[2]**
  - *Acidic impurities, e.g., $Al^{3+}/Fe^{3+} \Rightarrow$ unfavourable to selective oxidations*
- **Crystallite dimensions[3, 4]**
  - *Small crystallites offer better catalytic performance*
- **Catalyst polarity[5]**
  - *Enhanced mobility and adsorption of organics in hydrophobic channels*

[1] Camblor et al., 1993 [2] Selli et al., 2004 [3] Wilkenhöner et al., 2001 [4] van der Pol et al., 1992 [5] Blasco et al., 1998

SOLVENT COMPOSITION

Selectivity & Activity Effects

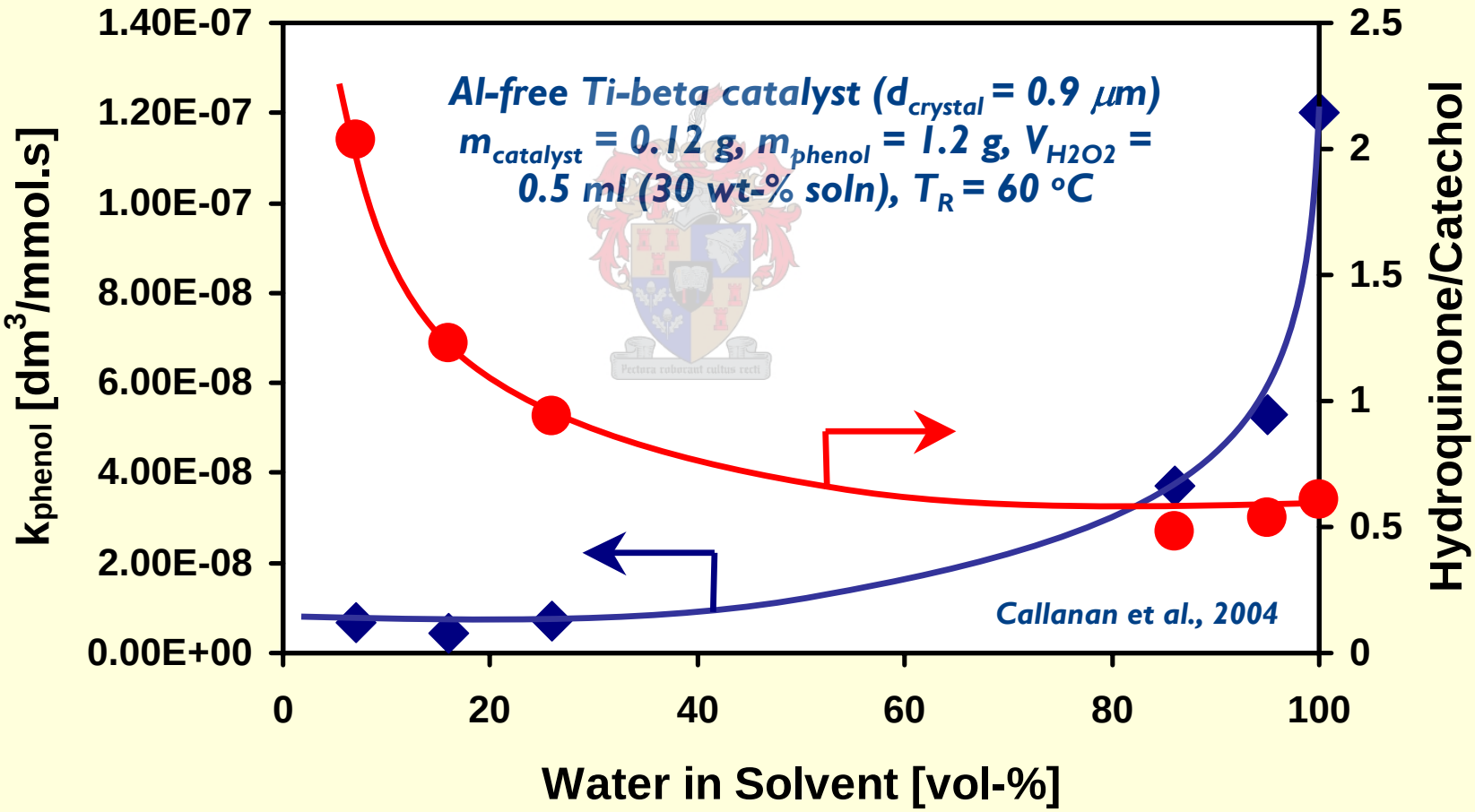

MECHANISTIC IMPLICATIONS

Active Site Formation & Coordinated Active Site Complexes

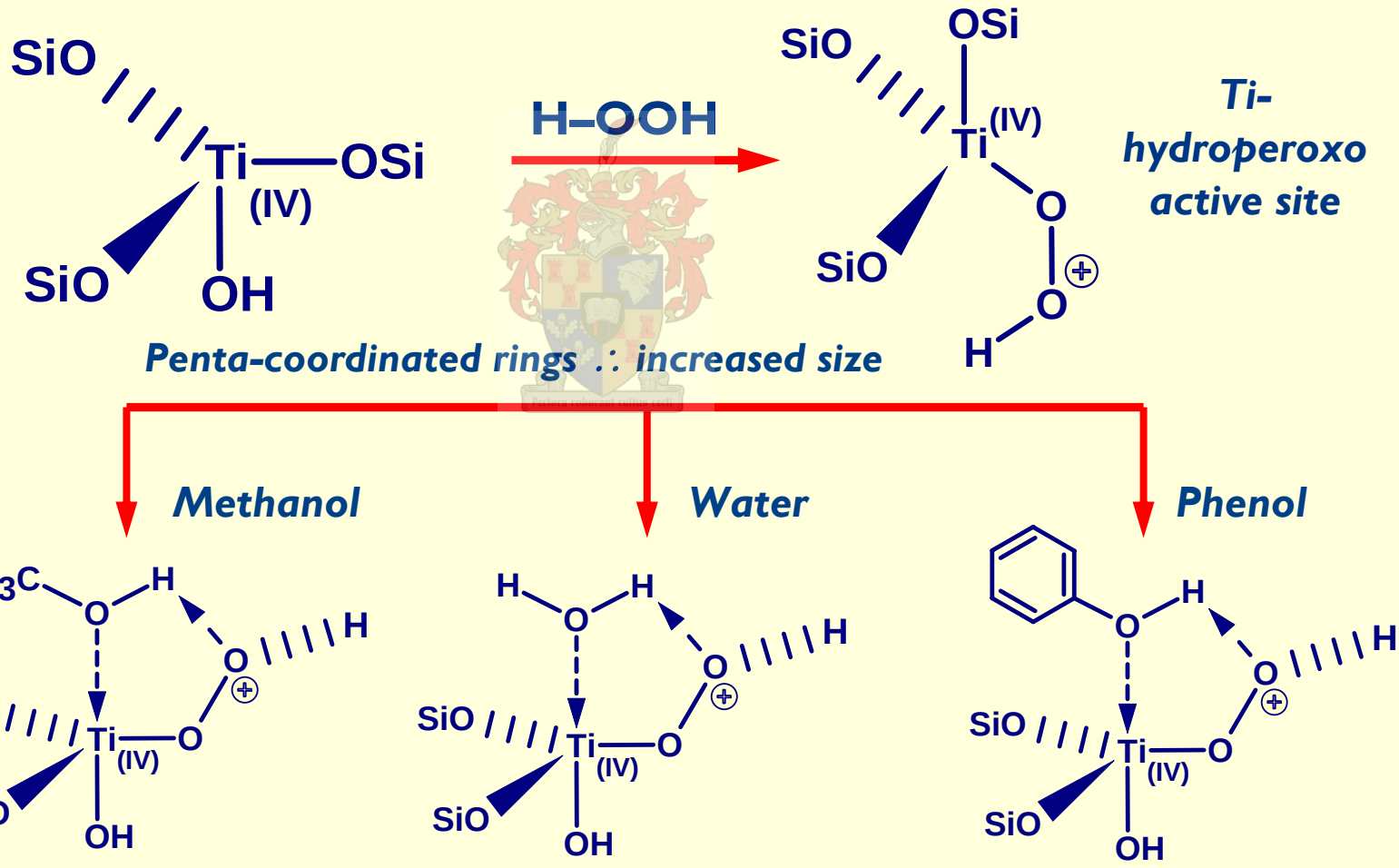

SPECIFIC OBJECTIVES

AIMED TO INVESTIGATE:

- **Peroxide concentration effects in methanol and water solvent over Al-free Ti-β and TS-1**
  - *Initial concentration varied in range 0.55 to 5 vol-% of total volume*
  - *Phenol-H_2O_2 ratio in range 10 to 1.1*
- **Combined effects of solvent composition and peroxide concentration on product selectivity and catalyst activity**
- **Method of peroxide addition in a pseudo semi-batch reactor**
  - *H_2O_2 added in discrete amounts over 4-4½ hours: 0.1 ml per hr & 0.05 ml per 30 min*

EXPERIMENTAL SETUP

Experimental Setup & Product Analysis

- **24 ml glass batch-reactor**
- **Continuous stirring (1000 rpm)**
- **0.2 ml samples at intervals**
  - *Reaction terminated after 12 h*
- **Analysis**
  - *HPLC → aromatics content*
  - *Iodometric titration → residual H_2O_2 concentration*
  - *TG analysis → tar attached to deactivated/used catalyst*

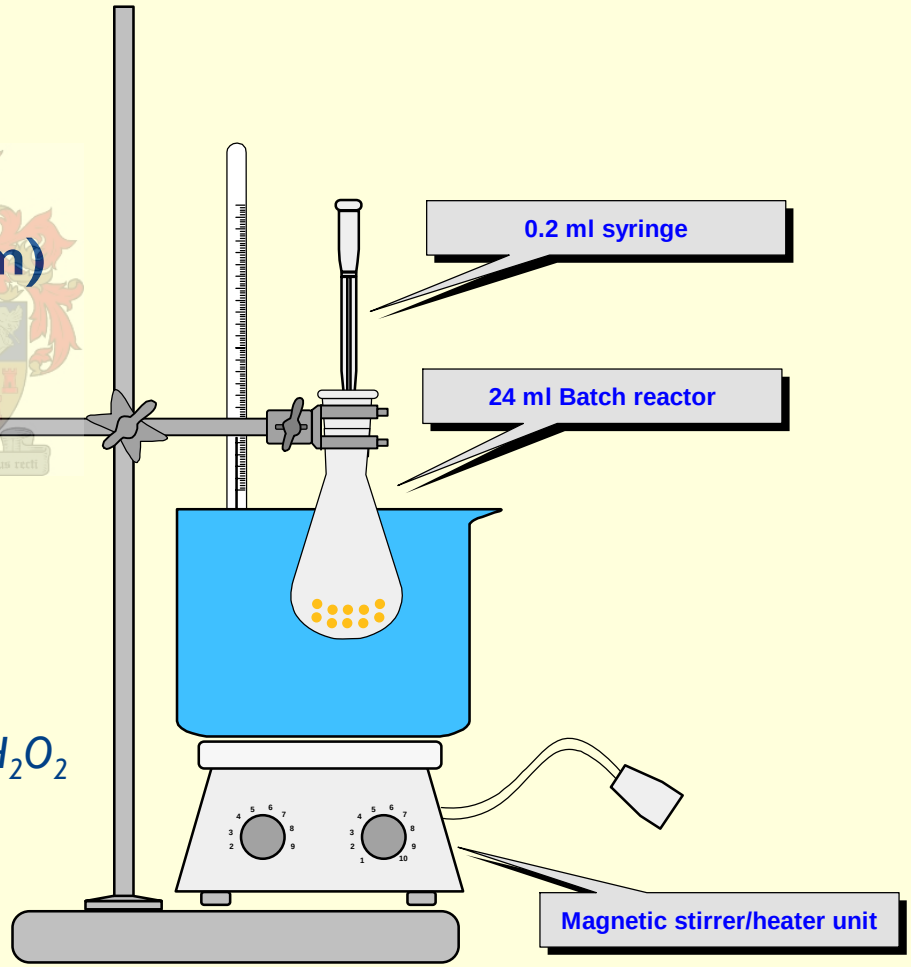

PHENOL CONVERSION

Al-free Ti-β Catalyst, Water Solvent

Phenol conversion vs. time for different starting volumetric fractions of H_2O_2 (WATER solvent)

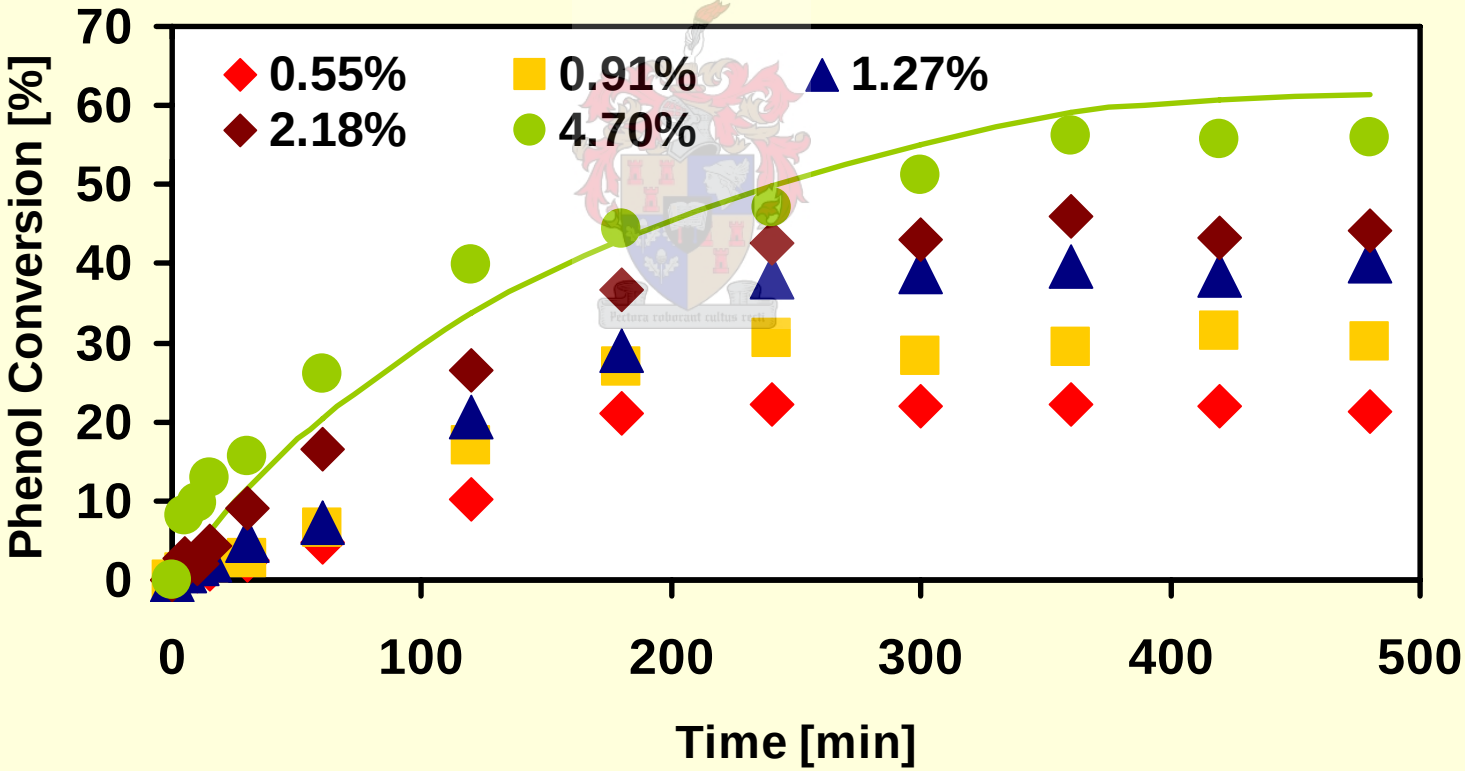

Al-free Ti-beta ($d_{crystal}$ = 0.9 μm), $m_{catalyst}$ = 0.12 g, m_{phenol} = 1.2 g, T_R = 60 °C

PHENOL CONVERSION

Al-free Ti-β Catalyst, Methanol Solvent

Phenol conversion vs. time for different starting volumetric fractions of H_2O_2 (METHANOL solvent)

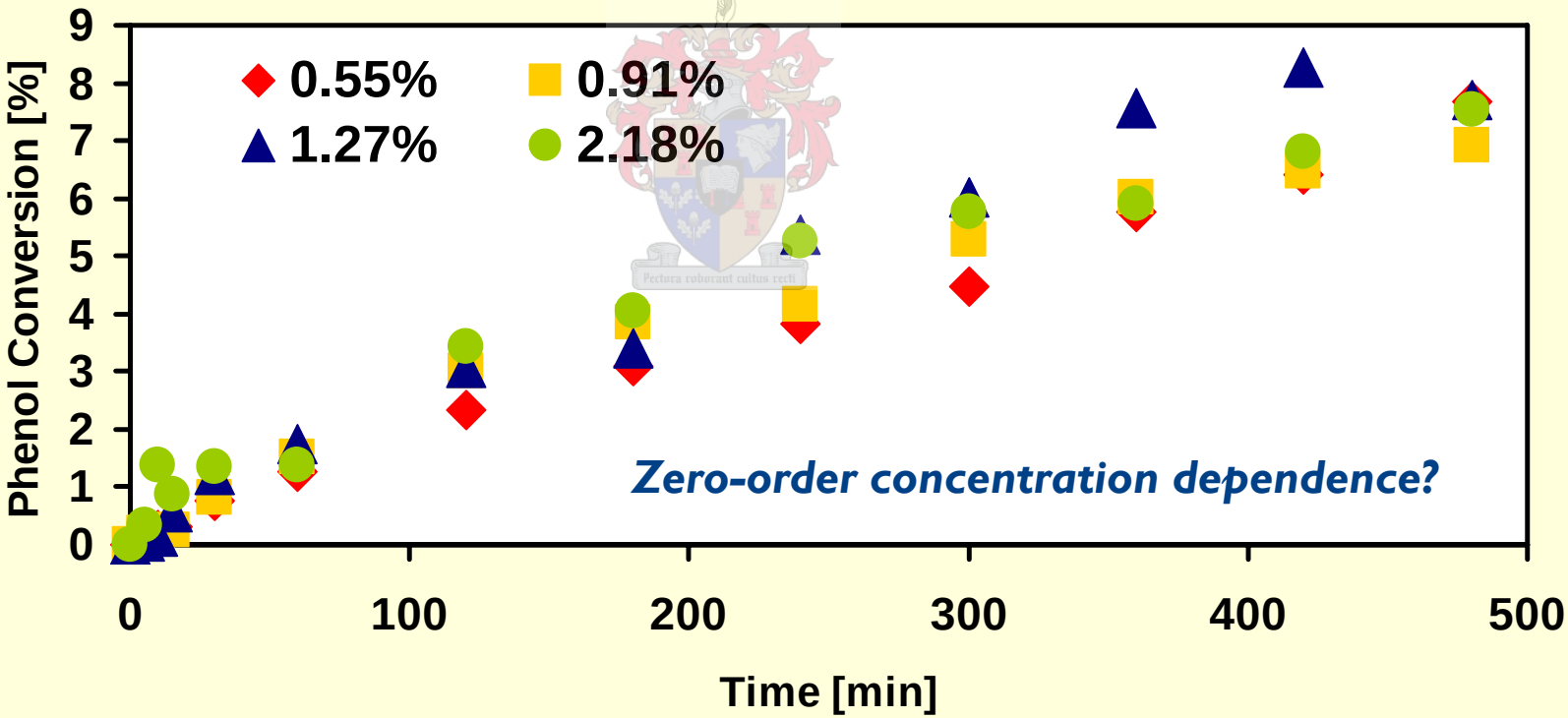

Al-free Ti-beta ($d_{crystal}$ = 0.9 μm), $m_{catalyst}$ = 0.12 g, m_{phenol} = 1.2 g, T_R = 60 °C

RATE FITTING & KINETICS (WATER)

Phenol Rate Constants for 2nd Order Reaction Kinetics

$$-r_{Ph} = k_{Ph} \cdot C_{Ph} \cdot C_{Ox} = C_{Ph,0} \cdot \frac{dX_{Ph}}{dt}$$

$$\Rightarrow \frac{dX_{Ph}}{dt} = k_{Ph} \cdot C_{Ph,0} \cdot (1 - X_{Ph}) \cdot (\theta_{Ox} - X_{Ph})$$

k_{Phenol} [dm³/mmol.s]		
H_2O_2 [vol-%]	Fitted for 480 min	Fitted for 120 min
0.55	1.256×10^{-7}	1.018×10^{-7}
0.91	1.358×10^{-7}	9.114×10^{-8}
1.27	1.275×10^{-7}	7.765×10^{-8}
2.18	1.050×10^{-7}	7.508×10^{-8}
4.70	1.010×10^{-7}	4.882×10^{-8}

- Overall 2nd order kinetics fit best in water solvent
  - *Better overall kinetic fit obtained over 480 minutes*

Rate constant is independent of changing H_2O_2 concentration

RATE FITTING & KINETICS (MeOH)

Phenol Rate Constants for 2nd and 1st Order Reaction Kinetics

$$-r_{Ph} = k_{Ph} \cdot C_{Ph} \cdot C_{Ox} = C_{Ph,0} \cdot \frac{dX_{Ph}}{dt}$$

$$\Rightarrow \frac{dX_{Ph}}{dt} = k_{Ph} \cdot C_{Ph,0} \cdot (1 - X_{Ph})$$

k_{Phenol} [dm^3/mmol.s]		
H_2O_2 [vol-%]	2nd order kinetics	1st order kinetics
0.55	1.729×10^{-8}	2.73×10^{-6}
0.91	9.766×10^{-9}	2.96×10^{-6}
1.27	7.4×10^{-9}	3.3×10^{-6}
2.18	5.540×10^{-9}	3.02×10^{-6}

- 1st order kinetics provides a good fit only for low initial H_2O_2 concentrations in methanol → 2nd order is overall best fit for all concentrations

HYDROQUINONE SELECTIVITY

Al-free Ti-β Catalyst

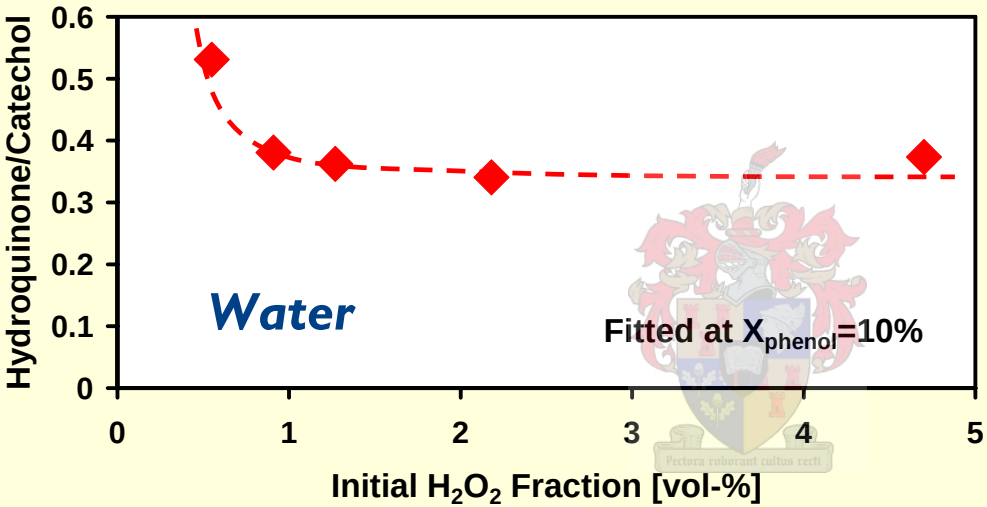

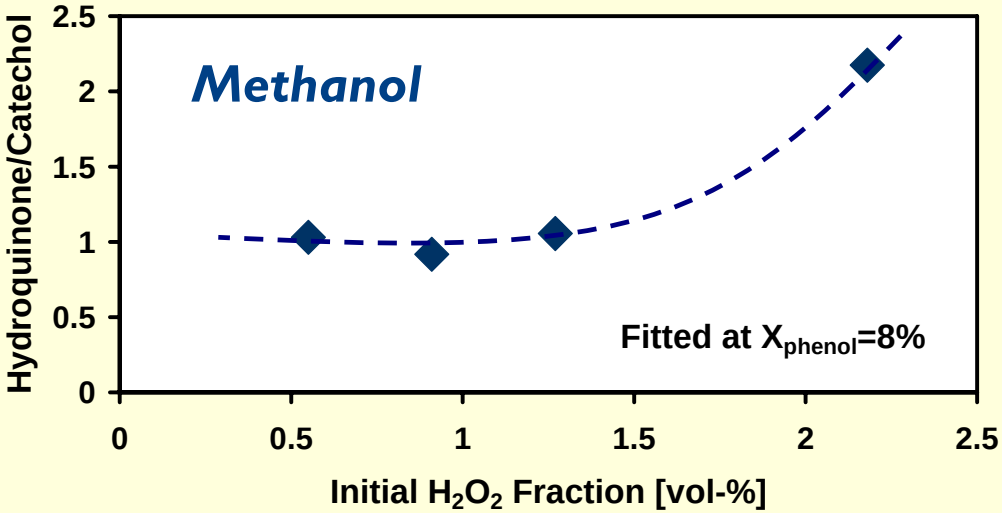

- *1.27 vol-% H_2O_2 appears to be a threshold concentration in both solvents*

- ***OPPOSITE** effects on selectivity in each solvent above this volume fraction*

***WATER:** const. selectivity*
***METHANOL:** selectivity ↑*

PHENOL CONVERSION

TS-1 Catalyst, Methanol Solvent

Phenol conversion vs. time for different starting volumetric fractions of H_2O_2 (METHANOL solvent)

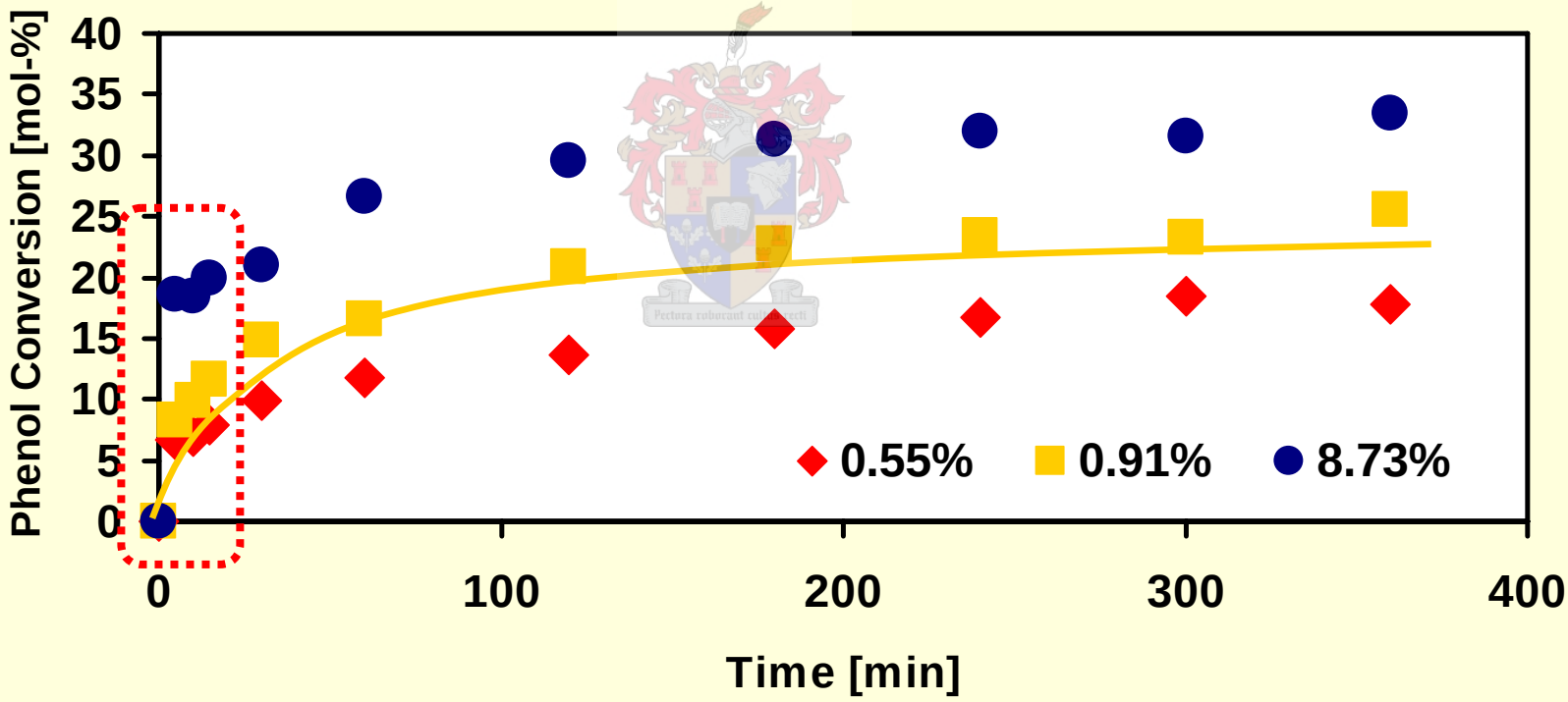

TS-1 ($d_{crystal}$ = 0.1 μm), $m_{catalyst}$ = 0.12 g, m_{phenol} = 1.2 g, T_R = 60 °C

More rapid phenol conversion as initial H_2O_2 concentration increases

HYDROQUINONE SELECTIVITY

TS-1 Catalyst

Hydroquinone selectivity vs. phenol conversion for different starting volumetric fractions of H_2O_2 (METHANOL solvent)

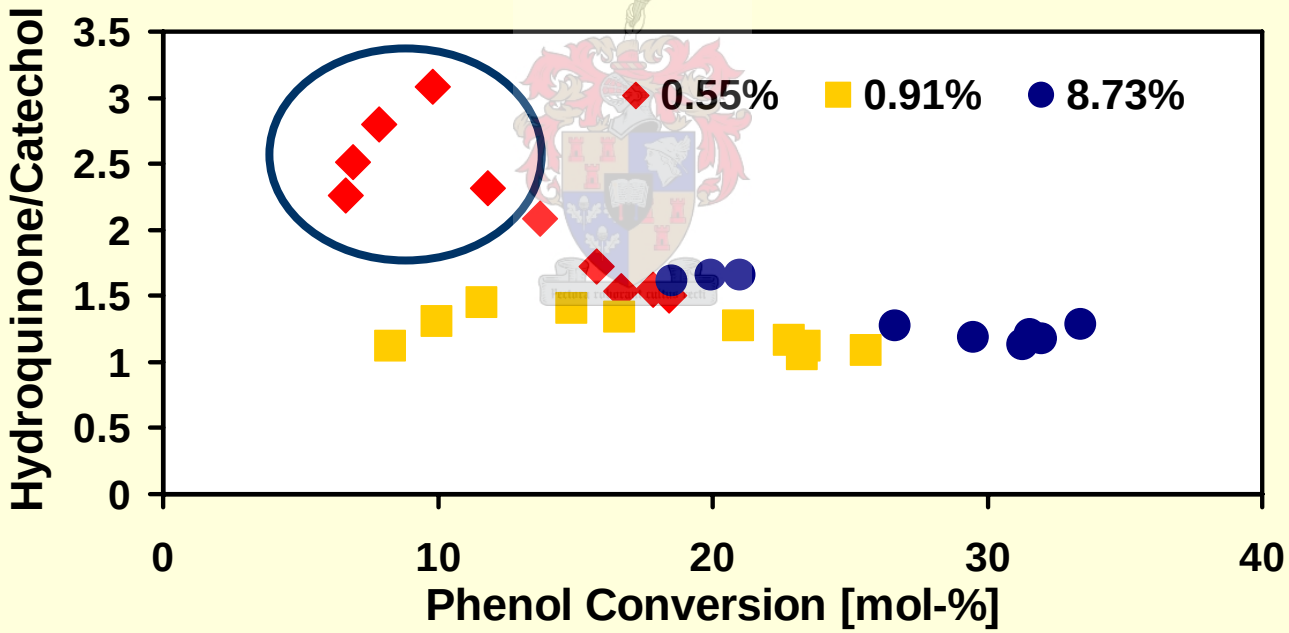

- Initial increase more pronounced at low initial H_2O_2 concentrations
- Constant selectivity approached at higher phenol conversions

PEROXIDE ADDITION EFFECTS

Phenol Conversions for Al-free Ti-β & TS-1 Catalysts

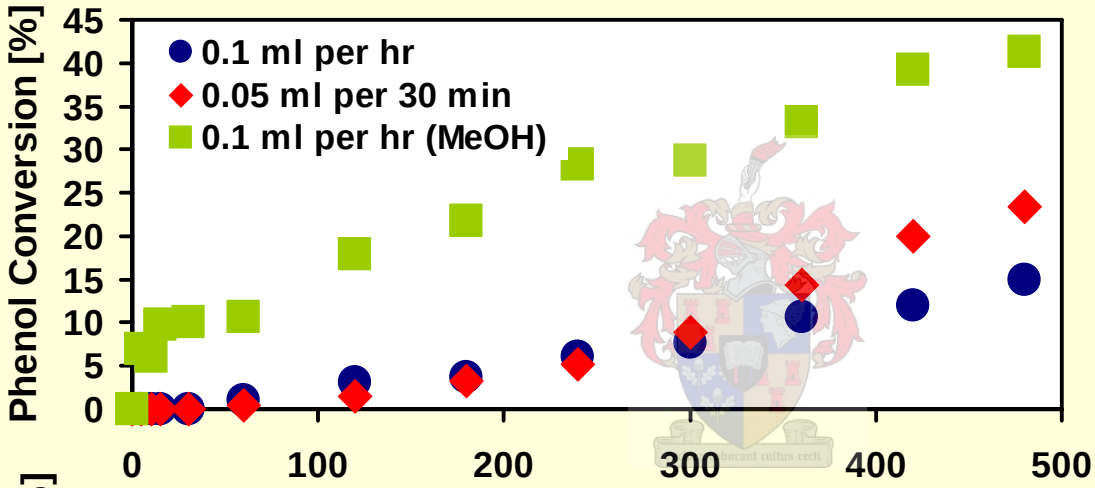

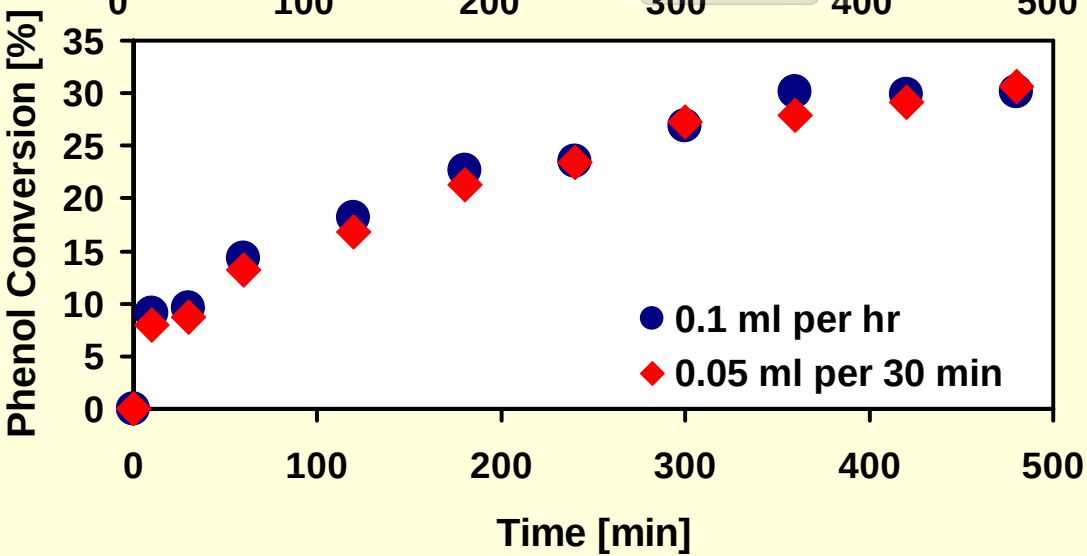

Al-free Ti-β

$d_{crystal}$ = 0.9 μm
$m_{catalyst}$ = 0.12 g
m_{phenol} = 1.2 g
V_{H2O2} = 0.5 ml (total)
T_R = 60 °C

TS-1

$d_{crystal}$ = 0.1 μm
$m_{catalyst}$ = 0.12 g
m_{phenol} = 1.2 g
V_{H2O2} = 0.5 ml (total)
T_R = 60 °C

PEROXIDE ADDITION EFFECTS

Product Selectivities

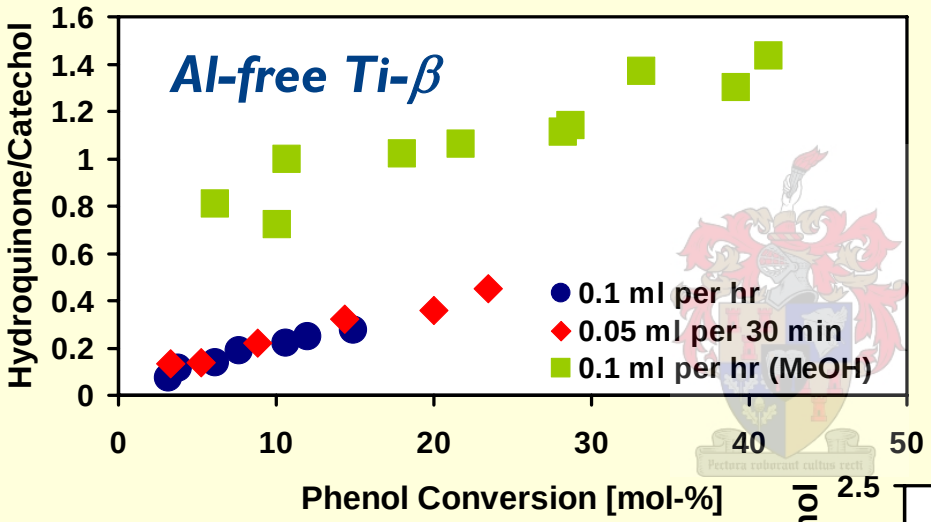

- *Ti-β:* *- p/o >1 in methanol*
  - p/o < 0.4 in water
  - selectivity ↑ as X_{phenol} ↑
- *TS-1:* *- selectivity ↓ as X_{phenol} ↑*

- *Methanol adsorption dominates at low conversions*
- *Favoured for more discrete H_2O_2 addition*
- *Constant selectivity is approached at high conversions*

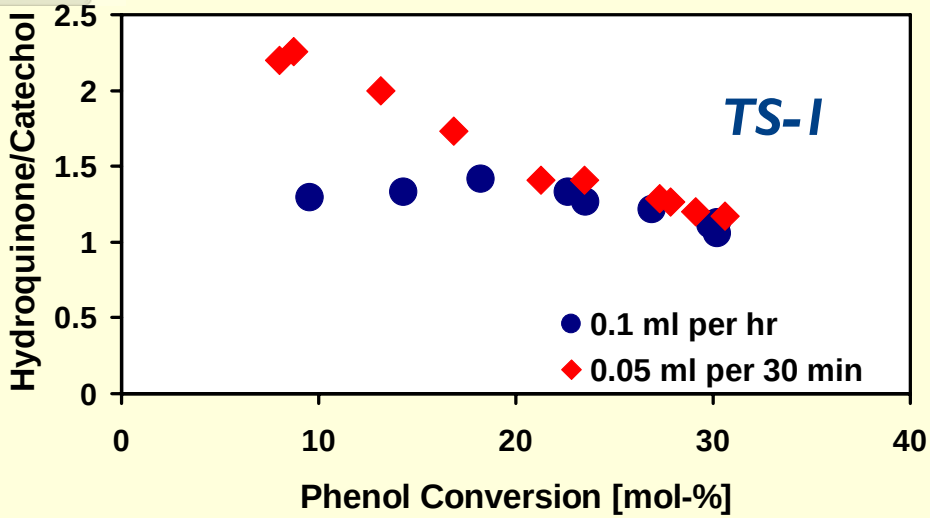

SUMMARISED CONCLUSIONS

- Reaction rate constant is independent of H_2O_2 concentration in water solvent over Al-free Ti-β (1.19×10^{-7} $dm^3/mmol.s$)
- Over Al-free Ti-β, hydroquinone selectivity in methanol is enhanced by higher initial H_2O_2 concentrations
- In water, hydroquinone selectivity is below *ca.* 0.6 for all H_2O_2 fractions over Al-free Ti-β → no positive influence on selectivity
- Over TS-1, higher selectivity is obtained at lower initial H_2O_2 concentrations; constant selectivity is reached at high X_{phenol}
- Discrete H_2O_2 addition favours phenol conversion, particularly in methanol
- Over Al-free Ti-β, hydroquinone selectivity increases, while over TS-1 selectivity to catechol increases with X_{phenol}

ACKNOWLEDGMENTS

- University of Stellenbosch and University of Cape Town
- NRF for financial assistance

QUESTIONS

Thank you

Questions ……

ADDITIONAL SLIDES

MECHANISTIC IMPLICATIONS

Hydroquinone Formation

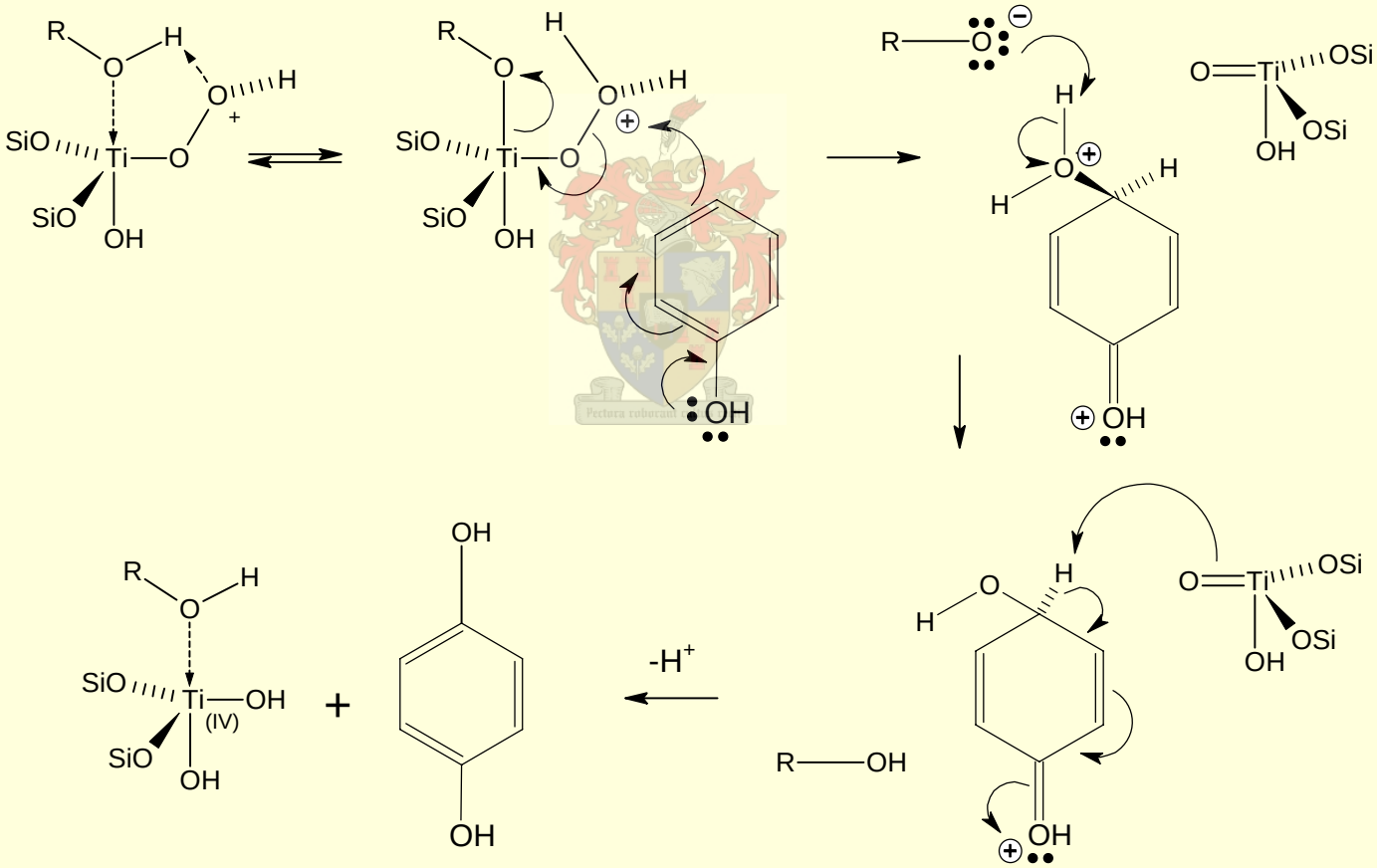

CARBOCATION INTERMEDIATES

Resonance Stabilisation at ortho and para positions

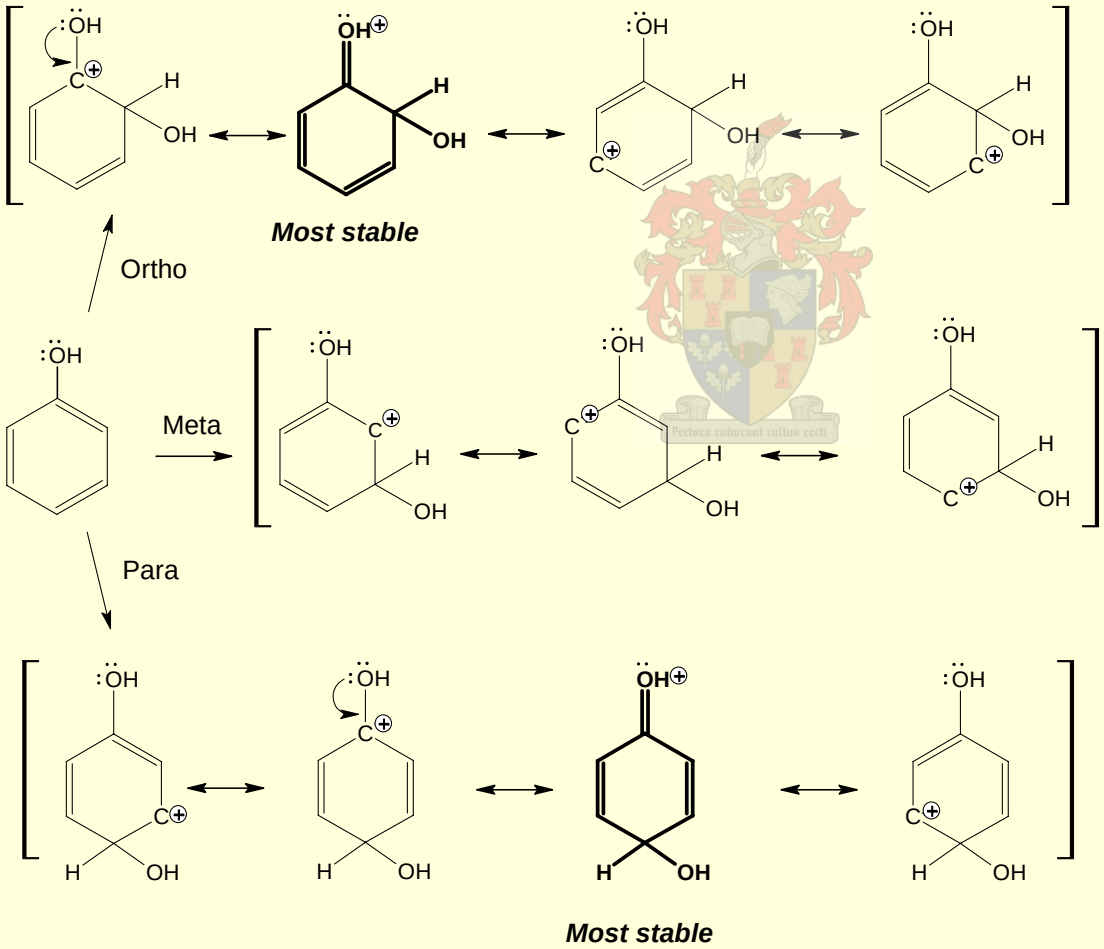

- *Ortho & para complexes are stabilised through delocalisation of the positive charge in the benzene ring*
- *These positions are lower in energy → form faster than meta-substituted complex*
- *Probability for resorcinol formation is thus lower than hydroquinone or catechol*

HYDROQUINONE SELECTIVITY

TS-1 Catalyst

Hydroquinone selectivity vs. time for different starting volumetric fractions of H_2O_2 (METHANOL solvent)

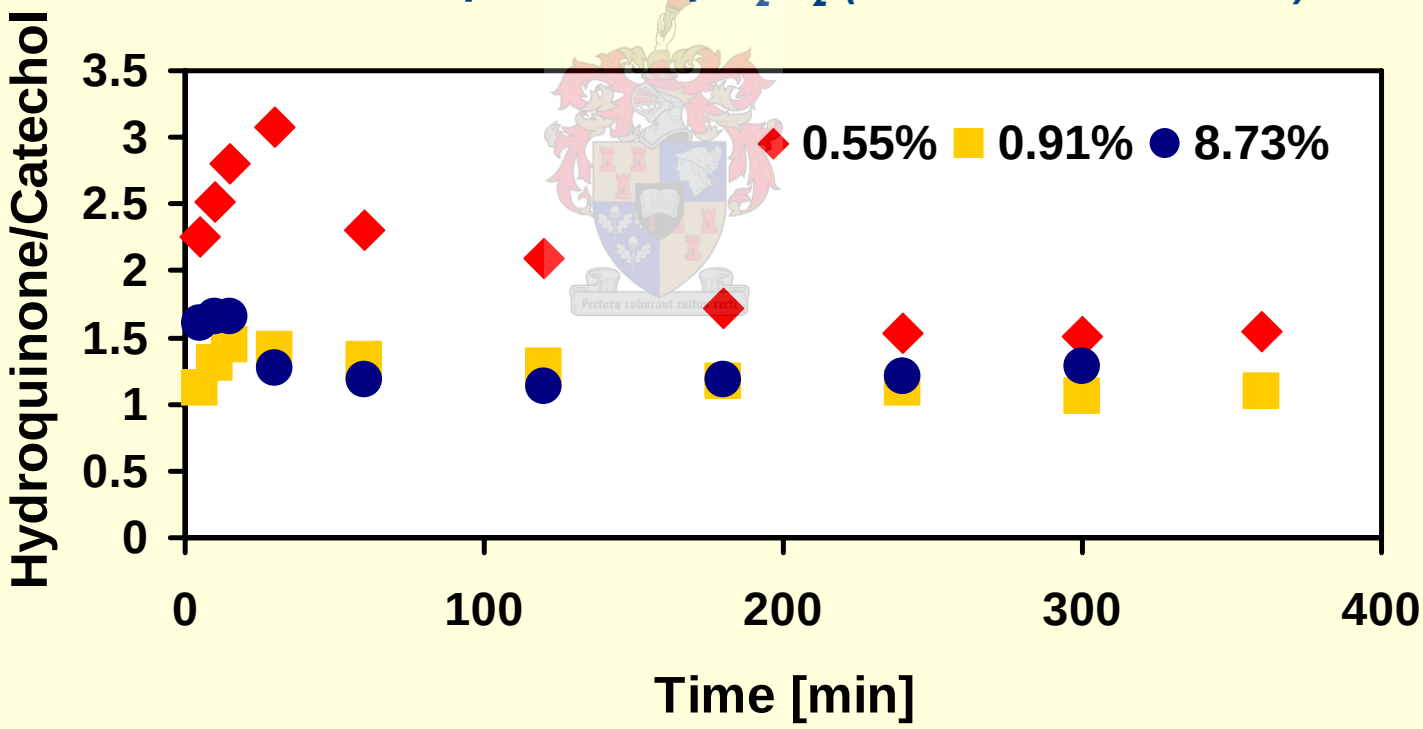

TS-1 ($d_{crystal}$ = 0.1 μm), $m_{catalyst}$ = 0.12 g, m_{phenol} = 1.2 g, T_R = 60 °C

CONCENTRATION-TIME PROFILE

TS-1 Catalyst, 0.55 vol-% H_2O_2, Methanol Solvent

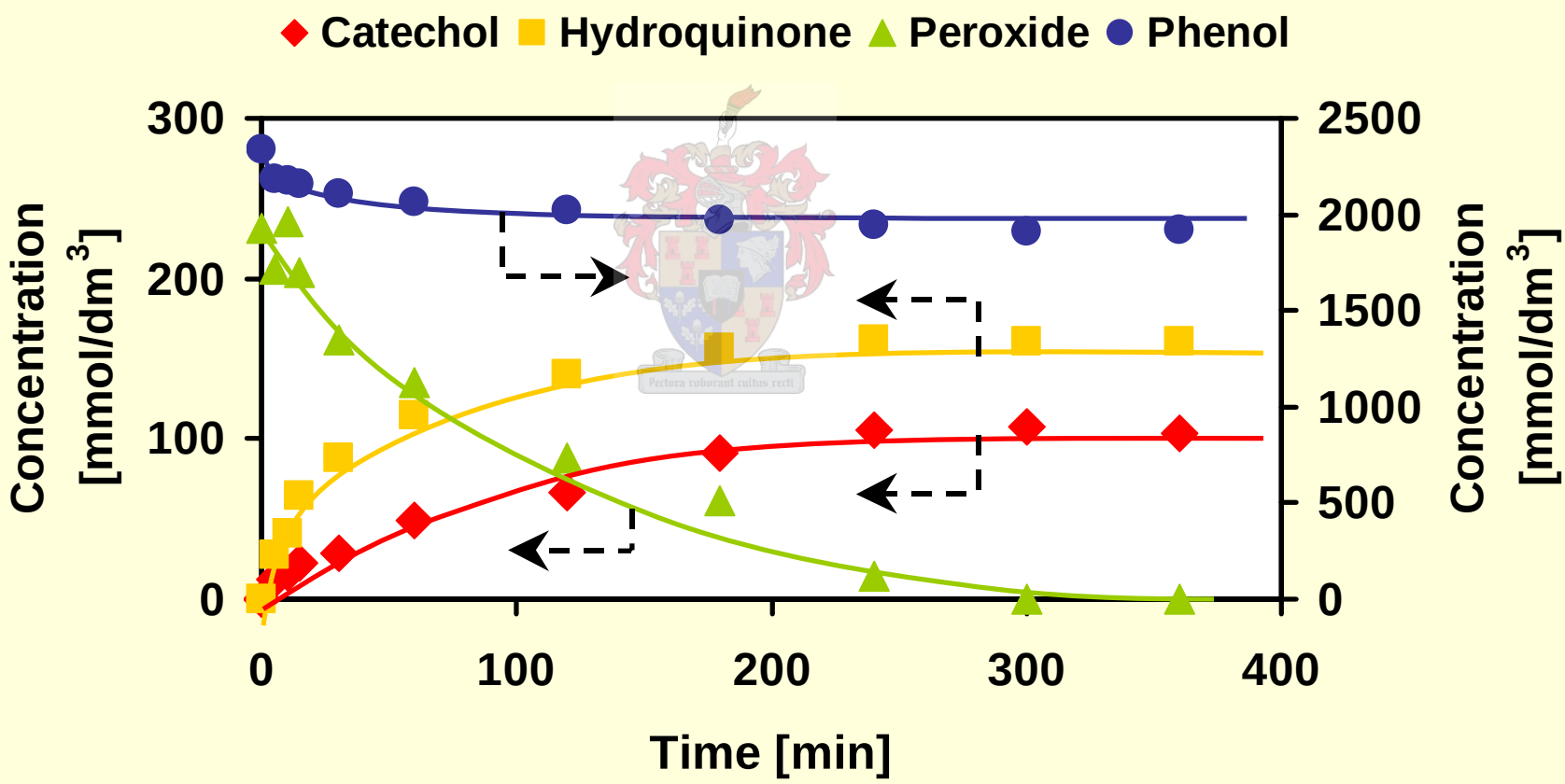

TS-1 ($d_{crystal}$ = 0.1 μm), $m_{catalyst}$ = 0.12 g, m_{phenol} = 1.2 g, V_{H2O2} = 0.15 ml, V_{MeOH} = 5.35 ml, T_R = 60 °C